Runoff controlling factors in various sized catchments in a semi-arid Mediterranean environment in Spain

Cover design: Kartlab, Faculteit Ruimtelijke Wetenschappen Universiteit Utrecht
Cover photos: A. de Wit and P. Burrough

ISBN 90-6809-318-5 (NGS)
ISBN 90-6266-198-X (Thesis)

Gedrukt door Drukkerij Labor – Utrecht

Runoff controlling factors in various sized catchments in a semi-arid Mediterranean environment in Spain

Factores que controlan la generación de escorrentía en cuencas de distinto tamaño en una ambiente semiárido mediterráneo en España
(con un resumen en castellano)

Runoff beïnvloedende factoren in stroomgebieden met verschillende afmetingen in een semi-aride mediterraan gebied in Spanje
(met een samenvatting in het Nederlands)

PROEFSCHRIFT

TER VERKRIJGING VAN DE GRAAD VAN DOCTOR AAN DE UNIVERSITEIT UTRECHT OP GEZAG VAN DE RECTOR MAGNIFICUS PROF. DR. W. H. GISPEN, INGEVOLGE HET BESLUIT VAN HET COLLEGE VOOR PROMOTIES IN HET OPENBAAR TE VERDEDIGEN OP DINSDAG 1 MEI 2001 DES NAMIDDAGS TE 4.15 UUR

DOOR

ARNOLDA MARIA WILHELMINA DE WIT

GEBOREN OP 5 SEPTEMBER 1968 TE HOUTEN

Promotoren: Prof. Dr. P.A. Burrough
Faculteit Ruimtelijke Wetenschappen Universiteit Utrecht
Prof. Dr. S.M. de Jong
Departement van Omgevingswetenschappen, Wageningen Universiteit
Faculteit Ruimtelijke Wetenschappen Universiteit Utrecht

Co-promotoren: Dr. H. Th. Riezebos †
Faculteit Ruimtelijke Wetenschappen Universiteit Utrecht
Dr. V.G. Jetten
Faculteit Ruimtelijke Wetenschappen Universiteit Utrecht

Deze publicatie werd mede mogelijk gemaakt door financiële steun van de Nederlandse Organisatie voor Wetenschappelijk Onderzoek, gebied Aard- en Levenswetenschappen (NWO/ALW)(750.294.03B), het MEDALUS project ('Mediterranean Desertification and Land Use')(EV5V-CT92-0128 en ENV4 CT95 0115) en het Utrecht Centre for Environment and Landscape Dynamics (UCEL).

This publication has been supported by the Netherlands Organization for Scientific Research, Council for Earth and Life Sciences (NWO/ALW) (750.294.03B), the MEDALUS project ('Mediterranean Desertification and Land Use')(EV5V-CT92-0128 and ENV4 CT95 0115) and the Utrecht Centre for Environment and Landscape Dynamics (UCEL).

Contents

Figures

In appendix

Tables

Dankwoord / Acknowledgements / Agradecimientos

Het werk is gedaan, het proefschrift is af maar dit was allemaal nooit gelukt zonder de hulp en steun van velen.

Op de eerste plaats wil ik graag mijn promotor Peter Burrough bedanken voor het delen van zijn kennis over semi-aride landschappen met mij en voor zijn inzet om mijn teksten te structureren en te corrigeren. Ook Steven de Jong wil ik graag bedanken voor de vele inspirerende gesprekken, vooral over remote sensing, maar ook voor zijn betrokkenheid bij het onderzoek en de onderzoeker. Hans Riezebos wil ik postuum bedanken voor zijn begeleiding, het in mij gestelde vertrouwen en het handig regelen van de financiën. Door zijn open benadering van het probleem verwoestijning gaf hij me veel vrijheid in de opzet van mijn onderzoek. Helaas heeft hij het eindproduct hiervan niet mogen meemaken maar zoals hij al voorzag bleef hij tot het einde toe 'aanwezig'. Verder wil ik graag Victor Jetten bedanken voor zijn betrokkenheid en zijn kritische op- en aanmerkingen en de momenten van ontspanning. Dit is het niveau van mijn proefschrift zeker ten goede gekomen.

Het onderzoek is uitgevoerd binnen een project dat geïnitieerd is door Anton Imeson. Samen met Erik Cammeraat en Hein Prinsen hebben we heel wat afgediscussieerd in het veld en op het terras. Ik wil hen graag bedanken voor de prettige samenwerking, Erik voor het delen van zijn kennis over het studiegebied en de meetopstellingen en Hein voor avondjes uit in La Parroquia. Rens van Beek, ook een lid van het onderzoeksteam, wil ik bedanken voor alle keren dat ik bij jou kon komen stoom afblazen van het veldwerk en weer heerlijk bijkwam.

Wat betreft de middelen om het onderzoek uit te voeren, was ik grotendeels afhankelijk van anderen. Ik mocht van Ben van de Weerd en Roel Dijksma (Wageningen Universiteit) een aantal (afgedankte) peilschrijvers meenemen om in Spanje te gaan meten. Professor Melia Miralles and Younis (Universitat de València) and afterwards Matthias Boer (EEZA/CSIC Almería) supplied me with satellite images to do my remote sensing analysis. Professor Joachim Hill (University of Trier) was willing to share his FieldSpec-II measurements with me. I am very grateful to all these people, these supplies have proven to be indispensable for the completion of this thesis.

Cees Klawer, Bas van Dam, Marcel van Maarseveen, Jaap van Barneveld, Wim Haak, Theo Tiemissen, en Marieke van Duin wil ik hartelijk danken voor hun inzet voor het helpen zoeken naar goedkope betrouwbare meetopstellingen, het verstrekken en het onderhoud van de apparatuur en het snel analyseren van monsters. Jeroen Schoorl (Wageningen Universiteit) wil ik heel erg bedanken voor zijn hulp bij het sjouwen van zakken cement en het bouwen van de meetopstellingen in het veld.

Soms vond ik het allemaal zo ingewikkeld dat ik er zelf niet meer uit kwam. Gelukkig waren Freek van de Meer (ITC/Technische Universiteit Delft), Edzer Pebesma, Theo van Asch, Martin Hendriks, Thom Bogaard, Marcel van de Perk en Simone van Dijck bereid om mee te denken en suggesties te doen voor

verbeteringen. Hiervoor mijn hartelijke dank. Lodewijk Hazelhoff wil ik bedanken voor het gebruik van zijn Iso2grid. Cees Wesseling, Kor de Jong maar vooral Derk Jan Karssenberg wil ik bedanken voor hun hulp bij het gebruik van PCRaster. Derk Jan, zonder jouw betrokkenheid, heldere geest en snelle oplossingen had het een eeuwigheid geduurd voor het model in elkaar stak. Ik ben je hiervoor erg dankbaar.

Estoy muy agradecido para la ayuda de Antonio Gomez Plaza, Victor Castillo Sanchez y Jose Ramon Rodriguez (CEBAS/CSIC Murcia), Gonzalo Gozales Barbera y Francisco Belmonte Serrato (Universidad de Murcia), Younis (Universitat de València), Matthias Boer (EEZA/CSIC Almeria) y Carolina Boix (Universitat de València, UvA Amsterdam). Especialmente Toni y Gonzalo para introducirme en varios institutos; sin vosotros no me podía enterarme nada. Además Toni ha traducido el resumen. Quiero agradecer todos para sus conversaciones en un ambiente agradable. Toni, me alegré mucho de mostrarte mi país, nuestra colaboración ha significado mucho para mí.

Al mijn collegae met wie ik gesquashed heb wil ik bedanken voor de ontspanning. Met Simone van Dijck, Oscar van Dam, Marcel de Wit, Nico Willemse en Jacob Wallinga was het erg gezellig op 'onze gang'. Celia Nijenhuis, Annina Andriessen en Irene Esser, bedankt voor alle ondersteuning die via jullie kreeg. Rens van Beek, Brigit Janssen-Stelder, Pim van Santen maar vooral met Simone van Dijck wil ik bedanken voor de prettige manier waarop we een kamer gedeeld hebben.

De dataset waarop dit proefschrift is gebaseerd, is mede tot stand gekomen door de inspanningen van Klaas Scholte, Marian Slenter, Sebastiaan van Bemmel, Martijn Odijk, Jeroen van den Brink, Michiel Dorresteijn, Wouter Dorigo en Yvonne Groenendaal. Ik wil jullie graag bedanken voor jullie inzet en het harde werken in de warme zon maar ook voor de gezelligheid. Mede door jullie was het veldwerk altijd leuk om te doen.

Quiero agradecer las familias Cabrera y Navarro en La Parroquia por su hospitalidad, gracias a ustedes mi estancia en La Parroquia estuvo siempre muy agradable. También quiero agradecer Andres, Santos, Inez, Marisol, Trini, Loli y Puri para su compañía. Con vosotros me he divertido muy bien y pienso mucho a nuestras conversaciones con bebidos y juegos en el O'KU.

Mijn vrienden wil ik bedanken voor de afleiding van het onderzoek. Mijn familie wil ik heel erg bedanken voor hun steun en meeleven in de problematiek van 'het promoveren'. Ik heb genoten van de keren dat mijn vader mee was in het veld; je was werkelijk de beste veldmaat die ik me kan wensen. Gijs wist op een heerlijke manier mijn gedachten van het proefschrift af te leiden; je bent een supervent! Tot slot wil ik Leo bedanken, je bent mijn rots in de branding geweest die altijd rustig bleef. Je weet wat promoveren inhoudt maar liet me hierin mijn eigen weg kiezen. Hoewel je kritisch was, bleef je me steunen in alles wat ik wilde of deed. Vooral de laatste periode van het afronden is voor jou en Gijs zwaar geweest. Nu het af is, kunnen we samen verder.

1 Introduction

1.1 The problem of land degradation

In 1998 newspapers reported that insurance companies had increased their payout from 30 billion dollar in 1997 to 90 billion dollar in 1998 for damage caused by natural disasters all over the world (*www.swissre.com*). Storms and floods caused most of the damage and to a lesser extent damage was caused by earthquakes, volcanic eruptions, drought, heat waves, landslides and avalanches.

In recent years the frequency of natural disasters due to excessive rainfall seems to have increased. Some scientists claim that the increase of the frequency of excessive rainfall is a result of climatic change due to global heating (Imeson & Emmer, 1992). For Europe, rainfall is expected to become more extensive and the area of unreliable, more irregular rainfall will shift northwards in the direction of Mediterranean Europe. Climatic change will also lead to an increase of evapotranspiration and decrease of the soil water retention in southern part of Europe, leading to an increase of the aridity in Mediterranean Europe (Imeson & Emmer, 1992) making it more vulnerable to land degradation processes. Based on Barrow (1991) and Thomas and Middleton (1994) land degradation is defined as the reduction of the potential of the terrestrial bio-productive systems (i.e. soil, vegetation and other biota) and includes the deterioration of the physical and chemical properties of the soil generally caused by a deficit or a surplus of water. Many scientists (e.g. Brandt & Thornes, 1996; Poesen & Hooke, 1997) are convinced that progressing land degradation processes will lead to the desertification of Mediterranean Europe; here the term desertification is defined as irreversible land degradation resulting from climatic change and human activities (Barrow, 1991; Thomas & Middleton, 1994).

During recent decades land degradation in the Mediterranean region is seen as a widespread problem. To combat this problem national governmental and non-governmental organisations have developed a wide range of political and scientific actions, an overview of which is given by Burke and Thornes (1998).

1.2 Contributing factors to land degradation in the Mediterranean

Land degradation in the Mediterranean is mainly caused by excessive runoff (Poesen & Hooke, 1997). The vulnerability of Mediterranean Europe towards land degradation can be explained by a variety of characteristic physical and climatic properties of the region. The combination and interaction of these typical properties result in complicated and strongly discontinuous hydrologic conditions. An additional problem is the temporal and spatial scales at which these conditions operate. Hydrological processes vary from the size of a raindrop, through hillslopes

and catchments to regions: numerous studies (amongst others, Gupta et al., 1986; Kalma & Sivapalan, 1995) have reported on this topic.
The main contributing factors towards land degradation in the Mediterranean are;

- Precipitation
- Infiltration
- Vegetation cover
- Discontinuity of flow.

1.2.1 Precipitation

Winter rainfall and dry hot summers are typical for the Mediterranean climate. In the semi-arid and arid parts of the Mediterranean periods of drought are not uncommon, both within and between years. These periods are interspersed by torrential rainfall events (Conacher & Sala, 1998).

In hydrological studies covering long periods of time, researchers often use the maximum daily precipitation and its intensity as measures for the occurrence of overland flow (Ahnert, 1987; de Ploey et al., 1991; de Jong, 1994). In a semi-arid Mediterranean climate that is characterised by short lasting, highly intense rainfall, it is questionable if the maximum rainfall amount per day has been properly measured or whether recorded values depend more on the format of the available rainfall data.

Besides the large variability in rainfall amounts and the temporal variability of the rainfall events, the spatial variability of rainfall events in Mediterranean arid and semi-arid regions is also known to be large. It is not unusual for the flood registered at the outlet of a catchment to be the result of an intensive partial-area storm over only a part of the catchment. Several studies (Butcher & Thornes, 1978; Pilgrim et al., 1988; Wood et al., 1988; 1990; Blöschl et al., 1995; Singh, 1997) stress the need to incorporate the spatial variability of rainfall in hydrological analysis and modelling.

1.2.2. Infiltration

In the Mediterranean, many soils have a loamy to loamy-sand texture (Poesen & Hooke, 1997) and are developed in limestone or marls. Apart from vegetation, the occurrence of sealing, compaction, crusts and the presence of stones all affect the infiltration rate. Sealing, compaction and crusting is generally assumed to reduce infiltration although some scientists claim that certain crusts increase infiltration (Thornes, 1994). In shrublands in southeast Spain, Cerdà (1997a) found that increasing bulk density resulted in reduced infiltration rates. The presence of rocks often increases the infiltration rate and reduces runoff due to stabilizing effect on the soil surface (Poesen 1996; Poesen & Hooke, 1997). It should be noted that the infiltration characteristics just described result from rainfall experiments at plot size and it is unknown whether they can be extrapolated to larger surfaces.

In the semi-arid Mediterranean where most rain falls in torrential events, the rainfall intensity often exceeds the limited potential rate of infiltration and the downslope flowing water is classified as Hortonian overland flow (Yair & Lavee, 1985; Pilgrim et al., 1988; Poesen & Hooke, 1997). Because of the spatial differences in infiltration capacity, the overland flow generated within the area covered by the rain may have infiltrated before it reaches the adjoining dry area downslope (Yair & Lavee, 1985; Pilgrim et al., 1988). Due to the disconnection of saturated areas, a significant subsurface flow may be lacking. According to Yair and Lavee (1985) a systematic downslope decrease of soil moisture can be noted in dry areas which is in contrast to the ideas behind the wetness index (explained in section 6.2). The estimated downslope decrease of soil moisture may result in dryer areas along the channel than on the hillslope. Because of this, Yair and Lavee (1985) state that the spatial distribution of soil moisture cannot be regarded as an important control of storm runoff generation in arid areas.

Due to the spatial variability of the infiltration capacities along hillslopes, the estimation of the infiltration for catchments is a problem. The infiltration measured in small plots (0.01-0.1 m) differs from the infiltration over larger areas and for this reason the total infiltration over larger areas can only be measured by runoff measurement (van Dijck, 2000). The infiltration estimated over larger areas is then called 'effective' infiltration (Binley & Beven, 1989).

1.2.3. The influence of vegetation cover on the water balance

In arid and semi-arid Mediterranean regions no closed natural vegetation cover exists due to the competition for water. The vegetation cover consists of a sequence of plant and bare interplant areas. In these regions interception is often highly significant in determining the micro-hydrology at a site (Pilgrim et al., 1988). The structure of the plant strongly determines the water availability of the plant. For example tussock grasses (*Stipa tenacissima*) with leaves that lead the water to the centre of the plant (figure 3.7, section 3.5), are known to have significantly higher interception than pine trees with their transparent canopy (Dorigo & Groenendaal, 2000).

Vegetation cover is of major importance for infiltration (Pilgrim et al., 1988). Lyford and Qashu (1969) measured three times greater infiltration rates underneath plants in a desert environment than in the openings between the plants. Combined with greater bulk densities of interplant areas, this implies that more water is available in the soil underneath the plant. In the southeastern part of Spain increasing biomass productivity has been shown to result in larger infiltration rates (Cerdà, 1997a) and other studies (Francis, 1990; Francis et al., 1986, Imeson et al., 1999) have shown that the steady-state infiltration rate on natural slopes of weathered unvegetated marls is significantly lower than on vegetated marls. The behaviour of the average rate of soil wetting in different soils developed in marl or in limestone, was examined by rainfall simulations in the Belmonte test site in eastern Spain (Bergkamp et al., 1996). For the soils developed in limestone major

differences were observed between the bare soils on one hand and the stony vegetated patches on the other. On the soils developed in marl, the differences in soil wetting rate between bare and vegetated patches were small (Bergkamp et al., 1996).

Vegetation cover is important for distribution and redistribution of the water. Thornes (1995) stated that in a semi-arid Mediterranean environment, the actual patchy pattern of vegetation cover may be the result of the former influences of concentrated water paths or erosion that have taken place. Subsequently this vegetation cover will affect the formation of concentrated water paths and control future erosion and sedimentation patterns. As a result of this bi-directional relation between vegetation cover and erosion rate an equilibrium exists that can be easily disturbed (Thornes, 1985). The exact interaction between these processes at subcatchment scale must still be clarified by further research.

Most important for the redistribution of overland flow are the plant's three-dimensional shape above and below the soil surface, the spatial distribution of plants and the species composition of the communities (Francis, 1994). In many parts of the semi-arid Mediterranean environment, trees have disappeared from the south facing slopes. The removal of trees will have taken place at both north and south facing slopes but the less favourable soil moisture conditions of the south facing slopes prohibit natural regeneration of trees. The resulting bare and sparsely vegetated areas make the hillslopes very vulnerable for concentrated water paths (López Bermúdez & Albaladejo, 1990). It is well known that the patchy distribution of *Stipa tenacissima L.*, which is characteristic for southeastern part of Spain, influences the distribution of water (Cerdà, 1997b). Its tussocks retain a large amount of dead leaves that can amount to six times the green leaf dry weight. This helps *Stipa tenacissima* to use topsoil water efficiently and to capture lateral runoff water and runoff-transported sediments (Domingo et al., 1998).

As described in this section, the cover of vegetation is important as it reflects favourable and less favourable soil moisture conditions and influences infiltration processes and concentrated water paths and controls the runoff on hillslopes. Apart from these general statements, little is known about the exact influence of vegetation cover on runoff in small catchments.

Catchment studies in recent years show a negative correlation between the forest cover and the water yield of catchments (Bosch & Hewlett, 1982). Therefore, in an attempt to reduce runoff, large regions in the arid and semi-arid Mediterranean have been afforested. But, especially in Southeast Spain the mechanical interference of slopes caused by terrace construction has had the opposite effect, and replacement of the natural vegetation cover by afforestation projects has increased the discharge of the treated catchments (Sorriso-Valvo et al., 1995, Ternan et al., 1997; De Wit & Brouwer, 1998). Recently it has become clear that the expected protective and erosion control effects of afforestation projects in non-cultivated semi-natural vegetated areas, have been less succesful than was intended (Francis & Thornes, 1990a; Quinton et al., 1997).

There are clear relations between land cover (plants) and susceptibility to land degradation, but these occur over a wide range of scales. On a small surface, individual plants control the hydrological conditions. Likewise land cover units and

land use will control the hydrological conditions in larger areas or regions. Between the size of an individual plant and a large region, several possibilities exist for the parameterisation of the vegetation cover like the Leaf Area Index (LAI) of a specific plant, the characterisation of a vegetation pattern, expressing the amount of surface cover per species per unit area or a simple land use classification. It remains unclear what a proper parameterisation of vegetation is at the size between plant and region in a semi-arid Mediterranean environment. This needs to be clarified in order to properly assess the effects of vegetation on hydrological response.

1.2.4. Discontinuity of flow

Due to short lasting rainfall events the length of slopes that are capable of contributing runoff to the channel, is often very short in the semi-arid Mediterranean. The slope angle and length of the slopes, determined by the geological and geomorphological setting, control the concentration of overland flow (López Bermúdez & Albaladejo, 1990). In the semi-arid Mediterranean most of the upper area of long slopes do not contribute water to the slope base (Yair & Lavee, 1985). This means that only a small proportion of the area contributes to storm runoff in the channels of small watersheds (Yair & Lavee, 1985; Puigdefabregas et al., 1999). This runoff is called partial-area runoff and the area from which this runoff originates is called the 'near-channel' area.

Discharge in channels in arid and semi-arid Mediterranean regions is mostly ephemeral (Thornes, 1977; Lane, 1982; Thornes, 1994; Poesen & Hooke, 1997) which means that the channel is dry for some period between the arrivals of runoff producing storms. The runoff volume and peak discharge are reduced substantially by infiltration losses in the initial dry stream channel. These losses are called transmission losses (Thornes, 1977; Lane, 1982; Yair & Lavee, 1985) and are related to network characteristics, channel widths, permeability and type of bed material (Butcher & Thornes, 1978).

This means that a larger channel width leads to an increase of transmission losses and a downstream increase of potential subsurface storage (Butcher & Thornes, 1978). This way the peak flow in the stream channel decreases downstream and flows survive a short distance without tributary inflows. Only high peaks can survive over long downstream distances. So both the survival length of the flow and the amount of runoff are controlled by these transmission losses (Thornes, 1977; Lane, 1982; Poesen & Hooke, 1997). Therefore runoff depths decrease when averaged over increasing catchment areas (Pilgrim et al., 1988; Thornes, 1994). The survival length of the flow is also determined by the pattern of the stream network because it determines the distance to the next tributary input (Thornes, 1977, Butcher & Thornes, 1978; Thornes, 1994).

The flood wave coming down the dry river results in an almost vertical rising limb of the hydrograph. Sharply peaked runoff hydrographs with short time bases are characteristic for the ephemeral streambeds in arid and semi-arid regions. Usually the time to peak of the rising limb is shorter than the recession time of the

falling limb of the hydrograph (Thornes, 1977; Lane, 1982; Pilgrim et al., 1988; Thornes, 1994; Poesen & Hooke, 1997). This results in asynchronous hydrographs. The flow may be generated over small areas. The flow of subcatchments resulting from different tributary systems may reach the main stream channel at different times, sometimes when the main channel is dry either before or after a flow has passed through (Thornes, 1977; Thornes, 1994).

Recently, improved understanding of the rainfall-related processes in catchments has led to the ability to model rainfall-runoff relations in ephemeral stream channels in arid and semi-arid regions (Thornes, 1977; Lane, 1982). A key issue of these models is that the survival length of the flow determines the amount of discharge. Especially in arid and semi-arid regions this is strongly influenced by transmission losses.

In the hydrological analysis of small catchments in the semi-arid Mediterranean, the catchment response is often complicated because the discontinuity of flow on both hillslopes and streambeds controls the hydrological conditions at the outlet. In small catchments local hillslope processes control the shape of the hydrograph (Beven & Wood, 1993; Blöschl & Sivapalan, 1995). Upland areas can produce large volumes of runoff but they do not always reach the outlet of large catchments (Poesen & Hooke, 1997). In large catchments, the role of the topology of the channel network in the hydrologic response increases (Beven & Wood, 1993; Blöschl & Sivapalan, 1995). Large volumes of water in the channels of large catchments can have catastrophic consequences (18 October 1978 in Puerto Lumbreras (Spain), 19 June 1996 in Tuscany (Italy), 7 August 1996 in Biescas (Spain), 6 May 1998 in Campania (Italy)) and can cause severe damage and disturbances of the landscape.

Knowledge is lacking how runoff of the upland areas is linked to the runoff in the channels. An understanding of this linkage should lead to improved soil erosion and channel models with varying resolution (Poesen & Hooke, 1997). Furthermore this knowledge will help to improve hydrological conditions thereby reducing the damaging effects of excessive floods.

1.2.5 The combined effect of Mediterranean characteristics

As described in the previous sections, the characteristics typical for a Mediterranean environment have impact on the hydrological conditions at different levels of resolution. Besides the problem of resolution, the factors interact. Climatic conditions influence the infiltration and flow conditions as well as the vegetation growth. On the other hand, vegetation growth also impacts on the infiltration and flow conditions and vice versa. Adding this set of complex interactions and their non-linearity and mutual feedback to the different resolutions at which the interactions take place, makes land degradation an even more complex problem.

When studying this problem, a major question is deciding at what resolution to collect data and do measurements. 'People sized' observations like soil core samples, rainfall measurements and the LAI of individual plants will provide a data

set from which other conclusions can be drawn than a data set based on 'landscape sized' observations like land unit classification, discharge measurements etc. How should one sensibly link observations at one level of resolution to another?

1.3 The problem of resolution

During the previous 10 years, the problem of resolution has become a research topic of growing interest. Numerous studies have examined the problem of 'scale' in the hydrological context. An overview of these studies is given by among others Blöschl and Sivapalan (1995). They claim that scale refers to a characteristic time or length of a process, observation or model. In the context of the study presented here, scale refers to the spatial and temporal resolution of a process.

Several theories have been developed to tackle the problem of differing resolution by 'upscaling' or 'downscaling'. 'Upscaling' means distributing the observation or process over a larger time or space and subsequently aggregating the distributed observations or processes into a single value. 'Downscaling' involves disaggregating and singling out (Blöschl & Sivapalan, 1995).

In the context of this study, hillslopes are part of catchments.Two theories that have been developed to link the runoff in hillslopes to streambeds based on patterns of soil, water and vegetation are discussed here because they provide a possible theoretical framework for the work carried out in this thesis. The DRU-theory and the REA-theory are both preliminary attempts to discretize the continua of runoff controlling factors so that;

- Rainfall-response modelling can be easily carried out realistically in complex environments
- Simple relations can be used (only REA)
- Computing remains tractable (not too much unnecessary data).

1.3.1 The DRU-methodology

In a semi-arid Mediterranean environment, the '*Desertification Response Unit*' (DRU) methodology has been developed to link hydrological processes from one temporal and spatial resolution to another (Imeson et al., 1995; Imeson et al., 1996). The DRU-theory has been adapted from the ecological hierarchy theory (O'Niell et al., 1996) which considers the landscape as a set of nested hierarchical levels of scale. Within the MEDALUS research project in the Guadalentín Basin, Spain, it is being used to assess the changes of water availability in land units caused by desertification (Imeson et al., 1996; Imeson et al., 1999).

The methodology encompasses the classification and description of desertification response units (DRU's) in the landscape. The size of a DRU covers a hillslope or part of it. The DRU classification is based on spatial patterns of soil, water and vegetation because these patterns are a result of the movement of water

and the water availability and redistribution. Furthermore these patterns are assumed to emerge from and to be influenced by the water dynamics between plant and interplant areas. They have come into existence by spatial variability of, for example, crust formation, soil aggregation or infiltration within a DRU. The patterns within a DRU are assumed to be constrained in their development by dictating boundary conditions that affect large areas like climate and geology (Imeson et al., 1995; Cammeraat, in press).

After the classification of DRU's, each response unit is described. The description of each DRU consists of a specific set of ecosystem characteristics that control the water availability. These ecosystem characteristics are different for each level of scale (Imeson et al., 1996). At the scale of a DRU the characteristics have to be chosen as being relevant for the water availability conditions of the DRU which means that not every response unit can be described by the same set of ecosystem characteristics (Imeson & Cammeraat, 1999).

Imeson et al. (1996) state that DRU's can be linked to larger spatial areas by development of a classification scheme in which the DRU's form the central units. This scheme reflects the structure of water reallocation processes that cause changes in land units with different resolution (Imeson et al., 1996). This way it provides information on how processes with a large spatial and temporal resolution have a feedback to a smaller spatial and temporal resolution and influence the dynamics of these units (Imeson & Cammeraat, 1999).

The most complete illustration of application of the DRU methodology so far, includes detailed descriptions of several response units (Imeson & Cammeraat, 1999). The hydrologic connectivity of runoff within and between DRU's, is defined by threshold rainfall amounts and intensities (Cammeraat, in press). Based on the soil, water and vegetation patterns of the described DRU's, DRU's can be identified in larger areas having comparable hydrological conditions. This method resembles previous techniques of aerial photo interpretation. Subsequently the earlier defined ecosystem characteristics of each DRU can be assigned to the DRU's classified in the larger area (Imeson & Cammeraat, 1999). For the exact application of the DRU methodology to larger resolutions than hillslopes, this methodology is currently under development.

Within the MEDALUS research programme (*www.medalus.leeds.ac.uk*) more work has to be done to improve and further develop the DRU methodology. This study tries to provide some new insights that can be used as tools for further development the DRU methodology.

1.3.2 The REA-concept

Patterns also form the key issue in the '*Representative Elementary Area*' (REA) concept, which is another approach to combining hydrological processes at various resolution. In this concept, spatial patterns of soil, topography, rainfall and vegetation are believed to control the hydrological response (Wood et al., 1988; Beven & Wood, 1993) as is assumed in the DRU methodology. The hydrological

response can be explained by soil, water and vegetation characteristics. On hillslopes and in very small catchments, the spatial variability of these hillslope characteristics caused by differences in the patterns leads to different responses even with identical underlying statistical distributions (Wood et al., 1988; Beven & Wood, 1993).

Wood et al. (1988 and 1990) introduced the REA-concept in the hydrological response of catchments by modelling the runoff production based on catchment topography. When the hillslope characteristics have only an idealised noise without spatial correlation structures (i.e. a homogeneous distribution) or they have correlation scales that are relatively small compared to the catchment, the differences in spatial patterns become less important and the variability of modelled hydrological responses of catchments decreases (figure 1.1). At certain catchment sizes, the catchment responses may appear to be almost identical for stationary distributions. Therefore, these catchments are considered to be representative of their particular physiographic province and for this reason are called '*Representative Elementary Area's*' (REA) being the smallest discernible point which is representative of the continuum (Wood et al., 1988; Beven & Wood, 1993).

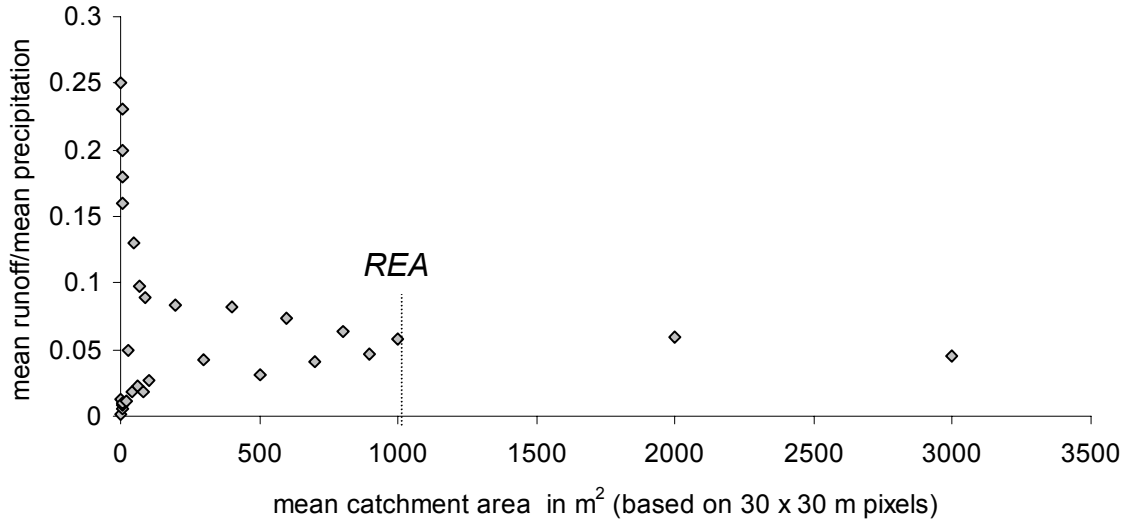

Figure 1.1 Runoff responses modelled by Wood et al. (1990) for different catchment sizes of Kings Creek, Kansas.

The REA is considered to be a fundamental building block for catchment modelling. It represents a threshold scale at which continuum assumptions and simple phenomenological equations for the quantification of runoff response can be used without knowledge of the actual patterns of small resolution of hillslope characteristics. Despite the unimportance of the patterns at the size of a REA, the statistical distribution of the characteristics is still important (Wood, 1998) and therefore it is necessary to account for the underlying variability of these parameters (Wood et al., 1988, 1990). The patterns representing inputs and parameters can be replaced by their distributional (statistical) representation in terms of their means and variances (Wood et al., 1990; Wood, 1995).

Summarizing, a REA is a catchment which fulfils the following constraints;

- The variability of runoff response has reached a low constant value compared to catchments with smaller dimensions. The average runoff response of these catchments is independent of the size of the catchment or varies only smoothly with further increasing catchment size.
- The range of spatial correlation of the variables that control runoff is smaller than the size of these catchments. The spatial distribution of these variables does not influence the runoff of these catchments.
- The runoff of these catchments can be predicted by simple equations based on the statistical representation of the variables that control runoff.

The REA concept has been developed based on model simulations. Although the work of Wood et al. (1988, 1990) suggests that the dimensions of the REA are of the order of 1 km^2, this size of a REA cannot be extended to other areas. The size can be invalidated by non-stationarity and correlation scales of soil, topography, rainfall and vegetation patterns larger than the size of a catchment (Wood et al., 1988; Beven & Wood, 1993). This means that the temporal resolution of for example rainfall, should be chosen to be meaningful for its influence on the runoff at the spatial resolution of a REA (Woods et al., 1995). It also implies that a REA cannot be simply defined for an area which has a spatial heterogeneity in features controlling runoff (for example land use) having a spatial correlation structure that is larger than the size of a REA (for example, if the study area straddles, two or more differing landscapes).

It should be taken into account that the REA concept is based on model simulations in which instantaneous runoff was estimated while neglecting the effect of routing on spatial variability. Wood et al. (1988; 1990) calculated the runoff of a catchment as the arithmetic mean of the runoff of each element located inside the catchment by which they neglected the importance of runoff routing. The concept has been developed, calibrated and validated for humid areas where streambeds always contain water (Wood et al., 1988; Wood et al., 1990; Wood, 1995; Woods & Sivapalan, 1995). So far it is unknown if this concept can be applied to catchments in a semi-arid Mediterranean environment where ephemeral flooding occurs and the runoff is highly discontinuous due to transmission losses and the contribution of near-channel areas.

The introduction of the REA-theory has lead to many discussions. Fan and Bras (1995) criticized the methodology of defining a REA based on model simulations because Wood et al. (1988; 1990) disregarded the routing component in their model. The approach by which Wood et al. (1988; 1990) estimate a REA is related to the resolution of the elements used, which determine the number of pixels needed for the model to reduce the spatial variability of the runoff (Fan & Bras, 1995). To overcome the problem of invalid model assumptions a REA should be defined based on field measurements instead of on the results of model simulations.

It is possible that different resolutions result in different REA's, that are determined by the spatial variability of features that control runoff in these spatial units. For example the spatial variability of features that control the runoff in large

areas, like land use, geology and other topographic features, can result in the definition of a new area size in which the variance of the runoff has decreased to a minimum (Woods et al., 1995). For this reason Fan & Bras (1995) state that the REA is a relative standard and a reference of the range of catchments sizes should be given by defining the lower and upper bounds for which a REA is a valid standard.

In the context of these remarks, the REA is not seen as a fundamental building block in a distributed hydrological model as it was meant to be by Wood et al. (1988; 1990) but as a range of catchments sizes at which simple equations can be used for runoff predictions. The use of these equations has several advantages;

- It provides a tool to overcome the problem of resolution of the runoff controls in the range of catchments sizes for which the REA has been defined to be valid
- Despite its lack of accuracy it provides a fast and easy tool to predict runoff in catchments with similar environmental conditions.

1.3.3 The combination of the REA concept and the DRU methodology

In previous sections I discussed the problem of differences in resolution of hydrological response on hillslopes and in catchments and how the hydrological response of hillslopes may be linked to the hydrological response of a small catchment in which they occur.

Table 1.1 Approaches of the DRU and REA-theory to describe water reallocation within the different units.

Water reallocation	On a hillslope (DRU)	In a catchment (REA)
DRU-theory	Described by a set of soil, water an vegetation characteristics, not uniformly applicable because not every response unit can be described by the same set of characteristics.	The water reallocating processes in a catchment are different from the water reallocating processes at a hillslope and should be described by different characteristics than for a DRU (Imeson et al., 1996). DRU-theory is under development for application at this resolution.
REA-theory	Described by the spatial distribution (mean and standard deviation) of soil, rainfall and vegetation characteristics	Described by the statistical distribution of soil, rainfall and vegetation (independent of its spatial distribution, given spatial correlation smaller than the size of the REA). Runoff described by simple equations and continuum assumptions.

Both theories assume that runoff on hillslopes is mainly controlled by the patterns of soil, water and vegetation (Imeson et al., 1996; Wood et al., 1988). Because of the similarities between the DRU and the REA theories (table 1.1), I have combined them as a means to find a range of catchments in which simple equations can be used to predict the runoff. The range of catchment sizes that fulfil the REA-constraints is taken as a starting point. In catchments that do not fulfil the REA-

constraints, I assume that the runoff is controlled by the spatial distribution of soil, water and vegetation characteristics. In catchments that fulfil the REA-constraints, runoff is best described by the statistical distribution of the characteristics and the information can be aggregated in terms of its mean and standard deviation. In this way the phenomenological equations used to describe runoff for a REA can provide us with the characteristics for describing the water reallocating processes according the DRU-theory.

1.4 Simple runoff assumptions valid for a REA

In catchments that fulfil the REA-constraints, it should be possible to simplify the representation of catchment responses, while still retaining the effects of heterogeneity in the hydrological processes. When this is possible, it provides a simple tool for describing the runoff in larger areas with a minimum of information. When this is not possible, the runoff is affected by the spatial variability of characteristics that control water redistribution on hillslopes of which additional information is needed to describe the runoff.

It remains difficult to formulate a set of equations for catchments fulfilling the REA-constraints because of the choice of appropriate variables that are continuous at the spatial and temporal resolution of a REA (Woods et al., 1995). However, it seems possible to unify and test key features of the spatial variabilities in rainfall, landforms, and runoff over successively larger spatial scales within a broad theoretical framework (Gupta & Waymire, 1998). Most important key features of catchments fulfilling the REA-constraints are related to the stream network such as topology and the cross-sectional geometry and hydraulic properties of the catchment (Blöschl & Sivapalan, 1995). Various authors (Thornes, 1977; Lane, 1982; Beven et al., 1988; Moore et al., 1993; Blöschl & Sivapalan, 1995; Blöschl et al., 1995; Gupta & Waymire, 1998) have tried to define exactly which stream network variables explain the differences in runoff for different sized catchments. Variables related to the survival length of the flow seem to satisfy most authors, being;

- Storm duration (Blöschl et al., 1995; Gupta & Waymire, 1998),
- The slope gradient and upslope contributing drainage area (Moore et al., 1993; Gupta & Waymire, 1998) combined in the topographic index or wetness index as used in the TOPMODEL (Beven & Kirkby, 1979) and
- The channel width (Thornes, 1977; Gupta & Waymire, 1998).

In the context of this thesis, these variables will be examined to see if they are applicable for the quantification of the mean runoff response in the study area.

Besides the different stream network variables vegetation cover is also known to influence the runoff of catchments (as discussed in section 1.2.3). To study the relation between the vegetation and catchment discharge, information is needed over large areas. According to the assumptions of the REA no information is needed on the spatial pattern of the vegetation cover within the REA but only on its statistical distribution. Such information may be provided by remotely sensed

images. With the applications of current imagery techniques it is possible to determine the distribution of the cover of the main vegetation types within raster cells. By using this information it may be possible to account for the vegetation's role in modifying the hydrologic response of catchments larger than a REA.

1.5 Runoff in catchments that do not match the REA-constraints

Processes governing land surface – atmosphere interactions are non-linear and heterogeneous (Beven, 1995). In catchments that do not fulfil the REA-constraints, the runoff is dominated by hillslope processes (Beven & Wood, 1993) and therefore is related to components of the water balance like precipitation, infiltration and routing as described in section 1.2.1 and 1.2.2. In arid and semi-arid areas like in SE Spain the 'non connected' runoff is controlled by contributions from near channel areas (Puigdefabregas et al., 1999). Blöschl et al. (1995) conclude from model simulations that the influence of the spatial variability of precipitation dominates infiltration and routing. They also show that different assumptions regarding the spatial variability of the hydraulic conductivity and the moisture saturation deficit do not affect the variation of the peak discharge in large catchments but significantly affect its variability in small catchments. Subsequently, the precipitation, infiltration and routing processes need to be quantified and interpolated over the total studied area to analyse the hydrological response of a small catchment.

As described in section 1.2.3 vegetation cover is widely accepted as a major control of runoff. Using a land cover classification seems to be the most obvious way to implement the spatial distribution of different vegetation cover in hydrological analysis. However at the scale of a hillslope not every plant has the same hydrologic response. For this reason it is also important to distinguish the main vegetation types.

On hillslopes and in small catchments the hydrological response is influenced by soil, rainfall and vegetation characteristics that control the water balance and have a spatial correlation structure smaller than that of a hillslope or small catchment. When studying the hydrological response for these smaller land units, knowledge about these characteristics is needed. The characteristics should be chosen based on their influence on the water balance and should be studied in the same way in the total study area, which is in contrast to the DRU-theory. This way the characteristics can be compared to each-other for different hillslopes and for different parts of the study area. Furthermore their spatial and statistical distribution is estimated for the total study area.

Differences in the variability of site characteristics and differences in hydrological response between different hillslopes and small catchments, support the use of a distributed model that accounts for spatial variability in inputs, processes or parameters (Wood, 1995). The question, "what is the effect of spatial variability on the parameterisation of hydrologic processes with varying resolution?" has become more and more important (Wood et al., 1990). A nested measurement set-up enables the detection of a minimum variability between

processes that cover a small area and period and a larger area and period. This way the catchments differ from each-other in terms of small spatial and temporal variability and the large spatial and temporal variability of the landscape is minimised (Blöschl et al., 1995). Another question that needs to be answered to fully understand the hydrological response at a small resolution i.e. smaller than a REA, is if it is possible to unravel the partial influence on the runoff of soil, rainfall and vegetation characteristics after its parameterisation.

1.6 The objectives of this thesis

Noting that in semi-arid Mediterranean environments upland hillslopes and upland areas can produce large volumes of runoff that do not always reach the outlet of the larger catchments in which they are situated (Poesen & Hooke, 1997), knowledge is needed on how the runoff of hillslopes controls the runoff in various sized catchments and how runoff in small catchments controls the runoff in larger catchments. The varying resolution and spatial variability of the characteristics that control the runoff at hillslopes and in catchments, makes the problem of hydrological linkage of runoff very complex.

For hillslopes with similar land cover and soil properties but a different underlying spatial distribution, the runoff has a large variability. In catchments defined as a REA, the mean runoff may be described by simple relations between runoff and stream network variables defined as storm duration, channel width and wetness index. The variability in runoff response decreases when the catchment size increases from hillslope to the size at which the variability has reached a minimum. This indicates the decrease of the influence of the spatial distribution of characteristics that control the runoff of hill slopes and the increasing effect of stream network characteristics on runoff by which the runoff can be predicted by simple equations. The use of these equations in various sized catchments implies that the definition of a REA provides a tool to overcome the problem of resolution of runoff controlling characteristics in these catchments.

As described in section 1.2.3, the vegetation also influences the rainfall-runoff response at several resolutions. Therefore, in catchments that do not fulfil the REA-constraints, the spatial distribution of vegetation may be a major factor controlling the runoff. In catchments that fulfil the constraints of a REA, the pattern of vegetation is assumed not to be important, only the statistical distributional representation (Wood, 1995).

For this reason, the definition of a REA is taken as a starting point in this study. Until now this theory has not been tested in a semi-arid Mediterranean environment with its specific hydrological characteristics as described in section 1.2. Within this context, I address the following questions;

1. Is it possible to quantify the relation between rainfall-runoff in various sized catchments and the amount of vegetation cover for different vegetation types

defined at different resolutions, classified by land cover or parameterised as surface cover per species per unit area? If so, what is this relation?

2. Is it possible to determine a range of catchment sizes that enable the definition of a REA for a semi-arid Mediterranean environment based on field measurements?

3. Is it possible to use dynamic distributed modelling to identify the driving factors in the scatter of hydrologic response for various sized catchments, including the spatial distribution of the variables? Do catchments that could be defined as a REA fulfil the constraint of having a runoff response independent of the spatial distribution of the runoff controlling variables?

4. Do the storm duration, the wetness index and the channel width control the rainfall-runoff relation in catchments defined as a REA? Do these variables also control the runoff in catchments not defined as a REA, which would imply that use of simple equations and continuum assumptions are also valid for these other-sized catchments?

1.7 Outline of this study

To fulfil the objectives, a semi-arid Mediterranean study area had to be found which corresponded with the characteristics described in section 1.2. This study area was described in chapter 2 which focuses on the climatic circumstances and the hydrological setting based on soil, land use and vegetation.

As described in this chapter, vegetation controls the runoff at different levels of resolution and therefore its spatial distribution should be parameterised. Because the study area covered 8 km^2, satellite images have been analysed to acquire information on vegetation at different levels of resolution. This is described in chapter 3.

To be able to carry out a hydrological analysis, the different components of the water balance are described in chapters 4 (precipitation), 5 (infiltration) and 6 (runoff) as shown in figure 1.2. In chapter 7 the field measurements are used to define a REA based on decreasing variability in runoff response with increasing catchment size. Subsequently the runoff controlling factors are defined for different scales of resolution and the runoff controlling factors that are independent of the resolution of the catchments. Equations are defined to describe runoff in terms of rainfall in combination with the storm duration, the wetness index, the channel width or catchment size. In this chapter the influence of the vegetation cover on runoff, based on variables of different resolution, have been also analysed.

Finally the results of the rainfall-runoff analysis in chapter 7 are used in combination with the hydrological variables as defined in chapter 3 to 6 to develop a hydrological model to simulate the runoff of different sized catchments. This model is presented in chapter 8. The model is used to test the REA-concept in the

catchments for the independency of the spatial distribution of runoff controlling variables. Furthermore the model was used to anticipate the effects of hypothetical land cover changes on runoff.

The results and conclusions are presented in chapter 9 followed by a summary.

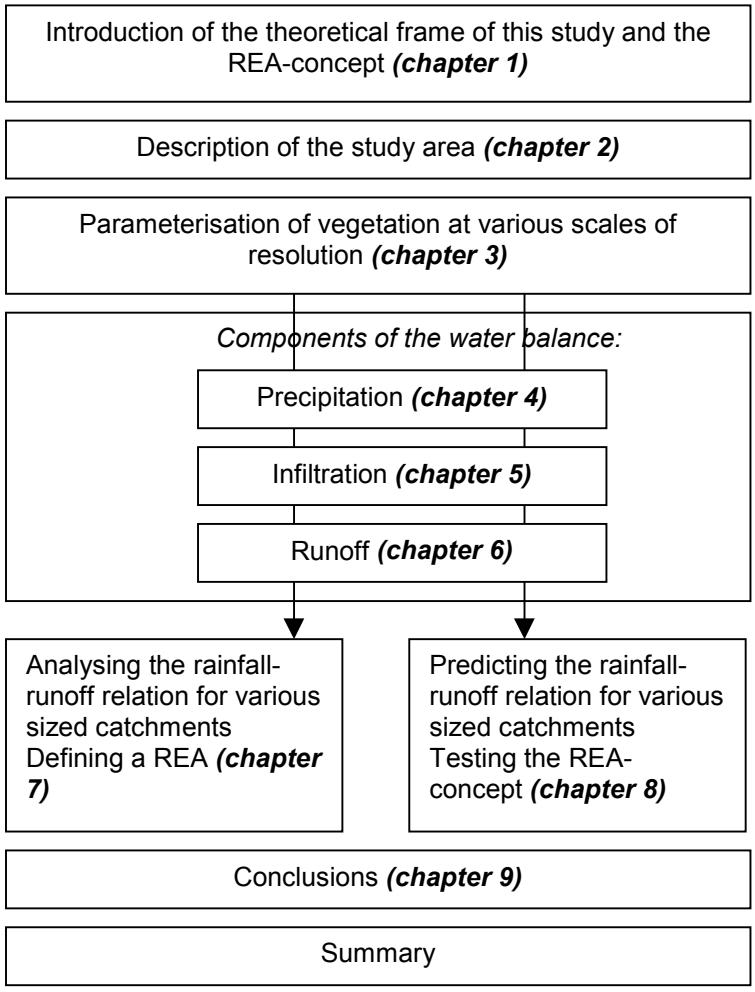

Figure 1.2 Outline of this study.

2 Study area

2.1 Introduction

For the work reported in this thesis, a study area was selected in the Guadalentín basin in southeast Spain which includes the typical characteristics of a semi-arid Mediterranean environment as described in section 1.2. The same area was also studied within the framework of the MEDALUS research project, which facilitated the logistic infrastructure of this study.

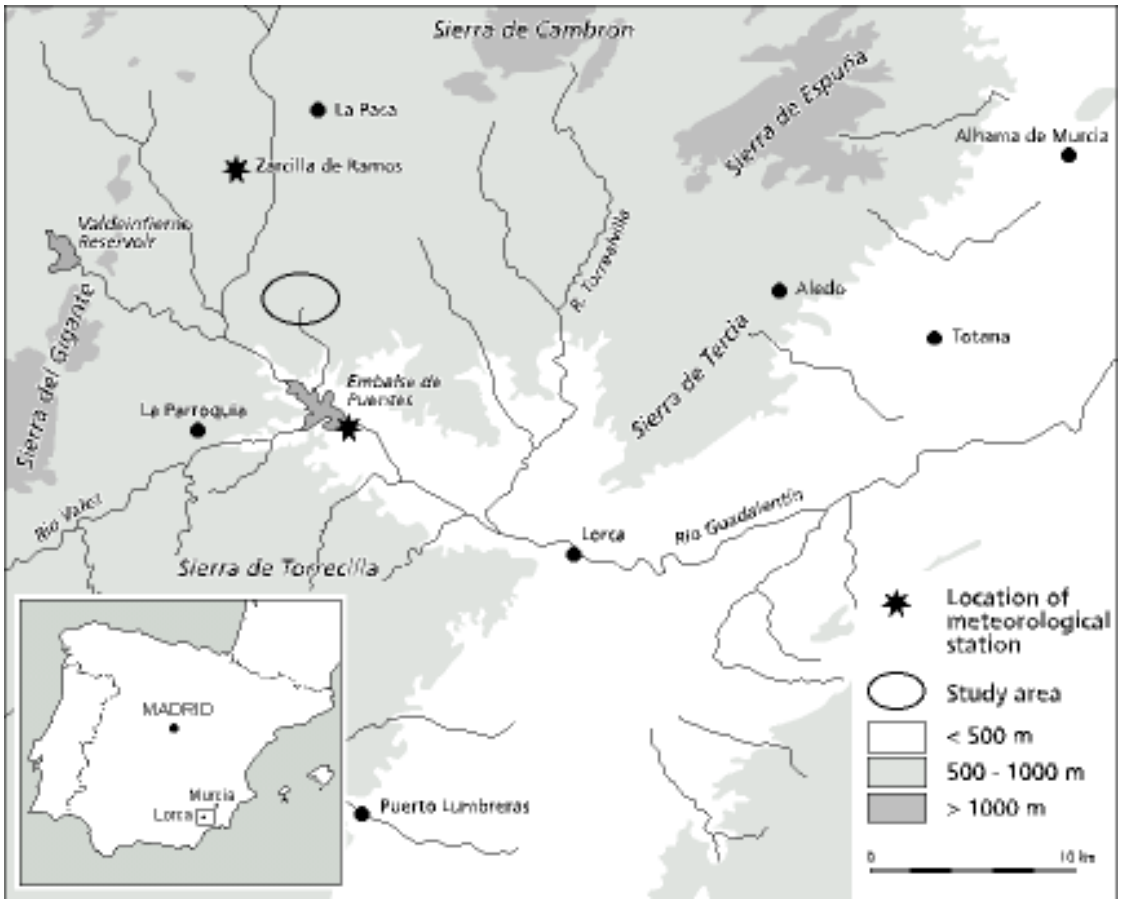

Figure 2.1 Location of the study area; the location of the map at the right is indicated by a square in the map at the left.

The Guadalentín river is said to be Europe's most irregular river (Hernández Franco et al., 1989). The Guadalentín basin suffers from dryland degradation mainly due to erosion caused by runoff and ephemeral flooding of different sized catchments. Sometimes the severe flooding has catastrophic effects such as in 1948 and 1973 (Navarro Hervás, 1991). With its strong seasonal contrasts in climate and vulnerable

lithology, this region has been subject to continuous erosion more or less intensively since Neolithic times (Romero-Díaz et al., 1988).

The natural vulnerability of this region has been exacerbated by governmental or European policies for implementing afforestation (Rojo Serrano, 1995; Ternan et al., 1997) which have led to questionable results (Francis & Thornes, 1990; Quinton et al., 1997). Combined with other social economic factors, the natural vulnerability and the enhanced erosion on afforested land have become more and more important causes for increasing erosion rates in recent years caused by ephemeral flooding. Field measurements of flood hydrology, however, are scarce.

To study the flood hydrology of the Guadalentín basin, a 8 km^2 large study area located in the semi-arid part, north of the Puentes reservoir was selected (figure 2.1). The reservoir and dam have occasionally been destroyed by excessive discharge (Hernández Franco et al., 1989). By selecting a study area upstream of the reservoir in the source area for runoff during excessive rainfall I hoped to improve understanding of the sediment accumulation in the reservoir.

The location of this study area is approximately seventy kilometres southwest of Murcia and about 18 kilometres northeast of Lorca (between 37º49'30" North, 1º53'50" West, 37º43' South and 1º45' East).

2.2 Climate

Dryland degradation problems in this area are triggered by short excessive rainfall events that alternate with periods of drought (Thornes, 1994); they are typical of a semi-arid Mediterranean climate. Not surprisingly, the climate in the selected study area has been classified as semi-arid Mediterranean (Navarro Hervás, 1991).

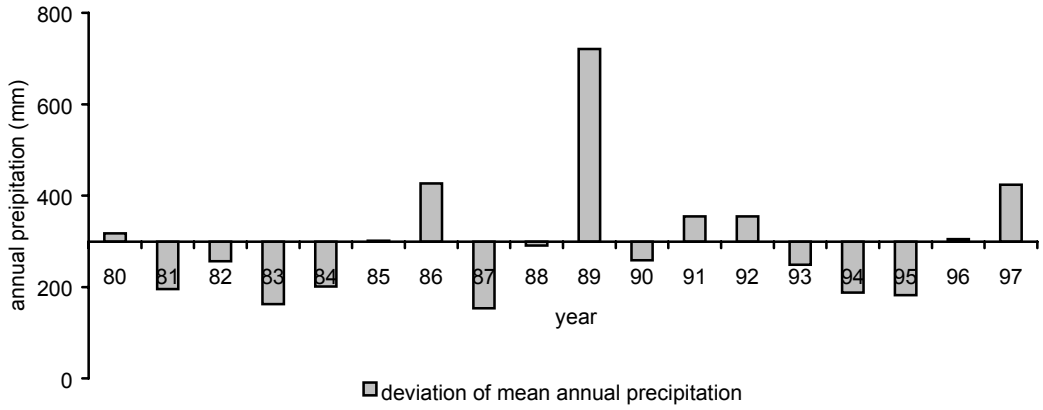

Figure 2.2 Long term variabilty in annual rainfall amounts recorded at la Zarcilla de Ramos (ICONA and Région de Murcia, Consejería de Medio Ambiente, Agricultura y Agua).

The mean annual precipitation varies between 299 mm at la Zarcilla de Ramos (recordings 1980-1998) to 278 mm at Embalse de Puentes (recordings 1951-1980) (Navarro Hervás, 1991). The locations of the meteorological stations la Zarcilla de Ramos and Embalse de Puentes are plotted in figure 2.1.

Precipitation recordings at la Zarcilla de Ramos underline Thornes' (1994) statement that the rainfall in (semi-)arid Mediterranean areas occurs with low overall amounts, at irregular intervals and usually with a very large interannual and inter-seasonal variability. The deviations in figure 2.2 indicate if a rainfall year is classified as 'dry' meaning a negative deviation, or 'wet' which implies a positive deviation. A large positive amplitude of the deviation indicates an extreme rainfall year. As discussed in chapter 5, the measured rainfall of the study area should match the range of precipitation deviations (figure 2.2) in order to be representative for the present climatic conditions. This is an important condition when the results of this study are used to make predictions for periods other than that of this study.

The mean monthly precipitation at la Zarcilla de Ramos and Embalse de Puentes show a maximum in April and October. The highest temperatures occur in July and the coldest in January (figure 2.3). The daily temperature amplitude throughout the year varies around 13 ºC, and is smaller in winter than during summer.

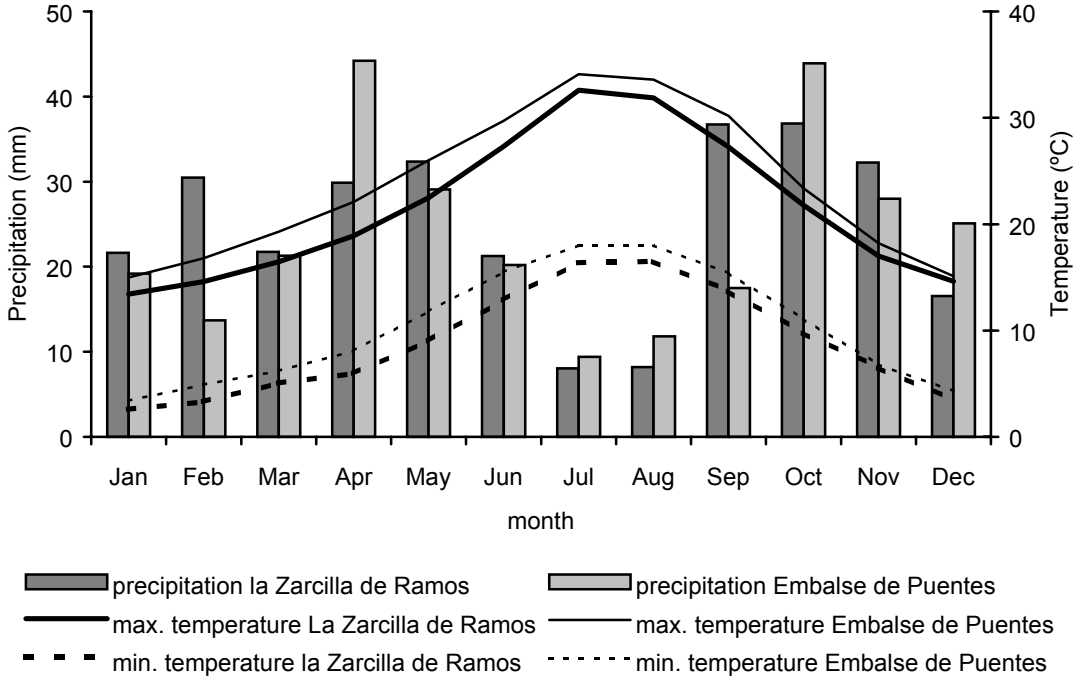

Figure 2.3 Climatic data of nearby located meteorological stations (after Navarro Hervás, 1991). The recordings la Zarcilla de Ramos cover 1951-1980 and the recordings of Embalse de Puentes cover 1951-1980.

The low amount of precipitation in combination with high temperatures results in a moisture deficit (calculated according to Thornthwaite & Mather, 1957) during most

of the year (figure 2.4). The moisture deficit determines the location of cultivated fields as described in section 2.6 and 2.8.

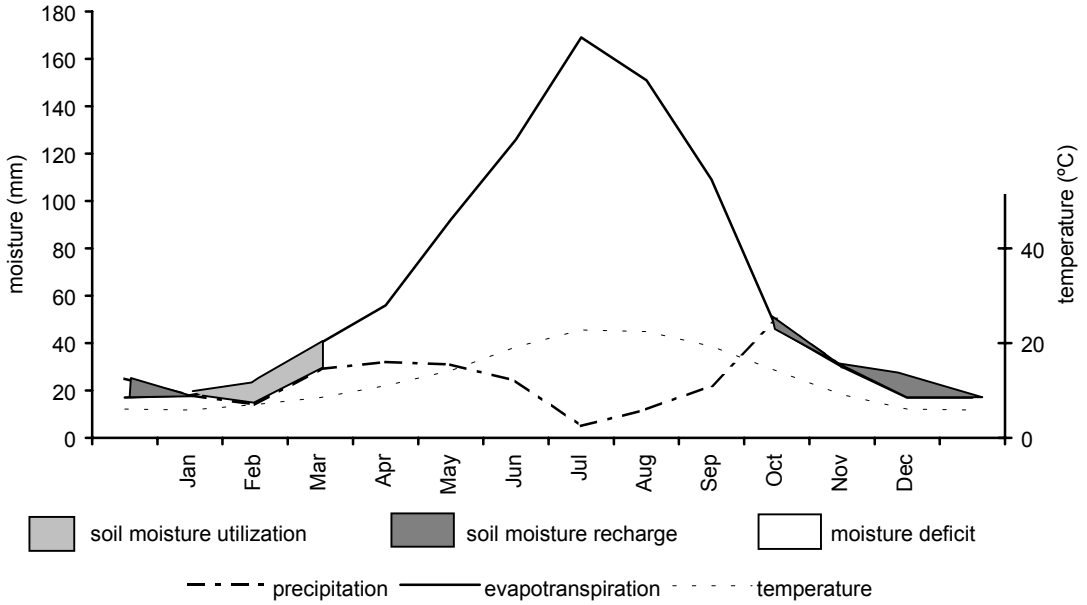

Figure 2.4 Water balance of Embalse de Puentes based on monthly averages (after Alías Pérez, 1989).

Certain catastrophic events are generated under conditions of *'la gota fría'* or the 'cold pool', caused by the onset of storms at the end of a summer anticyclone (Thornes, 1976). The restraining atmospheric conditions imply that at the earth's surface a high-pressure area is located in central Europe while a low-pressure area is located in the south of the Iberian Peninsula with wind coming from the east out of the Mediterranean Sea.

The phenomenon of the 'cold pool' occurs especially in September and October when the water of the Mediterranean Sea is still warm, driving water vapour to the east coast of Spain where the mountain belt causes advection of the humid air. Subsequently the cold depression cools the humid air, which causes instability and results in local heavy rainfall events (López Gómez, 1989). Such end of summer weather conditions cause severe rainfall events throughout Mediterranean Spain, France and Italy.

To know the frequency of excessive rainfall occurence, rainfall recorded at La Zarcilla de Ramos and Embalse de Puentes was used to calculate the recurrence interval using the Gumbel distribution (Buishand & Velds, 1980). Because the study area is located between these two meteorological stations, the estimated recurrence intervals were averaged to calculate the recurrence interval for the study area (figure 2.5) and assumed to be valid for the study area.

The 'cold pool' explains part of the strong seasonal bias that is present in the occurrence of torrential rain events (Thornes, 1994). For the period 1912-1977 of all rainfall exceeding 75 mm per day in southeastern Spain, 43.6% occurred in autumn, 29.5% in winter, 22.5% in spring and only 4.4% in summer (Gil Olcina, 1989). Near

the research area (Embalse de Puentes) most precipitation falls in autumn, which is 32.2% of the total annual amount: in winter 20.9% falls, in spring 43.1% and in summer 14.9% (Navarro Hervás, 1991).

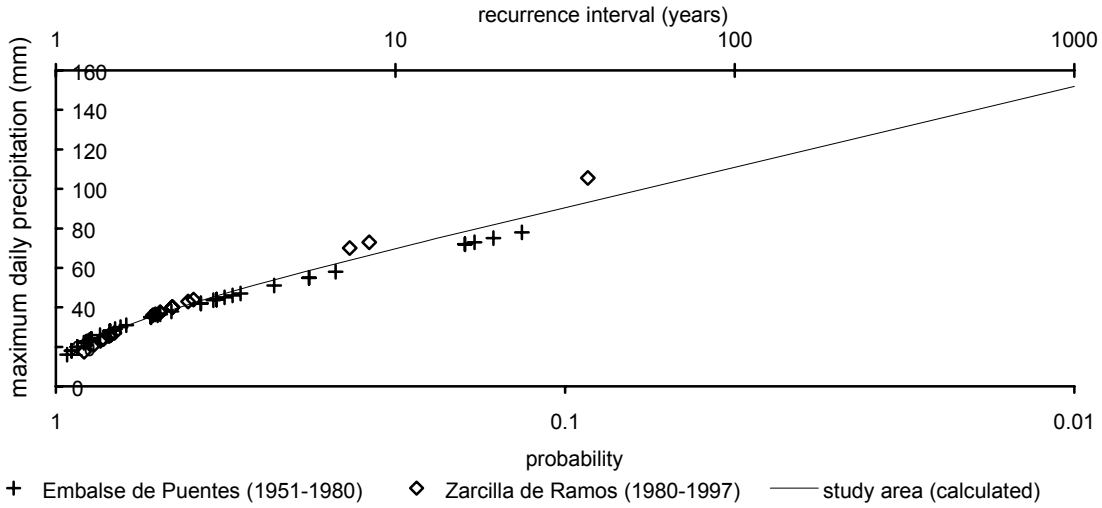

Figure 2.5 Recurrence interval of maximum daily precipitation.

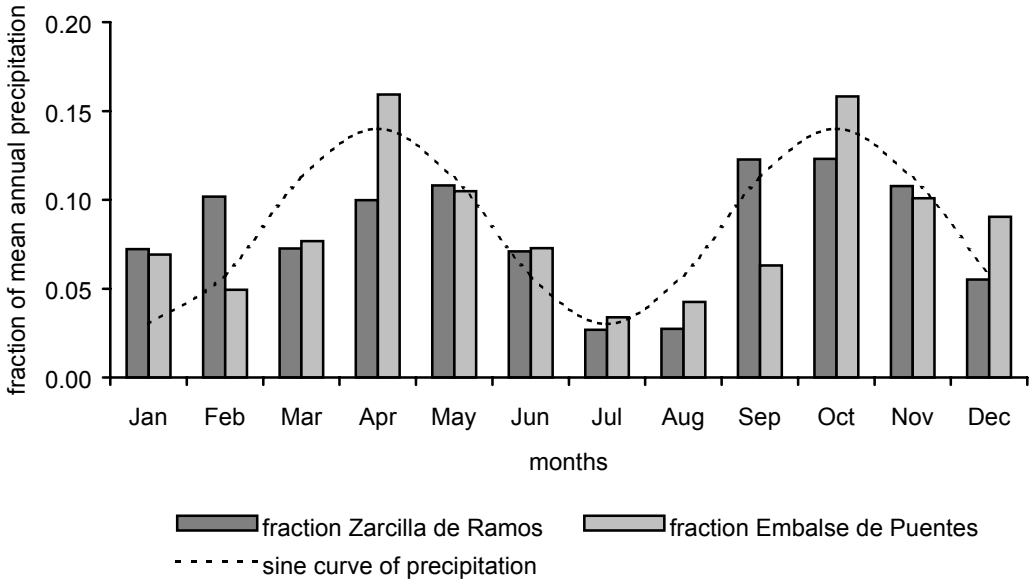

Figure 2.6 Temporal variability of precipitation through the year expressed as fraction of the mean annual precipitation.

The seasonal bias can be expressed as a sine curve when the fraction of rainfall on a monthly basis is used (figure 2.6). Because the study area is located between Zarcilla de Ramos and Embalse de Puentes, I assume that the mean of both precipitation recording locations is representative for the precipitation in the study area. Based on the sine-like representation of the temporal variability, the explained variance of

fraction of precipitation for both meteorological stations is not very high (Zarcilla de Ramos; R^2=0.55 and Embalse de Puentes; R^2=0.62) but significant ($p<0.05$).

Especially in desertified areas, the temporal variability of rainfall intensity is very important for its geomorphologic impact and hence its erosivity (Thornes, 1994). Unfortunately, information on rainfall intensities is lacking for most rainfall events. When only daily rainfall amounts are available, the mean rainfall per rain day is an index that can be used as a compromise and enables us to compare different rainfall recordings over long time spans.

This index gives lower intensities than if the absolute intensity (mm/h) is calculated over smaller intervals and illustrates its smoothing. Near the research area (la Zarcilla de Ramos) the largest amounts of precipitation per rainy day were recorded in June and after the summer drought in September and October (figure 2.7). In December the index was low which reflected periods of drizzle.

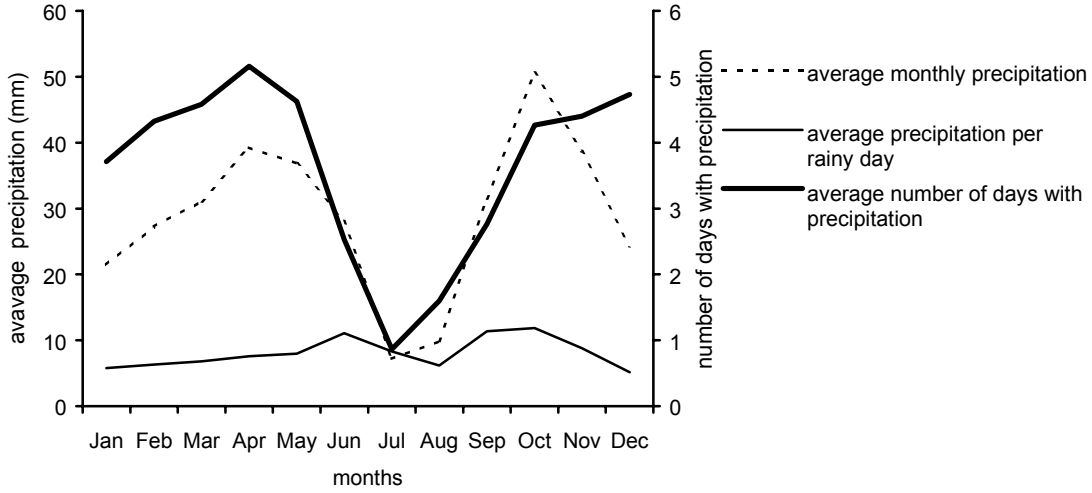

Figure 2.7 The mean monthly precipitation, the number of rainy days per month and the average precipitation per rainy day for every month in la Zarcilla de Ramos (source: ICONA and Región de Murcia, Consejería de Medio Ambiente, Agricultura y Agua).

2.3 Geology

The study area is dominated by limestone and marl that have been folded and faulted resulting in an undulating topography, ranging in altitude from 540 to 800 m. The landscape came into existence by sedimentation from the Trias to the Cretaceous (Vera, 1983). From the late Cretaceous to the Neogene the area was folded by the Betic orogenesis during which the African plate collided with the Eurasian plate (Biermann, 1995).

The resulting mountain range, called the Betic Cordilleras, stretches from Cádiz province (Southwest Spain) to the North of the province of Alicante (Eastern Spain). The Betic Cordilleras can be divided into the External Zone and the Internal or Betic Zone. The Internal or Betic Zone is located in the southern part of Spain. The External Zone can be further subdivided into the Prebetic Zone in the north and the

Subbetic Zone in the south (Soediono, 1971; Geel 1973; Navarro Hervás, 1991; Romero Díaz et al., 1992). Sedimentation continued in the Tertiary until the Miocene.

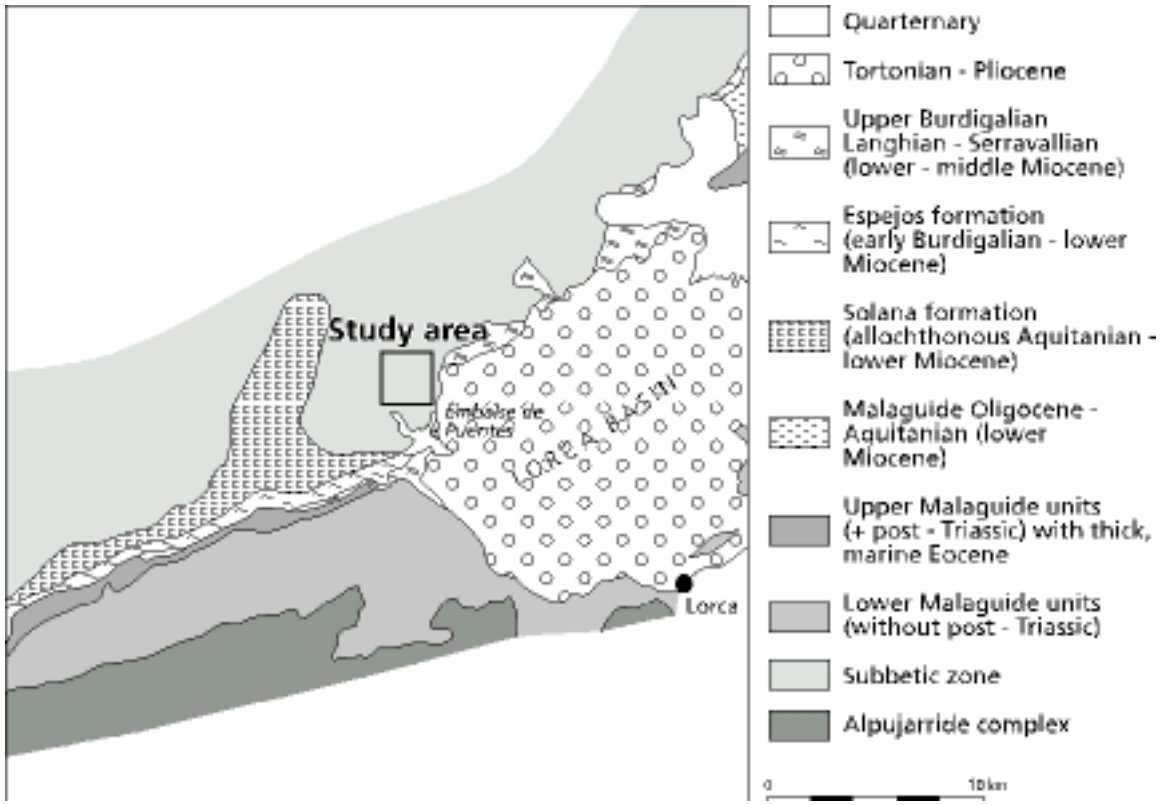

Figure 2.8 Geological setting of the Betic Cordilleras in Southeast Spain after Geel (1996).

The study area is located in the part of the Subbetic Zone (figure 2.8). Its lithology consists of Cretaceous-Paleogene red to white marly limestones and Paleogene marls that are overlain by massive limestones, marly limestones and green pelitic marls from the Eocene. During the Miocene a new sedimentation phase occurred during which more marls were deposited (Soediono, 1971; Geel, 1973, Geerlings, 1978; IGME 1981; Alías Pérez 1989; Geel et al., 1992). These layers were folded by the Betic orogenis (Geerlings, 1978; De Jong, 1991). Nowadays the topography in the study area is determined by mainly north-dipping limestone layers with green marl deposits in the valleys.

2.4 Geomorphology

From the Pleistocene until the present day several morpho-climatic periods have occurred in which periods of high morpho-dynamic activity alternated with periods of low morpho-dynamic activity (Romero Díaz et al., 1992; Faust & Díaz del Olmo, 1997). In periods with high morpho-dynamic activity processes like erosion, draining of sediments, pedimentation and locally shallow landsliding were quite

important, whereas in periods with low morpho-dynamic activity pedogenetic processes like calcrete formation were more prominent. The pediments are surfaces that are flattened and have been developed in bedrock. The partial cover of calcrete has fossilized the pediment surfaces and contributes to the actual preservation of the pediments because it offers resistance to current erosion processes.

The mountain ridges in the study area consist of limestone. The shallow slopes between the mountain ridges and the tributary fans also consist of limestone with marly limestone or marl and have been cut by gullies at several places and locally contain pediment surfaces. The valley floor in the research area is narrow and has developed in marls that are folded in between the limestone layers and are less resistant to erosion. Afterwards this valley filled with alluvial deposits of which the material ranges from a fine to coarse grained subangular texture (Mosch, 1999).

Neotectonics in the Quaternary caused a lowering of the erosion base and hence increasing erosion which led to the rejuvenation of the landscape (Mosch, 1999). The actual erosion processes in the study area are caused by torrential high energetic rainfall (Navarro Hervás, 1991; Romero Díaz et al., 1992), which generates drainage of water and sediment locally leading to the formation of rills. The ephemeral floods damage cultivated fields and undermine soil and water conservation structures that are frequently installed on the cultivated fields (section 2.6). Furthermore they favour further badland formation in the erodible marls.

2.5 Soils

The soils of the study area have been developed in limestone, marls and marly limestone, on fossilized calcretes and Holocene and Pleistocene clastic deposits (Cammeraat, in press.).

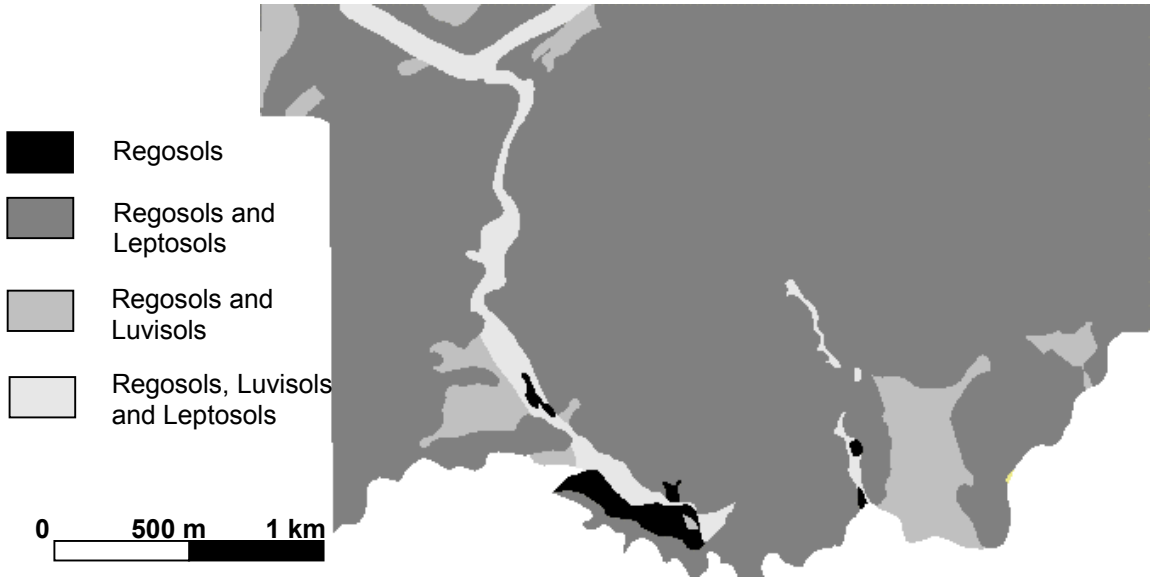

Figure 2.9 Soil map of the study area, after de Pijper (1999).

Dominant soil types in the study area are calcaric Regosol/haplic Calcisol and rendzic/eutric/lithic Leptosols according to the FAO/Unesco (FAO, 1988 used by Alias Pérez, 1989; Pérez Pujalte, 1993; de Pijper, 1999; Imeson et al., 1999) (figure 2.9).

Leptosols are shallow (less than 35 cm) soils on the hill slopes. Regosols are soils deeper than 35 cm. At the footslopes of the hills Calcisols can be found. In the valley bottoms and at the foot of the slopes of the larger valleys, Luvisols occur (Alias Pérez, 1989; Pérez Pujalte, 1993; de Pijper, 1999).

The soils have a weak structure and at several locations the soil is covered by a crust (de Pijper, 1999). The A-horizon of most soils consists of a texture of silty loam of which the silt content exceeds 50% of the total soil content (Odijk & van Bemmel, 1997; de Pijper, 1999; Imeson et al., 1999). Other soils have a texture of silt, sandy loam and loam (de Pijper, 1999; Imeson et al., 1999). The soils have a high $CaCO_3$ content (60 – 70%).

During this study soil samples were taken at 19 different locations in the study area, described in figure 5.1 in section 5.4. For the majority of these samples, the soil texture less than 106 µm consisted of silt (according to the European system) and the amount of clay was less than 10% (table 2.1). The texture did not significantly vary over the different types of parent material (figure 2.10).

Table 2.1 Descriptive statistics of the texture samples (n=19) ≤ 105 µm taken in the study area, analysed with a microscan (Cammeraat & Imeson, 1998). Note that with use of this methodology the $CaCO_3$ has not been removed from the soil samples.

Mass weight (%)	105-63 µm	63-32 µm	32-16 µm	16-8 µm	8-4 µm	4-2 µm	<2 µm
mean	0.4	30.8	30.7	15.0	8.7	5.6	8.6
standard deviaton	0.6	5.0	4.6	2.6	1.7	1.7	3.2

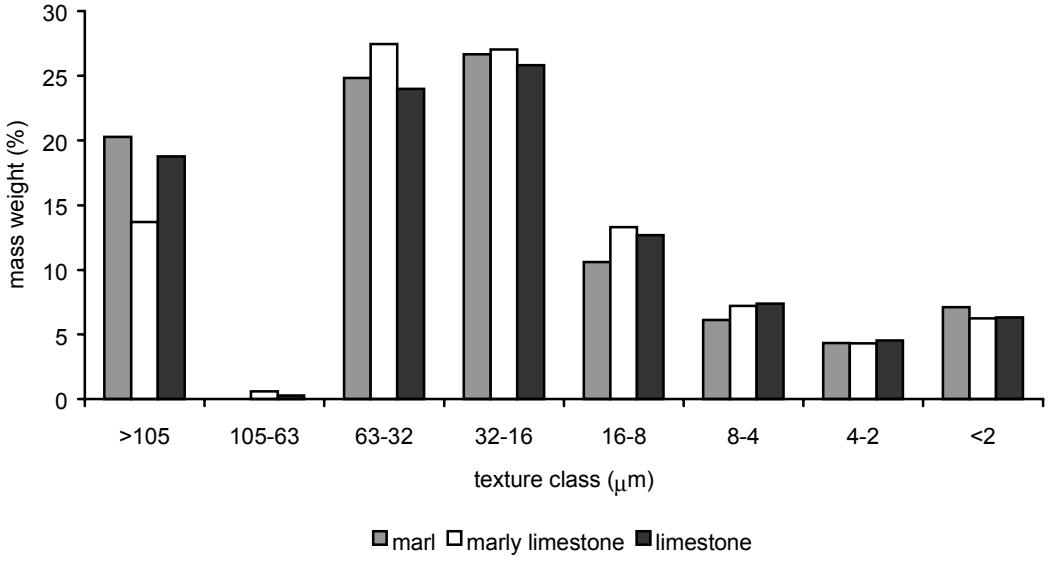

Figure 2.10 Percentage of mass weight per soil texture class of each type parent material. (n=2 for marl, n=4 for marly limestone, n=9 for limestone).

To estimate the soil depth up to bedrock or a petrocalcic horizon, 163 soil profiles divided over 5 transects were dug during this study. These profiles were located in the non-cultivated areas of the study area. In these parts the soil depth varied from 0 to 50 cm.

In the parts where terraces have been constructed to plant trees for afforestation, soil depths varied from 3 to 62 cm. The variability of soil depths in the afforested part was larger than in the non-cultivated area. No significant difference existed between the average soil depths of afforested and non-afforested areas (figure 2.11).

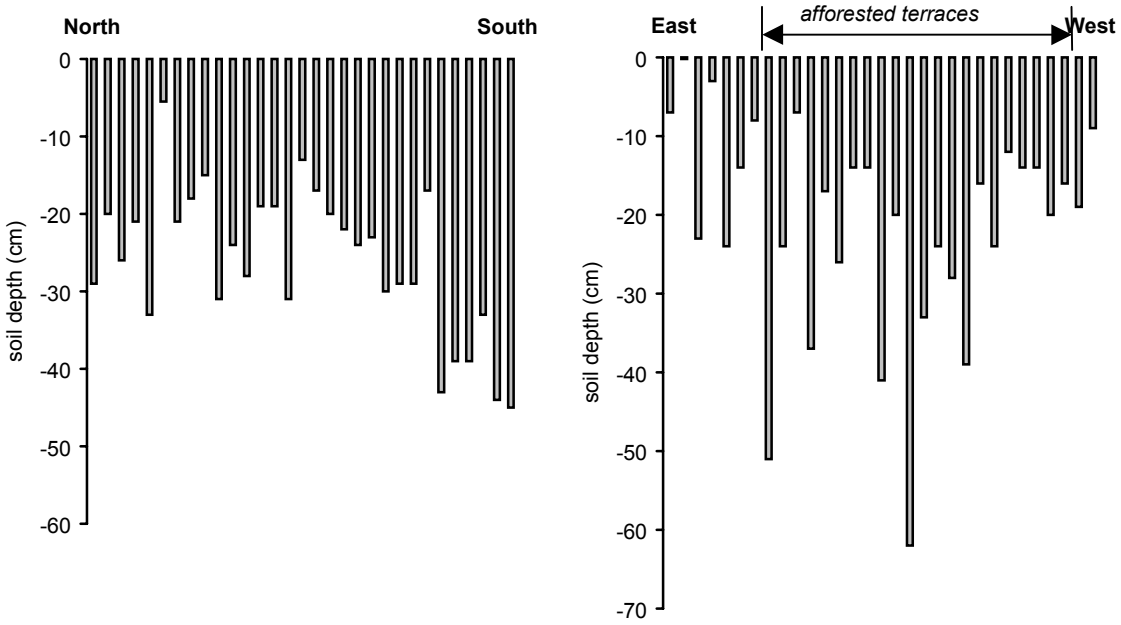

Figure 2.11 Soil depths along two transects on hill slopes from top (left in graph) to streambed (right in graph) in the Buitre catchment.

The organic carbon content under plants is significantly larger than in bare areas. The organic carbon content ranges from 2 to 4 %. However under pine trees and it soil pockets in limestones it can increase to even 14% (Imeson et al., 1999).

2.6 Land cover

The areas with steep slopes are not used for cultivation and are covered by natural vegetation. In the valleys with gentle slopes, the valley floor is cultivated with rain fed cereals (wheat, barley and at some places oats) or planted with almond and olive trees. In the study area almond trees are watered by drip irrigation, which is recently being increasingly applied (Boer, 1999).

Farmers within the study area have adapted their cultivation by locating their fields downstream of the small drainage basins. This way they enlarge the supply of water indirectly water harvesting of the drainage of these small catchments upstream. They have a large interest in the drainage of these basins because they

need the supply of water to compensate for the shortage of soil moisture in their cultivated fields.

Mechanization consisting of auxiliary equipment and harvest equipment has increased in the Guadalentín from 1989 to 1995 (López Bermúdez et al., 1999) and implementation of this equipment has lead to the enlargement of the cultivated fields. Since 1950 the emigration of people from the headwater regions within the Guadalentín Basin to other regions (López Bermúdez et al., 1999) has caused a decreasing demand for land in the study area.

Due to the mechanization and the low demand for land, small fields that are not easily accessible have been abandoned. Large fields used for the cultivation of cereals, are left fallow for one or more years to recover the nutrient and moisture status of the soil (Boer, 1999). Both the cultivated fields and the natural vegetated areas are used for grazing. Grazing in the study area is not as intensive as in many other Mediterranean areas (Imeson et al., 1999) with sheep and goat herds being present for only 4 months per year.

Figure 2.12 Part of the research area; in the foreground a north-facing slope dominated with Pinus halepensis fading into a south-facing slope dominated by Stipa tenacissima.

The natural vegetation in the study area has been characterized as the Meso-Mediterranean Murcian-Almerien vegetation series (Alias Pérez, 1989; Pérez Pujalte, 1993). The study area has a patchy vegetation cover that is dominated by the tussock grass *Stipa tenacissima* (figure 2.12). Other shrubs and grasses occuring *Thymus vulgaris*, *Rosmarinus officinalis*, *Antyllis cystisoides* and *Helictotrichon filifolium* (Alias Pérez, 1989; López Bermúdez & Albaladejo, 1990; Pérez Pujalte, 1993; Rojo Serrano

et al., 1993.). Typical for this vegetation series are forests that consist of *Quercus coccifera*, *Rhamnus lycioides* and *Pinus halepensis*. Because the lithology of the research area consists of limestone and marl, the forests are dominated by *Pinus halepensis*.

Trees are often located in terrain with alternating relief and at the origin of small streambeds. Hardly any pine trees are found on the south exposed slopes, which have dry soil moisture conditions. Re-vegetation of trees on these slopes is very difficult and degradation processes stimulate the prevailing alpha grasses like *Stipa tenacissima* to dominate the remaining patchy vegetation cover (Alias Pérez, 1989; Pérez Pujalte, 1993). Hence these slopes are very vulnerable to erosion (López Bermúdez & Albaladejo, 1990).

2.7 Soil and water conservation

Torrential rainfall can cause a lot of flood damage in the cultivated fields of the study area. For the Guadalentín basin Rojo Serrano et al. (1999) calculated that 0.03 euro is saved for every cubic metre of water that enters the soil and does not cause damage. Cultivated fields have a large socio-economic value i.e. 150 to 300 euro/ha/yr (Hein, 1997). Within the valleys of large drainage basins, farmers apply a variety of water harvesting techniques to protect the cultivated fields for severe erosion and to conserve the available water and soil. Measures taken include the construction of small dykes, the fortification of elevation steps in the terrain by the construction of stone walls and terrace bunds and the construction of small drainage trenches towards olive trees for water harvesting. The aim of these constructions is to minimize the incision of the fields and formation of rills by overland flow and to preserve fertile soil, especially the fine fraction of its texture. Furthermore to optimize the use of abundant water by water harvesting and collect it and lead it to cultivated areas.

During land abandonment the patterns of land use are important for the deterioration of the soil and water conservation structures. In marginal areas with steep slopes or with erodible soils, erosion processes accelerate (Rubio & Calvo, 1996). The development of gully and badlands through abandonment accelerating erosion has only affected small parts of the study area.

Part of the natural vegetation cover in the study area was removed and the land was afforested with Aleppo pine (*Pinus halepensis*). The main goal of afforestation is to control further land degradation by the improvement of water infiltration on hill slopes. By the increased infiltration rates on the terraces, more water is presumed to be stored in the subsoil and the growth of the vegetation is expected to improve (figure 2.13) (Martínez de Azagra Paredes, 1996; Rubio, 1998, Rojo Serrano et al., 1999).

Pinus halepensis is used for afforestation projects because it is an indigenous tree, which is very resistant for periods of drought and well adapted to high carbonate soil levels (Gandullo & Sánchez Palomares, 1994).

The first afforestation project in Murcia took place in 1889 (Rojo Serrano et al., 1993); by 1989 a total of 68 projects had been undertaken in the Guadelentín basin covering a total of 126000 ha. (Medalus, 1993). After 1939 efforts were made to restore degraded watersheds and the Spanish National Forest Administration was founded

(Rubio, 1998). In the early eighties, the afforestation activities were decentralized and the Forest Hydrologic Restoration (FHR) program was initiated by the Autonomous communities (Regional Governments) of Spain. This was part of the National Plan for Erosion and Desertification Control, meant to combat the problems of land degradation in Spain (Rojo Serrano, 1995; Rubio, 1998).

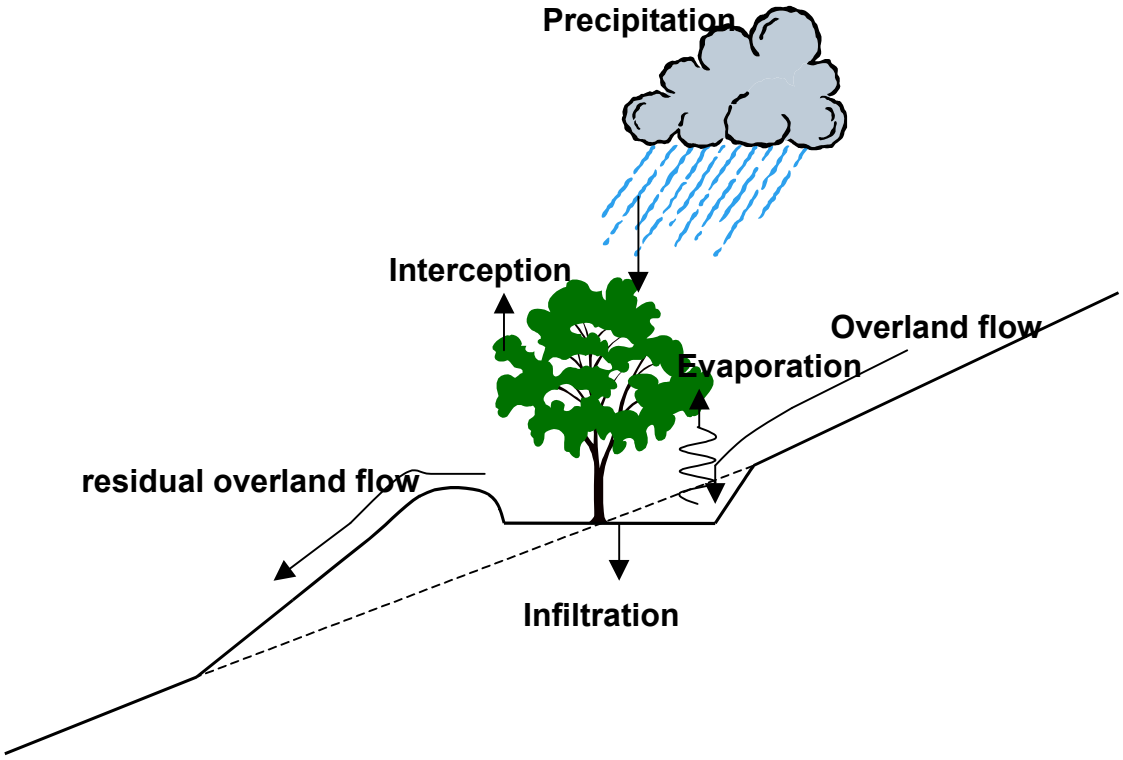

Figure 2.13 Concept of afforestation on terraces, after Martínez de Azagra Paredes (1996).

As a result of the FHR, in 1983 the study area was partly afforested with Aleppo pine on artificially created terraces. During the creation of the terraces, the existing vegetation cover on the terraces was removed. In this way the competition for water, nutrients, light and space was minimized. Between the terraces the vegetation was preserved. The terraces were constructed horizontally or inward to the slope, along the contour lines. Construction of this type of terrace is only possible with a heavy type bulldozer that can penetrate the rocky parent material. The width of the terrace is approximately the width of the bulldozer which is about 2.5 m. By this construction the water retention capacity should increase and runoff should be controlled (García Salmerón, 1990).

Field surveys in other areas where same kind of bench-terraced afforestation projects were carried out under corresponding conditions, showed that the expected protective and erosion decreasing effects were less than previously assumed (Francis & Thornes, 1990; Quinton et al., 1997; Ternan et al., 1997; González del Tánago et al., 1998).
In the study area, only non-cultivated public land was afforested in 1983 (figure 2.14). Before the afforestation the land cover consisted of semi-natural vegetation as described in the previous section. At the time of this study, the planted trees had only grown to heights of less than 80 up to 210 cm depending on their location. The location of the afforested areas was restricted to the occurrence of marly limestone and marl because these types of parent material were easily to penetrate by a bulldozer. Areas with only limestone were left out of the afforestation projects.

Figure 2.14 Afforestated terraces in the study area, orientation of the photo is from south (left) to north (right).

2.8 Hydrology

The topography of the study area is determined by the orientation of limestone strata. All streambeds in the study area are developed in limestone and drain ephemeral streams. Due to the orientation of the limestone strata, the main orientation of the stream network is East-West. The well-defined streambeds are found mainly in the higher areas covered with semi-natural vegetation or afforested terraces. The lower valleys in the study area have been developed in marls and are

filled with Pleistocene and Holocene deposits. By cultivation, water harvesting and other soil and water conservation measures in the valleys, water is collected for agriculture and no well-defined streambeds are found in the valleys of the study area. This means that the study area can be divided in two different types of areas;

- *discharge generating areas*, situated at higher topographical locations with moderately steep slopes and covered by natural vegetation and afforested terraces. Well-defined streambeds are found, cut in limestone with steep sides, that are initially dry but ephemerally drain water (figure 2.15). Water is stored in the discontinuities of the streambed after ephemeral discharge.
- *water harvesting areas*, situated at lower topographical locations with gentle slopes under cultivation. No streambeds are found because of ploughing and because soil and water conservation measures have been taken.

Figure 2.15 A streambed in the study area

This subdivision implies that during normal rainfall events within a catchment that contains both type of areas, only a part of the whole area contributes to the discharge of the catchment (figure 2.16). Infiltration and deposition processes dominate in the water harvesting areas. During most rainfall events the runoff in the subcatchments is not connected through the main valleys within a watershed. Upstream-located subcatchments, covered by semi-natural vegetation and afforested terraces, do not contribute to the discharge at the outlet of the whole catchment (figure 2.16). This

phenomenon is similar to the principle known as partial area runoff and typical hydrological behaviour of the study area (Pilgrim et al., 1988).
Cammeraat (in press.) states that runoff of partial areas in the study area (situation left in figure 2.16) occurs for rainfall amounts between 29 and 34 mm and rainfall intensities between 8 and 23 mm/h. For smaller rainfall amounts and intensities, runoff does not leave the partial areas because of infiltration and evapotranspiration. Only during extreme rainfall events like 'the cold pool', will the response of the catchment, dominated by Hortonian overland flow, be influenced by its total surface and will it react as a totally connected catchment (situation right in figure 2.16). According Cammeraat (in press.) this situation occurs when the initial condition of the soil is moist from previous rainfall events and rainfall amounts exceed 34 mm and the intensity is larger than 23 mm/h.

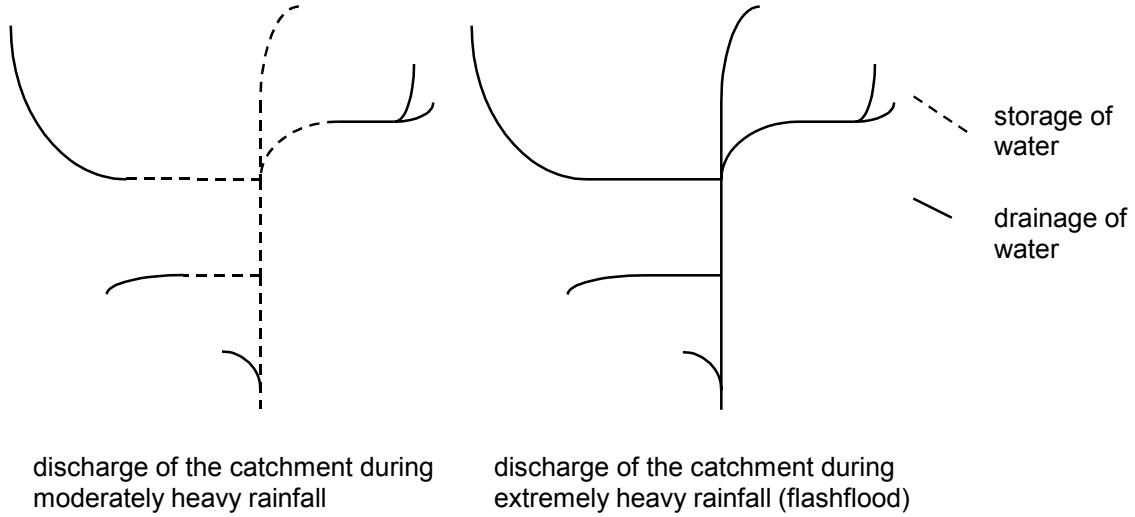

Figure 2.16 Schematic representation of the hydrological network in the study area covering about 14 km^2.

The non-stationarity of the 'water harvesting areas' and 'discharge generating areas' implies that a hydrological study to estimate a REA cannot be carried out in a region that covers both areas. This study where is aimed to understand the hydrological link between the runoff at hill slopes and in small catchments, focuses on the 'discharge generating areas' only.

2.9 The Buitre and Alquería catchments

Because 'discharge generating areas' control the runoff and discharge at both hill slopes and small catchments, given the framework of the objectives given in Chapter 1, this study should focus on these areas. The catchments selected for hydrological analysis should have characteristics that are representative for a semi-arid Mediterranean environment as summed in chapter 1. Another restriction was that the catchment should cover an area with a size large enough to use the REA concept

for the hydrological analysis. Although no arbitrary size is known, model simulations in humid areas often have indicated a size of 1 km^2 (Wood et al., 1988; Wood et al., 1990; Wood, 1998). To obtain the best results the analysis should be carried out on numerous independent catchments. Because of limited finance and resources this was not feasible in the framework of this study.

If two adjacent small catchments are compared to each other they differ due to small-scale variability but when they are located further from each-other the difference is due to both small-scale variability as well as large-scale variabilty present in the landscape. Blöschl et al. (1995) stated that large catchments will never appear more variable than widely spaced small catchments because the small-scale variability within each catchment is averaged out and only the large-scale variability remains. For this reason it is best to compare adjacent located subcatchments so the relative position of subcatchments is not ignored. The corresponding approach is a set of nested catchments in which a fixed reference point of a large catchment and variable sized subcatchments within it are considered (Blöschl et al., 1995).

In this study, the nested measurement setup is based on catchment sizeds and stream order. The most commonly used system to order stream channels is based on the topology of the stream network as developed by Horton (1945) and later modified by Strahler (1964). According this system, a stream of given order (u+1) is initiated at the junction of two streams of the next lower order u. This way the order number is directly proportional to the size of the contributing watershed and to the channel dimensions (Strahler, 1964). The order of the trunk stream u is not increased by the addition of tributary streams of lower order than (u-1) (Chorley et al., 1984, Selby, 1985).

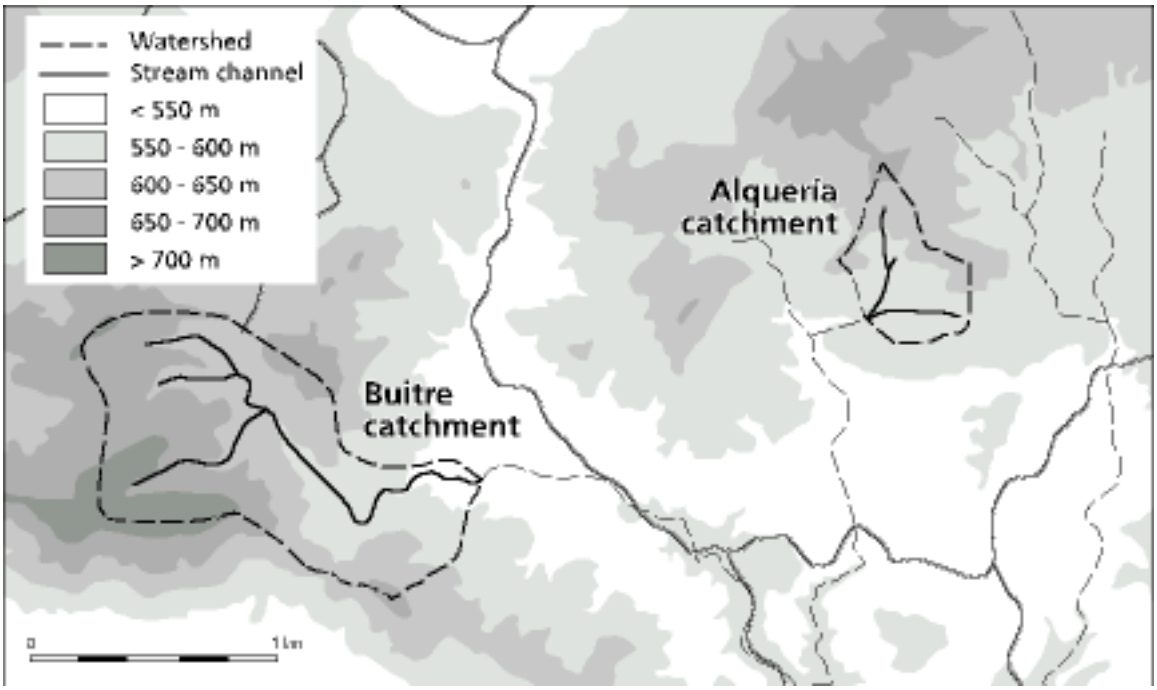

Figure 2.17 Location of Buitre and Alquería catchment within the study area.

Except for the constraints of the spatial location of the selected catchments, the catchments also needed to match the characteristics of a typical semi-arid Mediterranean environment as described in chapter 1. Furthermore I hoped to gain a better insight into the relation between vegetation cover and drainage at hill slopes and in catchments. To prevent introducing unnecessary variability in the runoff, the studied catchments had to be selected with various kinds of vegetation cover but with similar lithology.

Within the given constraints two catchments were selected for detailed investigation; the Buitre catchment and the Alquería catchment (figure 2.17) covering in total 129.6 ha. The measurement locations were located so that they best covered the spatial variability within the discharge regions.

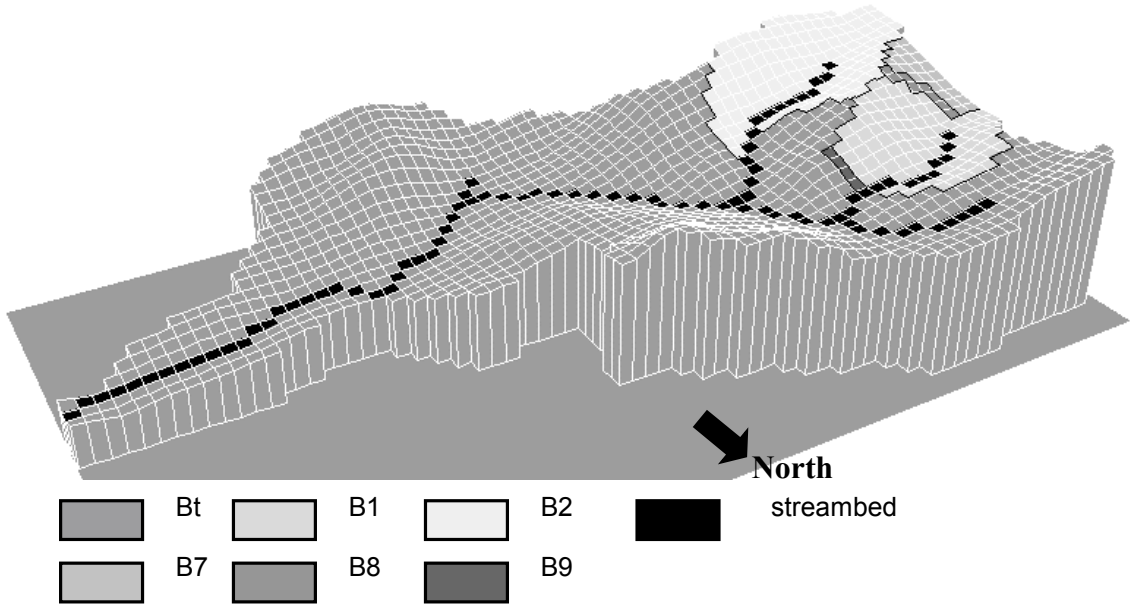

Figure 2.18 Digital Elevation Model of the Buitre catchment. The outlets of the monitored catchment and subcatchments are indicated with arrows (size of a raster cell is 30 x 30 m).

The Buitre catchment varies in altitude from 565 to 795 m. A set of nested subcatchments was selected in the Buitre catchment which covers a total surface of 1 km^2. By the nested distribution of the measurement locations in the Buitre catchment also information was obtained of the water redistribution within the total Buitre catchment during discharge. The nested measurement setup was based on catchment sizes and stream order. The order of the selected streambeds according Strahler (1964) is presented in table 2.2. The nested setup consisted of two subcatchments B1 and B2. Within subcatchment B1 three other sub-subcatchments were selected called B7, B8 and B9 (figure 2.18). As shown in table 2.2, the size of the sub-subcatchments B7, B8 and B9 is a magnitude 10 smaller than the subcatchments B1 and B2 that differ a factor 10 in magnitude of the largest selected catchment Bt in which they are located. The selected catchments are located on the same parent material and were covered by semi-natural vegetation consisting of different species as described in section 2.6. Parts of the Buitre catchment have been afforested.

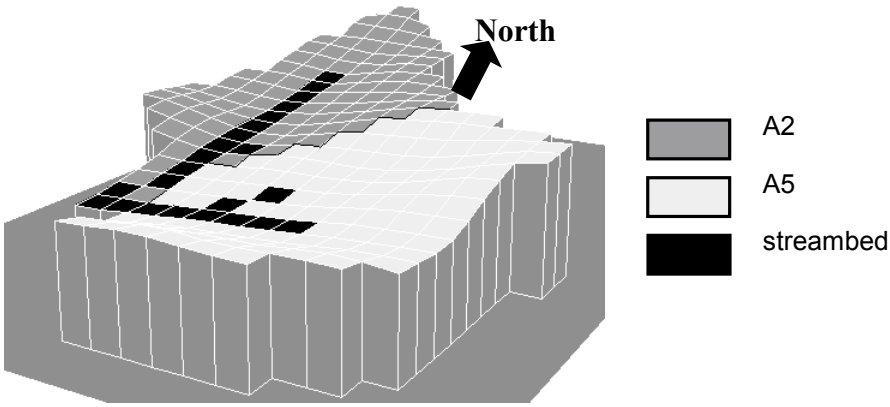

Figure 2.19 Digital Elevation Model of the Alquería catchment. The outlets of the monitored subcatchments are indicated with arrows (size of a raster cell is 30 x 30 m).

The Alquería catchment was selected to test if hydrological relations estimated in the Buitre catchment could also be applied in the Alquería catchment. The Alquería catchment is covered with a semi-natural vegetation and no afforestation has taken place in this catchment. The Alquería catchment varies in altitude from 614 to 709 m. Within this catchment two subcatchments A2 and A5 (table 2.2). were selected for hydrological monitoring (figure 2.19). The discharge of the total Alquería catchment has not been monitored due to financial and logistical constraints.

Table 2.2 Description of the selected catchments. The Buitre catchment is indicated with B and the Alquería catchment is indicated with A.

Catchment	Total surface (ha.)	Afforestated area (% of (sub)catchment)	Stream order
Bt	110.6	24	3
B1	13.0	51	2
B2	13.3	14	2
B7	2.2	83	1
B8	0.7	50	1
B9	0.4	25	1
A2	9.2	0	2
A5	9.8	0	2

2.10 Conclusion

The selected study area can be characterised as a 'typical' Mediterranean with highly irregular but violent rainfall events. Geomorphological setting, soil type occurrence and vegetation patterns are also representative for large areas in the Mediterranean basin.

If the hydrological system of the selected catchments is understood and can be captured in simple rainfall-runoff equations or a computer simulation model and the REA-concept proves to be valid, we will have a valuable tool to work out hydrologic scenarios for many other Mediterranean catchments.

3 Surveying vegetative cover using Spectral Mixture Analysis of earth observation imagery

3.1 Introduction

From previous rainfall-runoff studies (Francis, 1990; Sullivan et al., 1996; Cerdà, 1997; Gonzales del Tanago et al., 1997; Cerdà et al., 1998; Romero-Díaz et al., 1999) it is known that vegetation types control the runoff at different resolutions. In this study attention is focused on the runoff of different sized small catchments, in which the differences in hydrological response of plots are to a large extent controlled by different land cover types (discussed in chapter 1). To analyse the hydrological responses in the study area for the different sized catchments and to model the runoff of these catchments, information on the vegetation types is needed at different levels of resolution. When applied to small catchments both the DRU-methodology and the REA-concept (chapter 1) require information about the pattern of vegetation. In catchments that fulfil the REA-constraints, no information is needed about the spatial pattern of the vegetation cover within these catchments; only its statistical distribution is needed as input for a lumped model of the hydrological response. In this chapter the vegetation types are parameterized at different resolutions for use in the hydrological analysis of the studied catchments and to serve as input for a hydrological model.

Vegetation cover in this study is expressed as classified land cover types, which can be characterised by dominant vegetation species within the unit. In the study area, these land cover types comprise four dominant cover classes: woodland, grassland, afforestation and bare soil. Each vegetation species present within a land cover unit, has its own characteristic hydrological response (Imeson et al., 1999). In the framework of this study, vegetation cover is also expressed as surface cover being the fraction of dominant vegetation species and unvegetated soil. The dominant species are *Stipa tenacissima* and *Pinus halepensis* that each has its own hydrological response. *Stipa tenacissima* is known to have moisture pockets underneath the plant (Kirkby et al., 1996) which influences the microclimate around the plant (Bochet, 1996). Because of differences in canopy storage, the interception loss of *Pinus halepensis* is known to be negligible compared to *Stipa tenacissima* (Belmonte Serranto, 1997; Domingo et al., 1998; Dorigo & Groenendaal, 2000).

Land cover is frequently mapped in the field or by the visual interpretation of aerial photos. The problem of interpretative mapping is that the resulting choropleth maps are often only representative for a limited area and the method is not objective. Among other factors the results depend on the skills of the interpreter. Extrapolation of the measurements from local sites to larger areas may cause bias between the measured and the extrapolated values (Pickup & Chewings, 1996). Another problem is that the resulting choropleth maps are a static estimate of the land cover. Temporal changes due to seasonal fluctations or due to degradation or regeneration processes cannot be assessed except through repeated aerial photography.

In the research area, the precipitation is characterised by strong seasonal fluctuations (see chapter 2). Because of the complex relation between runoff response and land cover type, it is important to use data from seasons with a large chance of rainfall for the estimation of land cover type and the cover of the main vegetation species. Such data are provided by remotely sensed images of earth observation imagery and they may be used to estimate land cover types and the cover of the main vegetation species. Earth observation imagery from spaceborne sensors, including satellites, provide images with a multi-temporal cover from month to month, season to season or year to year. It allows the use of objective analysis methods to overcome the disadvantages of field surveys and aerial photo interpretations as discussed above.

By use of this information it may be possible to define vegetation cover as land cover with a coarse spatial resolution and as vegetation cover with a fine spatial resolution. Subsequently it may be possible to analyse how vegetation cover at different resolution controls runoff and to develop a model that includes the spatial distribution of vegetation cover for explaining the hydrologic response of various sized catchments. This chapter discusses whether remote sensing provides useful means to identify vegetation types defined as land cover units and surface cover units in the study area and to assess their spatial variability.

3.2 Using remotely sensed data for erosion studies

3.2.1 Choropleth maps resulting from image classification

In hydrological or erosion modeling, many input data are often obtained from choropleth maps having units that represent more or less uniform land cover, soil and vegetation types, which may be obtained by the classification of remotely sensed images.

Classification procedures for remotely sensed images are carried out either as unsupervised or supervised (Lillesand & Kiefer, 1979). Unsupervised classification means that the remotely sensed image is classified in a previously defined number of classes. Supervised classification implies that the image is classified according to previously defined training sets of areas with known land cover. The training set consists of ground truth polygons with known spectral reflectances that are assumed to be representative for the different types of cover present in the remotely sensed image. The choropleth maps resulting from classification often imply that structural properties such as vegetation species and cover are homogeneous within the mapping unit (figure 3.1). For most areas, especially in sparsely covered semi-arid areas, this assumption is often not valid.

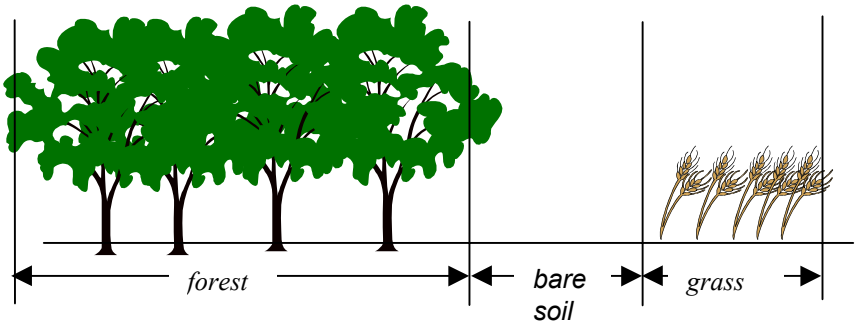

Figure 3.1 Choropleth mapping units, assuming homogeneity within the mapping unit.

The problem of these classification approaches is that the resulting mapping units may be composed of different entities. Also, because spatial variation within the mapping units has been suppressed, the results are likely to have a large and unknown within-unit variance of the entities covering the surface. If these results are used as the input to numerical models, they will yield results that do not account for short-range variability and have no guarantee of freedom from bias.

Two main disadvantages of classified choropleth maps are *a)* that the pixel will include reflections from a mixture of cover types such as different soil types, rock outcrops, vegetation species and shade (figure 3.2) and *b)* that all pixels falling in the same class contain exactly the same data. This is important if we want to relate variations of the vegetation types and amount of cover to hydrological processes.

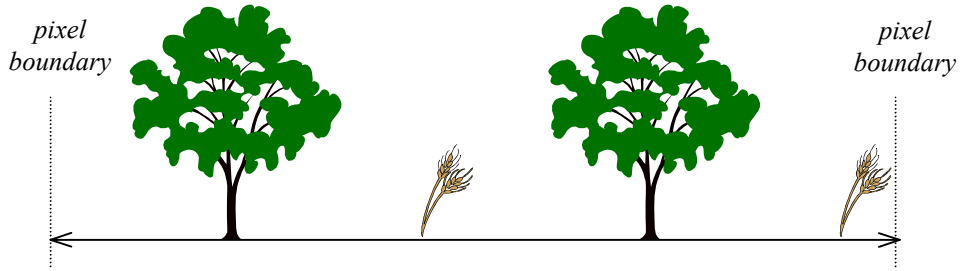

Figure 3.2 Contribution of vegetation and soil types to the total surface cover and hence, to the spectral reflectance within a pixel.

3.2.2 Vegetation Indices

Few studies have reported the incorporation of remote sensing information in rainfall-runoff modelling (Beven & Fisher, 1996). When vegetation cover is estimated by using remote sensing, an objective method needs to be selected. In the context of this study the common methods are reviewed and evaluated.

The vegetation cover is often estimated by using spectral vegetation indices (Lacaze, 1996; Yin & Williams, 1997; Moran et al., 1997) when it is surveyed as input for a hydrological or erosion model. Spectral vegetation indices have been developed to estimate to what extent green vegetation contributes to the overall

spectral reflectance as captured in satellite images. The indices aim at enhancing the spectral information of green coverage while the spectral contributions of soil background, the effect of sun angle and atmosphere are minimised. Over the years many spectral vegetation indices have been developed (Kauth & Thomas, 1976; Richardson & Wiegand, 1977; Tucker, 1979; Huete, 1988) and most are based on the differences in spectral reflectance of green canopy between the red and near infrared wavelengths. The indices can be divided into two groups; indices in the form of ratios of which the Normalised Difference Vegetation Index (NDVI) is the best-known example, and indices in the form of a linear combination based on sequential orthogonalisation. Of the last form the 'Tasseled Cap' transformation and the Perpendicular Vegetation Index (PVI) are frequently used (Perry & Lautenschlager, 1984).
When Landsat TM data is used, the NDVI is computed by equation 3.1 (Tucker, 1979):

$$NDVI = \frac{TM4 - TM3}{TM4 + TM3} \qquad \textit{equation 3.1}$$

in which:
TM4 : reflectance in near infra red, spectral TM band 4 (0.76-0.90 µm)
TM3 : reflectance in red, spectral TM band 3 (0.63 – 0.69 µm)

The 'Tasseled Cap' is a transformation similar to the Principal Component Analysis (PCA) to project information of soil and vegetation information of a Landsat image onto a single plane in the multi-spectral data space (Kauth & Thomas, 1976). The 'Tasseled Cap' transformation is based on user-defined points in the spectral space having a physical meaning such as 'dark soil', 'bright soil', 'green vegetation' or 'yellow vegetation'. In contrast to the 'Tasseled Cap', the PCA is a transformation based on the statistical distribution of the pixels. Crist & Cicone (1984), Crist et al. (1986) and Crist & Kauth (1986) extended the original 'Tasseled Cap' transformation from Landsat MSS to Landsat TM and introduced coefficients by which the resulting images represent the dimensions of 'brightness', 'greenness' and 'wetness' in the multi-spectral data space. The extent of 'greenness' computed by the 'Tasseled Cap' transformation of Landsat TM5 images is calculated by equation 3.2 (Crist et al., 1986);

$$\begin{aligned} Greenness = {} & -0.2728*TM1 - 0.2174*TM2 - 0.5508*TM3 \\ & + 0.7221TM4 + 0.0733TM5 - 0.1648*TM7 \end{aligned} \qquad \textit{equation 3.2}$$

in which:
TM1 : reflectance of spectral TM band 1 (0.45-0.52 µm)
TM2 : reflectance of spectral TM band 2 (0.52-0.60 µm)
TM3 : reflectance of spectral TM band 3 (0.63-0.69 µm)
TM4 : reflectance of spectral TM band 4 (0.76-0.90 µm)
TM5 : reflectance of spectral TM band 5 (1.55-1.75 µm)

TM7 : reflectance of spectral TM band 7 (2.08-2.35 μm)

Comparison of the NDVI index and the 'Tasseled Cap' index in the Ardeche test site used by de Jong (1994) showed that these indices have an large correlation because they are both based on the same principle of optimizing the contrast between green vegetation and bare soils (De Jong, 1994).

The 'Tasseled Cap' transformation was developed for application in a temperate climate scene where vegetation is continuously active (Crist et al., 1986). In semi-arid Mediterranean environment the vegetation commonly includes considerable amounts of dead material or dormant. In the study area (described in chapter 2) the dominant vegetation species *Stipa tenacissima* is known to consist for approximately 60% of dead material (Domingo et al., 1998). The large amount of dead material is part of the tussock and contributes to the infiltration of rainfall (Cerdà, 1997b; Bochet et al., 1998) in the tussock and controls the runoff by its cover (Puigdefábregas & Sánchez, 1996). For this study the cover is defined as all plant material (dead and alive) that covers the soil surface. Previous work has shown that the relation between field data and spectral indices is reliable for green vegetation estimates but is rather poor when the vegetation cover exists of vegetation in the senescent stage (De Jong, 1994; De Jong et al., 1999). For this reason the above described vegetation indices are not very suitable for accurately estimating vegetation.

The soil background in the reflectance signal of the vegetation will vary with the development stage of that specific vegetation. Therefore Richardson and Wiegand (1977) developed the Perpendicular Vegetation Index (PVI). This index is based on the same principle as the 'Tasseled Cap' transformation, in which the reflectance of the vegetation is transformed to same the spectral dimensions as the reflectance of the soil. For use with Landsat TM5 images the PVI is formulated such a way that the contrast of vegetative cover is enhanced (Richardson & Wiegand, 1977).

$$PVI = \sqrt{(0.355TM4 - 0.149TM2)^2 + (0.355TM2 - 0.852TM4)^2} \qquad \textit{equation 3.3}$$

in which:
TM2 : spectral reflectance in TM band 2 (0.52-0.60 μm)
TM4 : spectral reflectance in TM band 4 (0.76-0.90 μm)

The previously described vegetation indices, i.e. NDVI, 'Tasseled Cap', PVI, are well correlated with vegetation parameters such as biomass, green leaf area and percent green cover (Richardson & Wiegand, 1977). They all assume that the spectral features of soil, vegetation and other components do not interact with each other. However, when vegetation indices of an incomplete vegetation cover are calculated, the indices can be strongly influenced by the background signal of the soil that is underneath and in between the plants. This is caused by the near infrared part of the signal that scatters and is transmitted to the soil surface via the vegetation cover and

subsequently reflected by the soil, as a function of the optical properties of the soil surface (Huete, 1988). In the study area where bright marls and carbonate rocks are common, the soil background signal causes this index to give biased estimates of the vegetation. To correct for the influence of the soil background signal on the vegetation index, especially in areas with an incomplete canopy cover, the Soil-Adjusted Vegetation Index (SAVI) was developed by Huete (1988) (equation 3.4).

$$SAVI = \left\{ \frac{TM4 - TM3}{TM4 + TM3 + L} \right\} * (1 + L) \qquad \textit{equation 3.4}$$

in which:

TM4 : spectral reflectance in TM band 4 (0.76-0.90 μm)

TM3 : spectral reflectance in TM band 3 (0.63 – 0.69 μm)

L : adjustment factor, between 0.25 and 0.75 depending on the vegetation density and the Leaf Area Index

The detection of small amounts of vegetation still remains a problem because the spectral properties of sparse vegetation cover may be similar to the spectral signature of bare soils in the spectral dimensions of the red and near infrared wavelength space (Huete, 1988). In the study area, the soil is covered with tussocks of *Stipa tenacissima* consisting of large amount of dead material. So besides the small amount of cover in the study area, the reflectance of dry vegetation in the red and near infrared wavelength is very similar to unvegetated soil because of the large amount of dead material. For this reason, *SAVI* is insufficiently reliable for the estimating vegetation cover in the study area and was not used in this study.

The conclusion must be that the use of conventional remote sensing derived vegetation indices in the study area, can not result in proper estimation of the vegetation cover due to open canopy cover, the bright soils and the contribution of a relatively large amount of dead material to the canopy. Furthermore, for the application of vegetation indices, only two spectral bands are used. This means that only a small part of the information is being used of which is available in all spectral bands of the image. Finally, the information obtained by the use of vegetation indices has the resolution of one pixel while the resolution of interest is at sub-pixel level. Therefore we need a different approach.

3.3 Spectral Mixture Analysis

In arid and semi-arid areas, pixels may often cover areas including different vegetation species and unvegetated soil. In sparsely vegetated areas like the study area, the pixels have a rather heterogeneous composition of entities. Besides, all entities can mix in all proportions with shade (Gillespie et al., 1992). In fact the surface cover of a pixel is a function of ***m*** surface covering entities. As each of the ***m*** entities has its own spectral reflection, the spectral reflection of the whole pixel is a mixture of all contributing entities (Adams et al., 1993). If the mixed reflections from

a pixel could be decomposed into the separate ***m*** contributions, a better estimation of the ***m*** surface covering entities within the pixel would be established. Spectral decomposition should result in better estimates of the abundance of surfaces dominating the spectral response of a pixel than will be achieved by spectral indices. The abundance map of surfaces can be used for hydrological analysis and as model input.

Spectral Mixture Analysis or SMA (Gillespie et al., 1990; Adams et al., 1993; Settle & Drake, 1993) is a suitable technique for approaching the mixed pixel composition and hence, mapping vegetative cover at the sub-pixel level. It has been shown that especially in semi-arid areas with complex and sparse patchy vegetation this method yields better estimates of the vegetation cover than conventional methods like spectral indices (Smith et al., 1990; Pickup & Chewings, 1996).

SMA provides information about the fraction of vegetation cover at subpixel level (Melia, 1996; Smith et al., 1990). SMA requires well-calibrated remotely sensed images because laboratory or field spectral reflectances of 'pure surface cover' are commonly used for the pixel decomposition.

The linear spectral unmixing algorithm works as follows. It is assumed that there is no significant amount of multiple scattering between the different surface covering entities i.e. every photon reaching the sensor, has interacted with only one surface covering entity. The number of surface-covering entities should be limited (as will be discussed in this section). Furthermore, it is assumed that each characteristic type of surface cover has its own unique reflectance spectrum in the spectral bands recorded by the satellite or ground-based sensor, as shown in figure 3.3a.

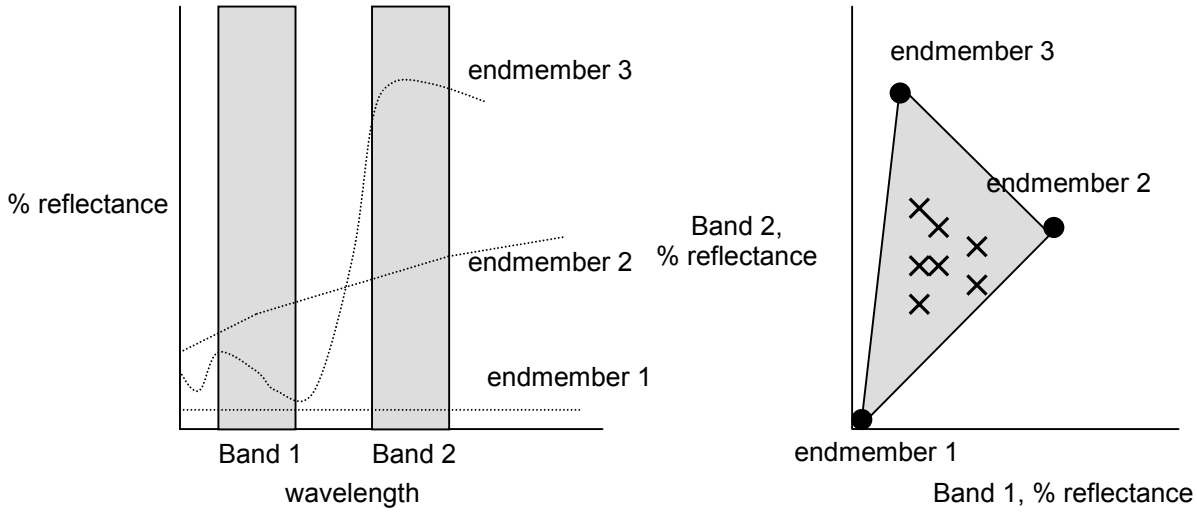

Figure 3.3 Two dimensional spectral data, reflectance spectra of the individual endmembers (left) and the endmembers in a two-band plot (right) in which the crosses indicate the reflectance of the pixels of the image. After Adams et al. (1993).

The reflectance spectrum is the reponse that will be received in the absence of noise from a pixel that contains only the component of interest (Settle & Drake, 1993). When the pixel comprises various surfaces, the spectrum is a linear mixture of the individual contributions of these surfaces. Therefore, mixed pixels have individual band values that fall between the extremes for each single cover as shown in figure 3.3b. For this reason the pure cover types define the extreme values of reflectance, and are called 'endmembers' (Adams et al., 1993).

Equation 3.5 defines how SMA unravels the spectral information of each pixel into the within-pixel abundance of a limited number of endmembers *m* by linear inversion in an iterative process while the error term is minimized (Smith et al., 1990; Gillespie et al., 1990). In order to solve this equation in a *n*-dimensional space, the maximum number of endmembers is the sum of the number of bands *i* plus one (figure 3.3) (Settle & Drake, 1988).

In the linear spectral unmixing procedure the coefficients of the linear reflectance combination are related to the fraction of the endmember in each pixel

$$R_i = \sum_{j=1}^{m} (F_j * RE_{ij}) + \varepsilon_i \qquad \textit{equation 3.5}$$

in which:

R_i = reflectance of the mixed spectrum in band *i*
RE_{ij} = reflectance in band *i* of endmember *j*
F_j = fraction of endmember *j*
m = number of endmembers *j*
n = number of bands *i*
ε_i = residual error in band *i*

This equation can be rewritten as the product of two matrices. One matrix (*n* x *m*) contains the spectral reflectance in every band for every endmember. The other column matrix (*m* x 1) gives the spectral reflectance of an image pixel (Settle & Drake, 1988). The equation can be solved by linear inversion techniques (Twomey, 1977). This way the endmember fractions are calculated by multiplying the inverse of the matrix that contains for every endmember the spectral reflectance in every band, with the column matrix (*n* x 1) of the recorded spectral reflectance of the image pixel in every band. The unmixing procedure results in *m* so-called abundance images that for each endmember *j* express the abundance *F* of the specific endmember on a pixel-by-pixel basis. The resulting endmember abundance maps provide an estimate of their spectral contribution to the real signal of each component (Settle & Drake, 1995). Besides the abundance maps for every endmember, a map with the residual error for every pixel is obtained.

In this study the quadratic matrix algebra of the SMA was carried out with the sum-to-one constraint (equation 3.6) (Twomey, 1977; Settle & Drake, 1993) by which the abundance maps are forced to sum to 1. This way the resulting fraction images represent the cover percentage of each selected endmember. Subsequently

the fraction images can calibrated with field estimates of the vegetation cover as described in section 3.11.

$$\sum_{j=1}^{m} F_j = 1 \qquad \textit{equation 3.6}$$

Generally, the reference spectra or endmembers used as input for SMA can be determined in three ways;

- Unsupervised by a selection of 'purest pixels' in the multi-spectral data space of the image by the 'purest pixel index' (Boardman et al., 1995). This method has the disadvantage that the physical appearance of the endmembers is unknown in terms of what they represent in reality and their cover percentage. The advantage is that the reference spectra is taken from a source from which the data are collected under the same atmospheric conditions and by the same sensor.
- Supervised by using a spectral library in which all characteristic reflectances of the selected endmembers have been assembled by selection of pixels in the image with a homogenous known cover (Kneubuehler et al., 1998).
- Supervised by using local field or laboratory observations to build a spectral library with information on known surface cover of the selected endmembers.

3.4 Field estimates of surface cover

In this study, field estimates of surface-covering entities were made to determine the most dominant vegetation species and to select the appropriate endmembers for the entire study area. After the SMA was applied, the results were calibrated using these field estimates.

For this purpose a field survey was made of the locations of vegetation types and their cover. The recordings were made at 72 locations. At each location the vegetation was measured along four line transects with a length of 30 metres each. Together the four line transects formed a square. Two sides of the square were oriented along the contour lines and two sides perpendicular to the contour lines. This way the total length of the transects equalled the length of all square sides, which totalled 120 metres. For the field recordings the vegetation was assumed to be equally distributed without any anisotropy. By using squared transects, the field recordings were assumed to be representative for the enclosed surface of the transect. The usage of transects makes that the viewing angle of the observations is consequently perpendicular to the soil surface for all recordings.

The variety of dominant vegetation species was limited; each had its own characteristic hydrological respons as described in chapter 2 and in section 3.1. Therefore the vegetation species were recorded in four classes;

- Unvegetated soil
- *Stipa tenacissima*
- *Pinus halepensis*

- Other vegetation species.

For each group the length of the canopy cover along the transect was recorded. The *Stipa tenacissima* grass was assumed to have a closed canopy cover but the canopy of other vegetation species had gaps between the leaves and branches, which made the cover semi-transparent. Because these recordings had to be compared with the SMA results of remotely sensed imagery, the semi-transparent canopies were recalculated to give the amount of unvegetated soil and 'real canopy' (figure 3.4).

For this reason the percentage semi-transparency was estimated and the full canopy cover was recalculated as the amount of unvegetated soil and the amount of 'real canopy cover' of the specific group by multiplying the length of the cover with the percentage of semi-transparency. For example if a Pinus halepensis had a full canopy cover of 1 metre along the transect line and a semi-transparency of 50% than the full cover was recalculated to 50 cm unvegetated soil and 50 cm 'real canopy cover'.

For each square the recorded lengths of canopy cover within each class, were expressed as the percentage of cover of the total length of the square sides. The cover percentages were assumed to be representative for the whole of the square surface of which the transects formed the sides.

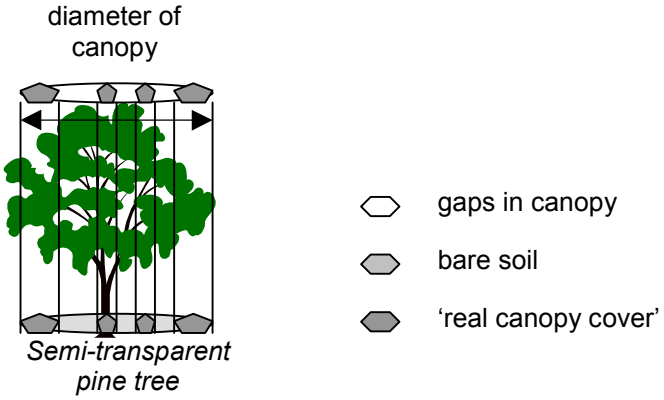

Figure 3.4 Semi-transparent cover of *Pinus halepensis*, divided in recalculated unvegetated soil and 'real canopy cover'.

3.5 Estimation of reference spectra for use of supervised classification and SMA

In this survey the reference spectra were used for *i)* supervised classification to estimate land cover types and for *ii)* SMA to estimate the amount of cover of the main vegetation species.

Two different methods were used to estimate the reference spectra. The first method was based on the available LandsatTM imagery. From the given images the pixel purity index was computed (Boardman et al., 1995). This index is based on the assumption that the purest pixels are located in the most extreme positions when the image is transposed in different spectral dimensions via an iterative process. The spectral data of the satellite images is repeatedly projected onto random unit vectors

(figure 3.5). During the iterations the extreme pixels in each projection are noted via a convex geometry argument. After the procedure, the number of times that a pixel was found to be extreme during each iteration, is counted. The purest pixels can be identified by the resulting extremity-score.

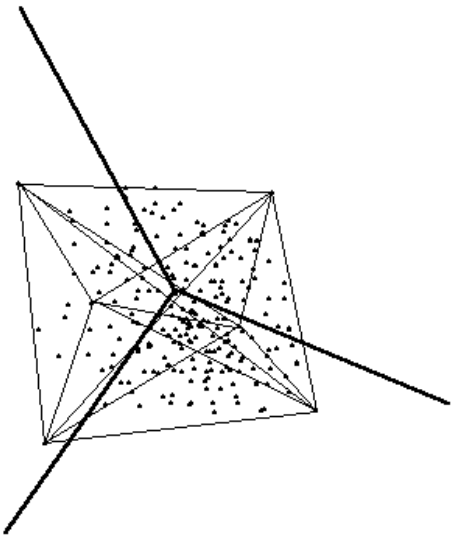

Figure 3.5 The spectral reflectance of pixels in a n-dimensional space projected on three random unit vectors.

The second method uses spectral reflectances from field and laboratory measurements. Based on field surveys, several surface covering entities were selected, for which was assumed that they contributed significantly to the spectral reflectance in the images of the study area. Their spectral reflectances were measured in the field using a portable Multispectral Radiometer (MSR5) of Cropscan Inc. (1994). The MSR5 was equipped with a sensor having a field of view (FOV) of 28 degrees. This means that when the sensor was mounted 2 metres above the ground, the measurement area was a circle of 0.78 m^2. The sensor simultaneously measures incoming solar radiance and reflected radiance from the surface, which is stored as a ratio and expressed in reflectance. The reflectance is measured in five spectral bands that exactly correspond to bands 1 to 5 of the Landsat TM5 sensor (table 3.1).

Table 3.1 Spectral bands and band width covered by the MSR5 sensor

Band	Wavelength (nm)
1	450 – 520
2	520 – 600
3	630 – 690
4	760 – 900
5	1550 – 1750

In order to use the SMA observations in a hydrological model, the selected surface covering entities or endmembers on which the SMA is based, need to be limited to easily recognisable objects that are related to hydrologic properties.

In the context of this study, such objects include trees, grass, soil. Shade must also be included because it is always a component in a nadir image (Adams et al., 1993). A problem with this approach, however, is that the entities themselves may not be homogeneous. For example, a plant consists of a heterogeneous mixture of green leaves, dead material and wooden parts (figure 3.6). However, using the SMA one seeks for results that comprise the spectral characteristics of a total plant.

During this part of the research, attention was focused on *Stipa tenacissima* because of its relevance for controlling the runoff. The spectral reflectance was measured in detail for 41 plants at different locations in the study area using the MSR5 sensor. In order to obtain the reflectance of *Stipa tenacissima* and to filter out background noise from shade and soil, the measurements of the vegetation species were carried out twice. The first measurement was made while the ground under the plant was covered with a black cloth. The second measurement was made the same way, but without the cloth which enables a correction for soil background.

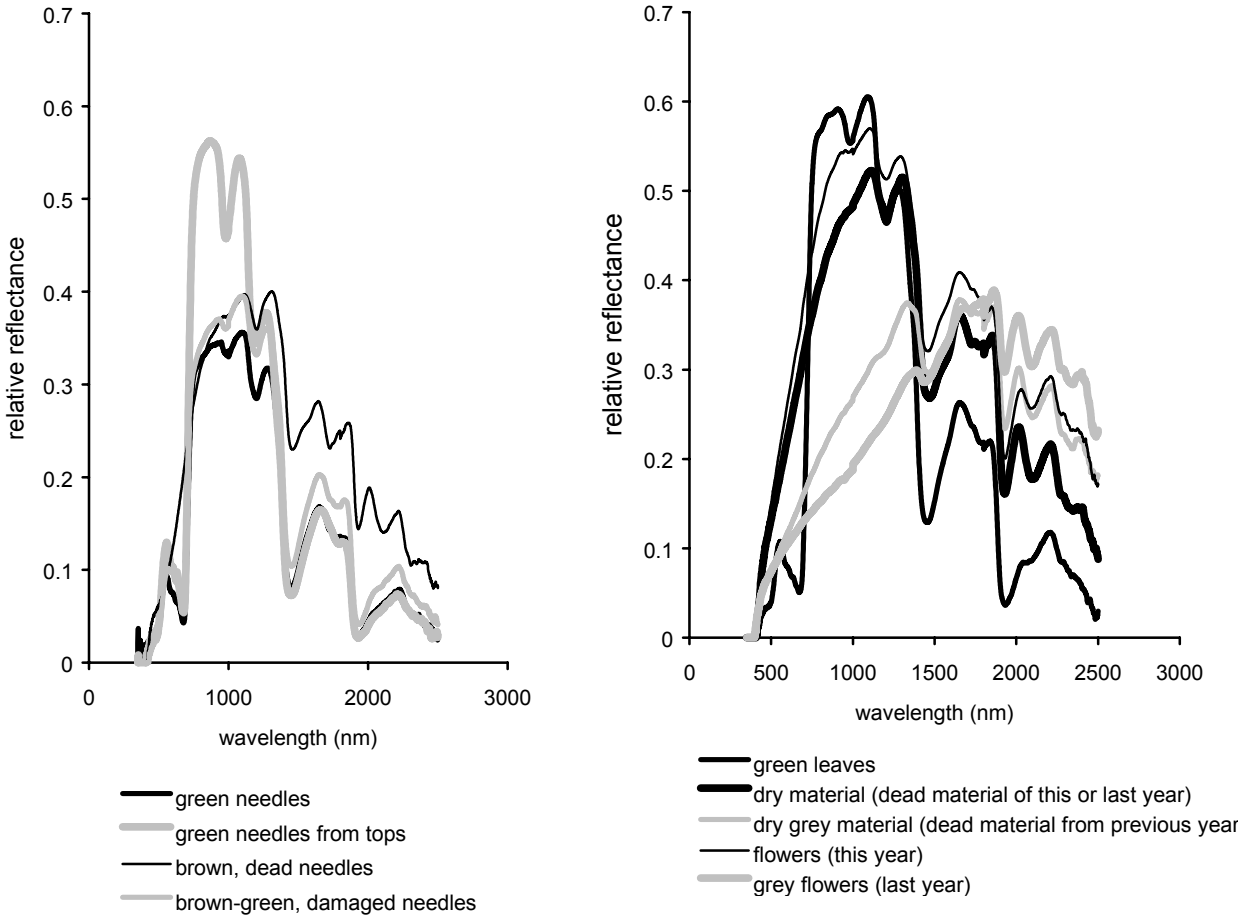

Figure 3.6 Spectral curves of *Pinus halepensis* (left) and *Stipa tenacissima* (right) (based on FieldSpec-II measurements of the University of Trier with spectral resolution of 1 nm).

Another possible cause for background signal is that the plant canopy of a single plant is smaller than the measurement area covered by the sensor (figure 3.7) and the measurement is influenced by the contribution of soil and shade in the surroundings of the plant.
To diminish the background noise additional measurements were carried out;

- Diameter (length and width) of plant canopy (cm)
- Height of sensor above canopy (cm).

Based on these measurements and the field of view of the sensor, I calculated the proportion of the surface covered by vegetation within the measurement surface of the sensor: this was defined as the 'canopy covered surface'.

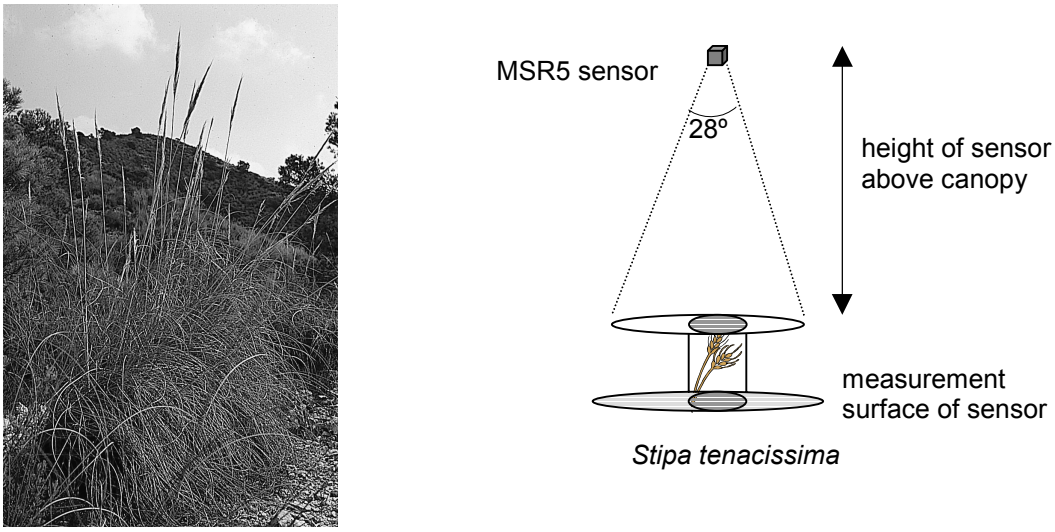

Figure 3.7 *Stipa tenacissima* (left) and measurement arrangement for the estimation of background with the MSR5 sensor (right).

For the hydrological study, *Stipa tenacissima* comprises all the components given in figure 3.6 (i.e. green leaves and dead material). The 'composite reflectance' of the plant is defined as not being influenced by background noise. When the canopy covered surface of the *Stipa tenacissima* plant increases, the spectral reflectance nears the 'composite reflectance' of the plant and is no longer influenced by background noise. Under these circumstances the spectral reflectance measurement with the black cloth will equal the spectral reflectance as measured without the black cloth. When the reflectance of the plant is influenced by background noise, the measurements with and without black cloth differ from each other as shown in figure 3.8.

The reflectance recordings were made by the MSR5 in multiple bands. For each of the five bands the composite spectral reflectance was estimated. For each spectral band the differences in the spectral reflectance between the measurements with and without cloth were plotted against the percentage of canopy covered surface of the plant.

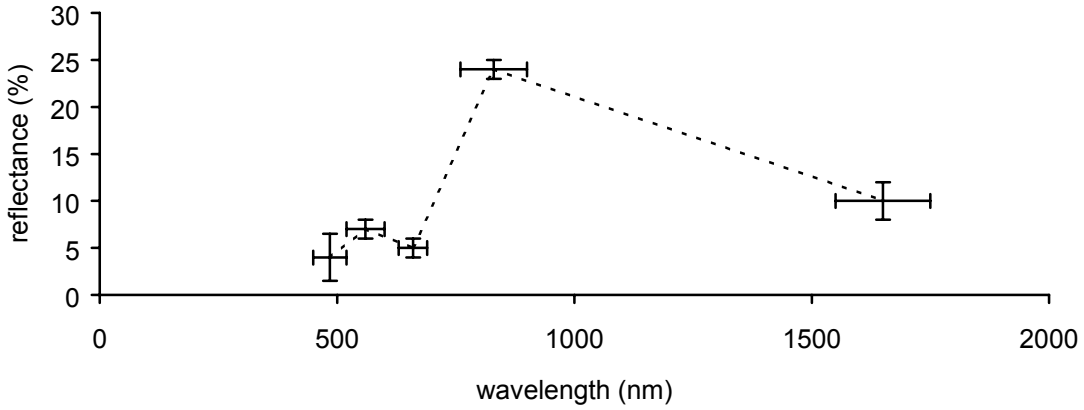

Figure 3.8 Theoretical spectral reflectance of the pure plant (dotted line) and the deviations caused by background noise (vertical error bars) measured in the spectral bands (horizontal error bars) of the MSR5. Note the limited spectral resolution of the MSR5 compared to Fieldspec-II measurements (fig. 3.6).

Next an exponential regression was computed for the relation between the difference in spectral measurements (the error bars in figure 3.8) and the surface covered by the plant canopy (figure 3.9). Subsequently for every spectral band the canopy covered surface was calculated that corresponded to zero background noise (figure 3.9). Note that the computed canopy covered surface exceeds one hundred percent when the canopy of the plant covers an area that is larger than the measurement surface of the sensor.

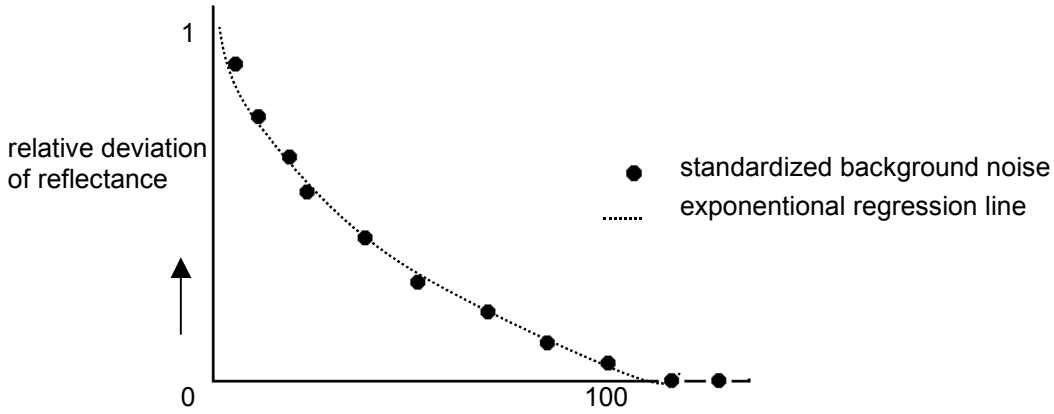

Figure 3.9 Scatter plot of the background noise as function of the canopy surface of *Stipa tenacissima* for spectral band i.

For a canopy covered surface of hundred percent background noise is still recorded. This is because spectral measurements and the measurement error in the estimates of the canopy covered surface are influenced by the noise at the border of the canopy surface. The composite reflectance of the plant was estimated by the reflectance of the plant canopy with zero background noise. To eliminate the influence of the noise at the canopy border from the spectral reflectance of the plant, the canopy covered

surface must be larger than hundred percent. This estimated composite spectral reflectance of the plant was assumed as being representative for the entire given *Stipa tenaccisima* plant.

3.6 Available Landsat TM5 imagery

For the assessment of vegetation cover, seven Landsat TM5 images were available (table 3.2). They were geometrically corrected by the EEZA (Boer, 1999). The satellite images were calibrated by using the standard pre-launch gain and offset values to convert raw digital numbers into exo-atmospheric reflectance values (Markham & Baker, 1986; Space imaging EOSAT, 1998). Visual inspection of the spectral curves of different target areas in the images, showed that no further correction for atmospheric interference was necessary.

Table 3.2: Available imagery.

Landsat TM5	Date of recording
TM070493	7 April 1993
TM140993	14 September 1993
TM031293	3 December 1993
TM290394	29 March 1994
TM270494	27 April 1994
TM280594	28 May 1994
TM310794	31 July 1994

The survey was carried out in the two selected catchments as previously described in chapter 2. For this purpose only the parts of the Landsat TM5 images that covered these catchments, were used.

To validate and calibrate the results from earth observation imagery analyses, the study area should not be too large because the field survey yields only calibration and validation areas of limited size. The land cover of the studied catchments consists of semi-natural and natural vegetation. The neighbouring areas with other type of land use, were excluded from the selections in the satellite image so they did not disturb the SMA analyses (like the pixel purity index) by their divergent spectral reflectance. For the validation and calibration, the area in and around the Alquería catchment was selected (covering 39 by 34 pixels). After validation the results were extrapolated to the Buitre catchment (covering 67 by 40 pixels) assuming that the spectral properties were similar.

The seasonal variation of the vegetation cover in the available imagery (1993-1994) is not very large as illustrated by figure 3.10, and smaller than the standard deviation in the individual images. The NDVI of the vegetation cover seems to respond to the precipitation but only monthly rainfall totals were available of the period preceding the date when the images were taken, and hence no further analysis was possible.

The histogram and the standard deviation of the 6 bands of spectral reflectance of Alquería covering part of the TM070493 show that the image is rather

homogeneous i.e. the spectral differences between the pixels are small (figure 3.11). The variance in the other available imagery is more or less the same.

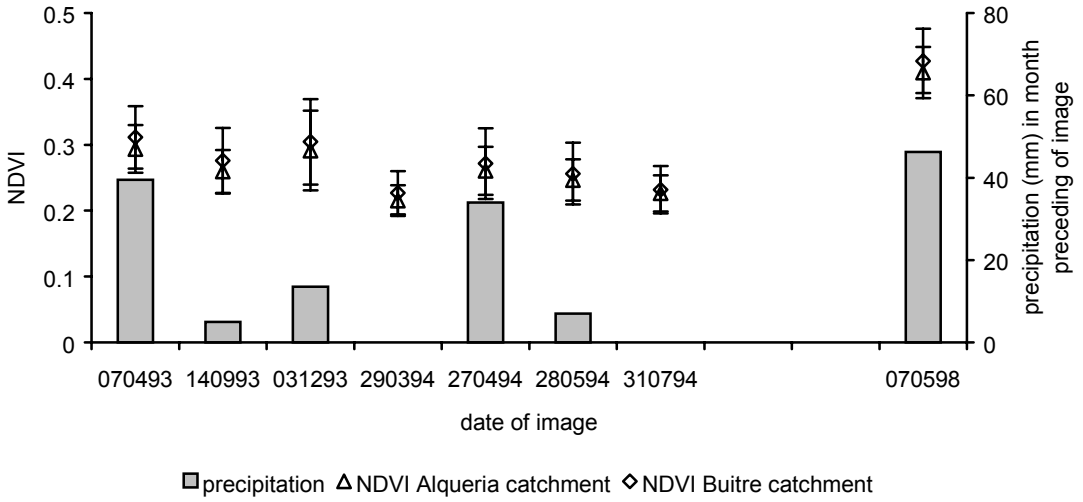

Figure 3.10 The mean NDVI of the Alquería and the Buitre catchment for the available imagery. The error bars indicate the standard deviation. Note that the image of 1998 became available after the field campaign of this study.

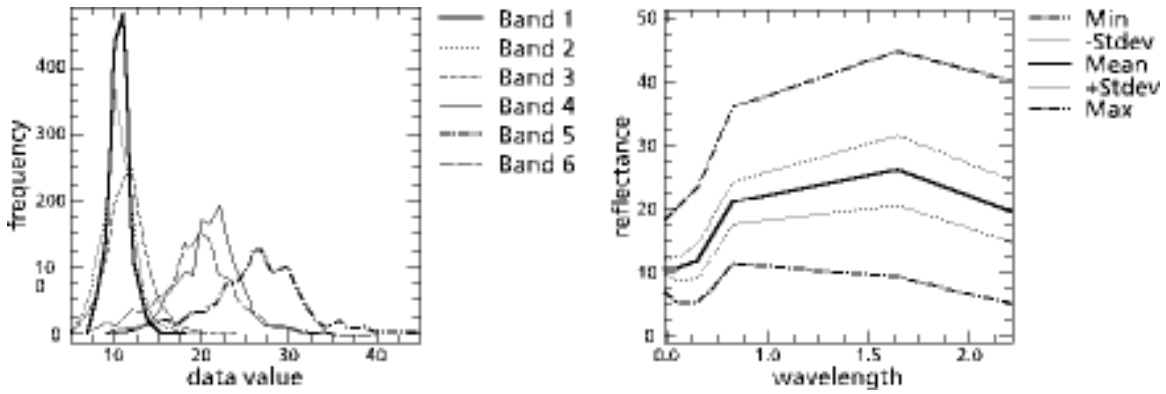

Figure 3.11 Results of statistical analysis of the spectral reflectance of the Alquería covering part of the TM070493 image.

3.7 Field inventory of surface cover

To calibrate and validate the SMA results the surface cover was estimated in the study area. The surface cover was mapped along cross-transects on 72 locations in and around the Alquería catchment (figure 3.12) and classified in four categories; *Stipa tenacissima*, *Pinus halepensis*, other vegetation types and unvegetated soil which includes rock outcrops.

The resulting surface cover percentages for all transects show a mean cover of 26% *Stipa tenacissima* and 60% of unvegetated soil with low amounts of 4% cover of *Pinus halepensis* and 10% of other green vegetation (figure 3.13).

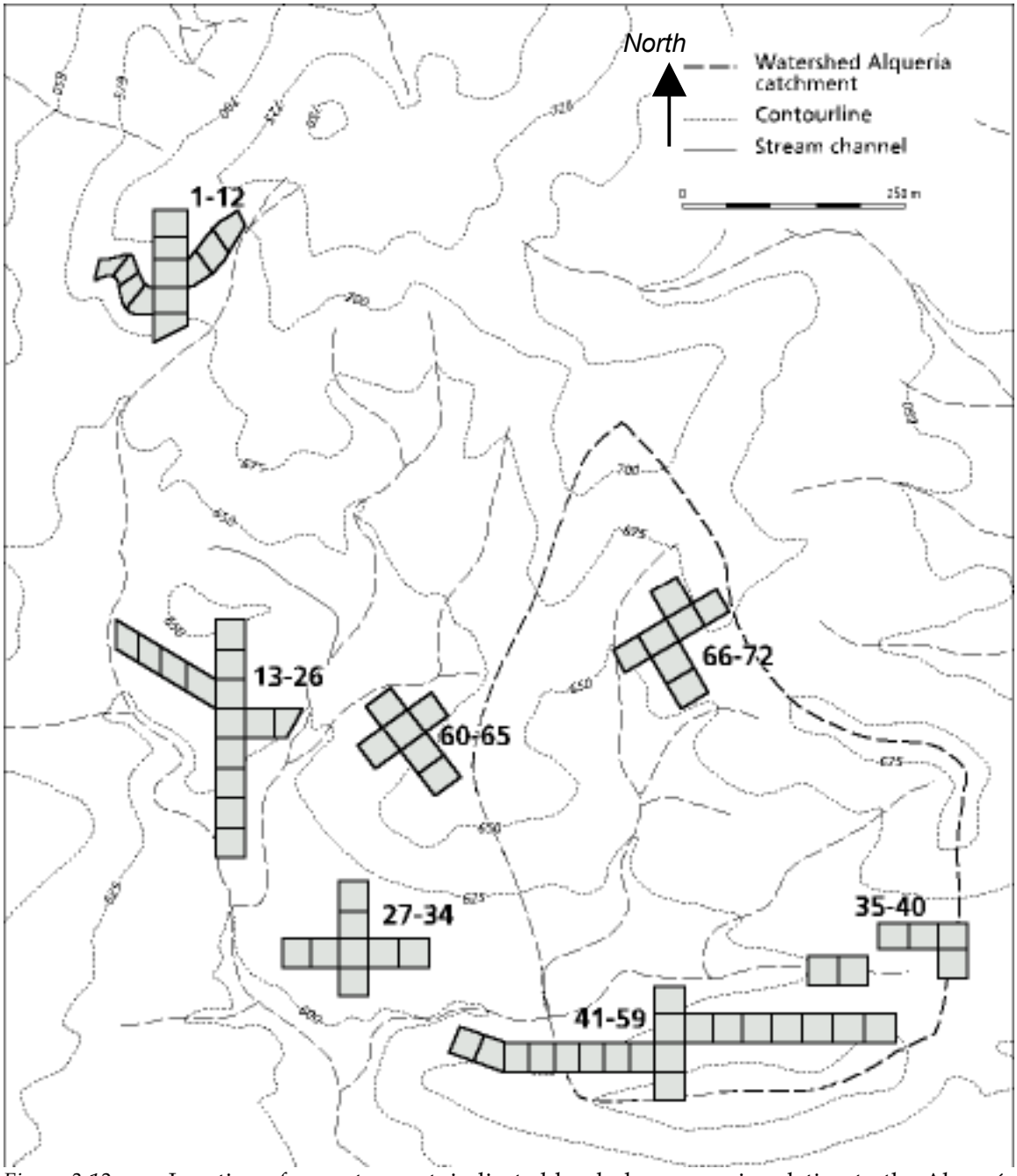

Figure 3.12 Location of cross-transect, indicated by dark squares, in relation to the Alquería catchment.

Locally the cover of the *Stipa tenacissima* increased to 58%. At other locations the surface consisted of 83% of unvegetated soil. On the north-facing slopes, the surface cover contained more *Pinus halepensis*, namely 9.5% and locally even 14%. At these locations the presence of other green vegetation increased locally to 42%. For semi-

transparent vegetation canopies these results were recalculated to give the amount of unvegetated soil and real canopy cover. For this reason the percentages of cover by *Pinus halepensis* and other green vegetation species are relatively low. If the canopies were not recalculated the amount of *Pinus halepensis* on north-facing slopes increased to 57 % and at some locations the amount of other green vegetation species not underneath the cover of pine trees reached 27 %.

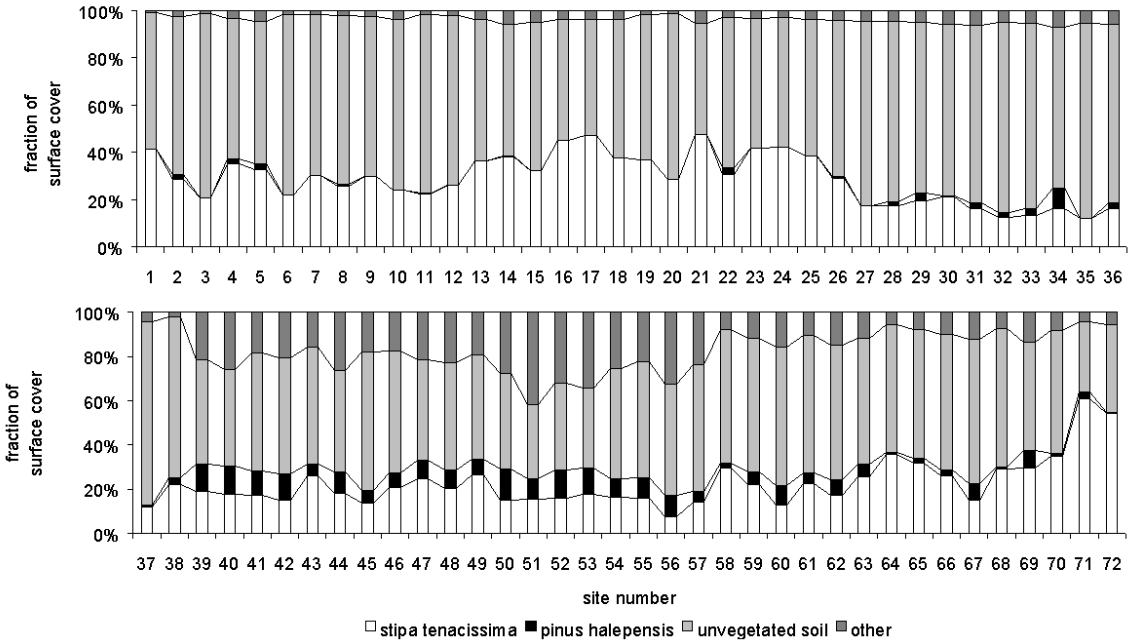

Figure 3.13 The fraction of different surface cover on field locations. Note that the sites are not located adjacent to eachother as shown by fig. 3.12.

3.8 Resulting reference spectra as representative for given imagery

From the field inventory, it was known that the main vegetation species consist of *Stipa tenacissima* and, to a lesser extent, *Pinus halepensis* alternated with unvegetated soil. For SMA, the reference spectra existed of a mixture of spectra, partly extracted from the available satellite image and if this was not possible, extracted from field spectra.

To estimate the reference spectra from the previously described images, the pixel purity index was calculated. The images appeared to be very homogeneous (figure 3.11) which was mainly due to the fact that only the studied catchments covered with semi-natural vegetation were used for analysis. The resulting purest pixels were interpreted as unvegetated soils and *Pinus halepensis* on shaded north facing slopes (figure 3.14). In a more humid environment than in which the study area is located, green vegetation would be also located at an extreme spectral location, however natural vegetation in an arid or semi-arid environment is not located at this position but somewhere in between (figure 3.14). The spectral

reflectance of the most extreme pixels was used as reference spectra for the SMA (table 3.3).

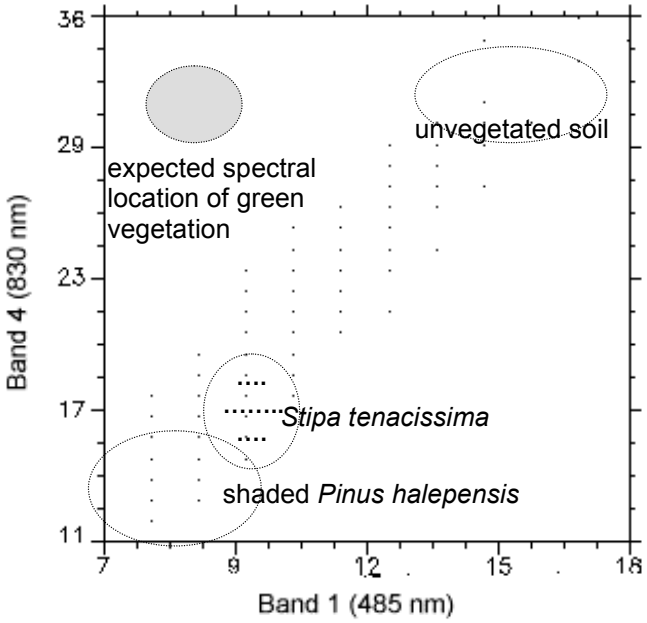

Figure 3.14 Scatterplot of the reflectance in the Alquería part of TM image in band 1 and 4 in which *Stipa tenacissima* is indicated with black dots (TM images was recorded on 7 April 1993).

Because *Stipa tenacissima* was the dominant vegetation species of the catchments, it was assumed to contribute significantly to the spectral reflectance of the satellite images. However, because the spectral reflectance of *Stipa tenacissima* is not spectrally unique (figure 3.14), it cannot easily be extracted from the images. For this reason its spectral reflectance was measured in the field with the MSR5 sensor for TM band 1 to 5, as previously described.

The spectral reflectance of 41 *Stipa tenacissima* tussocks with varying canopy diameter was measured with the MSR5 (Cropscan Inc., 1994). With an exponential regression model, the canopy cover within the field of view of the sensor was calculated under conditions of no background noise. Next the spectral reflectance of corresponding canopy cover was calculated as described in section 3.5 (figure 3.15).

The SMA was carried out on TM-images with six spectral bands but the MSR5, used to measure the ground truth spectral reflectances of *Stipa tenacissima*, was only recorded in the first five corresponding bands. Despite the absence of the sixth band, the field measurements were assumed to provide more reliable information than usage of an existing spectral library because in this study they were rectified for background noise. Spectral reflectances of a spectral library are taken under unknown conditions from only a part of the plant or from the total plant with an unknown background noise. For the sixth band, a ground truth measurement of *Stipa tenacissima* in an existing spectral library was used to calculate the spectral reflectance in TM-band 7 based on the MSR5 measurements.

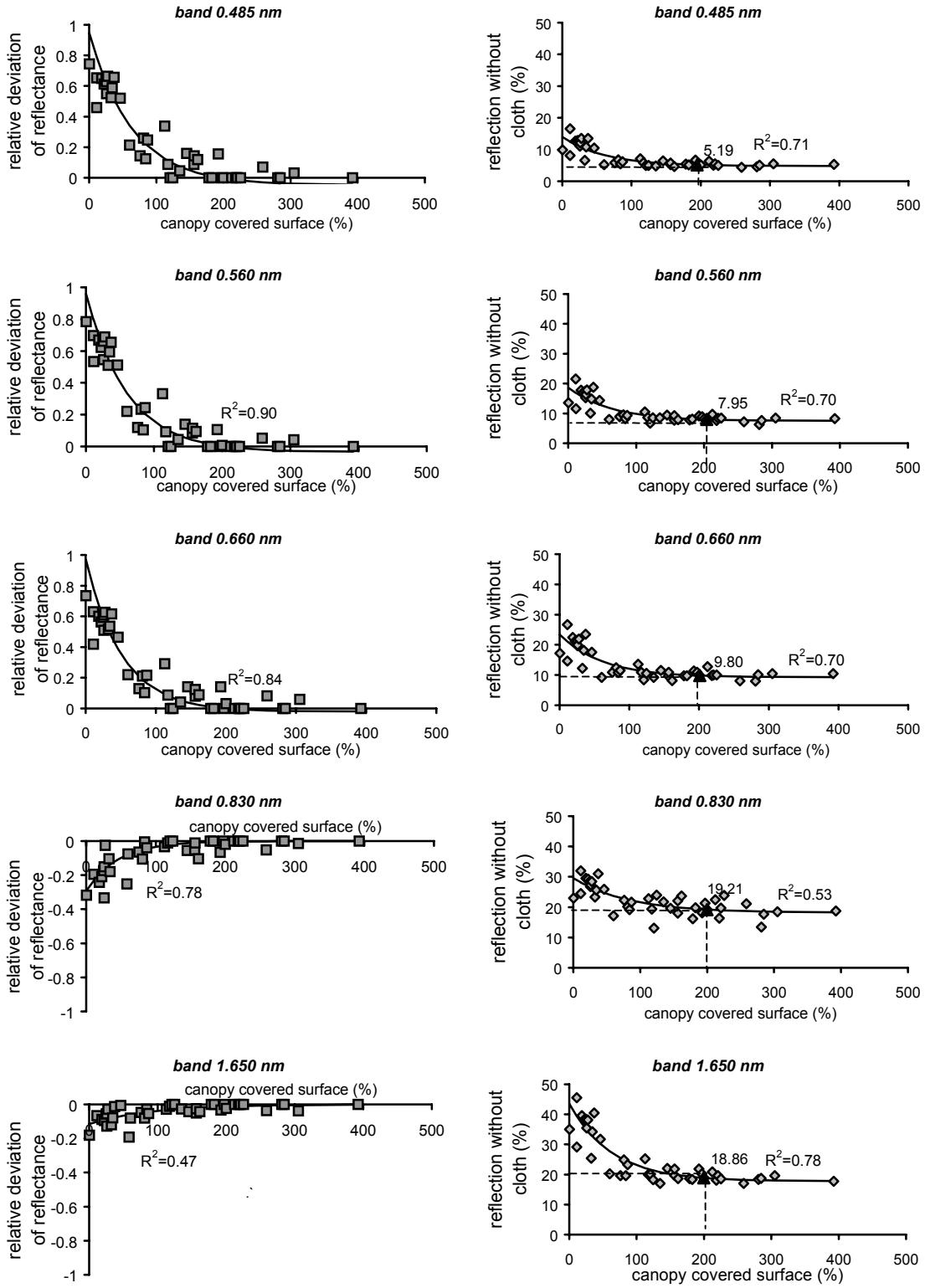

Figure 3.15 The spectral reflectance of *Stipa tenacissima* without background noise estimated by an exponential regression model for 5 different wavelengths.

Table 3.3 Reference spectra for given TM-images

TM band	Unvegetated soil reflectance (%)	*Pinus halepensis* reflectance (%)	*Stipa tenacissima* reflectance (%)
1	18	7	5
2	20	6	8
3	23	5	10
4	35	14	19
5	44	9	19
7	32	5	11

According to the soil classification in the research area (as described in chapter 2) the soil surface characteristics are very homogeneous and for this reason no further modifications were made to the unvegetated soil endmember. Furthermore, the spectral reflectance of shade was not selected as a separate endmember in spite of the suggestions in literature (Smith et al., 1990; Adams et al., 1993). Shade was included in the *Pinus halepensis* endmember because in the research area *Pinus halepensis* generally only grows on north facing slopes that are shaded due the sun angle and because its canopy structure contains the largest amount of shade compared to the canopy structure of *Stipa tenacissima*. Because of their scarce occurrence, other vegetation species were assumed not to contribute significantly to the hydrological response of the studied catchments and therefore not selected as an endmember for image analysis. In total no more than three endmembers were defined of which the resulting reference spectra are presented in table 3.3 and figure 3.16.

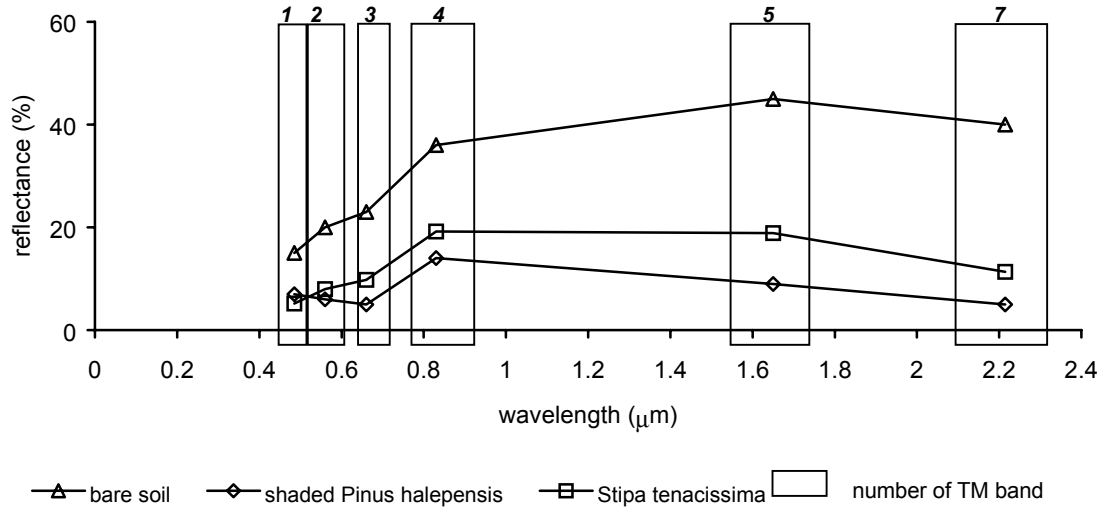

Figure 3.16 Spectral curves of reference sp ectra for given TM-images.

3.9 From spectral studies to land cover types

Previous studies have shown that the hydrological response of plots and hill slopes in a Mediterranean environment is for a significant part controlled by land cover (Francis, 1990; Sullivan et al., 1996; Cerdà, 1997b; González del Tánago et al., 1997; Cerdà et al., 1998; Romero-Díaz et al., 1999).

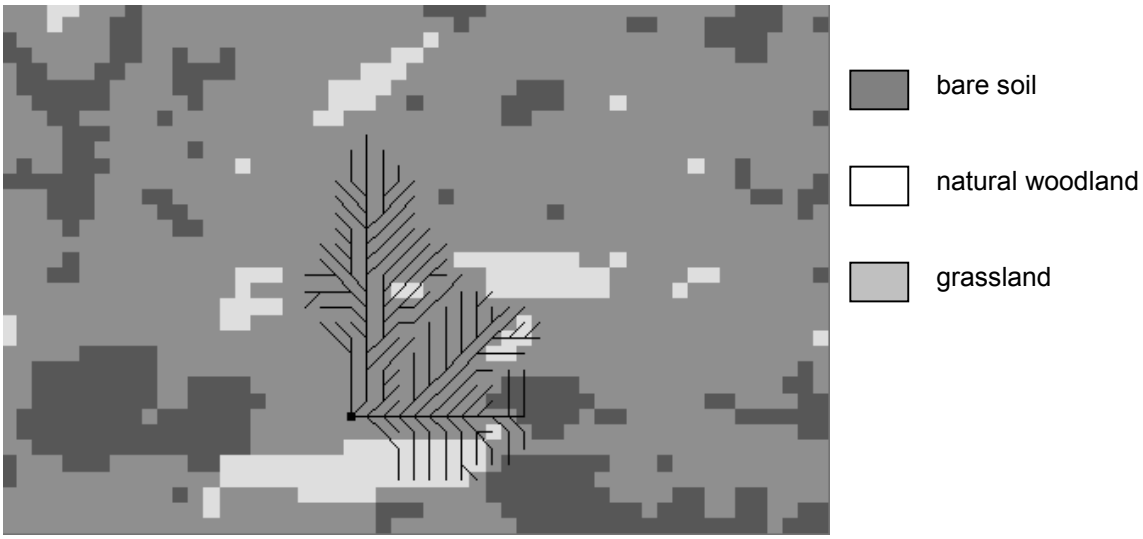

Figure 3.17 Land cover types in the Alquería catchment (indicated with the drainage pattern) and its surroundings, derived from TM070493.

The land cover types were classified to use them for hydrological analysis and to use them as inputs for a distributed hydrological model in which the components of the water balance (i.e. interception, infiltration and runoff) are related to land cover. For this reason it is important to determine the status of the land cover types from images matching the time of the year when extreme rainfall events occur. As discussed in chapter 2, the most precipitation occurs in April and October. Although the images showed little variation in reflectance values, for the determination of the land cover types TM070493 image was selected. The purest pixels of the pixel purity index were used as training set, completed with the reference spectra of *Stipa tenacissima*. For the Alquería catchment and its surroundings, the results are presented in figure 3.17.

Based on the field estimates of surface cover (figure 3.13), it was possible to assess the major vegetation species for each land cover unit, within and around the Alquería catchment. As well as through classification of a satellite image, the land cover can also be classified by visual interpretation in the field.

The classification result of the land cover units from satellite image analyses was validated based on the visual field interpretation. For this purpose the full non-recalculated canopy cover fractions as estimated in the field were related to the land cover estimated by classification of the satellite image (figure 3.18).

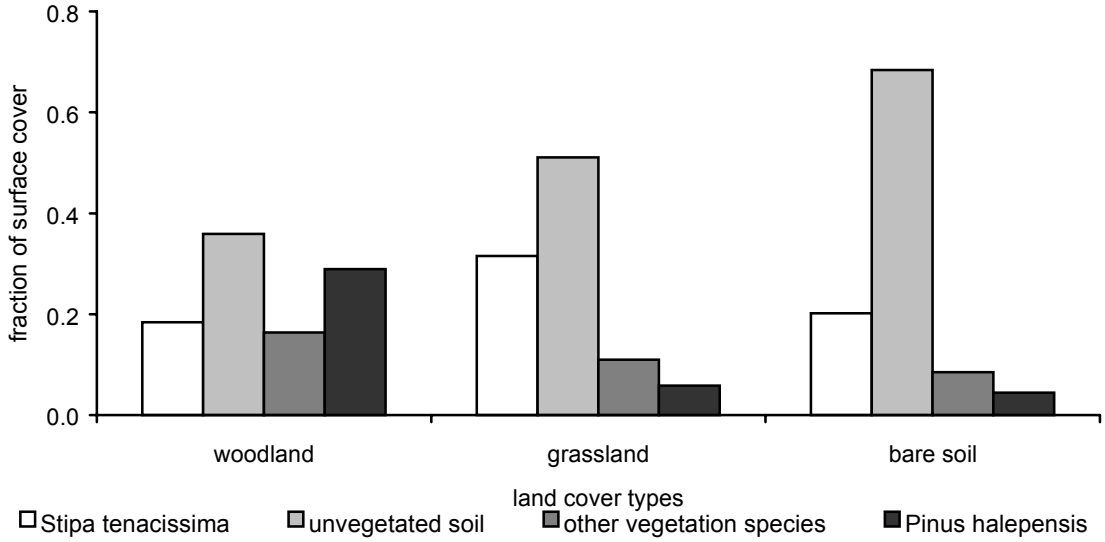

Figure 3.18 Fraction of surface cover for each entity within the three defined land cover units; woodland (n=30) grassland (n=22) and bare soil (n=17).

The results show that for each land cover unit, unvegetated soil makes the largest contribution to the surface cover. In the land cover unit woodland, the fraction of *Pinus halepensis* is largest, but in the other land cover units, *Pinus halepensis* is hardly present. The heterogeneity of vegetation species is largest on the north facing slopes that are classified as 'woodland'. Within the 'grassland' unit, the dominant vegetation species is *Stipa tenacissima* although it also contributes significantly in the unit of 'bare soil'.

The resulting land cover units of the supervised classification of the satellite image of the Buitre catchment are shown in figure 3.19.

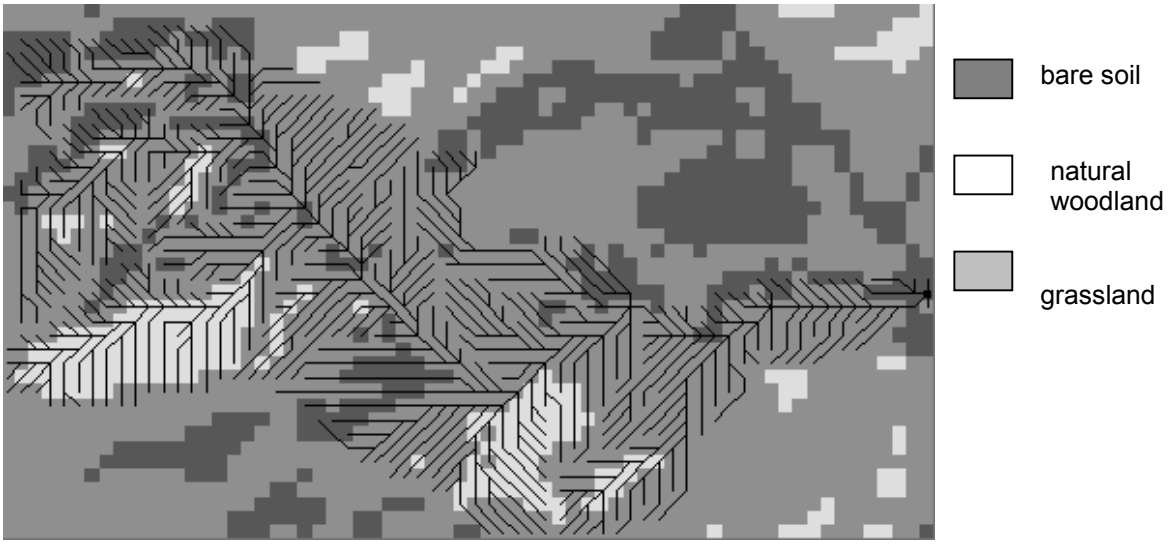

Figure 3.19 Land cover types in the Buitre catchment (indicated with the drainage pattern) and its surroundings.

Parts of the Buitre catchment have been afforested with *Pinus halepensis* planted on terraces. Although it is known that these parts have a different hydrological response, it was not possible to classify these land cover units separately by a supervised classification of satellite images. This is due to the fact that the small, planted trees are spectrally similar to the *Stipa tenacissima* and contribute for a small amount to the total land cover because of their large semi-transparency so their spectral reflectance consists to a significant degree of the background signal of bright marl soils. To implement these land cover units in the hydrological model, the afforested parts were mapped in the field and overlaid with the classified results (figure 3.20).

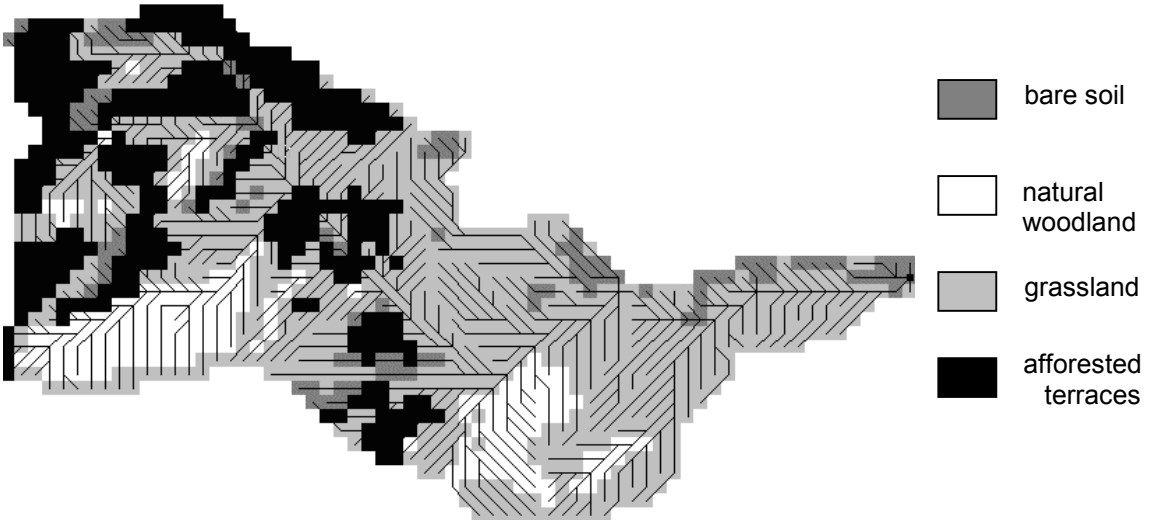

Figure 3.20 Land cover types in the Buitre catchment (indicated with the drainage pattern) including afforested terraces.

3.10 Surface cover from SMA

The parts of the Landsat TM images covering the Alquería catchment were linear constrained unmixed as explained in section 3.3. For the SMA the reference spectra of endmembers as presented in section 3.8 were used. The spatial pattern of the SMA resulting abundances looks promising (figure 3.21).

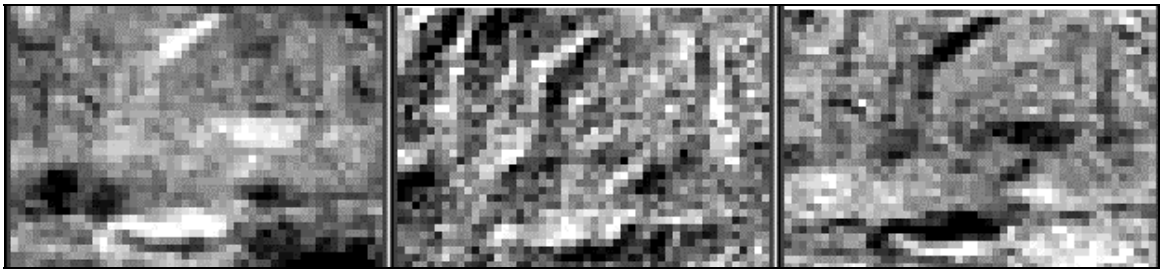

Figure 3.21 Fractions (0 – 1) of unvegetated soil (left) *Stipa tenacissima* (middle) and *Pinus halepensis* (right) resulting from SMA in the Alquería catchment. The largest fractions are indicated by black and the smallest by white.

The abundances resulting from SMA were calibrated with the surface cover estimates in and near the Alquería catchment, as described in section 3.7. During the field inventory the surface cover was classified in four classes of which one was 'other green vegetation'. Because during SMA the class 'other green vegetation' will be included in either *Stipa tenacissima* or *Pinus halepensis*, the fractions of 'other green vegetation' as mapped in the field, were proportional regrouped in the classes *Stipa tenacissima* (equation 3.7) and *Pinus halepensis* (equation 3.8) by;

$$St_{regr} = St_{field} + St_{field} * ogv/(St_{field} + Ph_{field}) \qquad \textit{equation 3.7}$$

$$Ph_{regr} = Ph_{field} + Ph_{field} * ogv/(St_{field} + Ph_{field}) \qquad \textit{equation 3.8}$$

in which:
St_{regr} = the regrouped fraction of *Stipa tenacissima*
St_{field} = the fraction of *Stipa tenacissima* estimated in the field
ogv = the fraction of 'other' green vegetation estimated in the field
Ph_{regr} = the regrouped fraction of *Pinus halepensis*
Ph_{field} = the fraction of *Pinus halepensis* estimated in the field

It was checked if the spatial correlation of the mapped fractions of vegetation cover corresponded with the SMA predicted fraction. For this purpose the fractions were analysed by exponential variogram models (figure 3.22) (Pebesma, 1995; Burrough & McDonnell, 1998) as described by (equation 3.9);

$$\gamma(h) = c_0 + c_1\{1 - e^{\frac{-h}{a}}\} \qquad \textit{equation 3.9}$$

in which:
$\gamma(h)$: semivariance
c_0 : nugget variance; the residual, spatially uncorrelated noise
$c_0 + c_1$: sill; semivariance at which no spatial dependence occurs
a : range; spatial dependency of inter-site differences
h : lag; distance vector

As pointed out in section 3.4, the field data were collected along square transects of which the surface cover along sides was assumed to be representative for the surface cover of the area inside the square. The results of a possible deviation between the surface cover along the sides of the transect and the area inside the transect are due to measurement errors and will result in a shift of the nugget but due not affect the range of the variogram models

These variogram models (appendix 1) showed that the spatial dependency of inter-site differences for *Stipa tenacissima* had a smaller range than either

unvegetated soil and *Pinus halepensis* for both the mapped cover fractions in the field as for the by SMA predicted fractions of surface cover (table 3.4).

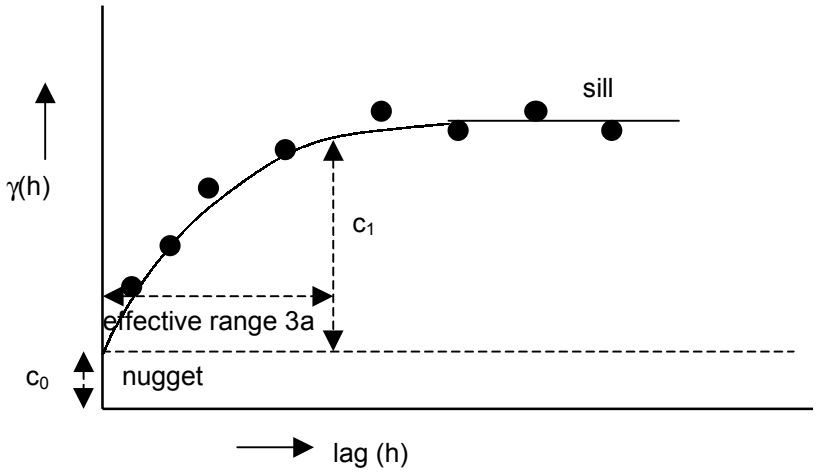

Figure 3.22 Example of an exponential semivariogram with range, nugget and sill. After Burrough and McDonnell (1998). Note that the effective range, where the variogram reaches 95% of its maximum, is 3*a, where a is the lag parameter in the exponential variogram model.

The range of the variogram of the field measurements, equaled more or less the range of the SMA fractions for all three endmembers. To determine the effective range of spatial dependency, the values of table 3.4 have to be multiplied by 3. The spatial dependency of a vegetation cover of *Stipa tenacissima*, occurred up to distances of 10 TM image pixels (with a size of 30 by 30 m.). Unvegetated soil occurred to be spatial dependent to maximum 13 - 22 pixels and the cover of *Pinus halepensis* had an even larger effective range of 18 – 27 pixels.

Table 3.4 Range a (in metres) of spatial dependency indicated by an exponential variogram model.

	Unvegetated soil	*Pinus halepensis*	*Stipa tenacissima*
Field cover measurements	160	271	79
SMA of TM070493	189	248	81
SMA of TM140993	181	183	111
SMA of TM031293	134	219	202
SMA of TM290394	134	200	100
SMA of TM270494	197	199	108
SMA of TM280594	213	224	103
SMA of TM310794	218	274	114

The results show that a spatial correlation exists for the surface cover types *Stipa tenacissima*, *Pinus halepensis* and unvegetated soil. The spatial independency of the field estimates occur at the same scale as the SMA predicted fractions (especially of image TM070493 in table 3.4) which suggests that the SMA had been applied successfully and the fractions seem reliable.

3.11 Calibrated fractions of surface cover for the study area

The resulting fractions of the SMA turned out not to correspond directly with the fractions of surface cover as measured in the field. This is shown in figure 3.23 for the seven available TM-images by absence of a $x=y$ relation between the fraction cover based on field measurements and on SMA. To calibrate the SMA fractions, a linear regression model (figure 3.23) was applied to the field measurements and the SMA results of the available images.

The results (figure 3.23) show a clear relation for shaded *Pinus halepensis* and unvegetated soil for which up to 55 % of the variance was explained for unvegetated soil and respectively 65 % for shaded *Pinus halepensis*. By a linear regression model, the fraction cover in the field could be predicted based on the SMA resulting fractions of unvegetated soil and shaded *Pinus halepensis*.

No relation was found between the SMA fractions and the measurements of *Stipa tenacissima* cover in the field. During the field survey the fractions of cover of different cover types at each measurement location summed together to 1. On this basis the cover of *Stipa tenacissima* could be calculated by the predicted fractions of unvegetated soil and *Pinus halepensis*. Negative fractions of cover, can be explained but cannot be interpreted and were reset to zero. The fraction of *Stipa tenacissima* based on SMA results, was recalculated by equation 3.10;

$$St_{SMApredicted} = 1 - us_{SMApredicted} - sPh_{SMApredicted} \qquad \textit{equation 3.10}$$

in which:

$St_{SMApred}$ = the by SMA predicted fraction of *Stipa tenacissima*
$us_{SMApredicted}$ = the by SMA predicted fraction of unvegetated soil
$sPh_{SMApred}$ = the by SMA predicted fraction of shaded *Pinus halepensis*

The relation between the recalculated fractions of *Stipa tenacissima* and the fraction of *Stipa tenacissima* cover estimated in the field, explained the variance for a maximum of 20%. The geometrical correction of TM images resulted in a horizontal RMS-error of 36 m and a vertical RMS-error of 62 m between locations of the topographical map and in the same locations in the images. This means that a certain location in the satellite image can theoretically deviate in average 1 to 2 pixels from its real geometrical position. This might explain why the correlation coefficients between the SMA resulting fractions and field cover fractions are so small. Another explanation might be that the assumption that the field cover fractions estimated along transects are representative for the content of a pixel, is not valid.

Nevertheless, the linear regression models with the largest correlation coefficients for all vegetation cover types between SMA (recalculated) resulting fractions and field cover fractions were used to estimate the surface cover fractions for the total study area.

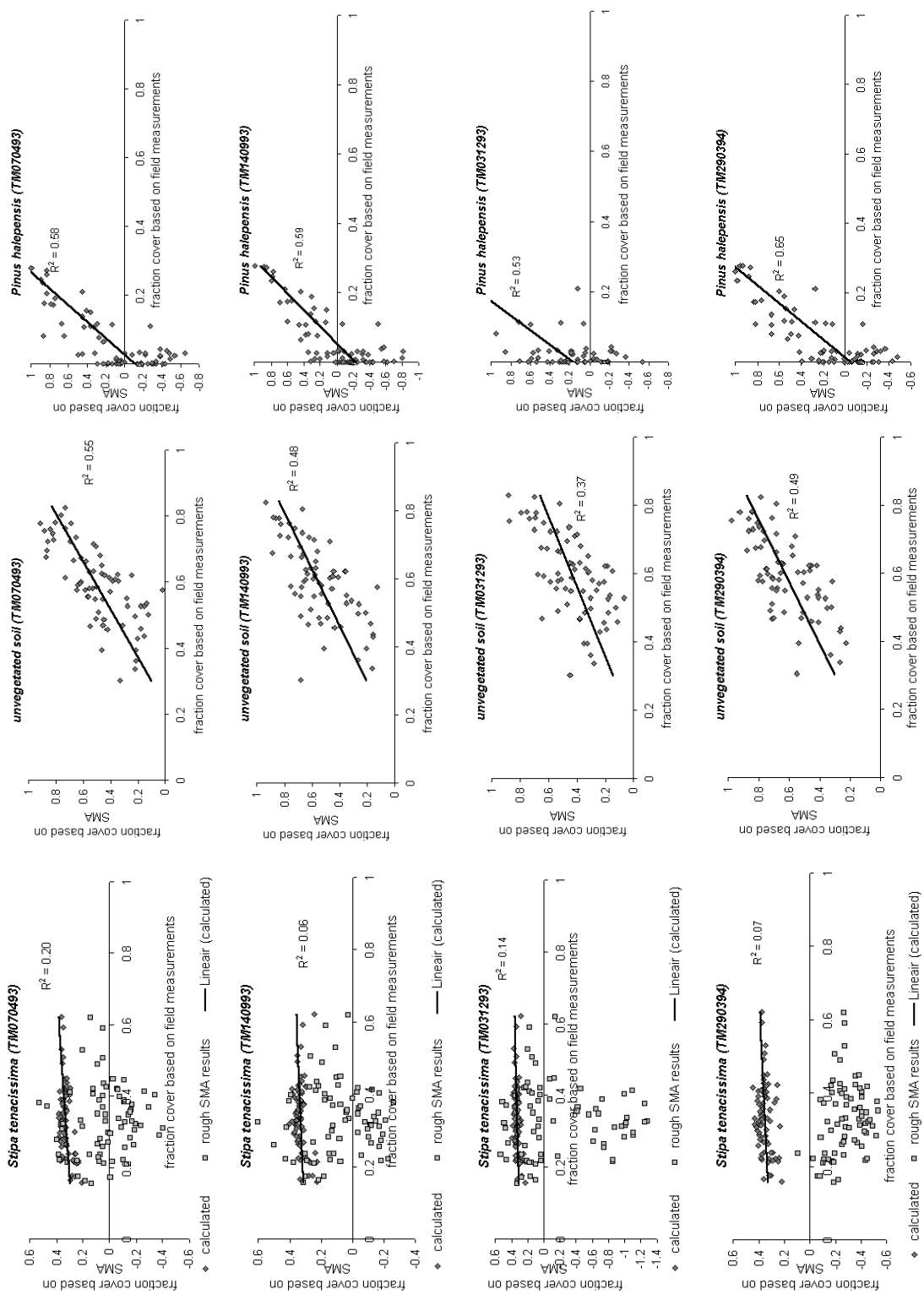

Figure 3.23 The calibrated fractions of surface cover for *Stipa tenacissima*, unvegetated soil.

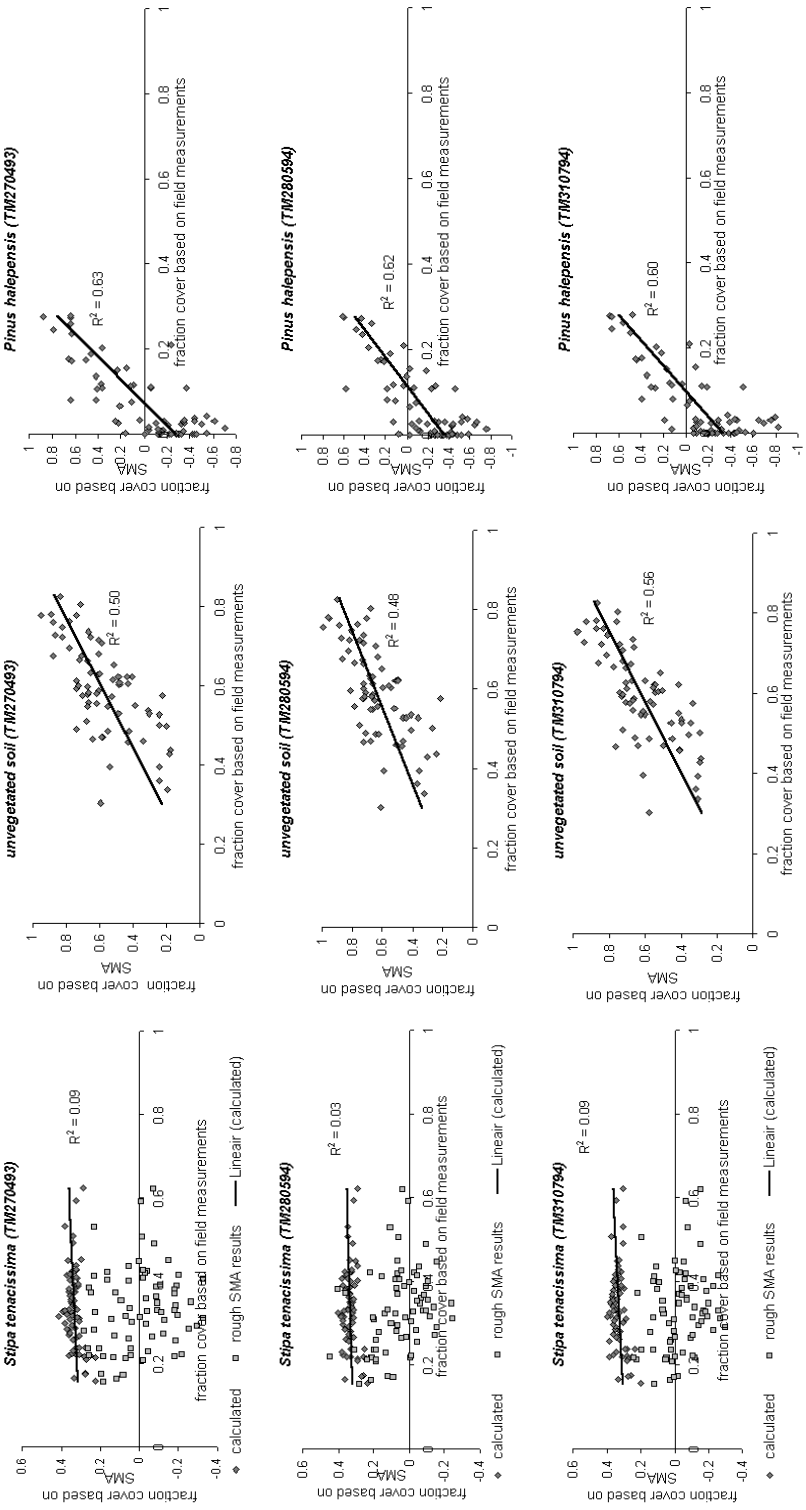

and *Pinus halepensis* estimated by an linear regression model for the seven available TM-images.

The largest correlation coefficients were all found for satellite images that had been recorded in humid seasons: these were TM070493 (unvegetated soil and *Stipa tenacissima*) and TM290394 (*Pinus halepensis*). The linear regression models of TM070493 were used to calibrate the fraction of surface cover of different entitites in both the Alquería catchment (figure 3.24) and the Buitre catchment (figure 3.25).

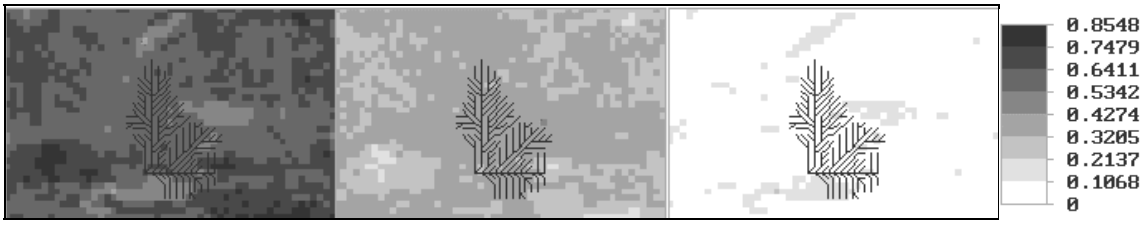

Figure 3.24 Fractions of unvegetated soil (left) *Stipa tenacissima* (middle) and *Pinus halepensis* (right) resulting from calibration in the Aquería catchment. The largest fractions are indicated by black and the smallest by white.

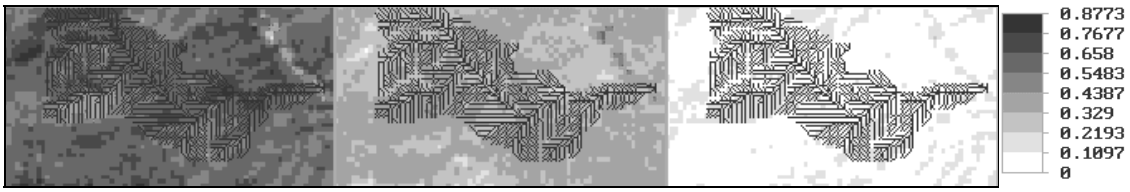

Figure 3.25 Fractions of unvegetated soil (left) *Stipa tenacissima* (middle) and *Pinus halepensis* (right) resulting from calibration in the Buitre catchment. The largest fractions are indicated by black and the smallest by white.

Table 3.5 The mean estimated fractions of surface cover for the different catchments with the standard deviation and the type of distribution.

Catchment	Amount of pixels	% *Pinus halepensis*			% *Stipa tenacissima*			% Unvegetated soil		
		Mean	SD	Distri-bution	Mean	SD	Distri-bution	Mean	SD	Distri-bution
Bt	1242	7.6	5.1	log-normal	33.5	4.4	normal	58.9	7.8	normal
B1	144	8.1	4.5	normal	31.7	3.9	normal	60.2	6.6	normal
B2	148	12.9	5.8	arcsine	37.1	3.9	arcsine	50.0	9.5	bimodal
B7	24	10.0	2.9	normal	29.0	2.7	arcsine	61.0	3.8	normal
B8	8	11.8	3.0	arcsine	34.7	3.9	arcsine	53.5	5.3	normal
B9	4	16.3	1.1	normal	38.4	1.7	bimodal	45.3	2.5	bimodal
A2	102	5.2	2.6	normal	35.6	2.0	normal	59.2	3.0	normal
A5	109	7.0	4.4	normal	35.0	3.0	normal	58.0	5.8	normal
Alquería total (A2+A5)	211	6.1	3.7	log-normal	35.4	2.6	normal	58.5	4.7	normal
Alquería field, after regrouping	72	5.3	4.2	log-normal	34.8	10.9	normal	59.8	12.1	normal

When the fractions of surface cover were calculated for the selected catchments (table 3.5), the differences between mean percentage of surface cover of the

catchments were small. The mean SMA estimated fractions of surface cover in the total Alquería catchment corresponded with the mean estimated fractions of surface cover in the field.

The predicted spectral reflection of the image and the spectral reflection as predicted by SMA, can be compared using the root-mean-square (RMS) error (equation 3.11);

$$RMS = \sum_{i=1}^{M} \{ \sqrt{\sum_{j=1}^{n} (R_{ij} - R'_{ij})^2 / n} \} / M \qquad \textit{equation 3.11}$$

in which:

R_{ij} = modelled or predicted reflectance of the pixel in band *i* for endmember *j*

R'_{ij} = measured reflectance of the pixel in band *i* for endmember *j*

n = number of spectral bands

M = number of pixels within the image

Iterative processing confirmed that implementation of a larger number of endmembers in the SMA resulted in a reducing RMS error but lead to unrealistic abundances for the selected endmembers, especially in rather homogeneous images as was the case for the selected study area. Although the resulting maps of the RMS error showed slight spatial patterns which looked similar to the distribution of *Stipa tenacissima*, no clear relation existed between the fractions of cover estimated in the field and the RMS error (explained variance varied between 0 and 14 %).

3.12 Discussion

During the analysis of data in this chapter, several assumptions have been made which may affect the quality of the results.

For the application of SMA, it was assumed that the signal received by the sensor has interacted with only one surface covering entity which means that the signal which is transmitted to the soil surface via the vegetation cover may affect the spectral reflectance of an image pixel. This way the spectral reflectance may be difficult to relate to surface covering entities, which have an assumed spectral reflectance without scatter. Because the leaves of the vegetation in the study area have a small width and are thick enough not to transmit the signal, the spectral reflectance will be without scatter.

The SMA was computed for TM images that had been recorded in 1993 and 1994 while field measurements were made in May 1998. As shown in figure 3.10, the vegetation cover did not vary much during the time span of the available imagery. However, the NDVI for May 1998 are significantly higher which indicate a more healthy condition of the vegetation. Under healthy conditions the spectral curves of the reference spectra are assumed to differ more from each other than under

moisture-stressed conditions. If the SMA had been carried out on the image of 1998, the calibration of the SMA-abundances by field estimates of the vegetation cover might have lead to better results. However in the given timeframe of this study, this was not possible. The deviation between the geographical position of the TM-pixels and the field transacts is assumed not to influence the results of the analyses because the vegetation cover is rather homogeneous.

The available TM-images had been corrected already. Only a standard pre-launch correction (section 3.6) was applied to convert raw digital numbers into exo-atmospheric reflectance values. This way the images were assumed to be corrected sufficiently which was confirmed by visual interpretation for the atmospheric interference and by calculation of the RMS for geometrical correction. However, if the atmospheric correction was insufficient, the SMA might have been improved after atmospheric correction. A RMS of 1 to 2 pixels seems reasonable but this may indicate a false position of the field measurements by overlaying them on the satellite image as described in section 3.10.

Settle and Drake (1993) suggested that SMA should be applied on the first four bands transformed by Principle Components Analysis (PCA) because of the intrinsic dimensionality of spectral data. PCA-transformed band 5 and PCA-transformed band 7 of the TM images mainly contain noise. Another reason to use only the first four PCA bands of the images, would be that the spectral reflectance of the selected endmembers in the PCA band 5 and 7 does not contribute to the spectral differences between the selected endmembers (figure 3.16).

Despite all arguments given in this section, the results are assumed to be the best possible because the main problems with application of SMA on TM-images maintain *a)* the limited spectral resolution of the TM-images existing of only six coarse wavelength bands and *b)* the spectral reflectance of *Pinus halepensis* is almost similar to the spectral reflectance of *Stipa tenacissima* (figure 3.16). It is believed that the suggestions given in this section will result in only slight improvements.

3.13 Conclusions

To study the influence of vegetation on runoff of different sized catchments, the vegetation types in the study area were parameterized at two different resolutions; as the amount of land cover and as the percentage of surface cover per unit area.

The spatial distribution of land cover units was classified from the Landsat TM images. By using the estimates of the canopy cover in the field it was possible to obtain a better definition of the land cover units. As expected in a semi-arid environment, the main vegetation cover within all land cover units was unvegetated soil. When the land cover was classified as grassland, the dominant species was *Stipa tenacissima* and the land cover classified as woodland was dominated by the species *Pinus halepensis*.

Spectral mixture analysis (SMA) was originally developed for hyperspectral data with information on a large number of narrow spectral bands. It has not been developed to use on data with a limited number of broad spectral bands, like

Landsat TM images, although numerous studies are known in which SMA has succesfully applied to such images. In several studies, the results still were classified as satisfactory mainly due to the fact that reference spectra were used to estimate the cover of entities that were spectrally very dissimilar and because sufficient reference field data were lacking.

In this study the SMA was applied to estimate the percentage of surface cover per entity per unit area. It was applied to parts of TM images that were only covered with semi-natural vegetation with a rather homogeneous cover. In spite of the limited number of reference spectra it was simply not possible to extract the quantitative amount of cover for different entities purely based on SMA. Only by the use of linear regression models and the estimates of vegetation cover in the field, could the SMA results be recalculated to amounts of cover for the selected entities in the whole study area. The resulting correlation coefficients were satisfactory due to the extreme spectral locations of two of the three selected entities; *Pinus halepensis* and unvegetated soil. For the third entity, *Stipa tenacissima*, both the mean fraction of surface cover and the range of spatial dependency of the in the calculated fraction corresponded with the field estimated cover. For this reason the error in the calculated cover of *Stipa tenacissima* was found to be acceptable.

Given the satisfying results of the calculated fractions of surface cover, SMA provides us with a good technique to estimate surface cover in a semi-arid Mediterranean environment. However, this technique should be applied to spectral images with a high number of narrow spectral bands. Applied to LandsatTM-images as used in this study, reliable results could only be obtained by recalculation procedures which makes application of SMA rather complicated.

4 Precipitation

4.1 Rainfall characteristics

As rainfall and rainfall properties are the main controlling factors in runoff production, the rainfall characteristics of the study area were carefully studied. Several studies (Blöschl et al., 1995; Gupta & Waymire, 1998) have shown that in catchments smaller than a REA, it is difficult to establish a simple relation between rainfall and discharge of similar sized catchments because the variability in discharge of these catchments is high. For catchments larger than a REA, discharge can be unambiguously related to rainfall characteristics, and if spatial correlation is absent the variability in discharge diminishes (Beven & Wood, 1993). One of these rainfall characteristics is storm duration, because it determines the survival length of the flow by controlling the amount of discharge (Blöschl et al., 1995; Gupta & Waymire, 1998). Next to the storm duration, rainfall intensity controls the runoff volume in a semi-arid Mediterranean environment (De Ploey et al., 1991; Poesen & Hooke, 1997). Therefore to quantify the storm duration and rainfall intensity that caused runoff in the study area, the rainfall in the study area was continuously recorded between November 1995 and October 1998.

It is widely accepted that it is important to incorporate the spatial variability of rainfall in hydrological modelling (Butcher & Thornes, 1978; Pilgrim et al., 1988; Wood et al., 1988; Blöschl et al., 1995; Lopes, 1996; Singh, 1997). Bull et al. (1999) illustrated this importance for areas located close to the selected research area. The spatial variability of precipitation is known to influence the size of a REA (Blöschl et al., 1995): its spatial correlation needs to be small or absent in order to apply the REA-concept. For the Guadalentín Basin, in which the study area is located, several relations between precipitation and altitude, longitude (Pérez Pujalte, 1993) and latitude (Boer, 1999) are described in the literature. It is not known a priori whether a relation between the amount of rainfall and topographical features like altitude and aspect exists in the study area, so this needs to be examined. If there is a significant influence of topography on the rainfall amounts then in absence of rain shadow effects, elevation may be used as aid for geostatistical mapping of rainfall (Goovaerts, 1999).

The two catchments studied are located close to each-other (as described in chapter 2) but even though they are only 2 kilometres apart, we need to know if they have the same rainfall characteristics so that the recorded rainfall can be treated as one data set. However, if the two catchments have different rainfall characteristics and the rainfall recordings only relate to a single catchment, the rainfall records should be treated separately during further analysis

The information collected on precipitation was used to analyse the discharge in the study area. The results were used to gain insight in how the hydrological model had to be adapted (i.e. timesteps and minimum amount of rainfall causing runoff in small streambeds) in order to simulate the superficial hydrological

response of the study area. The precipitation records serve as input data for this model (i.e. amounts of rainfall per event, rainfall intensity during an event and the spatial distribution of the rainfall during an event).

4.2 Continuous rainfall recording by tipping buckets

The rainfall intensities and duration of rainfall events in the two catchments (described in chapter 2) were monitored continuously by one pluviograph and four tipping buckets. A period of at least thirty minutes without precipitation was taken to indicate the separation of one rainfall event from the other.

The pluviograph was located near the outlet of the Buitre catchment. Two tipping buckets were installed, each at the centres of the Buitre and the Alquería catchments, respectively. The period of measurement is indicated in figure 4.1. Unfortunately the tipping bucket in the Buitre catchment had to be replaced halfway during the survey, and the tipping bucket in the Alquería catchment did not always function properly.

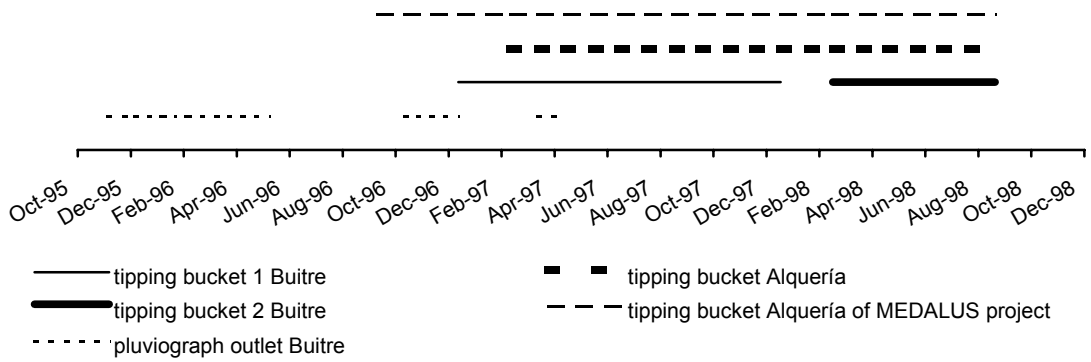

Figure 4.1 Period of rainfall measurements used for hydrological monitoring.

As part of the MEDALUS project (Imeson et al., 1999) a tipping bucket was placed in October 1996 near the centre of the Alquería catchment, approximately 50 m from the malfunctioning tipping bucket. This tipping bucket recorded precipitation over a larger time interval than the tipping buckets used for this survey.

Table 4.1 Resolution of measurement and monitoring of different used instruments.

	Buitre catchment			Alquería catchment	
Instrument	Pluviograph	tipping bucket 1	tipping bucket 2	tipping bucket	tipping bucket of MEDALUS
Resolution of measurement	1 cm = 1.32 mm	0.105 mm/tip	0.201 mm/tip	0.199 mm/tip	0.2 mm/tip
Time interval of monitoring	continuous 1 cm = 4.57 hours	5 minutes	2 minutes	1 minute	10 minutes

For intervals in which the tipping buckets malfunctioned, the measurements of the tipping bucket of the MEDALUS project were used. In order to be able to compare the different measurements (table 4.1), the maximum intensities were all recalculated to the largest interval of measurements of 10 minutes, which was the main interval used by tipping bucket of the MEDALUS project, located in the Alquería catchment.

4.3 Amount of rainfall

The precipitation in the study area was monitored almost continuously from October 1995 to December 1998 (as described in the previous section). The results are shown in table 4.2. For these records the rainfall event was defined as a period of rain with a dry period of at least 30 minutes before and after the rainfall event.

Table 4.2 Descriptive statistics of rainfall records during the study period.

Location	Number of rain events	Median amount (mm)	Minimum amount (mm)	Maximum amount (mm)
Tipping bucket Alquería catchment	125	1.4	0.4	28.8
Tipping bucket Buitre catchment	157	0.8	0.1	46.9
Pluviograph Buitre catchment	150	0.5	0.01	18.7

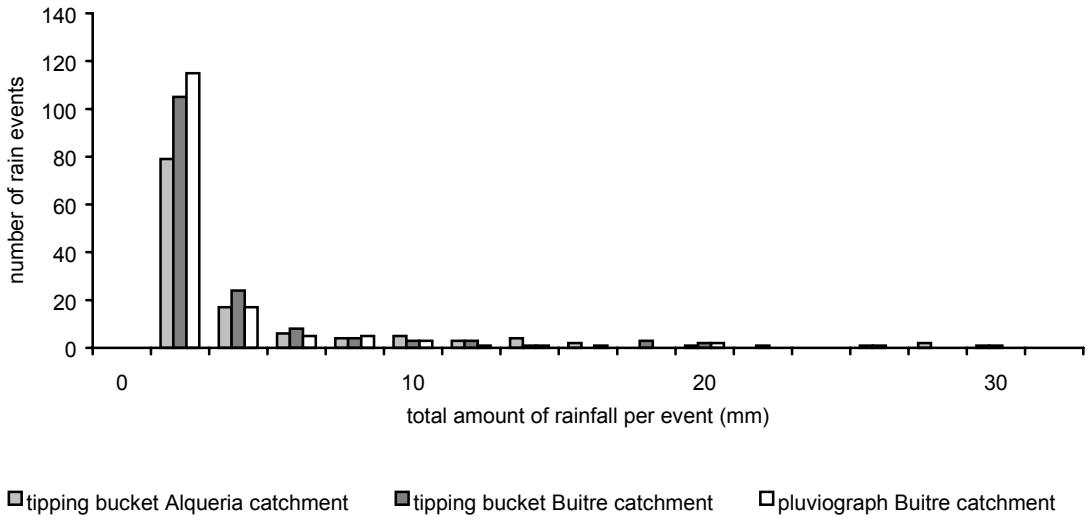

Figure 4.2 Rainfall events monitored during the study period; 1995-1998.

The majority of the recorded rainfall events are small and events with large amounts of rainfall (figure 4.2) have a large recurrence interval, giving a log-normal distribution. It should be noted that during the measurement period no extreme, violent event occurred. The lack of these extreme events hampers the definition of a REA for this area and the development of a representative runoff model.

4.4 Storm duration and rainfall intensity

To analyse the influence of storm duration and rainfall intensity on the amount of discharge in catchments smaller than a REA (i.e. all subcatchments of Buitre and Alquería), these rainfall characteristics were estimated during the study period.

- *Storm duration*

The recordings of the storm duration (table 4.3) show continuous rain for 24 hours was never recorded.

Table 4.3 Descriptive statistics of storm duration recorded during the study period.

Location	Number of rain events	Mean storm duration (min)	Median storm duration (min)	Minimum duration (min)	Maximum duration (min)
Tippingbucket Alquería catchment	125	82	46	6	995
Tipping bucket Buitre catchment	157	73	44	4	590
Pluviograph Buitre catchment	150	88	37	3	950

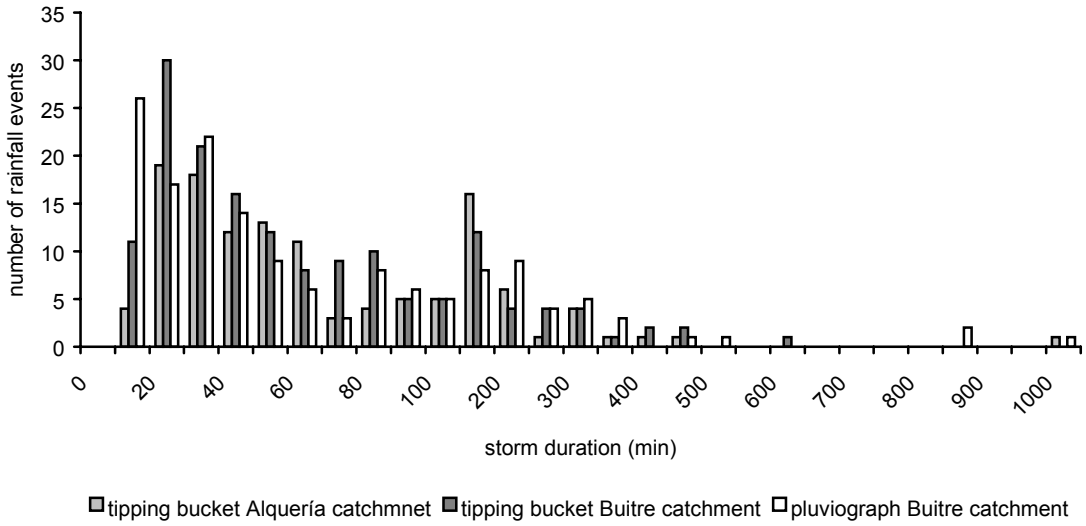

Figure 4.3 Storm duration recorded during study period; 1995-1998, note the non-linearity of the x-axis.

To study the surface runoff of the study area, rainfall should be analysed on event basis and not based on daily or monthly rainfall because this way the rainfall intensity will be underestimated. In the study area most rain falls in a short period (within 37 - 46 minutes, fig. 4.3) which is typical for rainfall in the semi-arid Mediterranean region.

- *Rainfall intensities*

To compare the rainfall intensities obtained from the different recording instruments, they were all standarized as rainfall intensity measured over 10 minutes.

Table 4.4 Descriptive statistics of the maximum rainfall intensity recorded during the study period.

Location	Number of rain events	Mean value of recorded maximum intensity (mm/h)	Median of maximum intensity (mm/h))	Minimum value of recorded maximum intensity (mm/h)	Maximum value of recorded maximum intensity (mm/h)
Tippingbucket Alquería catchment	125	12.4	4.8	1.2	120.0
Tipping bucket Buitre catchment	157	7.5	3.2	1.3	86.0
Pluviograph Buitre catchment	150	3.6	1.1	0.1	65.8

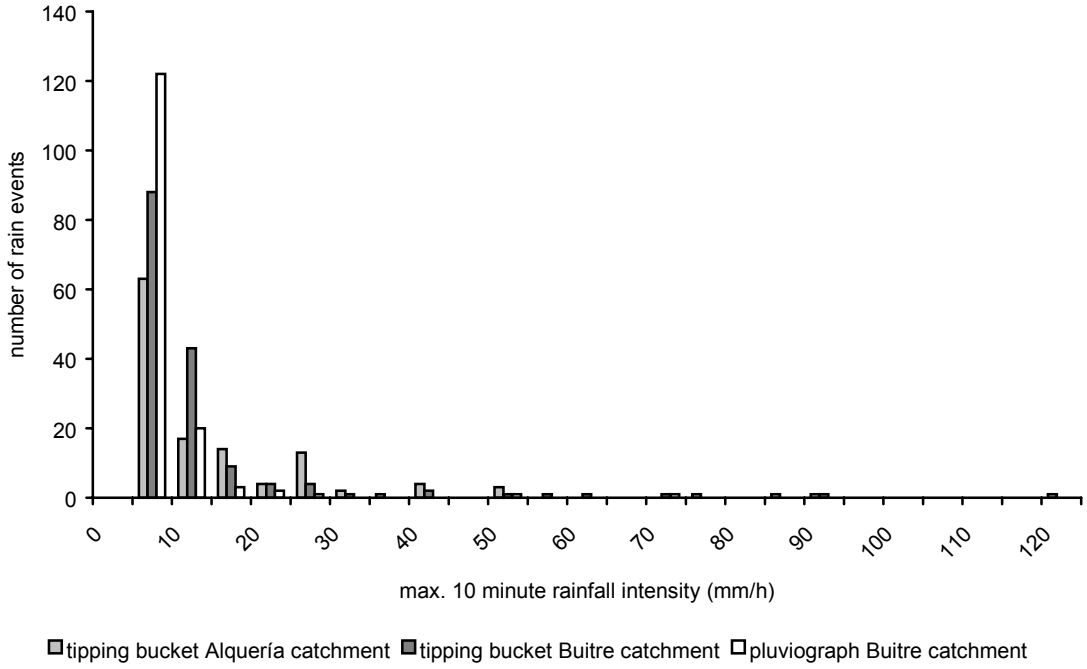

Figure 4.4 Maximum rainfall intensity recorded during the study period; 1995-1998.

The maximum rainfall intensity recorded during the study period was low, varying with maxima of 1.1 - 4.8 mm/h depending on the type and location of the recording instrument (table 4.4). Rainfall events with a maximum intensity that exceed 25 mm/h are rare (figure 4.4)

- *Threshold conditions for runoff generation in the Buitre catchment*

As previously mentioned storm duration and rainfall intensity control runoff (De Ploey et al., 1991; Poesen & Hooke, 1997). The log-normal distribution of the number of rainfall recordings with a long storm duration or with a large maximum intensity explains why the discharge in the semi-arid Mediterranean region is ephemeral.

An increase of the rainfall duration and/or rainfall intensity will result in an increase of the length of the contributing area. To analyse the influence of storm duration and rainfall intensity on the occurrence of discharge in the study area, the discharge measurements made in the first, second and third order catchments in the study area (described in chapter 6) were used. The relation between storm duration and rainfall intensity leading to discharge was calibrated for the Buitre catchment. For the rainfall recordings in the Buitre catchment, the maximum rainfall intensity, as measured during the event, was plotted on a logarithmic scale against the event's duration (figure 4.5).

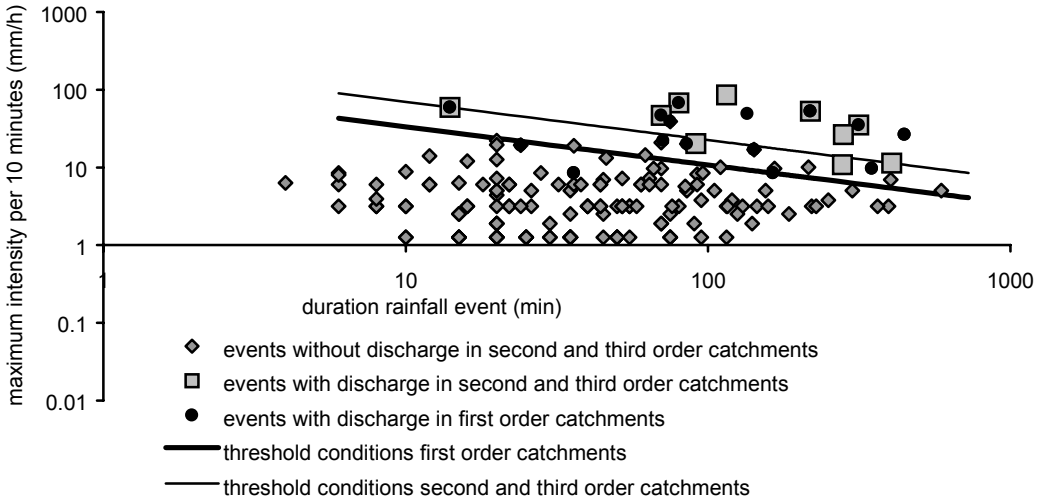

Figure 4.5 Maximum intensity and duration of total event as monitored by the tipping bucket (January 1995 – June 1998) in the Buitre catchment (Bt, B1, B2, B7, B8, B9).

This graph shows that a threshold condition exists above which discharge was generated. The combination of maximum rainfall intensity and duration of the event according to the power-law equation 4.1 determine this threshold condition for runoff in first order catchments, equation 4.2 determines the threshold condition for second and third order catchments;

$Log\ I_{max} = -0.491 * log\ d + 2.01$ *equation 4.1*

$Log\ I_{max} = -0.491 * log\ d + 2.51$ *equation 4.2*

in which:

I_{max} : is the maximum rainfall intensity (mm/h) as measured in a 10 minutes interval

d : is the duration of the total rainfall event (minutes)

When the critical combination of rainfall intensity and duration is exceeded, it is almost certain that discharge occurs in the channels of the catchments. The incorporation of storm duration in the threshold equations confirms that the storm duration of rainfall controls the survival length of the flow.

- *Validation of threshold equation in the Alquería catchment*

The threshold function for second and third order catchments (equation 4.2) was also applied to the rainfall data measured in the Alquería catchment (figure 4.6) to investigate whether the function is also valid for other semi-arid Mediterranean regions having the same characteristics. Although the rainfall events causing discharge in the second order Alquería catchments are all located above the threshold function, there were also rainfall events for which the second order stream channels did not flow. It seems likely that the occurrence of discharge in the Alqueria catchment not only depends on a combination of maximum rainfall intensity and duration of the rainfall event but also on other factors that have not been considered in this section, for example the vegetation cover in the near-channel areas.

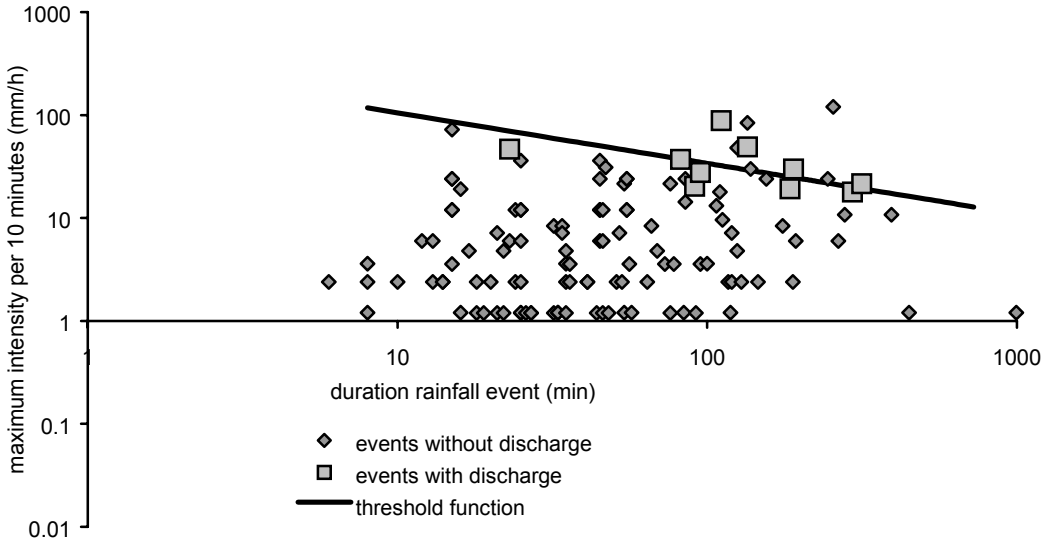

Figure 4.6 Maximum intensity and duration of total events as monitored by the tipping bucket (March 1996 – September 1998) in the Alquería catchment (A2, A5).

Applying equation 4.2 to the rainfall recordings of the Buitre and Alquería catchment suggests that for this study area the magnitude of the discharge (i.e. the peak discharge) is mainly controlled by storm duration and maximum rain intensity. For combinations of storm duration and maximum intensity that exceed the threshold intensity as calculated by equation 4.2 the channels of second and third order catchments will flow in most cases.

Scoging (1989 based on Lavee, 1985) reports a threshold for the rainfall characteristics of 45 minutes duration with an intensity of 9 mm/h for 90 m flow length on a hill slope in an arid environment. In the Alquería catchment, Imeson et

al. (1999) showed that with a minimum rainfall intensity of 6 mm/h and a rainfall amount of 5 mm, the individual bare areas between sparse patches of *Stipa tenacissima* on a hill slope, are connected. However, according to equation 4.1, these circumstances will almost certainly not result in runoff for the first order catchments. Imeson et al. (1999) also stated that on hill slopes with a relatively denser cover of *Stipa tenacissima* in the Alquería catchment, a larger rainfall amount i.e. at least 20 mm with a rainfall intensity of 6 mm/h, was needed to connect the individual bare areas. According equations 4.1 and 4.2, under these circumstances the all catchments will generate runoff.

In order to study discharge in the selected catchments it is only necessary to use combinations of rainfall intensity and storm duration to find which events yield runoff. Furthermore, if these functions relating the maximum rainfall intensity, the rainfall duration and the runoff occurrence can be established for larger catchments, they can be used for hazard assessment and early warning systems for flash floods when the rainfall conditions can be predicted for example by use of satellite images (Kniveton et al., 2000) or groundbased radar systems.

4.5 Spatial variability of rainfall estimated by pluviometers

For the assessment of the spatial variability of rain within the two studied catchments, the rainfall was monitored on an event basis from January 1996 until September 1998. The total volume of rainfall was measured with pluviometers (rain gauges) as described by Linacre (1992).

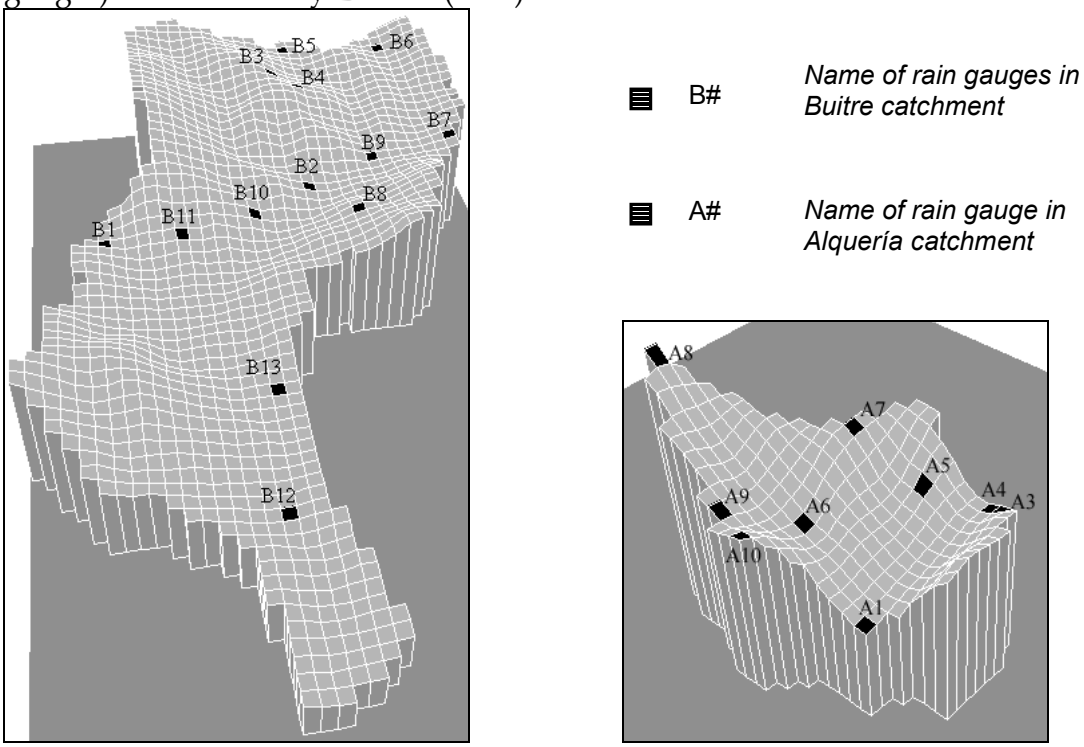

Figure 4.7 Location of pluviometers in Buitre catchment (left) and Alquería catchment (right).

He states that elevated gauges catch less rain than those located at ground level because the wind is stronger away from the ground. Nevertheless, for practical purposes the pluviometers were installed in the field within PVC tubes having a height of 50 cm and a slightly smaller diameter than the funnel.

In the research area 23 collectors were installed at randomly chosen locations, with diameters between 112 mm and 140 mm connected to containers of 2 liters. 13 Pluviometers were placed in the Buitre catchment and 10 pluviometers were placed in the Alquería (figure 4.7 and table 4.5).

Table 4.5 Geographical location of rain gauges B in the Buitre catchment and A in the Alquería catchment, 1) indicates the tipping bucket location before 15 April 1998 and 2) indicates its position after 15 April 1998.

Rain gauge	Location Longitude (UTM)	Latitude (UTM)	Altitude (m above sea level)	Aspect (degrees from North)
B1	600940	4181780	657	107.5
B2	600640	4182360	658	1.2
B3	600270	4182266	751	97
B4	600318	4182410	733	201
B5	600080	4182390	718.5	42
B6	600030	4182610	722	109
B7	600500	4182740	696	94.5
B8	600780	4182460	689	238
B9	600480	4182540	673	108.5
B10	600720	4182220	655	22
B11	600865	4182100	640	83
B12	601550	4182160	580	151.5
B13	601240	4182230	607	97
Tipping bucket1) Buitre	600080	4182360	721	11
Tipping bucket2) Buitre	600570	4182315	669	110
A1	603140	4182880	616	231
A2	603110	4182740	638.9	12
A3	603480	4182820	642.2	356
A4	603480	4182870	635.8	269
A5	603400	4182980	641	253
A6	603210	4183100	639	191
A7	603380	4183140	676	277
A8	603170	4183440	724.6	172
A9	603080	4183180	656	116
A10	603040	4183100	670.9	166
Tipping bucket Alquería	603140	4182880	616	231

For 21 events, the mean precipitation of the study area was calculated using both pluviometers within the Buitre and the Alquería catchments. The normalized deviations from the mean precipitation of all rain gauges were also calculated as well as the 95% confidence interval. Because of time and logistic constrains more than 23 pluviometers in the two catchments could not be installed.

The results were used to map the spatial distribution of rainfall in the study area. These maps have a form suitable for use in the distributed hydrological model.

4.6 *Variability of precipitation between the studied catchments*

The rainfall amounts of the Buitre and the Alquería catchments, the rainfall amounts measured by the pluviometers and the continuous rainfall recordings of the tipping buckets were analysed and compared. The total rainfall amounts recorded by the tipping bucket show the absence of a relation between the two catchments. For larger rainfall amounts the difference between the rainfall amount in the Buitre and the Alquería catchments is larger (figure 4.8).

The rainfall amounts of the 21 events recorded by pluviometers in the Buitre and Alquería catchment, were statistically analysed. The rainfall amounts were normally distributed. For 14 of the total of 21 events, the average values of the recorded rainfall amounts of the Buitre catchment differed from the means of the recorded rainfall amount of the Alquería catchment (t-test for independent samples, $p<0.05$). To also test if the shape of the distribution of the rainfall amounts differed between the two catchments, the Kolmogorov-Smirnov test was used. It appeared that during 13 of the 21 events the rainfall amounts in the Buitre catchment were significantly ($p<0.05$) differently distributed from the rainfall amounts in the Alquería catchment.

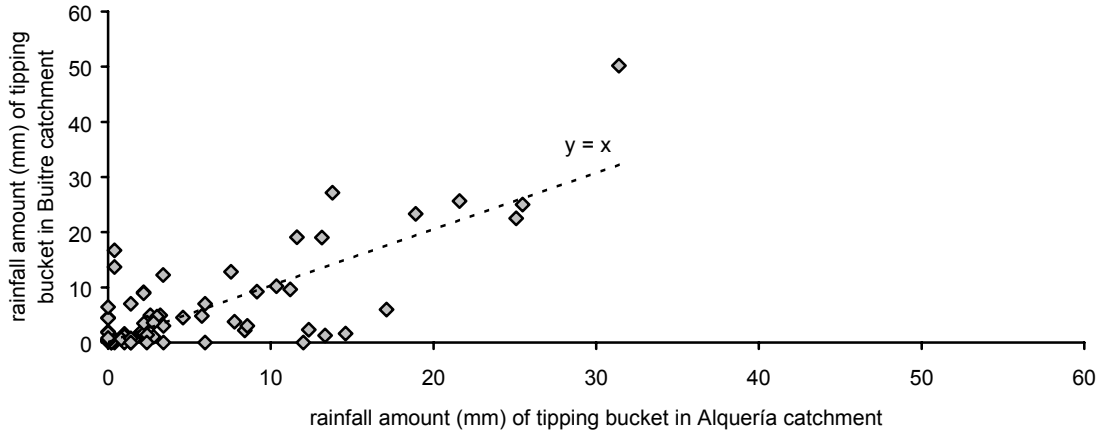

Figure 4.8 Rainfall amounts of 72 events recorded by tipping buckets in the Buitre catchment and the Alquería catchment.

The results of the pluviometer recordings show that the differences in rainfall recorded by the tipping bucket between in the Buitre and Alquería catchments are larger than the spatial variability of rainfall within the studied catchments. The rainfall amounts of the two catchments recorded by tipping buckets also indicate the difference in recorded rainfall. Therefore rainfall measurements in one of the studied catchments cannot be used for analysis in the other catchment, especially because the differences are largest for rainfall events that cause runoff: these events will be used for further rainfall analysis.

4.7 *Spatial variabililty of precipitation within the studied catchments*

It was examined if the spatial variability of rainfall could be explained by the topography of the study area. The spatial variability of frontal and convective rainfall that results in heavy, short thunderstorms is assumed to be influenced by the aspect (wind- or lee-ward side of hill slope) of the rainfall recordings, due to orographic influence (Boer & Puigdefabregas, 1995). Long lasting showers often originate from low hanging clouds. For this reason it would be plausible to suppose that the spatial variability of these long lasting drizzling events is influenced by the altitude of the rainfall recordings in the terrain.

Before further analysis, the recordings of pluviometer B13 and A2 were removed from the data set because of their deviation from the rest of the data caused by local wind conditions.

By multiple regression, for every rain event the correlation coefficients were calculated between the deviation from the mean precipitation recorded with the pluviometers and respectively the altitude and aspect. To obtain proper results and to correct for adjacent aspect angles of 0° and 359°, the multiple regression was carried out with the altitude and the sine transformed aspect and subsequently with the altitude and cosine transformed aspect as independent variables. The deviations from the mean precipitation were significantly influenced by altitude when estimated the p-level was under 0.05 and for aspect when the p-level was under 0.05 for the sine or cosine of the aspect.

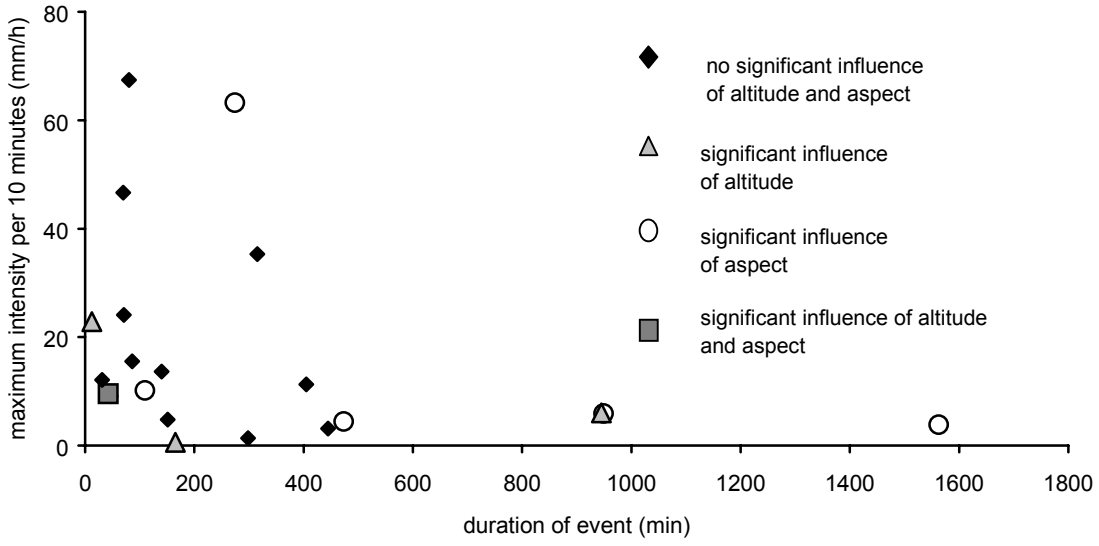

Figure 4.9 The relation between different types of rainfall events and altitude and aspect for the Buitre catchment.

The results of the statistical analysis do not support the assumed relations with topography and orographic impact as pointed out at the beginning of this section. Both for the Buitre (figure 4.9) and the Alquería catchment (figure 4.10), the number of rainfall events was limited to 21 and the number of significant relations between

rainfall amount and altitude or aspect was low (maximum 4). No clear distinction could be made between the type of rainfall event and the influence of topography within the Buitre or Alquería catchment.

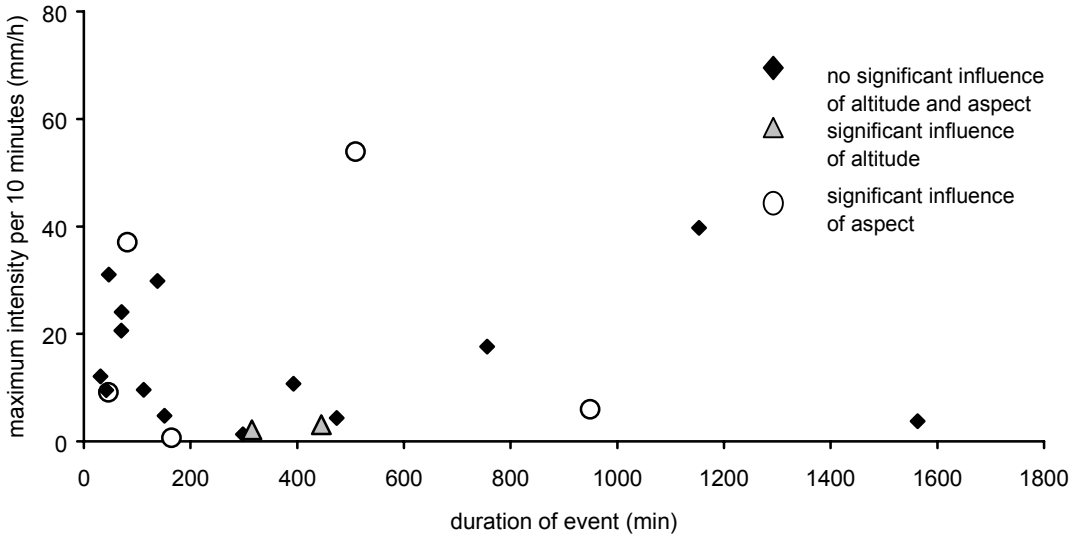

Figure 4.10 The relation between different types of rainfall events and altitude respectively aspect for the Alquería catchment.

The spatial variability of the rainfall could not be explained by the topography because the above described results show that neither altitude nor aspect form a good basis to interpolate the rainfall amounts over the study area. To fulfil the need to incorporate the spatial variability of rainfall in discharge modelling, the pluviometer recordings were used on basis of which the mean amount of rainfall was calculated for every event. Subsequently for every pluviometer location, the deviation of the mean rainfall was calculated and expressed as the fraction of the mean rainfall. After this procedure was carried out for all events, for every pluviometer location the average deviation of the mean precipitation was estimated as well as the standard error. This way the spatial distribution of rainfall amounts in the study area becomes clear.

Figures 4.11 and 4.12 present the standardised rainfall anomalies for the Buitre and Alquería catchments. In spite of the range of values, very little spatial correlation was observed in the Buitre catchment (figure 4.11) or in the Alquería catchment (figure 4.12)

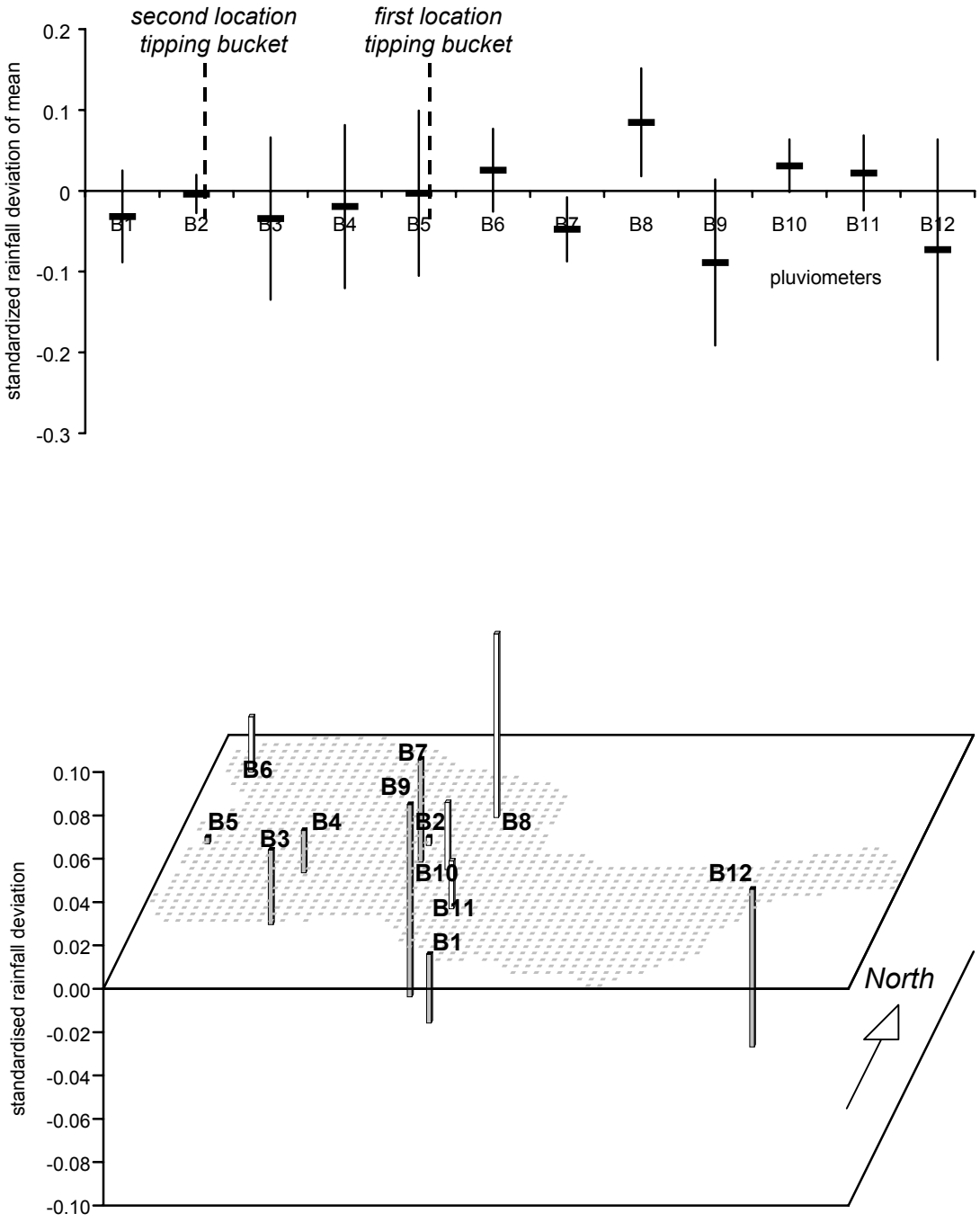

Figure 4.11 Standardised rainfall deviation and its standard error (upper graph) and its spatial distribution (lowest graph) in the Buitre catchment.

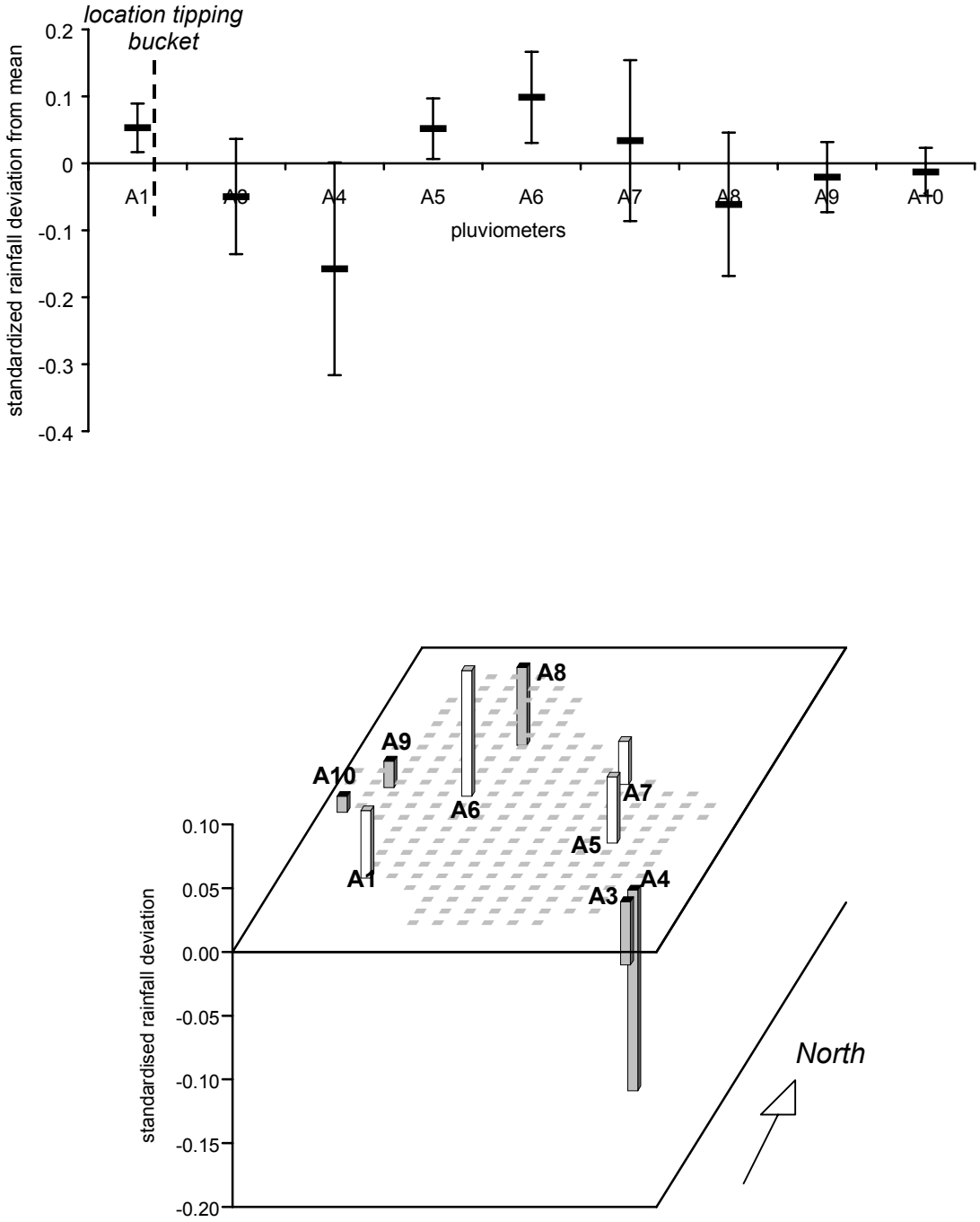

Figure 4.12 Standardised rainfall deviation and its standard error (upper graph) and its spatial distribution (lowest graph) in the Alquería catchment.

Based on the spatial distribution of the rainfall amounts in the Buitre and Alquería catchments, the rainfall recordings of the tipping buckets can be interpolated over the catchments. Not enough measurement locations were available to compute a variogram and hence kriging could not be used to interpolate the rainfall recordings. Because no significant influence of topography on the rainfall amounts could be

proved, it was not possible to use elevation as aid for geostatistical mapping of rainfall (Goovaerts, 1999). Therefor simple inverse distance interpolation was applied to estimate the spatial distribution of rainfall on the selected catchments Buitre and Alquería (figure 4.13)

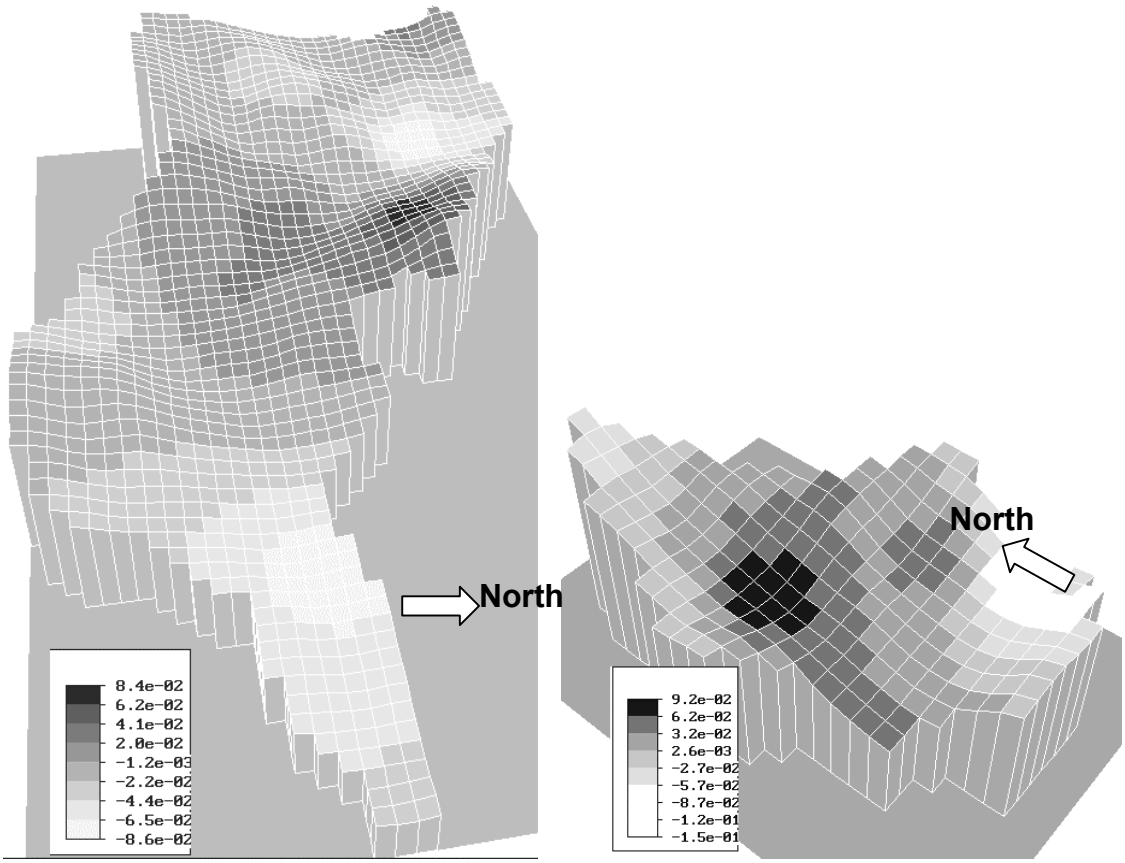

Figure 4.13 Estimated fraction of spatially distributed rainfall amount in the Buitre catchment (left) and the Alquería catchment (right).

4.8 Quality of the rainfall data

The resolution the rainfall measurements by the tipping buckets and the pluviograph has been discussed in section 4.2. The pluviograph recordings had such a bad time resolution that a large error originated in the estimation of the rainfall duration. The data of the pluviograph were only used for events for which no other continuous rainfall data were available.

To evaluate the quality of the rainfall recordings, the pluviometer recordings were compared with the continuous recordings of the pluviograph and the tipping buckets (figure 4.14). Despite the bad temporal resolution of the pluviograph, the recordings did not show a deviation from the rainfall amount measured by the pluviometers (R^2=0.92). For almost all rainfall events, the total amount recorded by the tipping bucket fell within the range of rainfall amounts measured by the

pluviometers (R^2=0.95 for the Buitre catchment and 0.99 for the Alquería catchment). For the events for which the tipping bucket recordings fell outside the range, the local wind circulations might have caused this deviation. Based on these results, it was concluded that the pluviometer measurements were reliable.

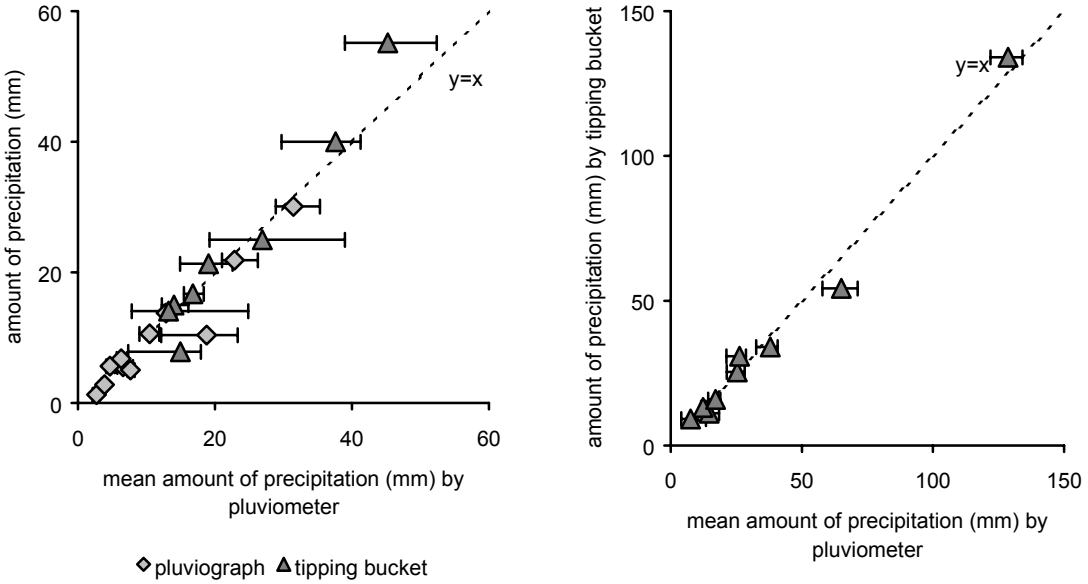

Figure 4.14 Amount of rainfall recorded by different methods for the Buitre catchment (left) and the Alquería catchment (right). The error bars indicate the range of the rainfall amounts measured by the pluviometers.

4.9 Discussion and Conclusions

Detailed rainfall data is required for the analysis of discharge in the channels of the selected catchments. Furthermore it serves as input for a discharge model (chapter 8). Based on former studies (as discussed in section 4.1) three rainfall characteristics were selected for analysis in this study; rainfall amount, rainfall intensity and rainfall duration. Additionally the spatial distribution of the amount of rainfall was studied because of its importance in controlling the spatial distribution of the discharge production.

- *Rainfall amount, intensity and duration*

Most rainfall events in the study area consist of small amounts, last a short period and have low intensities. Scoging (1989) found that 80% of the rainstorms in southern Spain last less than 30 minutes. In the study area 77% of the rainstorms lasted less than 100 minutes. These short-lasting rainfall events make it essential to record rainfall recording with a detailed temporal resolution. The frequency of the rainfall amounts is logarithmically distributed. Former studies in the Guadalentín Basin (López Bermúdez, 1971; Navarro Hervás, 1991) also show that events

consisting of extremely large amounts occur rarely and therefore have a large recurrence interval.

In this study the rainfall was recorded continuously so that the rainfall amount, its intensity and duration were known for every event. In other runoff analysis and hydrological models (Ahnert, 1987; de Ploey et al., 1991; de Jong et al, 1999) daily totals of rainfall amounts were used after which these amounts were transformed to rainfall intensities per day. The short duration of the recorded events in this study indicates that rainfall intensities derived from rainfall amounts per day lead to a serious underestimation of the rainfall intensity in the study area. In this chapter the rainfall intensities were recalculated to 10 minute intervals. This time interval was regarded as large. Imeson et al. (1999) recorded a total of only 7 hours of overland flow in 1.5 years, which indicates the short duration of the discharge in the channels of the study area. The median storm duration in the study area was found to be about 45 minutes. Scoging (1989) even found 80% of the rainfall to last less than 30 minutes in southern Spain. For this reason a small time interval for rainfall recording in a semi-arid environment is preferred. The temporal resolution of the rainfall recordings should be as small as logistically possible when the rainfall is used as input for a dynamic discharge model. Although extreme rainfall conditions of large successive rainfall events with a large recurrence interval known to occur, unfortunately these events were not recorded during the measurement period. This hampers the definition of a REA and the development of a distributed discharge model in the study area.

- *Threshold rainfall conditions for runoff*

To determine the occurrence of discharge in second and third order catchments in the study area, a threshold equation was defined based on the combination of storm duration of the rainfall event and maximum rainfall intensity per 10 minutes. This implies that the peak discharge in the studied catchments is influenced by the combination of rainfall characteristics (the storm duration and maximum rainfall intensity of the rainfall event). The threshold equations (equation 4.1 and 4.2) define those rainfall conditions that are threshold conditions that lead to runoff connection of bare surfaces within patched vegetation on a hill slope and of streambed parts by which runoff reaches the outlet of the catchment.

- *Spatial variability of rainfall*

Due to the spatial variability of rainfall in the study area, the rainfall events of the Buitre catchment could not be compared with the rainfall events in the Alquería catchment. This large spatial variability of rainfall in the study area is also known from other studies (Bull et al., 1999). Published results from other studies (Pérez Pujalte, 1993; Boer & Puidgdefabregas, 1995; Boer, 1999) have shown that relations between topography and rainfall amounts in the Guadalentín Basin hold for a larger region than the study area. The spatial distribution of rainfall in the study area had a pattern that was not related to topographic features such as aspect and altitude. The spatial pattern had a relative small standard error of the standardised rainfall

deviations. The spatial invariance of rainfall implies that as far as rainfall variability is concerned, the REA-concept can be applied in the study area. The absence of spatial correlation in rainfall was also experienced by Thornes (1994), who found a poor correlation of rainfall amounts over distances of 5 km. Despite the absence of spatial correlation of the rainfall in the study area, the small standard error indicates its importance.

Inverse distance interpolation was used to interpolate the rainfall based on the measurements of the pluviometers. These kind of interpolation methods are questioned by Lopes (1996) who concluded that the spatial rainfall distribution was not correctly described by these methods for computational elements that are required as input of a distributed discharge model. He based his conclusions on differences in modelled runoff response caused by the exclusion of one or more raingauges. Lopes used 10 rainfall gauges in a catchment of 673 ha for his rainfall recordings. I considered the inverse distance method to be a proper and acceptable method because the installed raingauge network was denser, the studied catchments were smaller, the results are based on more events (23) and the standard error of the mean rainfall deviation for all pluviometer locations was small (<15%).

- *Rainfall as input of distributed discharge model*

The results of this chapter underline the need to incorporate the following in the hydrological response model;

- Only rainfall data that exceed the threshold function of equation 4.1 for the occurrence of discharge in catchments B7, B8 and B9 and equation 4.2 for the occurrence of discharge in catchments A2 A5, B1, B2 and Bt, will be used as input data for the model simulations in these catchments because events that do not produce discharge are not interesting for runoff modelling.
- The time steps of the discharge model need to be equal or smaller to the time interval of the rainfall recordings.
- The spatially distributed rainfall in the study area was established by inverse distance interpolation of the precipitation measurements of the pluviometer locations.

5 Infiltration

5.1 Introduction

The infiltration characteristics of the soil are an important component of the hydrological conditions in small catchments. They are one of the components of the water balance and are necessary to describe the runoff response by a runoff model as outlined in section 1.7. The semi-arid Mediterranean environment is characterized by torrential rainfall altered by periods of drought. Under these conditions the soil is dry before the rainfall starts and is not saturated during the rainfall event. For this reason the runoff is almost always Hortonian which means that the infiltration capacity of the soil is less than the rainfall intensity.

The infiltration rate depends of the hydraulic conductivity of the soil. The hydraulic conductivity K depends on the soil moisture content of the soil, which changes during the infiltration process. Only when the soil is saturated does the hydraulic conductivity become constant; the saturated hydraulic conductivity K_s. The saturated hydraulic conductivity is a property, which can easily be measured in the field and enables the researcher to collect a large amount of data in a relatively short period and to compare different types of soils with varying moisture content. This property was therefore estimated in the study area and used to describe the infiltration process.

Certain studies (Woolhiser et al., 1996; Merz & Plate, 1997; Cerdà, 1997b) suggest that the redistribution of texture along a hill slope due to surface processes like sheet flow, might influence K_s. Various authors (Lyford & Quashu, 1969; Pilgrim et al., 1988; Seyfried & Wilcox, 1995, Fitzjohn et al., 1998; Imeson et al., 1999) describe the differences in infiltration under vegetation and interplant areas, estimated at plot scale. Generally, infiltration rates increase under vegetation compared to interplant areas. This is caused by the difference of the organic material, micro-topography, bulk density, aggregate stability and penetration resistance underneath plants from these in bare soil between plants (Bochet, 1996).

Vegetation is also known to influence the infiltration rate over larger areas. Francis, 1990; Sullivan et al., 1996; Cerdà, 1997b; Gonzáles del Tanago et al., 1998; Cerdà et al., 1998 discuss the effect of land cover on the infiltration. Bare soil is known to have a smaller infiltration rate than vegetated areas (Francis, 1990; Cerdà, 1997b). Woodland is known to have a larger infiltration capacity than grassland and afforestation reduces the infiltration capacity significantly (Gonzáles del Tanago et al., 1998).

Infiltration is a complex process that varies for every event and it is difficult to achieve proper estimates that cover the whole study area in time and space. Nevertheless, because of the aim to construct a spatial-temporal response model, I hoped to be able to map variations in the infiltration capacity over the area. In the study area, the saturated hydraulic conductivity K_s was measured at many locations to quantify the infiltration process.

5.2 *Estimation of the saturated hydraulic conductivity*

The saturated hydraulic conductivity of the soil was estimated by the inverse auger hole method. The procedure is as follows; first a hole with radius r (cm) and depth D (cm) is augered. The hole is prewetted for 30 minutes during which it is filled with water and the head of the water level is kept constant. After 30 minutes the walls of the hole are assumed to be saturated with water and the fall of the head is measured. Subsequently, the quantity of water infiltrated under saturated conditions is measured based on Darcy's law, using equation 5.1 (Kessler & Oosterbaan, 1974).

$$Q(t_i) = -\pi r^2 * dh/dt = K_s Area(t_i) = 2K_s \pi r (h(t_i) + r/2) \qquad \text{equation 5.1}$$

in which
$Q(t_i)$: quantity of infiltrated water (mm^3)
r : radius of auger hole (mm)
t_i : elapsed time at moment i (s)
h : water level in hole (mm)
K_s : saturated hydraulic conductivity (mm/s)
$Area(t_i)$: surface over which the water infiltrates into the soil at time t_i (mm^2)

Rearranging equation 5.1 yields the saturated hydraulic conductivity (equation 5.2).

$$K_s = r/2 \{[ln(h(t_1) + r/2) - ln(h(t_2)+r/2)] / (t_2-t_1)\} \qquad \text{equation 5.2}$$

Under saturated conditions, the relation between $log(h(t)+r/2)$ and elapsed time is linear, so the saturated hydraulic conductivity is estimated by linear regression through the measurement points.

5.3 *Spatial variability of the saturated hydraulic conductivity*

5.3.1 Strategy for mapping K_s

As outlined in section 1.7, I intend to use a spatial hydrological model and therefore hope to be able to map the K_s over the study area. Bierkens & van der Gaast, 1998 discuss that it in a humid climate it is difficult to use the results of core measurements of K_s at local scale (10^2-10^3 m). This is mainly due to the large spatial variability of the K_s, which is a widely recognised problem (Williams & Bonell, 1988; Loague & Gander, 1990; Sullivan et al, 1996; Turcke & Kueper, 1996; Singh, 1997; Bierkens & van der Gaast; 1998). To overcome this problem geostatistical methods are sometimes used to characterise the infiltration variability at a local or catchment scale (10^2-10^3 m). However, these methods are based on a semivariogram model like kriging (Loague & Gander, 1990) or stochastic upscaling (Bierkens & van der Gaast, 1998), which assumes that the data are statistically stationary over the total study area or stationary over homogeneous classified units. Previous research in humid

areas has shown that the range of spatial correlation of K_s, as established by semivariograms, is often very small, ranging from. 4.8 to less than 20 meters, depending on the deposits (Loague & Gander, 1990; Turcke & Kueper, 1996; Corradini et al., 1998). The K_s estimates of point locations, by for example ring infiltrometer tests or inverse auger hole tests, have a larger spatial variability than the K_s estimates derived from continuous runoff recording at plots of 250 m^2 under ponding conditions (Williams & Bonell, 1988). Because the correlation range of the spatial variability of K_s point estimates is generally smaller than the size of these plots K_s cannot be mapped by interpolation. Although this conclusion is based on studies that were carried out in a more humid area than the semi-arid Mediterranean, it is asumed to be valid for the study area.

A possible alternative strategy for mapping K_s is to reduce the spatial variability by bulking (Williams & Bonell, 1988) and by using a possible relationship between K_s and environmental controls that vary over larger distances, like soil texture, topography and land cover (Wood et al., 1990; Loague & Gander, 1990; Sullivan et al., 1996).

5.3.2 Using proxies to map K_s

- *Texture and K_s*

Texture is known to influence the K_s. The texture can be redistributed by topography controlled surface processes like sheet flow, which might affect the K_s. To account for the influence of soil texture and topography, the sites of the K_s measurements in this study were selected to have different upstream slopelengths and parent material. At each K_s site soil texture was determined to see if a relation between the saturated conductivity and topography and/or texture could be established for the study area. The results are discussed in section 5.5.1.

- *Vegetation cover and K_s*

The locations of the K_s measurements were spread over the land cover types in the two selected catchments. These land cover types were described in section 3.9. Section 5.1 discusses the effect of vegetation on the infiltration rate at various levels of resolution. The K_s is known to vary between plant- and inter-plant areas and for this reason surface cover is assumed to control the K_s at a fine resolution.

Table 5.1 Measurement locations for saturated hydraulic conductivity within each land cover type.

	Land cover type			
Vegetation type (surface cover)	Shrub/woodland	Open grassland	Bare soil	Afforestated terraces
no vegetation	X	X	Lambregts (1999)	X
Pinus halepensis	X			X
Stipa tenacissima	X	X		

A measurement scheme was developed to see if it was possible to find a level of resolution at which spatial variation of K_s could be distinguished from noise. Therefore measurements (table 5.1) were made in various land cover types, both between and underneath vegetation.

- *Surface crusting and K_s*

Because the crust is destroyed by using the inverse auger hole method, this method does not account for the presence of surface crusting which commonly occurs on bare soil. Insight into this problem in the study area is given by data from Lambregts (1999). His measurement sites were not located inside the selected Alquería catchments but near enough to be representative for the environmental conditions of the Alquería catchments His measurements were carried out using the ring infiltrometer method (Chow et al., 1988). Although it is difficult to preserve the crust during the installation of the ring, these measurements will give a better estimation of the saturated conductivity than the measurements with the inverse auger hole method because by applying the inverse auger hole method the topsoil and the crust are removed for the experiment and with the ring infiltrometer the crust is left intact. When the ring infiltrometer test and the inverse auger hole method are applied at a surface with similar dimensions, the quality of the measurements will be similar. The differences in magnitude between the K_s measurements by use of ring infiltrometer method and the K_s measurements by use of the inverse auger hole method, will be discussed in section 5.7. The choice of the inverse auger hole method for the K_s measurements in all land cover types other than 'bare soil', is based on the simplicity of the method and because it does not take much time. This way it enables the researcher to make many measurements in a short period of time.

5.3.3 Locations of the K_s measurements

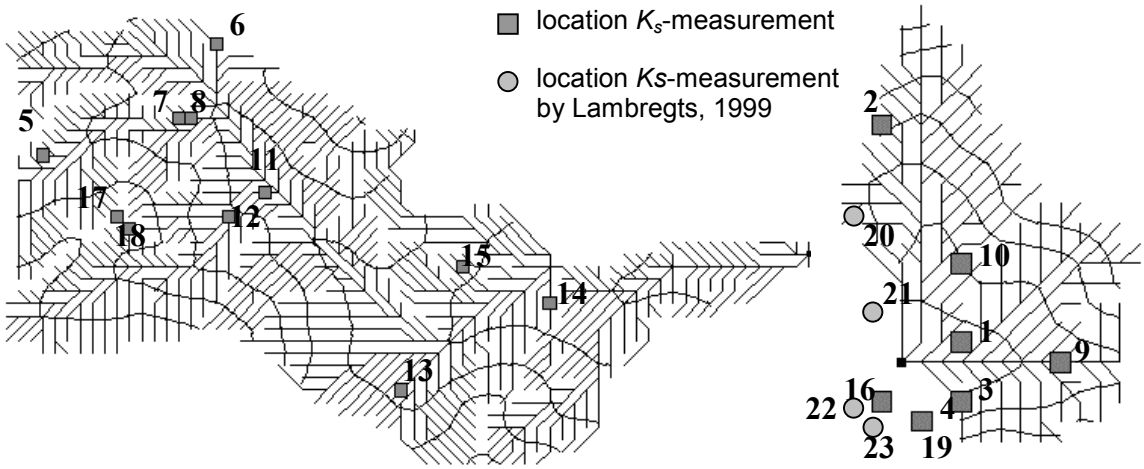

Figure 5.1 Locations of K_s measurements in a drainage network and contour lines of the Buitre catchment (left) and the Alquería catchment (right).

The measurements (table 5.1) were carried out in duplicate or triplicate to reduce the known large measurement error. In total 118 K_s measurements were done, spread over 19 different locations (figure 5.1) divided over the Buitre and Alquería catchments.

5.4 Results

5.4.1 Saturated hydraulic conductivity in the study area

The results of the field measurements by the inverse auger hole method are presented in table 5.2. The K_s estimates are log-normally distributed (figure 5.2) and show a large variability. For further analysis the log-transformed values of the K_s will be used. The K_s estimates varied strongly per site but also the total range of the estimates was large (figure 5.3).

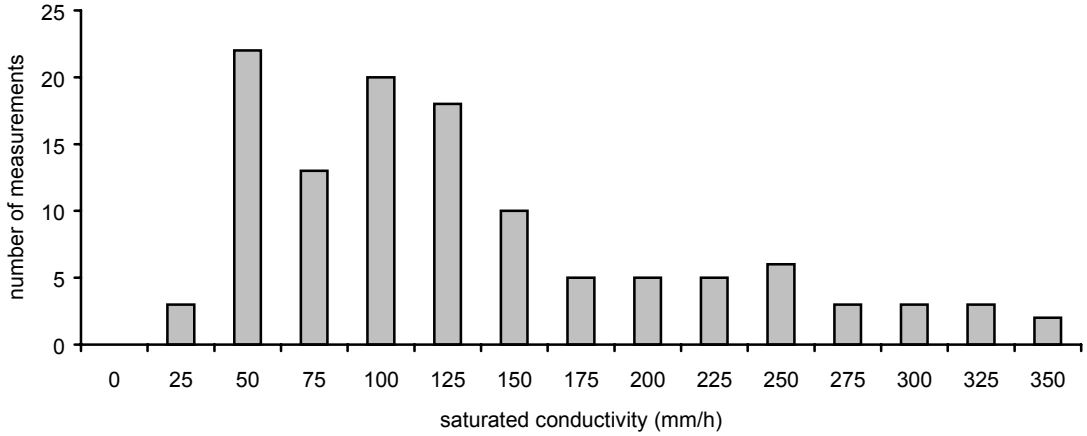

Figure 5.2 Saturated hydraulic conductivity estimates, measured in the study area.

Table 5.2 Descriptive statistics of saturated hydraulic conductivity estimates.

	Number of measurements	Mean	Median	Minimum	Maximum
K_s (mm/h)	118	121.6	103.8	18.4	345.8

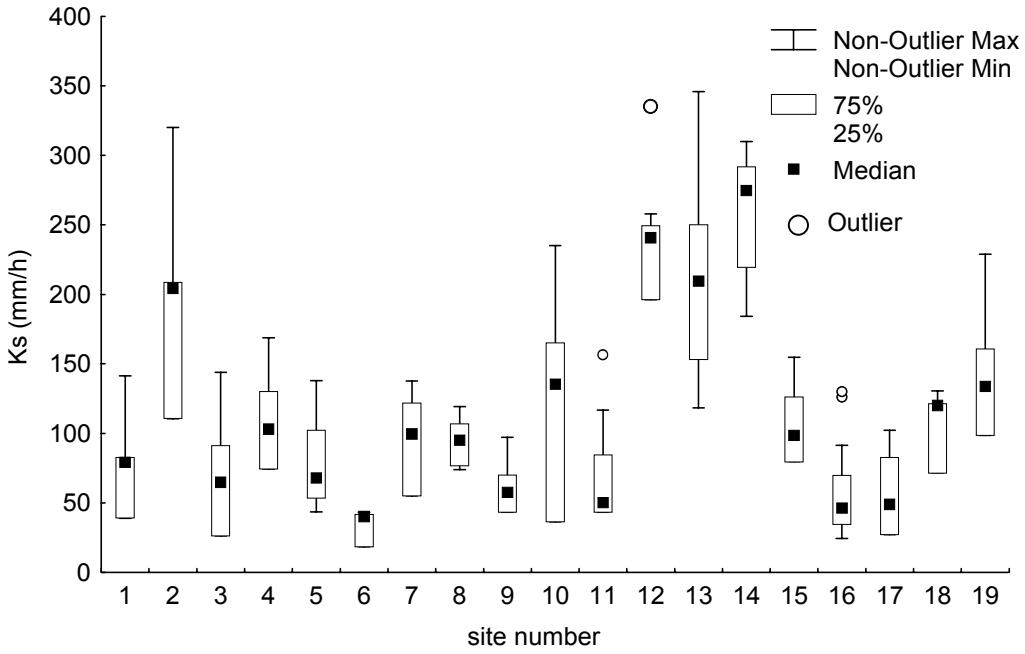

Figure 5.3 The saturated hydraulic conductivity estimates per site (based on 5 to 9 estimates per site), outliers (indicated by a circle) differ more than one standard deviation from the mean.

5.4.2 Spatial variability of the saturated hydraulic conductivity in the studied catchments

As discussed in section 5.3 I attempted to find a relation between K_s measurements and environmental controls like soil texture, topography, parent material and land cover. If such a relation exists, these controls can be used to map the K_s estimates over the research area.

- *Texture, topographic position and K_s*

No relation (explained variance < 0.05) was found between the soil texture at the site and saturated hydraulic conductivity (figure 5.4). Loague & Gander (1990) and Sullivan et al. (1996) explained their results by the absence of a relation between texture and Ks by limited variations in soil type, which are less than the variability of the saturated hydraulic conductivity.

The same explanation holds for my study area. A redistribution of texture along a hill slope might explain why a relation between K_s and slope length should exist (Woolhiser et al., 1996; Merz & Plate, 1997) but the absence of any relation between K_s and texture already indicates that a relation between K_s and slope length will be is absent as well.

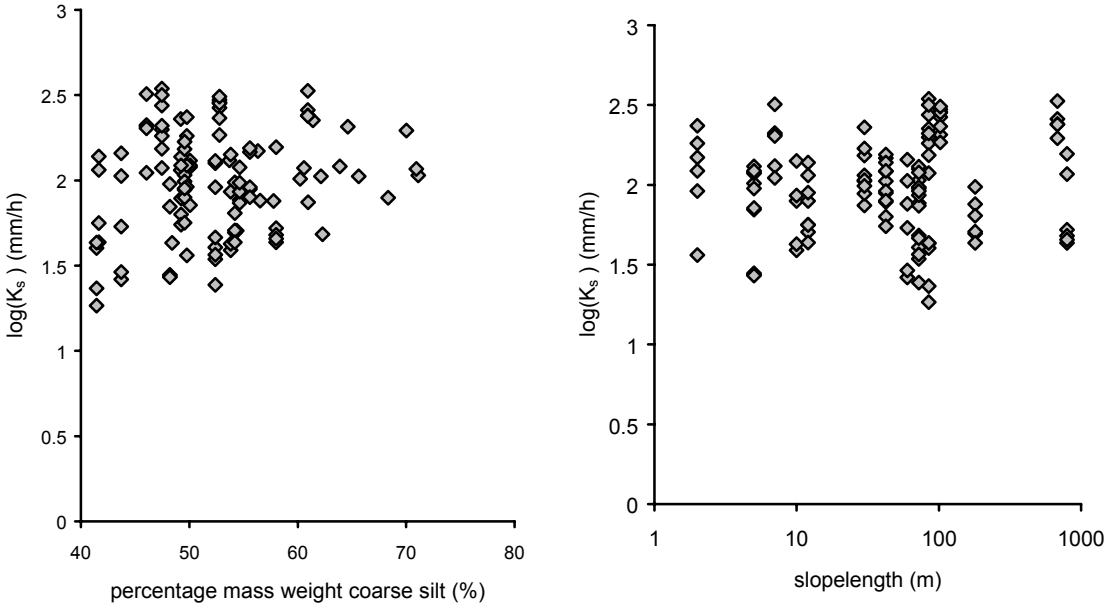

Figure 5.4 Logarithmic-transformed saturated hydraulic conductivity in relation to coarse silt texture class (60-20 μm) (left) and to the upstream slopelength (right). Of all texture classes the texture class coarse silt gave the best correlation (R^2<0.05) and the correlation between K_s and slopelength was smaller (R^2<0.01).

- *Parent material and K_s*

It was also examined if the K_s measurements could be divided into significant different classes based on the type of parent material.

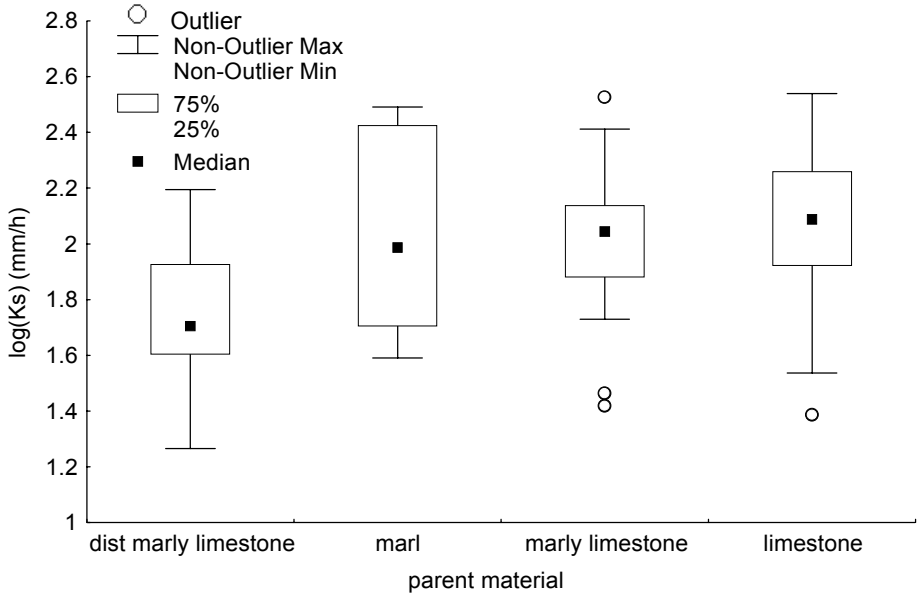

Figure 5.5 Box-Whisker plot of the logarithmic transformed saturated hydraulic conductivity for type of parent material; disturbed marly limestone (n=25), marl (n=19), limestone (n=48) and marly limestone (n=26), outliers (indicated by a circle) differ more than one standard deviation from the mean.

Parent material in the study area was classified as marl, limestone or marly limestone. Afforested areas were mainly on marly limestone that had been severely disturbed. For this reason this unit was classified apart from the other units, as 'disturbed marly limestone'. With non-parametric statistical testing (the Mann-Whitney U test and the Kolmogorov-Smirnov test) there were no significant differences in the log-transformed K_s measurements between parent material (figure 5.5) except for the log-transformed K_s measurements on the 'disturbed marly limestone' ($p<0.05$).

- *Land cover and K_s*

The infiltrometer estimates by Lambregts (1999) were added to the field estimates of the saturated conductivity for the land cover type 'bare soil'. The saturated conductivities of all land cover types differed significantly from each other, except for the saturated conductivity of grassland and natural woodland (figure 5.6). The results show that natural woodland has the largest saturated hydraulic conductivity. The smallest saturated conductivity was found on the 'bare soil'. The largest K_s-values were estimated in 'grassland' and 'natural woodland'.

With statistical non-parametric tests (Mann-Whitney U test for difference in means and Kolmogorov-Smirnov test for difference in means and distribution) significant differences in the log-transformed K_s estimates for the different types of land cover could be distinguished ($p<0.05$). However, it was not possible to distinguish the log-transformed K_s estimates on 'grassland' from 'natural woodland'.

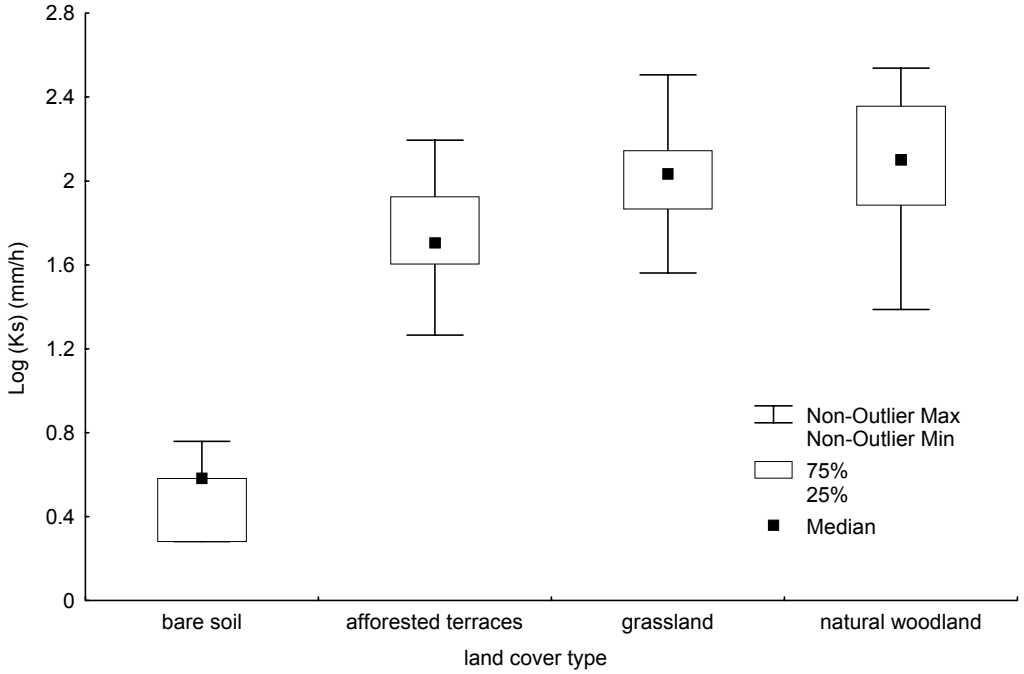

Figure 5.6 Box-Whisker plot of the logarithmic transformed saturated conductivity for different types of land cover; bare soil (n=7), afforested terraces (n=25), grassland (n=40) and natural woodland (n=53).

As discussed in chapter 2, the study area has a patchy vegetation cover, which means that at a fine resolution the vegetation cover consists of a alternating soil surfaces covered with vegetation and unvegetated soil surfaces. These locally unvegetated soil surfaces are classified differently from the large land cover units of 'bare soil' as explained in chapter 3.

To estimate the difference in K_s between vegetated soil surfaces and unvegetated soil surfaces at a fine resolution within the land cover units, the measurements were carried out according to the scheme in table 5.1.

Both parametric (t-test for independent samples) as non-parametric statistical tests (Mann-Whitney U test and Kolmogorov Smirnov test) showed that the log-transformed K_s under vegetation did not differ significantly ($p>0.05$) from interplant areas within the same land cover unit (figure 5.7). These results are in contrast with the results in other studies in comparable natural settings (Francis et al., 1986; Seyfried & Wilcox, 1995; Puigdefábregas et al., 1996; Imeson et al., 1999). The log-transformed *Ks* estimates underneath *Stipa tenacissima* were also not significantly different from the ones underneath *Pinus halepensis*.

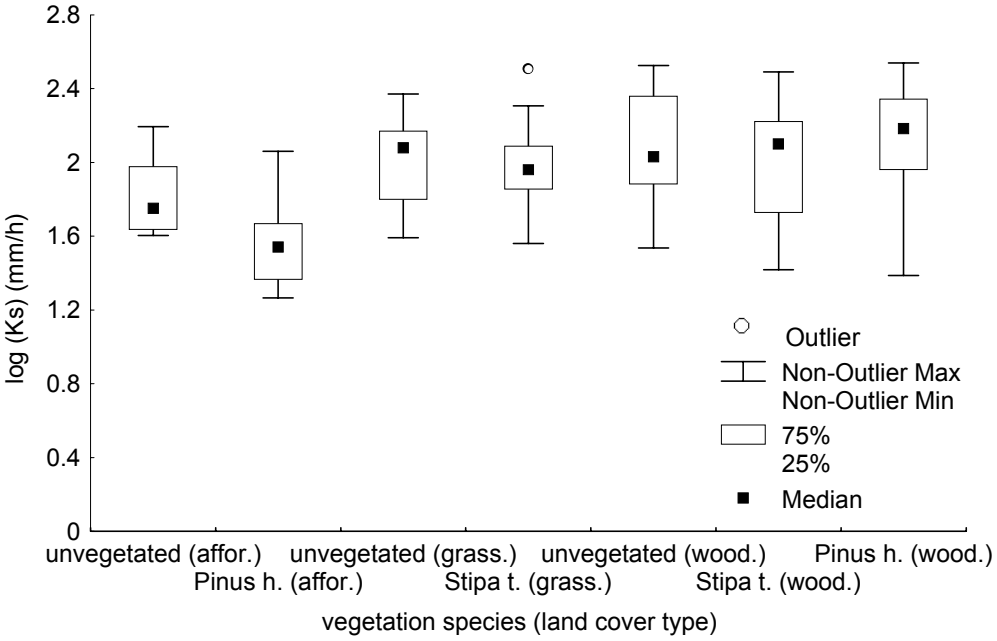

Figure 5.7 Box-Whisker plot of the log-transformed saturated conductivity for the dominant vegetation species in different types of land cover (excluding 'bare soil'); unvegetated on afforested terraces (n=15), Pinus halepensis on afforested terraces (n=10), unvegetated on grassland (n=21), Stipa tenacissima on grassland (n=19), unvegetated on natural woodland (n=23), Stipa tenacissima on natural woodland (13) and Pinus halepensis on natural woodland (n=17), outliers (indicated by a circle) differ more than one standard deviation from the mean.

Based on these results the vegetation cover at the plot scale does not seem to influence the K_s estimates. However for larger surfaces, the K_s estimates seemed to be related to a specific land cover type. For this reason the K_s was mapped over the

study area according the land cover types (figure 5.8). Between land cover type grassland and natural woodland no difference was found so the mean value of the total of K_s estimates was assigned to these two land cover types (table 5.3).

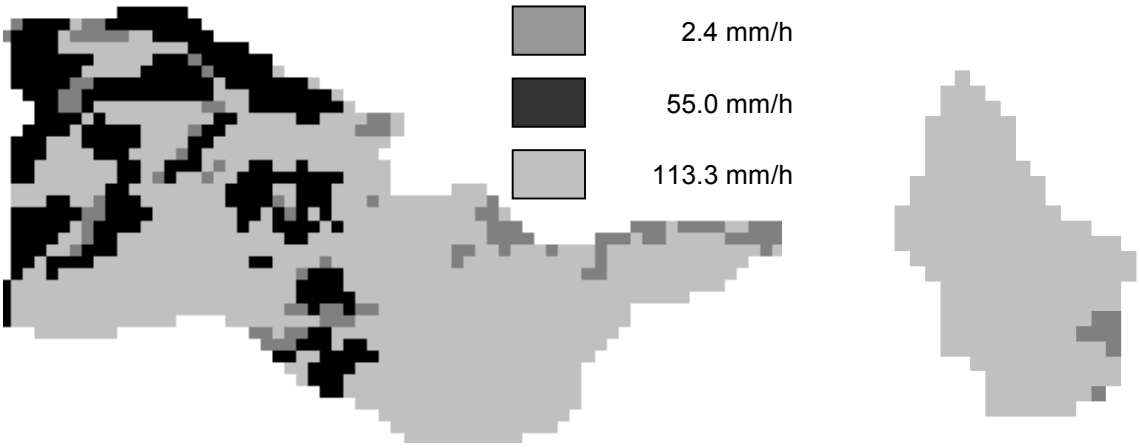

Figure 5.8 The variation of the saturated hydraulic conductivity for the Buitre catchment (left) and the Alquería catchment (right).

Table 5.3 The assigned values for the saturated conductivity in the study area.

Land cover unit	K_s (mm/h)	Standard deviation	Distribution
Bare soil	2.4	1.3	lognormal
Afforested terraces	55.0	38	lognormal
Grassland/Natural woodland	113.3	82	lognormal

5.5 Quality of the saturated hydraulic conductivity measurements

The auger hole method was used in this study to estimate the saturated hydraulic conductivity. These measurements were supplemented by the K_s estimates of crusted bare soils (Lambregts, 1999) measured by the ring infiltrometer method at two hill slopes in the Alquería catchment. In both methods the soil is saturated before the K_s is estimated. For measurement locations with similar site characteristics (soil texture, slope exposition and under or between vegetation) the estimates of both methods were compared with each-other. By use of statistical testing (Kolgomorov-Smirnov test) the means and distribution of the K_s estimates by both methods did not significantly differ from each-other (figure 5.9). Based on these results, the estimates by the ring infiltrometer for crusted bare soil (Lambregts, 1999) were used in this study.

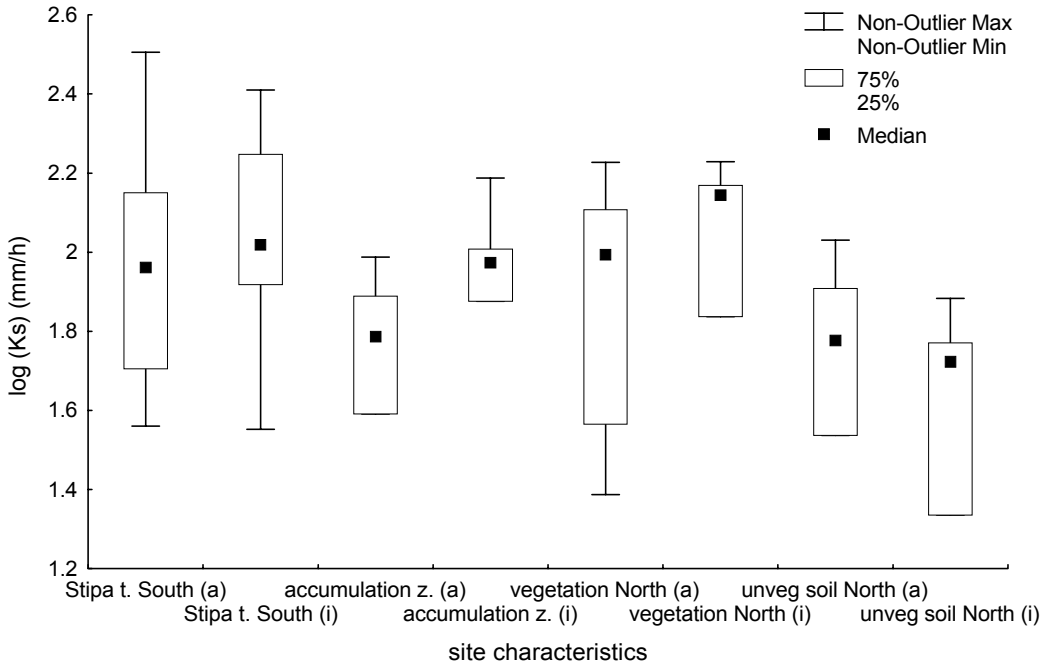

Figure 5.9 Log-transformed K_s estimates for sites with the same characteristics by different methods; a=auger hole method and i=ring infiltrometer method. South and North stand for the aspect of the site.

5.6 The K_s results in a larger perspective

There are many different ways to quantify the infiltration process. In this study the saturated hydraulic conductivity was estimated by use of the inverse auger hole and K_s measurements by the ring infiltrometer were added. K_s can also be determined in the laboratory on saturated soil samples. Another characteristic that often is measured by use of rainfall simulations, is the steady state infiltration rate f_c. To place the K_s results of this study in a larger context of the results of previous studies, this section discusses the transformation of K_s into f_c.

Both parameters are derived from *Darcy's law* (equation 5.3). During the infiltration process the advancing wetting front causes a decrease of the gradient of the pressure head.

$q = KS_f$ *equation 5.3*

In which;
q ; volumetric flux
K ; hydraulic conductivity
S_f ; head loss of flow per unit length of medium

From *Darcy's law* (equation 5.3) it can be shown that the flux density or infiltration rate decreases and approaches asymptotically a constant value with gravity as the

main driving force. This infiltration rate is called the steady state infiltration rate f_c or the final infiltration rate because it is achieved at the end of the infiltration process. Unlike the K_s, the steady state infiltration rate f_c is not obtained in a fully saturated soil. Nevertheless the steady state infiltration rate f_c can be converted into the saturated hydraulic conductivity K_s by a dimensionless material coordinate m as in equation 5.4 (Kutílek & Nielsen, 1994). The value of m depends on the substrate and is smaller than 1.

$f_c = m^* K_s$ *equation 5.4*

This conversion enables us to compare results of K_s and f_c estimates from former studies that used different methods (i.e. inverse auger hole method, ring infiltrometer method and rainfall simulation).

In the study area the K_s and f_c were estimated at the same location (Odijk & van Bemmel, 1997; Prinsen, in prep). By combining these data, the material coordinate is determined as 0.3 (figure 5.10). This value is estimated by an insignificant linear relation with a explained variance of only 0.13.

In general K_s values obtained with the inverse auger hole method or with the ring infiltrometer test are known to be much larger than estimates obtained from plot studies (Williams & Bonell, 1988). In an area with sandy loam soils on limestone Cerdà (1997a) found a material coordinate of 0.1 to transform the K_s of ring infiltrometer tests into the final infiltration rate f_c obtained from rainfall simulations. So, although the material coordinate of 0.3 obtained in this study is not a reliable value, it gives an indication how the K_s estimates of this study correspond with the K_s and f_c estimates of other studies (table 5.4).

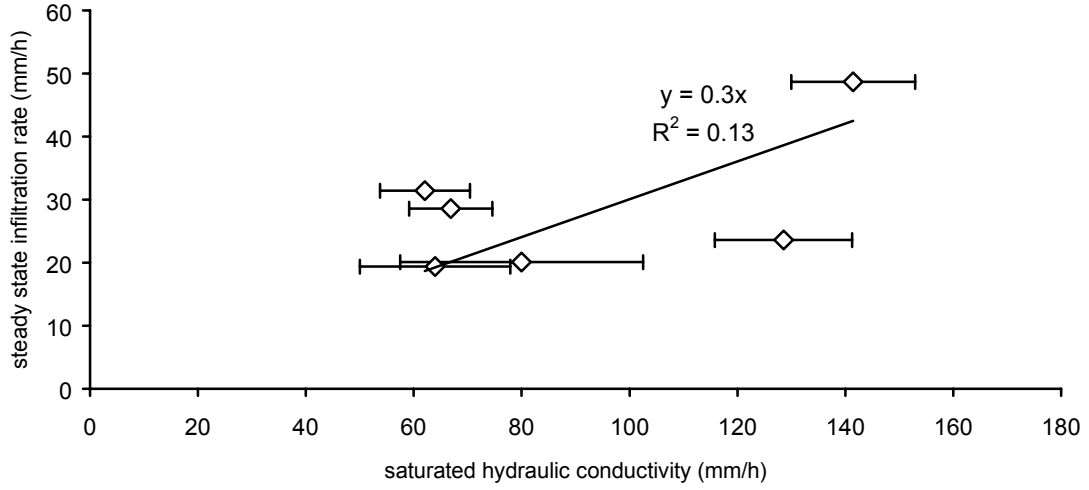

Figure 5.10 The steady state infiltration rate f_c as a function of the saturated hydraulic conductivity, based on data of Odijk & van Bemmel (1997) and Prinsen (in prep.). The error bars indicate the minimum and maximum values.

The saturated hydraulic conductivity as estimated during this study appears to be slightly larger than estimates from former studies (table 5.4). Despite the information given in table 5.4, the dimensions of the test surface used for rainfall simulations, inverse auger hole test and ring infiltrometer tests are rarely published. The logarithmic distribution of the K_s estimates (figure 5.2) indicates that on a larger surface, the chance increases that the infiltration capacity is completely utilised. This may result in smaller f_c or K_s estimates when they are estimated over larger test surfaces (Karssenberg, in prep.). The 'effective' saturated hydraulic conductivity K_{s_eff} is a parameter used to account for larger areas than the support size of the saturated hydraulic conductivity, which is the surface of the field measurement (Kabat et al., 1997). The value of an 'effective' K_{s_eff} representing the saturated hydraulic conductivity of the classified land cover units will be smaller than the K_s measured by the methods given in this chapter (Williams & Bonell, 1988).

Despite the slightly larger values of the K_s point estimates, the relative differences between the estimates for the classified land cover units were found to be reliable and the K_s; point estimates were used for further hydrological analysis and modelling.

5.7 Conclusions

The results show that the saturated hydraulic conductivity K_s is not significantly influenced by texture, topography or parent material. The parent material that was disturbed by afforestation had a significantly smaller K_s than the undisturbed parent material of the study area.

Although the vegetation at a fine resolution is known to control the K_s, the estimates of this study showed no significant differences between the K_s under vegetation and the K_s of inter-plant areas. The variability of K_s within a land cover unit was larger than the variability of the K_s between plant and inter-plant area. For this reason the K_s could not be related to the vegetation cover of the study area when the vegetation cover was parameterised at a fine resolution as the percentage surface cover per unit area (as described in chapter 3).

At a larger resolution, within the land cover units 'bare soil' and 'afforested terraces' the K_s was smaller than within the land cover units 'natural woodland' and 'grassland'. The K_s in land cover unit 'bare soil' was smallest. Although the K_s estimates were rather large, the results corresponded with the results of other studies with regard to the relative differences between the classified land cover units and the magnitude of the K_s. For this reason the land cover units were used to map the K_s results.

The K_s estimates were lognormally distributed which results in smaller K_s values when estimated on larger plot surfaces. For this reason the K_{s_eff} that represents the saturated hydraulic conductivity of a land cover unit will be smaller than the mean of the field estimates in that specific land cover.

Table 5.4 Overview of saturated hydraulic conductivity K_s and steady state infiltration rate f_c

Para-meter	Unvegetated soil				Vegetated soil (by natural vegetation; shrubland/herbs and grasses			
(mm/h)	mean	min	max	n	mean	min	max	n
K_s					199.6			u
					109.0			u.
					92.5			u.
K_s	u.	60	174	u		138	894	u.
f_c	12.59	7.13	18.74	5	44.53	41.17	47.7	3
f_c	24.44	13.62	37.96	6	52.99	50.93	54.75	3
K_s					72.9	1.1	712.7	51
K_s					91.3	38	164.1	10
K_s					77.1	2.8	55.4	42
K_s					70.2	18.8	158.5	10
K_s					102.8			u
K_s					7.29	0.06	110.7	16
K_s					8.77	0.12	34.93	16
K_s					13.21	1.06	70.23	15
K_s					97.71	59.17	141.3	4
f_c						23.6	28.6	2
K_s					102.71	50	152.9	4
f_c						19.4	48.7	2
K_s					71.04	57.5	102.5	4
f_c						20.1	31.4	2
K_s	2.4	1.3	3.8	7				
K_s					55.0	18.4	156.5	25
K_s					113.3	24.4	345.8	93

estimates of former studies, u stands for unknown.

Para-meter (mm/h)	Soil description	Method	Source
K_s	Gypsiferous marls with marly regosols, 20 yrs fallow	Ring infiltrometer	Francis, 1990
	idem, 5 yrs. Fallow, spur	idem	Francis, 1990
	idem, 5 yrs. Fallow, hollow	idem	Francis, 1990
K_s	marls	Ring infiltrometer	Lopez-Bermudez et al., 1984
f_c	Hard and compacted mudrock in marls, calcareous, dominantly silt-size	Rainfall simulation	Solé-Benet et al., 1997
f_c	Marls with regosols/leptosols	Rainfall simulation	Cerda, 1997b
K_s	Silty clay loam soils developed in marls, open shrubland	Falling head of saturated soil sample in laboratory	Martinez- Mena Garcia (1995)
K_s	Marl with sandy texture covered by dense shrubland	idem	Martinez- Mena Garcia (1995)
K_s	Clay loam soils developed in marls; open shrubland	idem	Martinez- Mena Garcia (1995)
K_s	Sandy loam soils developed in quaternary sediments; Stipa t.	idem	Martinez- Mena Garcia (1995)
K_s	Clay and silt dominated soils in limestone/limestone conglomerate; shrubland	Inverse auger hole	Lopez-Bermudez et al., 1996
K_s	loamy soils on marls and quaternary deposits	Falling head of saturated soil sample in laboratory	Gómez-Plaza (2000)
K_s	silty loam soils on marls and quaternary deposits	idem	Gómez-Plaza (2000)
K_s	silty loam soils on marls and quaternary deposits	idem	Gómez-Plaza (2000)
K_s	silty loam on marls, downslope of	inverse auger hole	Odijk & van Bemmel
f_c	*Stipa tenacissima* tussock	rainfall simulation	(1997) Prinsen (in prep.)
K_s	silty loam on marls, upslope of	inverse auger hole	Odijk & van Bemmel
f_c	*Stipa tenacissima* tussock	rainfall simulation	(1997) Prinsen (in prep.)
K_s	silty loam on marls, between *Stipa*	inverse auger hole	Odijk & van Bemmel
f_c	*tenacissima* tussock	rainfall simulation	(1997) Prinsen (in prep.)
K_s	Crust on silty loam on marls	Ring infiltrometer	Lambregts, (1999)
K_s	Silty loam on marls and limestone, afforested terraces	Inverse auger hole	De Wit, this thesis
K_s	Silty loam on marls and limestone, grassland and natural woodland	Inverse auger hole	De Wit, this thesis

6 Discharge

6.1 Introduction

As explained in chapter 1, this study focuses on the runoff of various sized catchments. The discharge of catchments is a function of rainfall properties as discussed in chapter 4 and of infiltration properties of the soils as presented in chapter 5. In a semi-arid Mediterranean environment the discontinuity of runoff on hill slopes and in streambeds controls the discharge at the outlet of catchments. To analyse the runoff of various sized catchments, the discharge was recorded in the selected catchments described in chapter 2. The methodology and the results of the runoff records are discussed in this chapter. In chapter 7, the measured runoff will be used to estimate a REA for the study area and to support further hydrological analysis.

6.2 The measurement of discharge

In order to determine the hydrological behaviour of the survey area, the rainfall-runoff relation was estimated. In the study area, the discharge was measured in different streambeds. For every rainfall event the discharge was measured by monitoring the water level in the streambed, which was transformed into discharge by calibration. For this calibration the researcher has to be present at the measurement location at the time of the discharge to measure the discharge next to the normal recording by the installed instruments. In a semi-arid environment with infrequent rainfall this is often a problem (Thornes et al., 1999). If calibration is not possible a theoretical relation is used. The collected data were used for the hydrological analysis of the study area and served as input for the hydrological model (chapter 8).

Measurement weirs were built in the studied streambeds. This way the exact area of the artificial cross-section is known and, more importantly, the water is brought to a critical flow condition (Froude number Fr = 1). Before the cross-section the flow will be subcritical (Fr < 1) and tranquil, while by passing the structure, it changes to a rapid, shooting or supercritical flow (Fr > 1). Under critical flow conditions a linear relation exists between the depth of the flow and its average flow velocity. Moreover, under these conditions the depth of the flow is directly related to the specific energy level by equation 6.1 (King, 1954; Bos, 1978).

$$Q = C\,H^{c} \qquad \textit{equation 6.1}$$

in which:
Q : discharge (m^3/s)
C : coefficient depending on the cross-section and energy losses

H : specific energy height approximated by the water level upstream of the weir (m)
c : general exponent estimated by calibration

At a certain distance upstream of the weir, a slight drop of the water surface starts to develop and the specific energy height starts to differ from the water level. This certain upstream distance is defined as two times the water head in the weir (figure 6.1). Upstream of the drop, the head of the water level *h* equals the specific energy height *H* and the head of the water level can be used as input for equation 6.1. For this reason the water level *h* is measured at a location 2.5 times the maximum measurable head (or the depth of the control section) upstream of the weir.

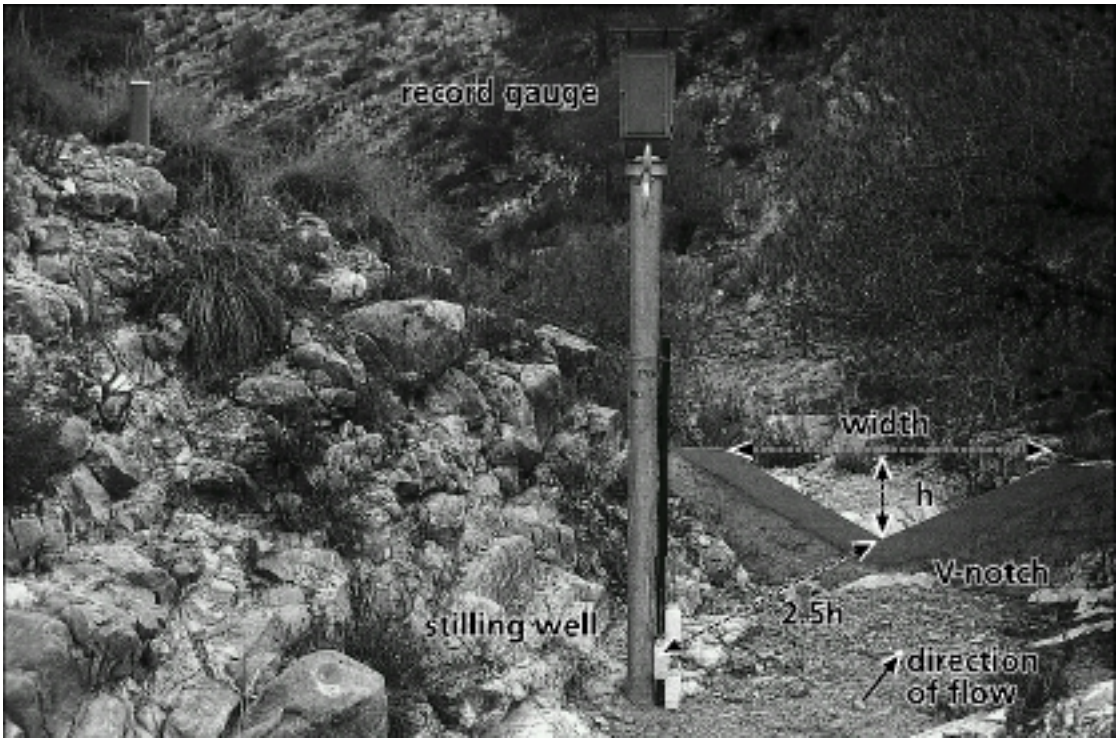

Figure 6.1 Schematic view of measurement location.

The monitoring program aimed at short-period, low discharge events in ephemeral streams, which were expected to take place frequently in the study area. For this reason it was decided to use sharp crested V-notches or Thomson weirs (Bos, 1978). For this weir, equation 6.1 has been rewritten in discharge form as equation 6.2 (Shaw, 1988).

$$Q = K \tan(\theta/2)\, h^{5/2} \qquad \text{equation 6.2}$$

in which:
K : coefficient based on analysis and experiment ($m^{1/2}/s$);

h : height of water level (m)
θ : angle of V-notch

The V-notch weirs in the survey area were each constructed with an angle of 126.8 degrees (width to depth of control section is 4:1). The head h was recorded in a stilling well that was installed by the placement of a pierced iron pipe (figure 6.1). This way, the recorded water level is not disturbed by wave action. The head of the water level is recorded by record gauges. At some locations a pressure sensor was installed next to the record gauges to monitor with a higher resolution and to have a backup if the record gauge malfunctioned.

Table 6.1 Resolution of discharge measurements by pressure sensors and record gauges.

Measurement location	All except B2, B7,B8	B2	B7, B8	B1	B2, B7	Bt
Instrument	Ott record gauge	Seba record gauge	Seba record gauge	SEWER pressure sensor	DRUCK pressure sensor	SEWER pressure sensor
Resolution of measurement (cm)	1: 5 in reality	1: 5 in reality	1: 5 in reality	± 0.5	± 0.35	± 0.5
Time interval of monitoring	continuous 1 cm = 5 hrs	continuous 1 cm = 10.4 hrs	continuous 1 cm = 20.2 hrs	0.5 min (July 1996–Oct.1997) 1 minute (Oct. 1997–Sep.1998)	2 min	0.5 min

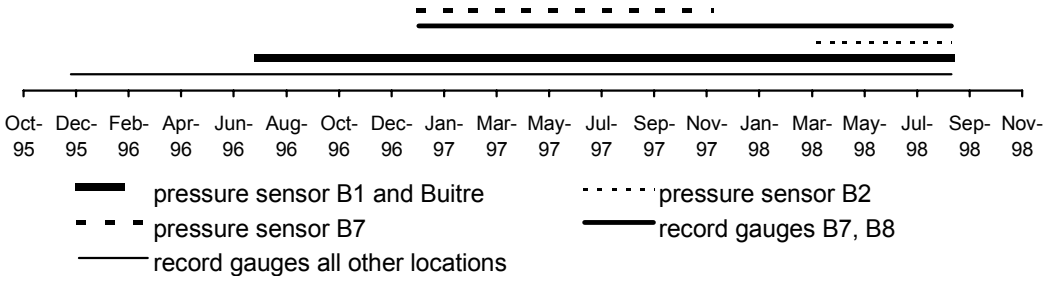

Figure 6.2 Measurement period of different discharge measurements.

The period of discharge measurements during the survey is indicated by figure 6.2 and the resolution of the pressure sensors used is given in table 6.1. The spatial distribution of the discharge measurement locations is shown in figure 6.3.

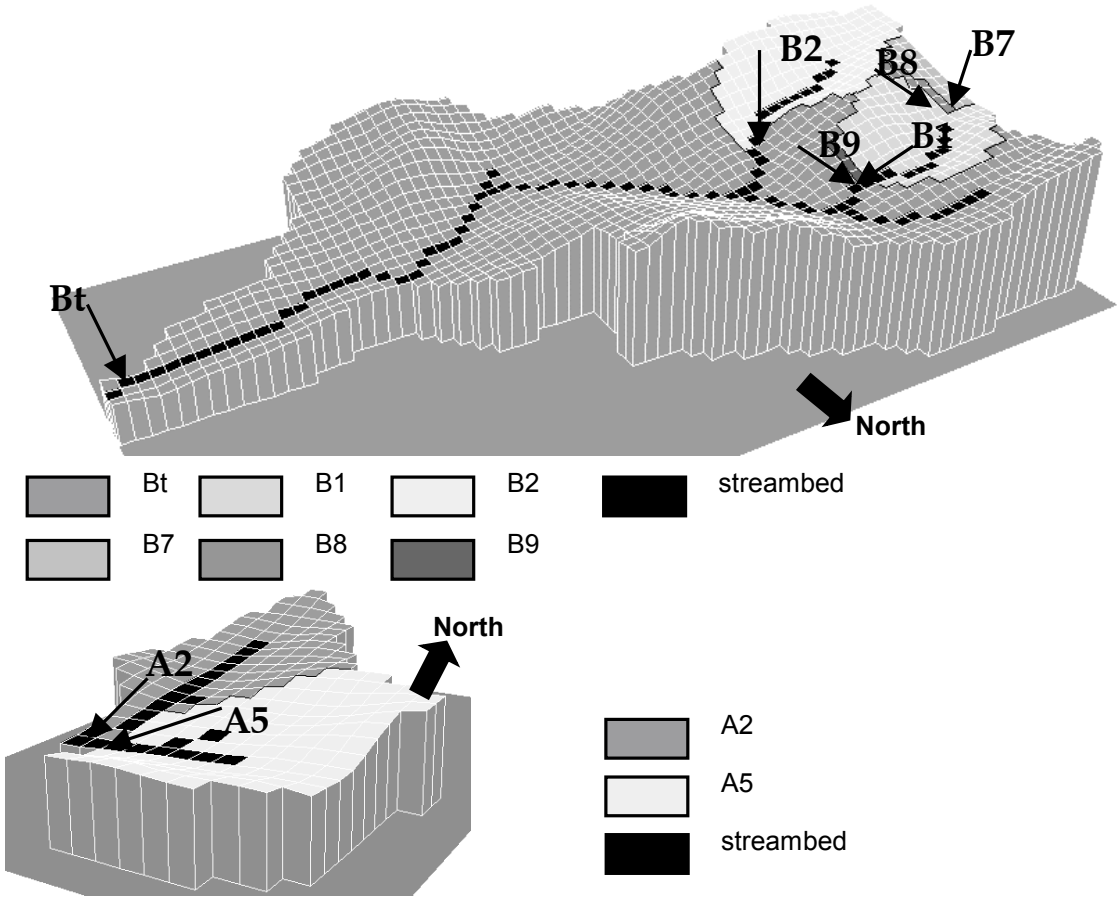

Figure 6.3 Location of discharge measurements in Buitre catchment (upper figure) and Alquería catchment (lower figure).

6.3 Calibration of the discharge equation

The previous section explained how discharge was measured and estimated. To transform the height of the water level recorded by the pressure sensor or record gauge into discharge, equation 6.2 needs to be adjusted to the specific circumstances of the measurement location.

By calibration (figure 6.4) at the outlet of the Buitre, the following discharge equation (6.3) was determined;

$$Q = 1.288 * h^{2.27} \qquad \textit{equation 6.3}$$

in which:
Q : discharge (m^3/s)
h : height of water level (m)

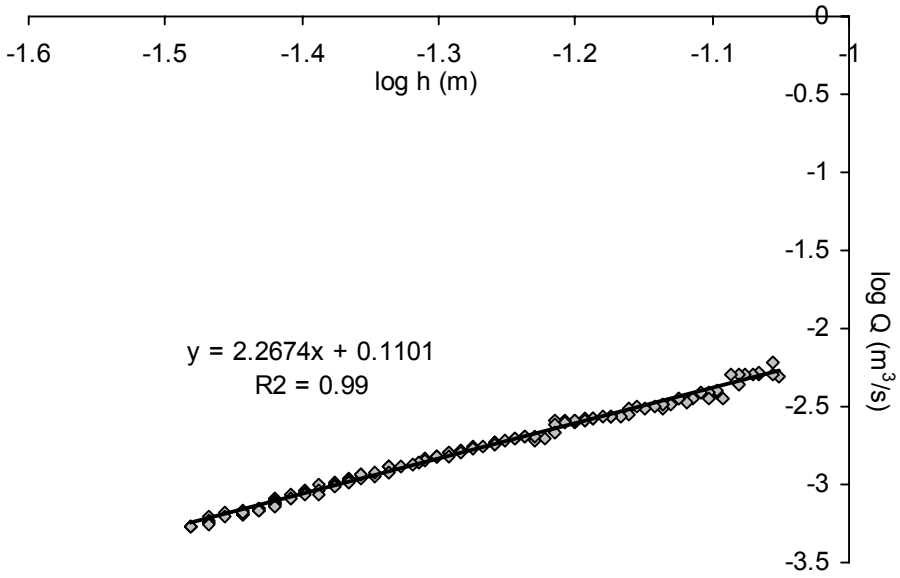

Figure 6.4 Calibration curve of log-transformed discharge (l/s) depending of log-transformed water level (m) at the outlet Bt during the event of 5 June 1998.

To estimate if this equation was valid for all measurement locations in the study area, measurements of the water height and the corresponding volumetric amount of water were taken at the A2 V-notch weir during event 6 May 1996, located in the Alquería catchment.

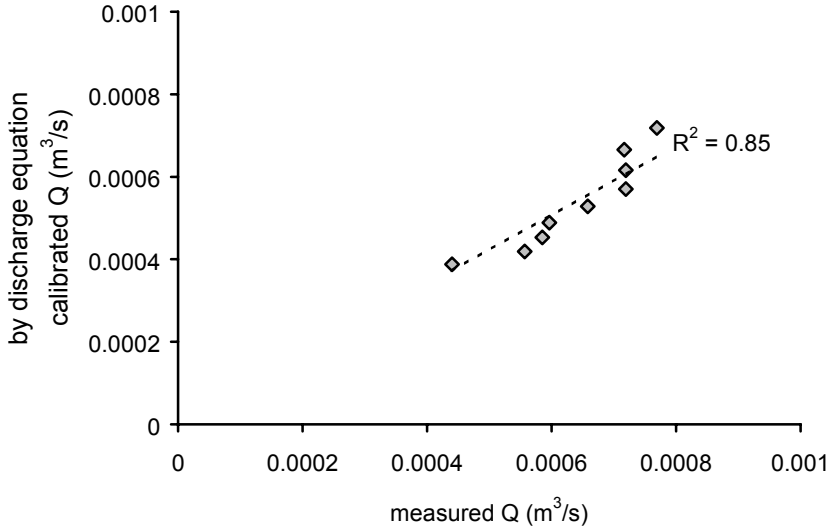

Figure 6.5 The measured discharge in catchment A2 versus the calibrated discharge computed with equation 6.3 for the rainfall event of 6 May 1996.

When equation 6.3 was applied to the measurements, the estimated deviation between calculated and measured discharge was smaller than the deviation due to measurement errors (figure 6.5). Hence, the discharge equation 6.3 was applied for

all measurement locations to estimate the discharge of all catchments in both the Buitre and the Alquería catchment.

6.4 Calibration of the record gauges

As shown in table 6.2, several instruments were used for discharge recordings. These instruments had different spatial and temporal resolutions. The recordings of the record gauges had to be scaled to enable the recording of the total range of the discharge duration and magnitude. The pressure sensors had a much smaller measurement error than the record gauges and were therefore assumed to be more accurate.

In several catchments (i.e. B1, B2, B7, Bt, see table 6.2) both pressure sensors and record gauges were used at the same time to record the discharge. The magnitude of the water level recorded by the pressure sensors and the record gauges corresponded with each other.

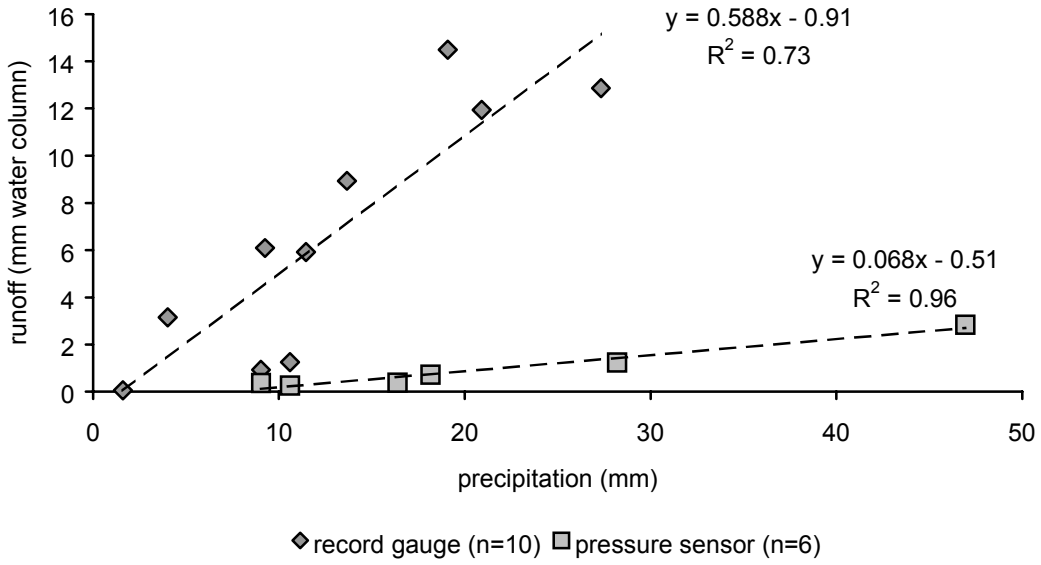

Figure 6.6 The total amount of runoff (mm) recorded in catchment B7 depending of the total amount of precipitation (mm).

The temporal resolution of the record gauges used appeared to be sufficient to obtain accurate estimations of the temporal recordings of the discharge events in all catchments except for the catchments B7 and B8. A deviation in the temporal resolution leads to a deviation in the estimation of the total amount of runoff. To transform runoff estimates of the record gauge recordings into accurate runoff estimates, the recordings of both the pressure sensor and the record gauge installed in catchment B7 were used (figure 6.6). Because the pressure sensor was relocated during the study, only two events were recorded by both the pressure sensor and the record gauge. All recorded events were used to estimate the total runoff amounts recorded by the record gauge and the pressure sensor. These recordings of mainly

non-corresponding events, were significantly related ($p<<0.001$) to the total amount of precipitation of a rainfall event.

Using the relations between total runoff amount and precipitation as calculated by linear regression, the runoff recorded by the record gauge was transformed (equation 6.4) into runoff recorded by the pressure sensor.

$$RO_{ps} = 0.116*RO_{rg} - 0.401 \qquad \textit{equation 6.4}$$

in which:
RO_{ps} : total amount of runoff recorded by pressure sensor (mm water column)
RO_{rg} : total amount of runoff recorded by record gauge (mm water column)

The estimated runoff amounts of catchments B7 and B8, in which the record gauges with the coarse temporal resolution were used, were all transformed using equation 6.4. These runoff estimates were used for the hydrological analysis in chapter 7 except the smallest runoff amounts. The smallest runoff amounts of B7 and B8 neared zero after calibration and are therefore not incorporated in the further analysis.

6.5 Discharge estimates

The recorded water level over time was transformed into discharge using equation 6.3, which resulted in hydrographs. From the resulting hydrographs two quantities were estimated; the total amount of runoff (m^3) and the peak discharge (l/s).

6.5.1 The number of runoff events

In the Buitre catchment discharge was recorded during 17 rainfall events during 2 years of recording. Due to malfunctioning of the instruments and later installation of the instruments in subcatchment B7 and B8, it was not possible to obtain recordings at all measurement locations during all rainfall events. Eleven recorded runoff amounts in the B7 and B8 were excluded from analyses because they were near zero after calibration.

In 40 cases the rainfall in the Buitre catchment could be related to the discharge at a measurement location (figure 6.7). After recalculation the runoff amount of 29 events and the peak discharge of 35 events were used for further analysis. The largest total runoff and peak discharge were estimated at the outlet of Bt. At the outlet of B9 discharge was only measured for 1 rainfall event.

In the Alquería catchment, discharge was recorded during 8 rainfall events during two years of measurement. In 11 cases the rainfall could be related to discharge at measurement location A2 or A5 (figure 6.8).

Unfortunately, during the two events with a recurrence period of more than two year, the instruments malfunctioned. The result was that during the two and a

half years of measurement only a few moderate runoff events were recorded in the Buitre and Alquería catchments. This indicates that a longer measurement period is needed to obtain an adequate impression of the hydrological response of the studied catchments.

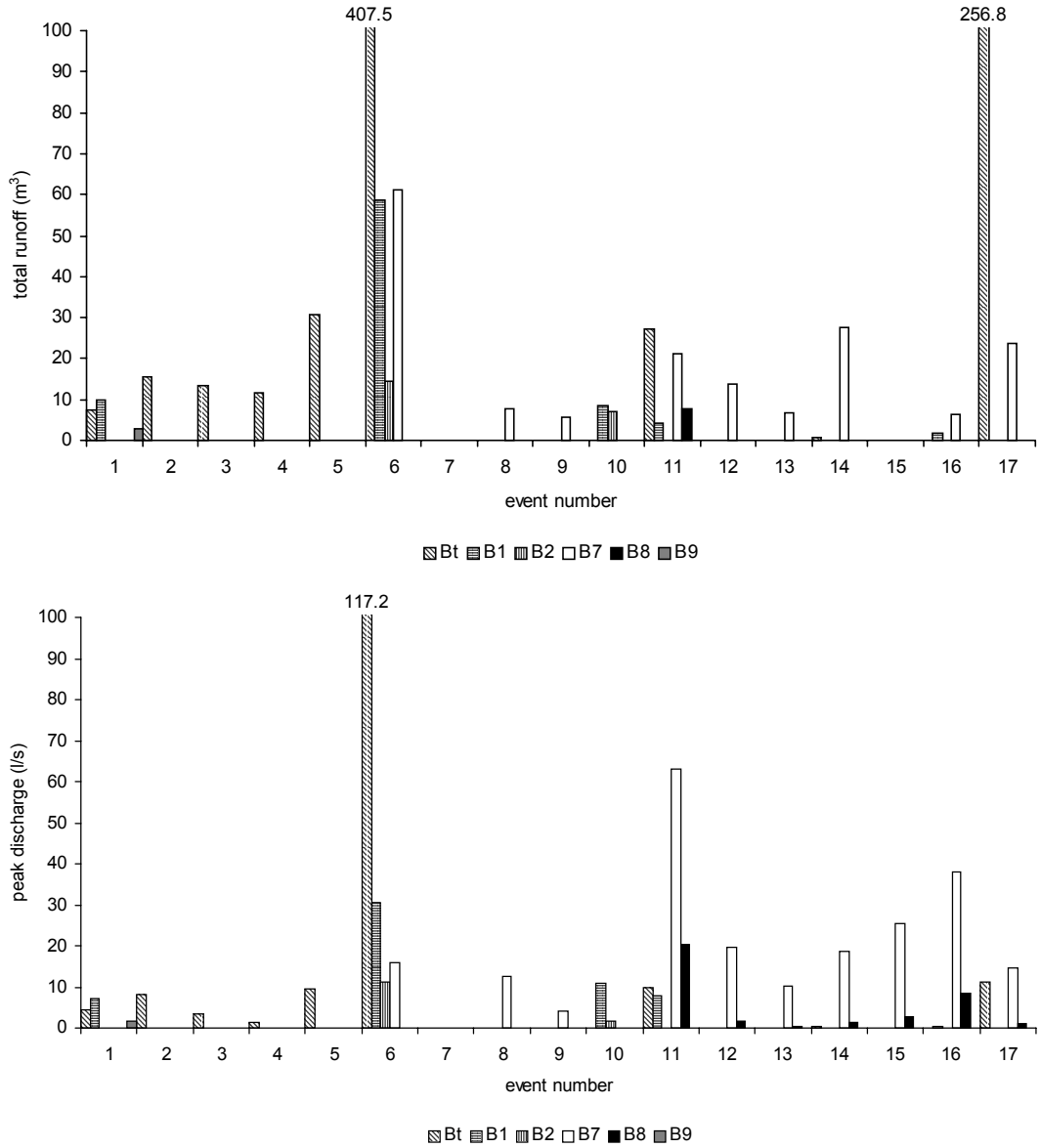

Figure 6.7 Total amount of runoff (upper graph) and peak discharge (lower graph) measured at different outlets in the Buitre catchment. Note, if no bar is given no discharge occurred, or the instruments malfunctioned.

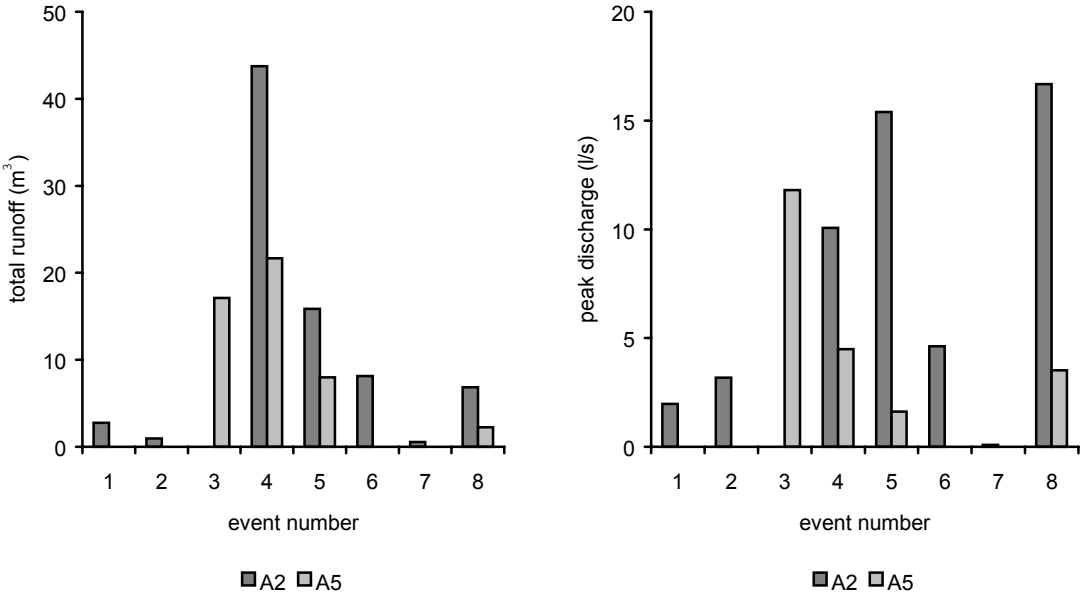

Figure 6.8 Total amount of runoff (left) and peak discharge (right) measured at different outlets in the Alquería catchment. Note, if no bar is given no discharge occurred, or the instruments malfunctioned.

6.5.2 The runoff coefficients

The range of the recordings in the Alquería catchment is smaller than in the Buitre catchment. The runoff coefficients (discharge expresses as percentage of precipitation) from the Alquería catchment fit in the range of the runoff coefficients of the Buitre catchment (table 6.2).

Table 6.2 Mean and maximum runoff coefficients of the studied catchments.

(Sub) Catchment	Number of events	Mean runoff coefficient (%)	Standard deviation	Max. runoff coefficient (%)
Bt	9	0.25	0.32	0.85
B1	6	0.47	0.42	0.96
B2	3	0.14	0.12	0.23
B7	9	4.10	1.37	6.72
B8	1	1.71		
B9	1	9.76		
A2	7	0.78	0.60	1.65
A5	4	0.66	0.28	0.93

The largest runoff coefficient estimated in subcatchment B9 corresponds with the runoff coefficients of subcatchments under corresponding conditions that are ten times smaller than B9 (Martínez-Mena et al., 1998). The runoff coefficients from subcatchments B7, B8 and B9 correspond with runoff coefficients derived from plot studies (Puigdefabregas et al., 1996; Lopez-Bermudez et al., 1996). The coefficients of

the other catchments in the study area are smaller than runoff coefficients known from hill slope or plot studies under conditions corresponding to the study area (Puigdefabregas et al., 1999).

The mean runoff coefficient of Bt is smaller than the runoff coefficient of subcatchment B1 and the mean runoff coefficients of the sub-subcatchments B7, B8 and B9 are all larger than the runoff coefficient of subcatchment B1 in which B7, B8 and B9 are located. This indicates that not all runoff that leaves the small catchments reaches the outlet of the larger catchment in which the smaller catchments are located. The decrease of runoff coefficients with increasing catchment size can be explained by transmission losses in the streambed as discussed in chapter 1.

6.5.3 The recorded hydrographs

The subcatchments B1 and B2 in the Buitre catchment Bt were almost equal in surface area., Sub-subcatchments B7 and B8 were located within the B1 subcatchment and their surface areas are of similar magnitude. In the Alquería catchment subcatchments A2 and A5 were also almost equal in surface area. To compare the hydrographs of all catchments, the discharge was standardised as the discharge per hectare.

As shown in figure 6.9 and 6.10, all hydrographs had a steep rising limb and a short duration which is characteristic for discharge in a semi-arid environment. The amount of discharge in sub-subcatchments B7 and B8 was far larger than in the other catchments. Runoff was also recorded in B7 and B8 during the event of 22 April 1998, but these data have been excluded here because they exceeded the recorded discharge in Bt, B1 and B2 by a factor 100 when the discharge was standardised per hectare. If these data from B7 and B8 were to be plotted on the middle graph of figure 6.9 using the current y-scale, the other recordings would not be visible.

Clearly, catchments B7 and B8 responded quickly to rainfall but it should be taken into account that the temporal resolution of the record gauges used in these catchments is very coarse and therefore the response time is not a reliable parameter for the comparison of different catchments. The response time in the remaining catchments was recorded at a finer temporal resolution and therefore was a more reliable parameter.

During the events of 22 April 1998 and 20 April 1997 catchment Bt responded later than the stream-upward located catchments (middle graphs in figure 6.9 and 6.10) and during these events it is likely that part of the runoff that left the smaller catchments reached the outlet of catchment Bt.

During some rainfall events, however, discharge was recorded at the outlet of Bt while B1 and B2 did not generate runoff (upper graph in figure 6.9) so the runoff in the streambed was generated in nearby areas. At the time of this event, the record gauges of B7 and B8 had not been installed.

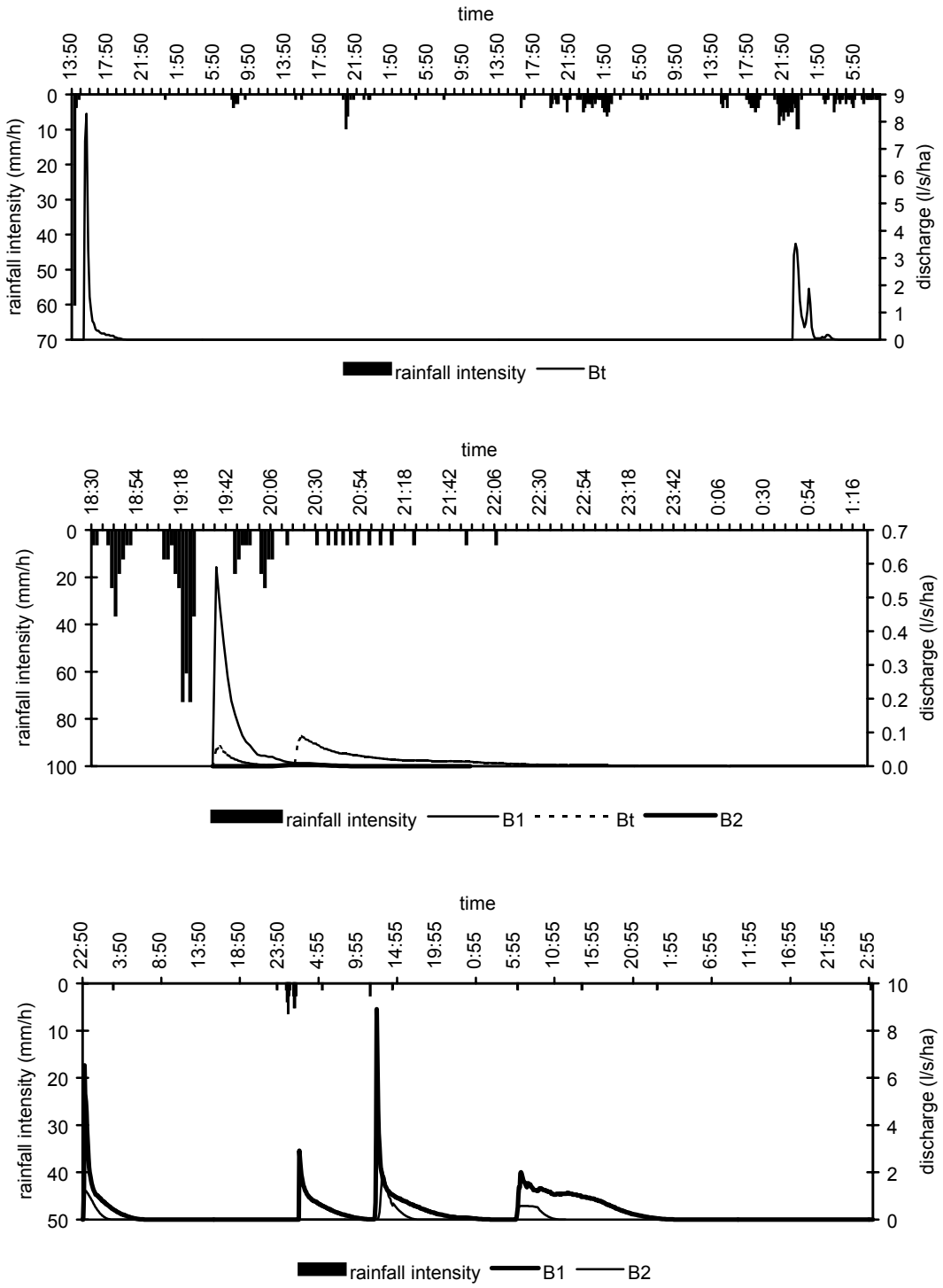

Figure 6.9 Discharge recorded in the Buitre catchment (B#) during 8-12 September 1996 (upper graph), 22 April 1998 (middle), 27-30 September 1997 (lower graph). For further explanation, see text.

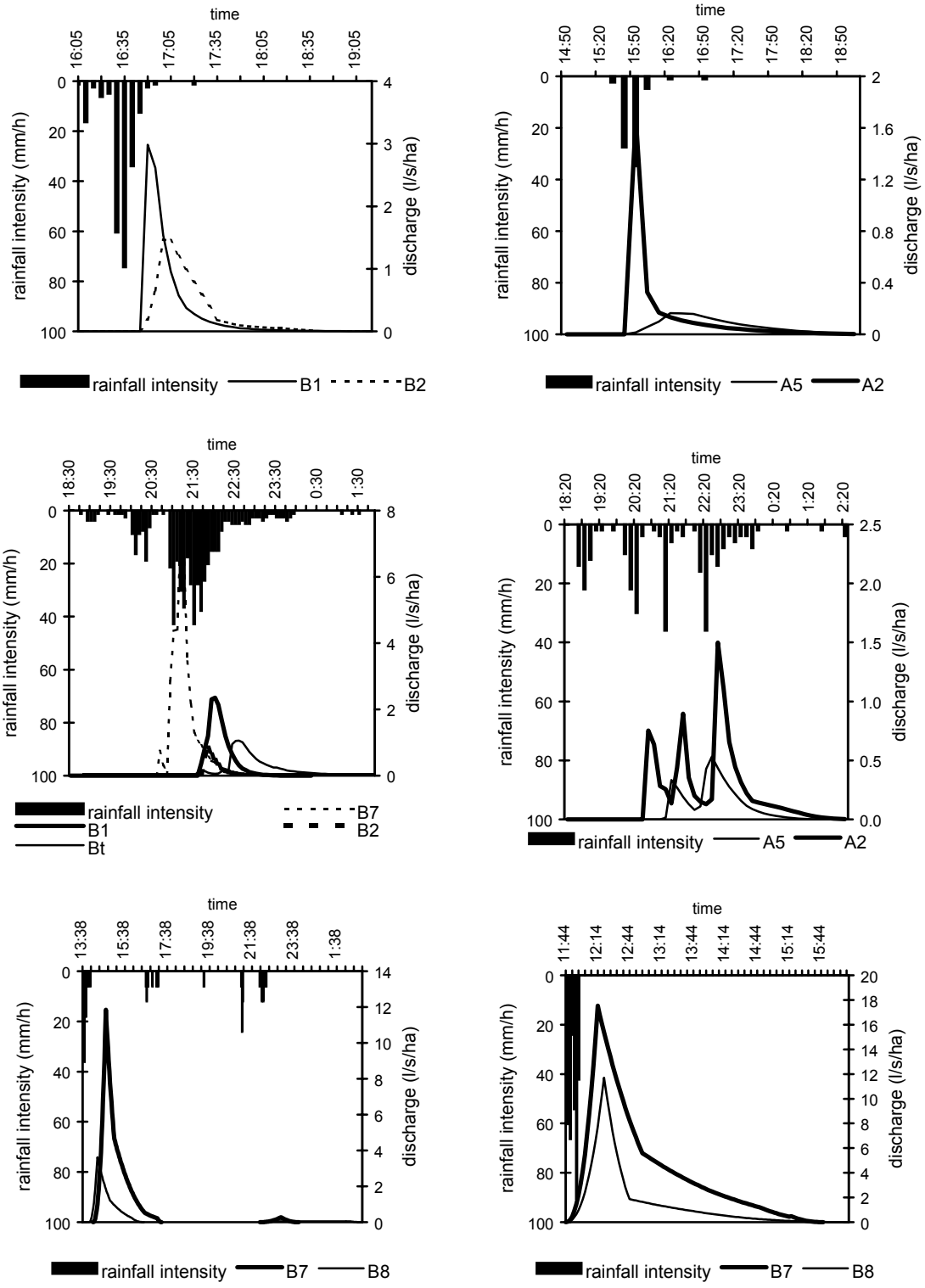

Figure 6.10 Discharge recorded in the Buitre catchment (B#) and the Alquería catchment (A#) during 31 May 1997 (upper graph), 20 April 1997 (middle), 24 May 1998 (lower left), 4 June 1998 (lower graph right), for further explanation, see text.

The upper and middle graphs in figure 6.10 illustrate that rainfall recorded in the Buitre catchment differed from rainfall recorded in the Alquería catchment. Nevertheless, the rainfall recordings were assumed to cover the separate catchments.

6.5.4 Different runoff response in equal sized catchments

Figure 6.7 and 6.8 show that in the pairs of equal sized subcatchments, the catchments B1, A2 and B7 responded with a larger runoff than the catchments B2, A5 and B8. This is illustrated by several events shown in figure 6.9 and 6.10. Note that the event of 27-30 September (figure 6.9, lower graph) is a heavy rainfall event with a recurrence interval of approximately five years (Cammeraat, in press). During this event much sediment was transported and terrace bunds in the downstream agricultural fields were damaged. Unfortunately the tipping bucket recorder broke down and the record gauge of Bt malfunctioned. Imeson et al (1999) and Cammeraat (in press) described this event in detail for the Alquería catchment.

After a rainfall event that caused runoff in subcatchment B1 and no runoff in subcatchment B2, field observations showed that the surface water in parts of the streambed of B2 had not connected with surface water in other parts of the streambed and therefore runoff had not reached the outlet of subcatchment B2. This might have been caused by the better infiltration conditions of the soils under the 'woodland' in catchment B2 in contrast to the compacted soils without any vegetation, except for small trees of the 'afforested terraces' in subcatchment B1. Another reason is that the 'afforested terraces' in subcatchment B1 are located near the streambed. Because these terraces are not situated parallel to the contour lines and at some locations they are situated even perpendicular to the contour lines, the 'afforested terraces' contribute to the routing of surface water. When the 'afforested terraces' end in the streambed, which is the case at some locations, the runoff of these terraces increases the runoff in subcatchment B1.

These observations also explain the differences in runoff in the sub-subcatchments B7, in which the 'afforested terraces' were located near the outlet and the sub-subcatchment B8 in which the 'afforested terraces' were located more upstream of the outlet. In catchment A5, the area near the streambed is covered by 'woodland' while the catchment A2 is almost not covered by woodland. In catchment A2 more runoff is generated which is routed quickly over the unvegetated surface between the tussocks of *Stipa tenacissima*.

The nonparametric Wilcoxon matched pairs test was used to test if the response between the two subcatchments that formed a pair, was significantly different. In general this test is used to analyse if the variables of one group had a consistently larger value than the variables of another group. It assumes a rank ordering of both observations based on each variable, and magnitude of the differences between the variables. When these constraints are met, this test is almost as powerful as a parametric t-test. For this test, the variables were defined as the amount of runoff, the amount of runoff as fraction of precipitation and the peak discharge. The groups were formed by the set of subcatchments which means that

the runoff recordings of B1 were tested with the runoff recordings of B2, A2 with A5 and B7 with B8 (table 6.3).

Table 6.3 Significance (p-level) of differences in simultaneous events (n is number of events).

Significance of Wilcoxon matched pairs test				
Signficance; horizontal Studied catchments; vertical	Amount of runoff (mm)	Amount of runoff (as fraction of precipitation)	Peak discharge (l/s/ha)	Level of scale
B7 > B8	p<0.05 (n=5)	p<0.05 (n=5)	p<0.05 (n=7)	I
B1 > B2	p<0.05 (n=5)	p<0.05 (n=5)	p<0.05 (n=5)	II
A2 > A5	p<0.05 (n=5)	p<0.05 (n=5)	p<0.05 (n=5)	II

The results (table 6.3) show that the assumed differences between the subcatchments were significant. Further analysis of the discharge recordings as given in the next chapter, will be used to find an explanation for these differences.

6.6 Conclusions

By calibration in the field it was possible to relate the water level in the streambeds to the discharge by a calibrated discharge equation. Due to the coarse temporal resolution of the recording instruments of one measurement location, the recordings of this location had to be transformed in order to be reliable. The estimated discharge recordings show runoff coefficients that are very small. The runoff coefficients decreased with increasing catchment surface. The standardised discharge recorded in upstream located subcatchments was larger than the standardized discharge recorded at the outlet of the larger catchment that enclosed the smaller catchments. This indicates that transmission losses in the streambed controls the runoff. Due to this phenomenon the sediment transported out of the largest catchments will be far less than the sediment transported out of the smaller catchments, as can be seen by the shallow soils on the upper slope and sediment blankets in the bottoms of the valleys to which the catchments drain.

The transmission losses, very small runoff coefficients and steep rising limbs of the hydrographs are characteristic for runoff in small catchments located in a semi-arid Mediterranean environment.

The total amount of runoff and the peak discharge of the catchments B1, A2 and B7 was always significantly larger then of catchments B2, A5 and B8 respectively, eventhough the catchments had been selected based on similar environmental conditions like soil, topography and a (semi-)natural vegetation cover.

Further hydrological analysis and the estimation of the REA based on the recorded runoff will be discussed in chapter 7.

7 Hydrological response of various sized catchments

7.1 Introduction

As stated in chapter 1, the definition of a REA is useful because for catchments that fulfil the REA constraints, the mean runoff can be quickly estimated using simple linear equations without a detailed inventory of characteristics at various levels of resolution in the study area. Because a range of catchments sizes can be found that match the REA-constraints, the simple linear equations can be applied at the catchments within this range. This way, these equations can be used to overcome the problem of resolution of characteristics controlling the runoff in different sized catchments.

This chapter aims to define the size of a REA for the study area based on the runoff recordings of the selected catchments. Furthermore this chapter aims to define the simple equations based on characteristics defined as bottom width of the streambed, catchment size, land cover and rainfall characteristics to estimate the runoff and to investigate whether these equations can be applied to the REA-sized catchments or also to other catchments. The field measurements collected over the almost three years measurement period yield a good basis for the definition of a REA in this semi-arid Mediterranean area although the dataset lacks extreme events and the measurement period is fairly short.

In chapter 1 I noted that previous studies have shown that the runoff is controlled by vegetation cover at various levels of resolution. In chapter 3, the vegetation cover was estimated as land cover units and as surface cover per unit area. This chapter aims to quantify the influence of vegetation at vaying resolution by the definition of a simple relation by which the runoff can be estimated as with the other catchment characteristics.

7.2 Explanation of applied statistics

Statistical analysis was used to examine relations between rainfall characteristics, runoff amounts, peak discharges and the variables bottom width, wetness index, storm duration, catchment size, land cover and surface cover.

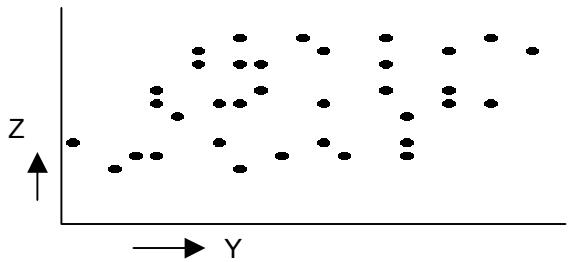

Figure 7.1 Two dimensional plot of dataset that is controlled by the interaction of a third variable.

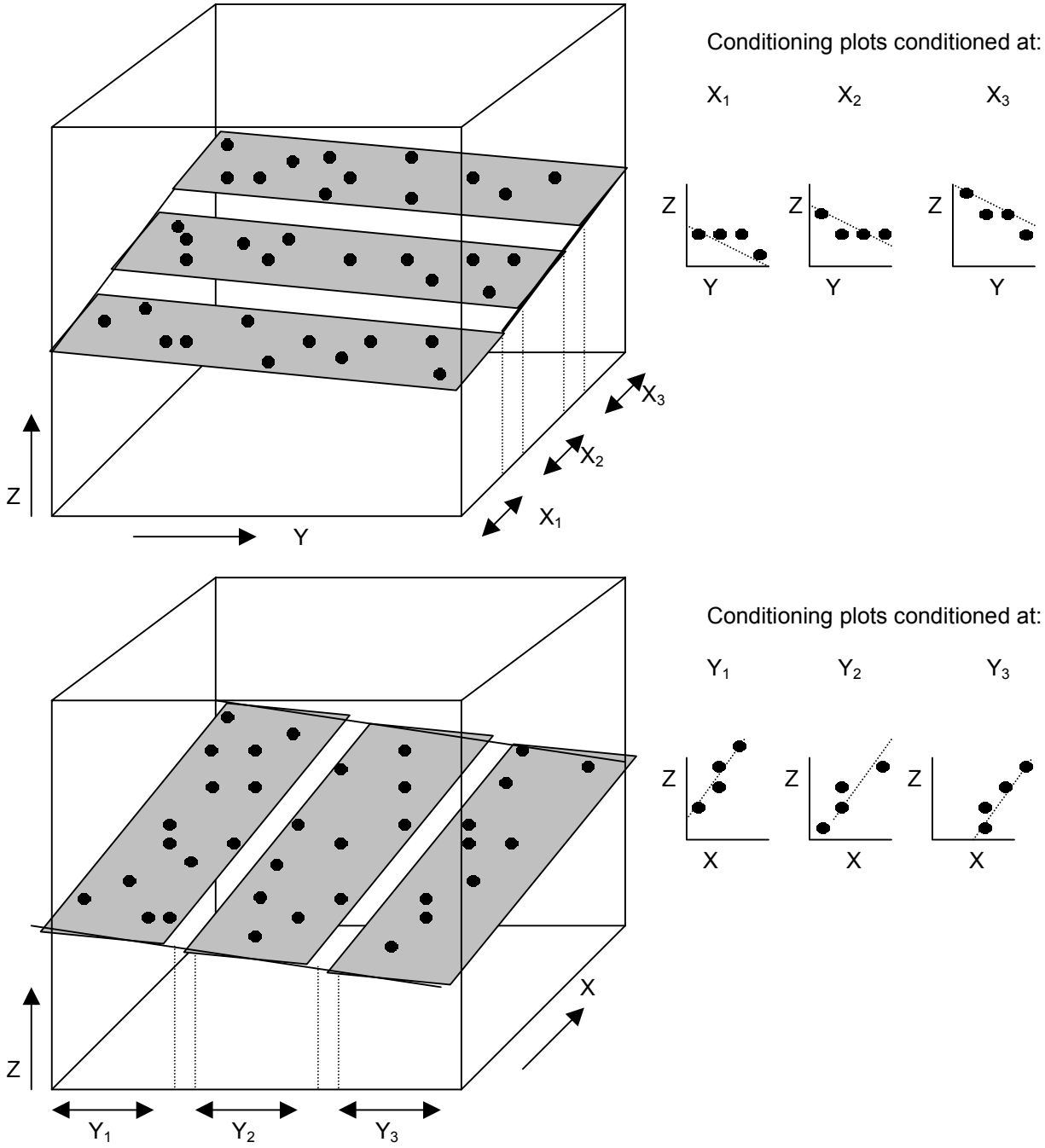

Figure 7.2 Conditioning plots of a dataset (of figure 7.1) in which Z is described by the variables X and Y (in 3 ranges).

In most cases simple linear correlations were calculated or linear (multiple) regression analysis was used. Prerequisite for applying these statistical methods is a normal distribution of the variables. When a regression analysis is done, the regression residuals should be normally distributed (Blalock, 1981). When the variables did not have a

normal distribution and a parametric test was used, the variables were transformed for example by a log-transformation, by which a normal distribution of the transformed variables was obtained.

For multiple linear regression analysis, the data is assumed to be described by a plane in a three-dimensional space described by $Z=aX+bY+c$. If the data is projected in a two-dimensional graph (figure 7.1), the relations may not be clear. However when the data in two dimensions are conditioned by the third variable, a 'conditioning plot' is created (figure 7.2). From such a plot it may easily be seen if the variables are linearly related to each-other, over several range intervals. If these constraints are fulfilled, the assumed linear relation exists and multiple linear regression analysis is allowed (Blalock, 1981).

If these constraints are not met, linear regression analysis is not allowed and the relation between the variables can be better studied using non-parametric tests. These tests are distribution-free which means that the regression residuals do not need to be normally distributed and the assumed relation does not have to be linear. The Spearman R correlation test was used to examine if the analysed variables had a corresponding ranking. It assumes a linear relation between the variables and accounts for the proportion of variability in the data. The Kolmogorov Smirnov test is sensitive for the mean and the general shape of the distribution of the selected variables and tests the difference between cumulative distributions of the variables. This test is especially appropriate for grouped variables.

7.3 Estimation of the wetness index and the bottom width

In the studied catchments the bottom width and the wetness index were estimated to investigate whether these variables give a proper explanation for the discharge in various sized catchments in order to fulfil the aims of this research.

7.3.1 Bottom width

The bottom width is a property, which depends on the runoff because the extent of the runoff forms the streambed. As discussed in chapter 2, the streambeds of the study area have developed in bare limestone. Because the shaping of the streambed is a process that takes place over a long period of time, the bottom width may be used as an indicator of the extent of the runoff. For this reason bottom width is used for inverse modelling of runoff in the runoff analysis described in section 7.5.

For the channel bottom width B_w, the definition of Chow et al. (1988) was used in which B_w is the width of the horizontal part of the streambed, perpendicular to the stream flow over which the water flows. In the study area, the hydrographs had steep rising limbs which indicated a rapid runoff response. Field observations showed that during the runoff, the total width of the streambed was used for runoff. For this reason, the Chow et al. (1988) definition of bottom width seemed to be correct and was used for the measurements. The bottom width of the each streambed was measured at the outlet

or at the location of the discharge measurements of the selected catchments. The results are listed in table 7.1.

7.3.2 Wetness Index

The topographic index or wetness index (equation 7.1) was first introduced by Beven and Kirkby (1979) who used it to represent a theoretical estimation of the accumulation of flow at any point. The wetness index is defined as:

$$Wetness\ Index = \ln (a/\tan\beta) \qquad \text{equation 7.1}$$

in which:
a : upslope area drained per unit contour length at a point of flow
β : local slope angle

This equation is very sensitive to the break in slope at the lower hill slope on to the valley bottom, but the topographic index can easily be achieved from a gridded DTM in a raster GIS. a is the sum of gridcells draining towards a point and β the local slope angle of the cell. A pixel resolution that is too large results in a bias towards a large $\ln(a/\tan\beta)$ (Quinn et al., 1995).

The wetness index was estimated by use of a raster GIS. The values of the gridcells at the location of the outlet of the studied catchments were used for the analysis (table 7.1). Both the bottom width and the wetness index were linearly related to the log-transformed total surface area of the studied catchments. The bottom width correlated with the wetness index (fig 7.3). Because a proper estimation of the wetness index strongly depends of the pixel resolution of the DTM and in this thesis catchments of different size are studied, the bottom width based on field measurements provides a better parameter for further analysis than the wetness index.

Table 7.1 Catchment characteristics of the studied catchments, note that the surface cover the percentage *Pinus halepensis* has been recalculated and indicates in this table the total surface cover of the three including its transparency, in contrast to table 3.5.

Catchment	Surface area	Bottom width channel (m)	Wetness index	Stream order	Land cover (% of catchment surface)				Surface cover (% of catchment surface)		
					natural woodland	grassland	bare soil	afforested terraces	*Pinus halepensis*	*Stipa tenacissima*	no vegetation
Bt	110.60	1.9	16.56	3	13	55	8	24	24	34	42
B1	12.96	1.4	13.85	2	9	34	6	51	26	32	42
B2	13.32	1.55	13.51	2	56	27	14	3	42	37	21
A2	9.20	1.60	13.67	2	2	98	0	0	17	36	47
A5	9.81	1.50	14.30	2	22	72	6	0	23	35	42
B7	2.16	1.00	12.54	1	0	17	0	83	32	29	39
B8	0.72	0.95	10.92	1	12	38	0	50	38	35	27
B9	0.36	1.05	9.73	1	25	50	0	25	53	38	9

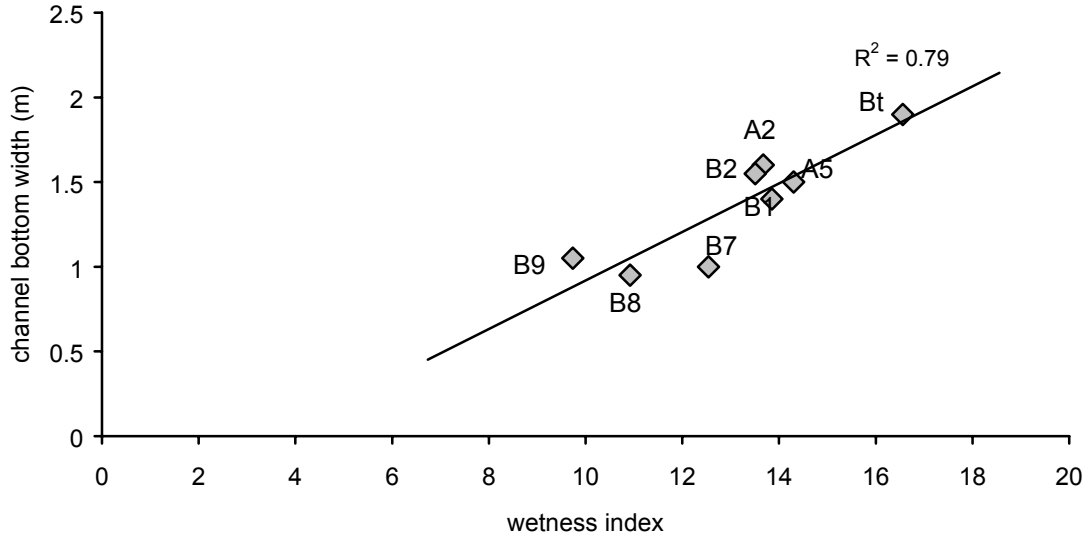

Figure 7.3 Bottom width as a function of wetness index at the outlet of the studied catchments.

Problems arise when the wetness index is used to calculate the channel network (Quinn et al., 1995). These include artefacts in the variable source areas and difficulties with correct averaging of multi-directional flow. For this reason the wetness index should not be used to define the streambed. In the selected catchments, the streambeds were defined based on field measurements as explained in chapter 8.

7.4 The rainfall-runoff relation

For the analysis of the rainfall-runoff relation every rainfall-runoff recording at a specific measurement location was regarded as a separate event. Rainfall events that did not result in discharge in the selected streambeds were disregarded. A definition of a rainfall event is given in section 4.2. In total 51 rainfall-runoff recordings from all selected catchments were combined in one group and used for further analysis.

Of the runoff recordings, both the total amount of runoff (figure 7.4) and the peak discharge (figure 7.5) were analysed for their relation with rainfall characteristics. To compare all records properly, the parameters were transformed to one-dimensional units i.e. mm water column and l/s/ha respectively. For the analysis, the total runoff amounts smaller than 0.005 mm water column (11 events) were disregarded because these estimates have a high degree of uncertainty due to the measurement error.

The relation between runoff and one or a combination of rainfall characteristics (i.e. total amount, storm duration, maximum intensity) was analysed by linear multiple regression. To meet the requirements of linear regression, both the total amount of runoff and the peak discharge were logarithmically transformed to obtain a normal distribution of the regression residuals. Also the storm duration was logarithmically transformed for this purpose.

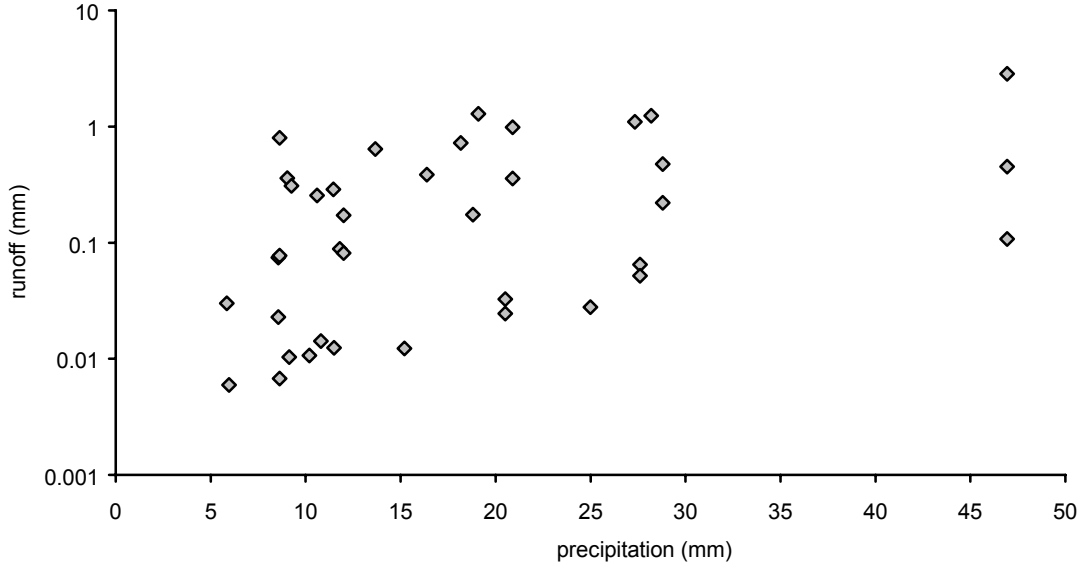

Figure 7.4 The recorded runoff amounts with corresponding rainfall in the selected catchments during the study period.

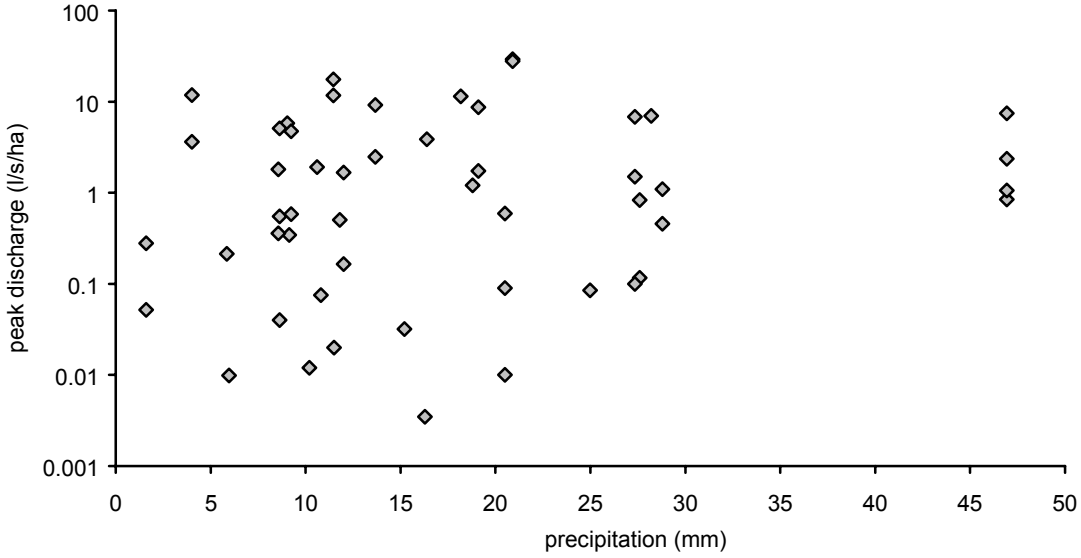

Figure 7.5 The recorded peak discharge with corresponding rainfall in the selected catchments during the study period.

The results showed that a rainfall-runoff relation valid for all studied catchments was absent. A significant relation was found ($p<0.05$) between the log-transformed runoff amount and the amount of precipitation, but the explained variance was very low ($R^2=0.12$). No statistical significant relation was found between the log-transformed runoff and storm duration and/or the maximum intensity, or between the log-transformed peak discharge and one or a combination of the selected rainfall

characteristics. So, based on the available data, there is no clear relation between runoff and rainfall characteristics when all observations are combined in one group.

7.5 Runoff influenced by catchment characteristics

7.5.1 Bottom width and wetness index as indicator for runoff

As noted in chapter 1, in catchments larger than a REA, the rainfall-runoff relation is characterized by the wetness index and the bottom width of the stream channel (Thornes, 1977; Beven & Kirkby, 1979; Gupta & Waymire, 1998). The area range of a REA in the study area is unknown. For the selected catchments it is unknown if the runoff is controlled by the wetness index and if the runoff in the selected catchments is indicated by the bottom width.

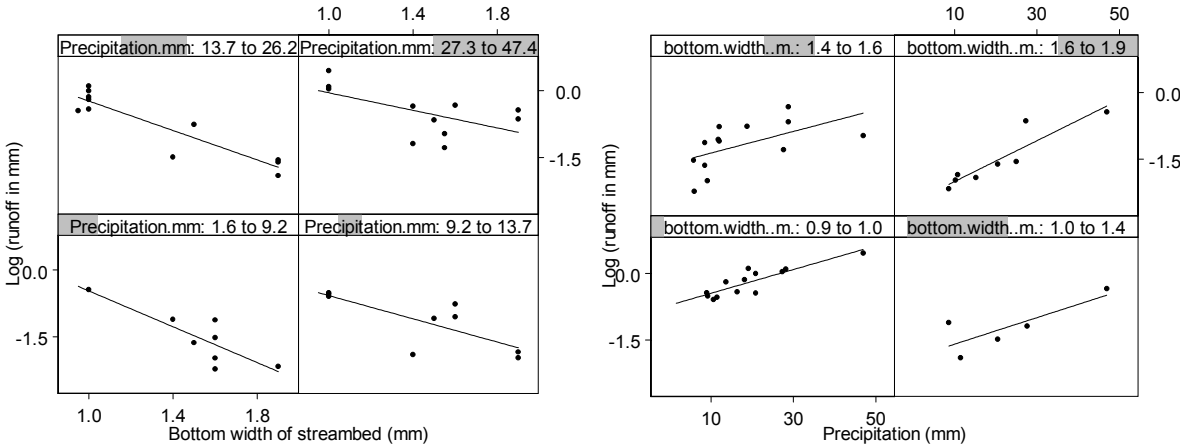

Figure 7.6 The estimated log-transformed runoff as a function of the measured bottom width conditioned at the precipitation (left) and as function of the precipitation conditioned at the bottom width of the streambed (right).

Linear multiple regression was used to see if the bulked measured rainfall-runoff events in all selected catchments were related to the wetness index and the bottom width (m) of the stream channel (table 7.1). First conditioning plots were made of the peak discharge or runoff amount depending on the precipitation and bottom width or wetness index (figure 7.6). It should be noted that in this analysis bottom width is used as an independent variable because it is used to indicate the extent of the runoff. All plots showed that the constraints for applying a multiple linear regression as defined in section 7.2, were fulfilled. Subsequently the contribution of the independent variables to the explained variance were estimated by stepwise multiple regression.

Between the log-transformed runoff (total amount and peak discharge), the bottom width and wetness index, significant relations ($p<0.05$) were found (table 7.2). The corresponding explained variances (R^2) indicate that the runoff (total amount and peak discharge) is better indicated by the bottom width and the wetness index than by

the rainfall amount once rainfall exceeds a threshold. The rainfall amount only contributes a small amount to the explained variance. The linear relations are based on all catchments including the smallest catchments B7, B8 and B9. In the previous section was explained that the wetness index and the bottom width of the stream channel are related. The accuracy of the wetness index in small catchments is less than in larger catchments and therefore analysis using the bottom width of the stream channel will give more reliable results. This might explain the differences in the explained variances of table 7.2 between the wetness index and the bottom width as independent variable.

Table 7.2 Explained variances between runoff and both the amount of rainfall and bottom width (BW) or Wetness Index (WI). Between brackets the R^2-change due to precipitation. Note; runoff amounts smaller than 0.005 mm were excluded from analysis and for rainfall conditions that exceed the threshold equation (4.1 and 4.2).

Explained variance (R^2) of multiple regression analysis ($U=ax_1+bx_2+c$)		
dependent variables (horizontal) independent variable (vertical)	Log (Runoff (mm)) (*LRO*) (n=40)	Log (Peak discharge (l/s/ha)) (*LPD*) (n=51)
Wetness Index (*WI*) + Precipitation (*P*)	0.49 (0.17) *LRO=* *2.792-0.316*WI+0.031*P*	0.46 (0.08) *LPD=* *4.430-0.372*WI+0.025*P*
Bottom Width (*BW*) + Precipitation (*P*)	0.61 (0.14) *LRO=* *0.942-1.744*BW+0.028*P*	0.59 (0.07) *LPD=* *2.321-2.126*BW+0.023*P*

7.5.2 Catchment surface as indicator for runoff

Another catchment characteristic is the surface area of the selected catchments. This variable is incorporated in the wetness index and its influence has as such been analysed. The catchment surface itself however is a variable which can easily be estimated unlike the wetness index. In the previous chapter it was concluded that the mean runoff coefficients decreased with increasing catchment size. This was illustrated by the hydrographs in figures 6.9 and 6.10. In chapter 4 the rainfall conditions were defined to generate runoff. To exclude the effect of the amount of precipitation on the amount of runoff for different catchment surfaces, the total amount of runoff was expressed as a fraction of the precipitation. A larger runoff fraction was observed within smaller catchment surfaces (figure 7.7). Also larger peak discharges were observed in smaller catchments than in the larger catchments. An example of such an event is given in figure 6.9 of the previous chapter.

The values of the runoff amount and the peak discharge in figure 7.7 show a decreasing variability with an increasing catchment size which is conform the REA-concept. The remaining variability of catchments B1, B2, A2, A5 and Bt suggests that all these catchments match the REA-constraints and catchment A2 can be defined as a REA because this catchment is the smallest catchment that fulfils the REA-constraints. However, these conclusions are based on a relative small number of measurements and

measurements of catchments with a size equal to or larger than Bt are lacking. Catchments consisting of a mixture of natural land cover and cultivated land will not fulfil the constraints of the REA because of the spatial heterogeneity caused by the water conservation measures in the cultivated fields, as discussed in chapter 2.

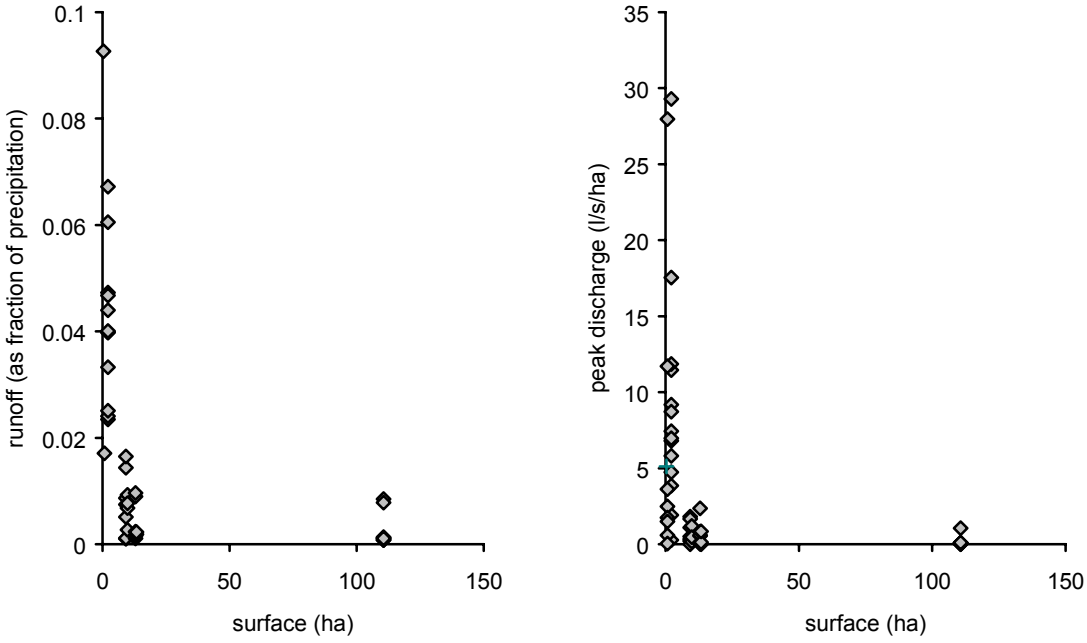

Figure 7.7 The runoff as fraction of precipitation (left) and the peak discharge (right) as function of the catchment surface.

Because of the small number of studied streambeds, the non-parametric Spearman R correlation test was used to estimate the relations between surface area and the fraction of runoff and the peak discharge respectively. For this analysis, the catchment size and average peak discharge were log-transformed. The runoff expressed as fraction of the precipitation was logit transformed by *ln(fraction/(1-fraction))* (Webster & Oliver, 1990).

The results (figure 7.8) show that the surface area of the studied catchment as a bounding polygon indeed influences the mean total amount of runoff and the mean peak discharge. The explained variances were reasonable, respectively 0.81 for the logit runoff and the log-transformed surface area and 0.69 for log-transformed peak discharge and surface area, they were significant ($p<0.05$) for both the peak discharge and the fraction runoff (figure 7.8). The decreasing amount of runoff and peak discharge in larger catchments indicates that hydrological processes on a small surface cannot be extrapolated to a larger surface simply by summation of the discharges of smaller surfaces.

The plots in figure 7.8 show a power law relationship between the runoff (defined as average standardised runoff amount) and respectively, the average peak discharge and the catchment size. The power-law relation indicates a log-log linearity over all

scales and is evidence of a pseudo-fractal behaviour (Burrough, 1993), in this case of the runoff.

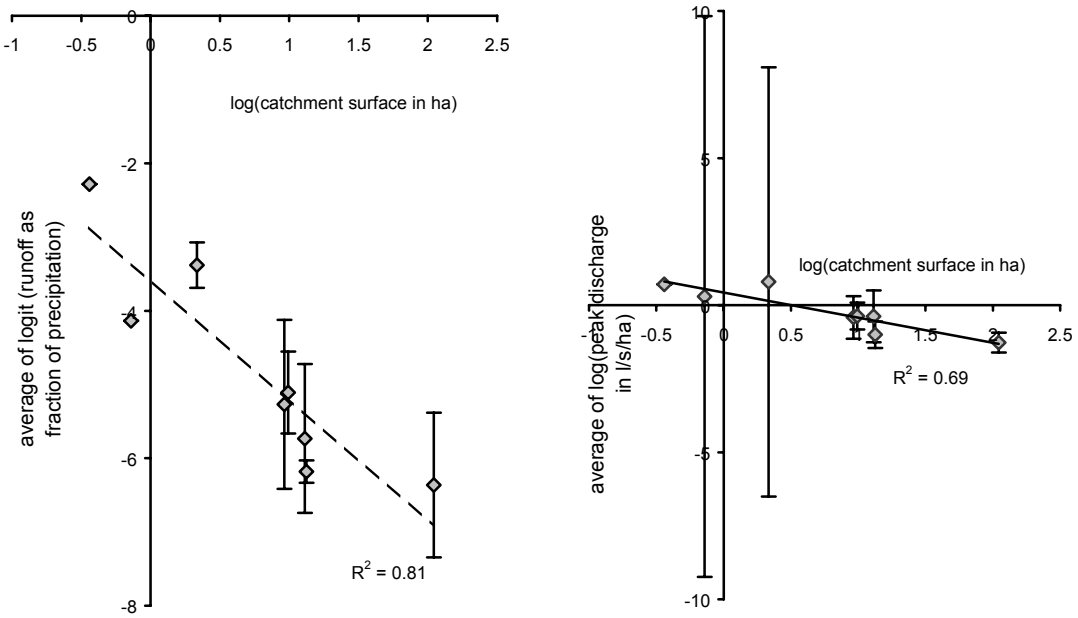

Figure 7.8 The average values of the logit runoff fraction (left) and the log-transformed peak discharge (right) as a function of the log-transformed catchment size. The error bars indicate the standard deviation.

A fractal is defined as an object which has variation that is self-similar at all scales, in which the final level of detail is never reached and never can be reached by increasing the scale at which observations are made (Burrough, 1993). This means that the variation in runoff is not linked to a single, dominant scale but is similar for all catchments sizes when it is transformed by a simple scaling parameter. A pseudo –fractal is a fractal for which the range of resolutions over which the variation is self-similar is limited. Based on the results in figure 7.8, the power-law relation was found for catchment sizes ranging from 0.36 to 110.60 ha. It seems likely that this power-law relation is valid for these catchments and all other catchments with a size between 0.36 and 110.60 ha given corresponding environmental controls and rainfall exceeding the threshold conditions (equation 4.1 and 4.2). If this is so, the power-law relation provides a tool to predict the average runoff quickly by calculating simple relations. When these equations are estimated from all recorded rainfall-runoff events instead of the mean values, they are:

$Logit(RO_p)= -1.70* log(CS) -3.28$	$(R^2=0.63)$	*equation 7.2*
$Log(PD)= -0.93*log(CS) +0.62$	$(R^2=0.47)$	*equation 7.3*

in which:
RO_p : runoff amount as fraction of precipitation
PD : peak discharge (l/s/ha)
CS : catchment surface (ha)

The fact that power-law relations were found for all catchments, invalidates the existence of a REA. In theory, the variation in runoff response of a REA should reach a minimum with increasing catchment size but the power-law relation indicates that the variation is not constant but varies with the scale of resolution. This is illustated by catchments B7, B8 and B9 for which the runoff response has not reached a minimum. Therefore these catchments cannot be defined as a REA. However, the power-law relation was found in rainfall-runoff recordings in which the recordings of catchment B7, B8 and B9 were included. The REA-concept will be further tested in the next chapter.

It is unknown whether the relations (equations 7.2 and 7.3) can be extrapolated to catchments smaller than 0.36 ha or larger than 110.60 ha. In study area, catchments with a size larger than the Bt catchment, consists almost always of a mixture of natural land cover and cultivated land cover. Because the cultivated areas in the study area are often located in the lowest parts of the catchments, the discharge of the largest catchments will strongly be controlled by the water conservation measures in the cultivated field as was discussed in chapter 2. For this reason the relations in equation 7.2 and 7.3 will not be used to predict the runoff in catchments that consist of natural land cover and cultivated land cover.

As was noted in chapter 6, the decrease of runoff with a larger catchment surface indicates transmission losses, which are known to play a major role in semi-arid flood hydrology of initial dry stream channels (Thornes, 1977; Butcher & Thornes, 1978; Lane, 1982, Thornes, 1994). Because the runoff in larger catchments is transported over longer distances along the stream channel, more water infiltrates in the stream channel, which is mostly before the start of rainfall events. This causes a redistribution of sediment within the catchment and only a part of the transported eroded material in the catchments will leave the largest catchment and is deposited in the valleys. Another reason for the decrease of runoff in larger catchments is the spatial variability in infiltration at a small scale of resolution (Yair & Lavee, 1985) which leads to a redistribution of water along the hill slopes (Puigdefabregas et al., 1999). Due to this phenomenon the fraction of precipitation that reaches the stream channel is lower with longer hill slopes because more water can infiltrate (figure 7.9). The sum of all sinks and the loss by evapotranspiration is calculated as (1-runoff fraction) in which the effect of transmission losses and discontinuous runoff at hill slopes are combined.

In the study area more than 90% of the precipitation infiltrated or evaporated before reaching the outlet. For the largest catchments the fraction of precipitation that infiltrated almost reached 100%. These results correspond with the results of a hydrological response study in south-eastern Spain (Puigdefabregas et al., 1999) in which the annual runoff coefficients decrease strongly with slope lengths up to 10 to 15 m. and remain less than 4% for greater slopes. This implies that near-channel areas probably form the main sources for runoff in the stream channel (Puigdefabregas et al., 1999).

Based on the average of the recorded events the average fraction of precipitation that infiltrates was calculated as the precipitation minus the runoff. A simple linear regression gives the average fraction of infiltration as a function of the maximum hill slope in the studied catchments being 0.74+0.043Ln(hill slope length in m). Note that the average infiltration in the largest catchment does not seem to differ from the mid-sized

catchments so an average infiltration of 99.7 % of the precipitation infiltrates along hill slopes of more than 650 metres in the study area.

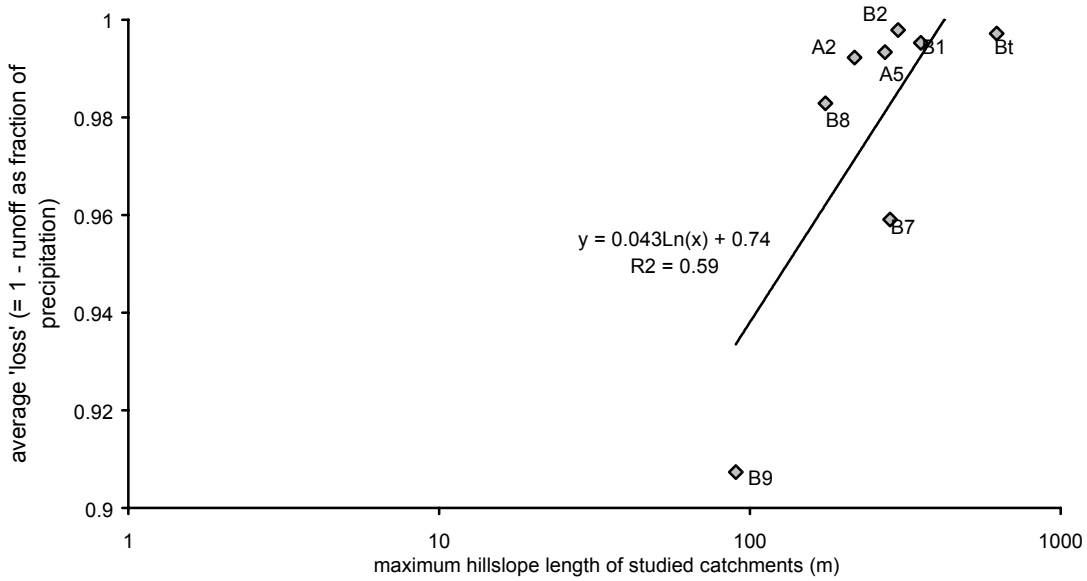

Figure 7.9 The average fraction of precipitation that infiltrated or evaporated during the recorded events depending on the maximum hill slope length of the studied catchments.

Unfortunately not enough simultaneous events were recorded at different levels of scale to analyse the exact amount of water that infiltrates between the outlets of the studied catchments at the successive levels of scale. Due to a lack of field data it was not possible to quantify the reduction of water in a more detailed manner than by average values as given in figure 7.9.

7.6 Runoff influenced by vegetation

In the previous section, it was shown that significant relations could be established between runoff and catchment characteristics. As discussed in section 1.4, vegetation cover is assumed to influence the rainfall-runoff response. The vegetation cover was estimated in chapter 3. Although in this study, no infiltration differences were measured between plant and inter-plant areas, previous research (Lyford & Qashu, 1969; Francis et al., 1986; Francis, 1990) showed a significantly higher infiltration under vegetation than in the bare soil between the plants at plot scale. This has lead to a widely accepted idea that vegetation cover controls the runoff at plot scale. However, the influence of vegetation cover on runoff in small catchments has not received the attention in research that it deserves. In this study vegetation cover is classified by land cover type and expressed as percentage surface cover per unit soil surface. Section 5.5 showed that almost all infiltration estimates, based on point measurements, could significantly be

related to the land cover type except for 'grassland' and 'woodland'. Vegetation cover at a small spatial resolution did not influence the infiltration estimates. In this section the influence of vegetation cover on the rainfall-runoff response is analysed, in which the interception, the infiltration as well as the redistribution of water along the hill slopes are included.

In section 6.5.3 (figure 6.9 and 6.10) of the previous chapter some of the hydrographs of the catchments of table 7.3 were presented. In section 6.5.4 it was tested and concluded that the peak discharge and runoff amount in sub-subcatchment B7 in all cases were significantly larger than in subcatchment B8. The peak discharge and runoff amount of subcatchment A2 were always larger than of subcatchment A5 and of subcatchment B1 always larger than of subcatchment B2. Table 7.3 shows that the land cover unit 'afforested terraces' in catchment B7 covers more surface as in catchment B8. Also the unvegetated soil surface covers a larger surface in catchment B7 than in catchment B8. The same differences in land cover and vegetation cover exist between catchment B1 and B2. The amount of unvegetated soil surface in catchment A2 equals more or less the unvegetated soil surface in A5 but catchment A5 included more 'natural woodland' while catchment A2 is almost entirely covered by 'grassland'.

Table 7.3 Vegetation cover (from table 7.1) in the catchments with different runoff response.

Catchment, large runoff response		Vegetation cover (%)	Catchment, small runoff response	Vegetation cover (%)
A2	Natural woodland	2	A5	22
	Grassland	98		72
	Bare soil	0		6
	Afforested terraces	0		0
	Unvegetated soil surface	47		42
B1	Natural woodland	9	B2	56
	Grassland	34		27
	Bare soil	6		14
	Afforested terraces	51		3
	Unvegetated soil surface	42		21
B7	Natural woodland	0	B8	12
	Grassland	17		38
	Bare soil	0		0
	Afforested terraces	83		50
	Unvegetated soil surface	39		27

Preliminarily to further analysis, the vegetation cover seems to explain why the rainfall-runoff response is different for the selected catchments. The results of section 5.5 show a smaller saturated conductivity for 'bare soil' and 'afforested terraces' than for 'grassland' and 'woodland'. Previous research (Nonhebel, 1999; Houkes, 1998) showed a larger infiltration in the land cover unit 'woodland' than in other land cover units. The afforested terraces in the study area consist of terraces of by bulldozers disturbed soil vegetated with only small planted indigenous pine trees. The disturbance of the soil has resulted in deterioration of the soil condition towards infiltration and growth. Therefore the land cover units 'afforested terraces' and 'bare soil' are presumed to contribute to faster routing of runoff than 'grassland' and 'woodland'. For this reason the surface

covered by the land cover units 'afforested terraces' and 'bare soil' was used as variable for multiple regression analysis together with precipitation. Furthermore unvegetated soil is assumed to contribute to faster routing of water because of the low resistance between the plants. Therefore unvegetated soil was selected as variable for multiple regression analysis together with precipitation.

Both the amount of land cover and soil surface were calculated as the mean percentage of a catchment by which they did not account for the surface of the studied catchments and expressed as the logit transformed percentage cover of the catchment.

As assumed for the REA-concept, the pattern of soil, topology and vegetation is not important in controlling the runoff in catchments. For this reason it was expected that the percentage of vegetation cover (expressed as land cover units or as surface cover) can be used in the same way catchment characteristics were used (section 7.5). In catchments smaller than a REA the vegetation pattern and hence its spatial variability is important and should be incorporated as will be discussed in the next chapter.

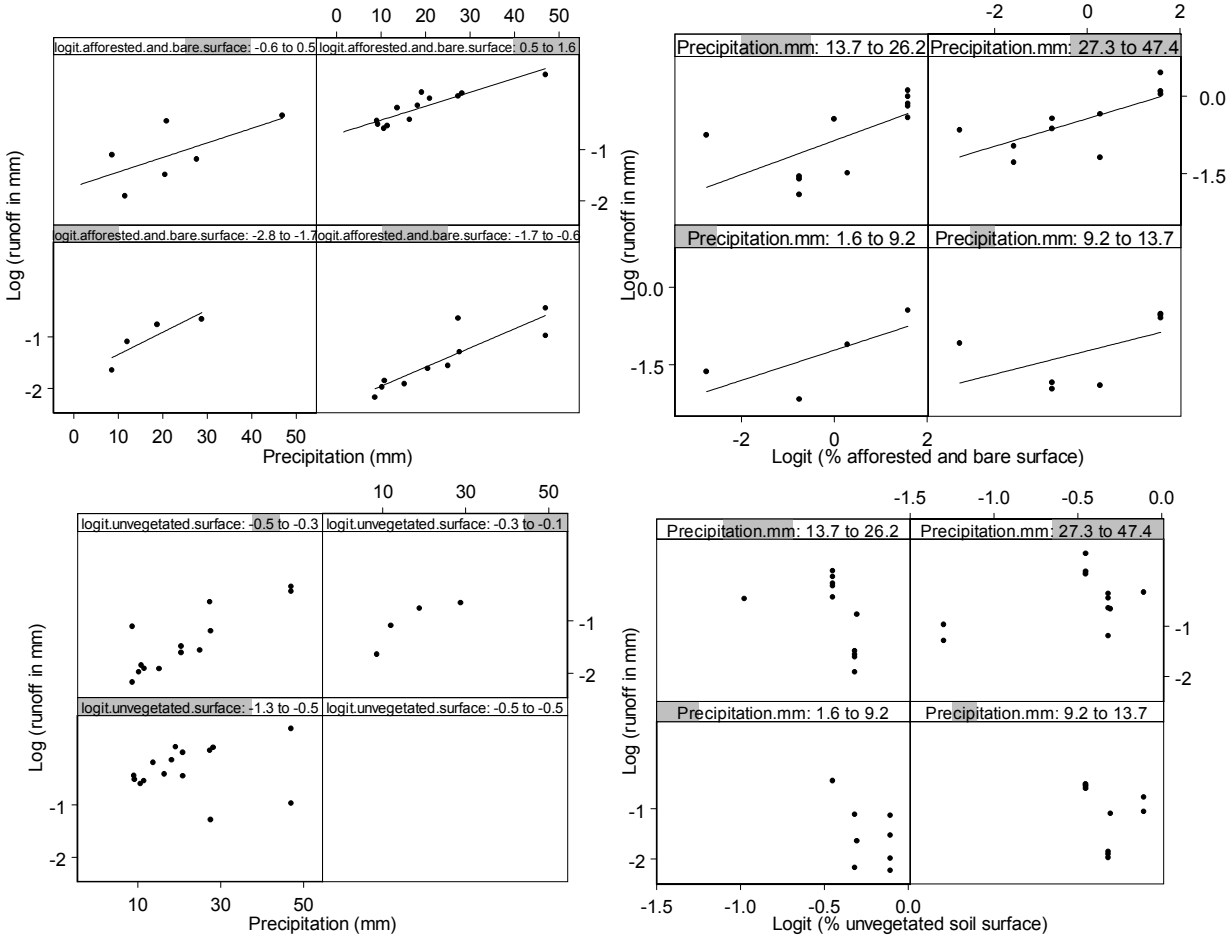

Figure 7.10 The log transformed runoff amount as function of precipitation and land cover units 'afforested terraces' and 'bare soil' (upper scatterplots) and as function of precipitation and unvegetated soil surface (lower scatterplots).

First conditioning plots were made of the bulked estimated runoff amounts as function of precipitation and land cover or surface cover and bulked estimated peak discharges as function of precipitation of land cover or surface cover.

The conditioning plots of the log transformed runoff amount as function of precipitation and unvegetated soil surface did not show linear relations (figure 7.10). This is probably due to the small variation in unvegetated soil surfaces between the selected catchments and the small number of observations (table 7.1). The runoff estimates for catchments with the smallest unvegetated soil surfaces (B9 and B2) have the largest deviation from the residual scatter in the plots. Only few estimates have been made in these catchments.

From the conditioning plots (figure 7.10) it is concluded that at the scale of a catchment, the classified land cover units 'afforested terraces' and 'bare soil' control the runoff amounts to a larger extent than the summed unvegetated surface cover at pixel basis. The conditioning plots of the log transformed runoff as function of precipitation, land cover 'afforested terraces' and 'bare soil' show a linear relation and suggest multiple linear regression analysis may be worthwhile. The results of multiple regression analysis are presented in table 7.4. The explained variance is modest (0.39) but significant which means that the regression residuals have a large dispersion.

Table 7.4 Explained variances between runoff amount and both the amount of rainfall and land cover 'afforested terraces' and 'bare soil' for rainfall conditions that exceed the threshold equation (4.1 and 4.2). Between brackets the R^2-change due to precipitation.

Explained variance (R^2) of multiple regression analysis ($U=ax1+bx2+c$)	
Dependent variables (horizontal) Independent variable (vertical)	Log (Runoff (mm)) (*LRO*) (n=33)
Logit (% afforested terraces and bare soil) (*LAB*) + Precipitation (*P*) in mm	0.39 (0.14) *LRO=-1.289 + 0.264*LAB+0.023*P*

The conditioning plots of the log transformed peak discharge as function of precipitation and unvegetated soil surface did not show linear relations (figure 7.11). The unvegetated soil cover estimates do not show much variation. They were calculated as the sum of the fraction unvegetated soil cover per pixel of the selected catchments and the estimates include a considerable amount of uncertainty as described in chapter 3.

The unvegetated soil cover estimates do not include the pattern of the vegetation cover. From the conditioning plots in figure 7.10 and 7.11 it is concluded that at the scale of a catchment, unvegetated soil surface is not a proper variable to estimate to what extent the vegetation cover controls the runoff. This is due to the use of the total amount of unvegetated soil per catchment by which the influence of surface cover on runoff is 'smoothened' and because the unvegetated soil controls the runoff in an area smaller than the cell size of which the amount of unvegetated soil was calculated.

Also the log transformed peak discharge as function of precipitation and the land cover units 'afforested terraces' and 'bare soil' did not show a linear relation (figure 7.11). Because former analysis showed no relation between precipitation and peak discharge (section 7.4) the non-parametric Spearman r correlation was used to estimate the

correlation coefficients between ordinal ranked peak discharges and the logit percentages cover of land cover 'afforested terraces' and 'bare soil'. The results, based on 51 estimates, showed a significant correlation coefficient of 0.58 between peak discharge and the logit of the summed land cover units 'afforested terraces' and 'bare soil'.

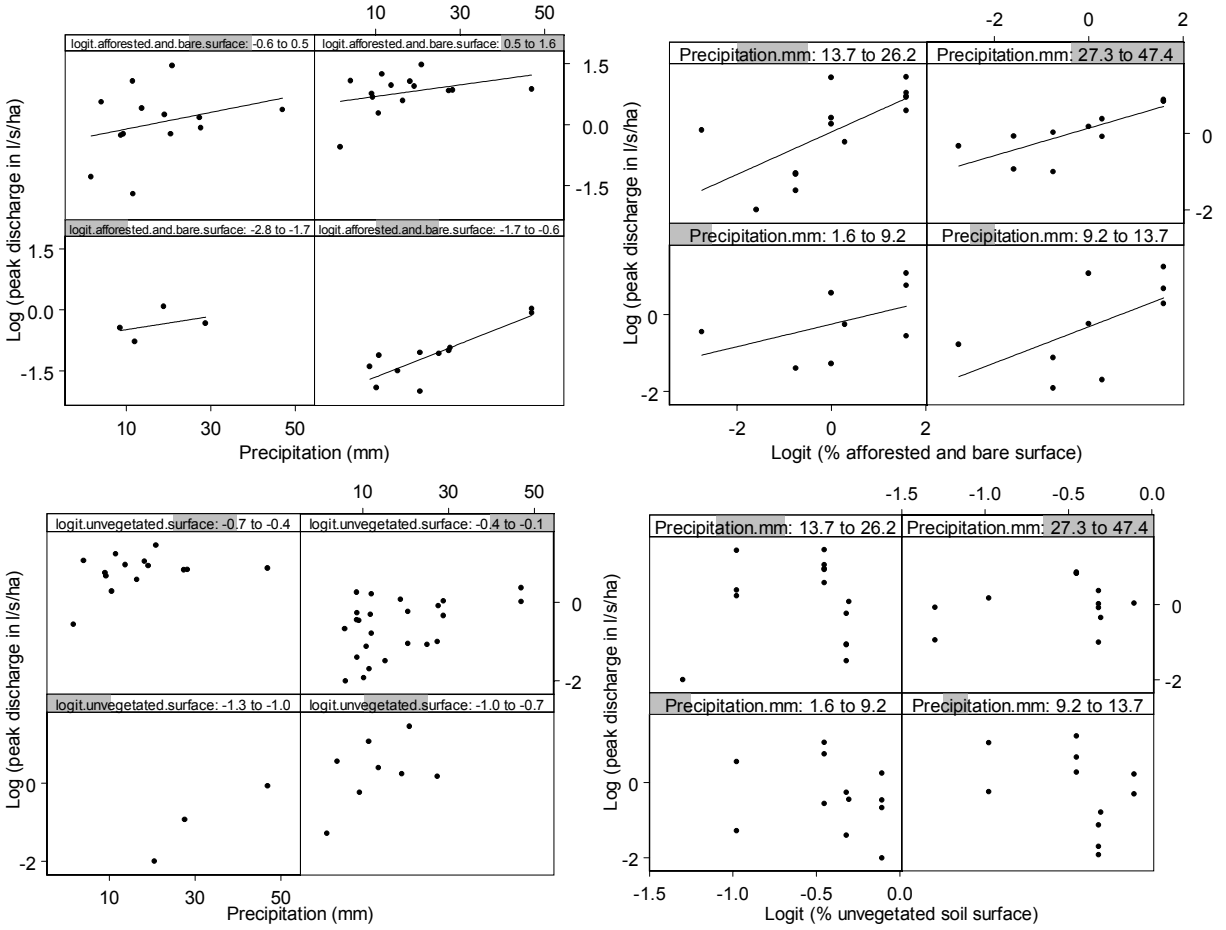

Figure 7.11 The log transformed peak discharge as function of precipitation and land cover units 'afforested terraces' and 'bare soil' (upper scatterplots) and as function of precipitation and unvegetated soil surface (lower scatterplots).

The results of this section show that the influence of land cover on runoff amount and peak discharge respectively is theoretically sound and assumable but could only be proved by weak correlations. This might be due to the limited number of studied catchments i.e. 8, with corresponding limited variation in vegetation cover and no significant different infiltration capacity for 'grassland' or 'natural woodland'. Next to the small number of measured catchments, the weak correlations might be the result of the combination of other factors that also control the runoff like the bottom width of the streambed (section 7.5) rainfall characteristics (as discussed in the next section) and other unknown variables. Outlined against the clear difference in hydrological response of catchments with the same catchment size (section 6.5.4), the influence of vegetation cover needs to be further examined.

7.7 The rainfall-runoff relation at different resolutions

In chapter 4, the most important runoff controlling rainfall characteristics were defined as rainfall amount, maximum rainfall intensity and storm duration. Chapter 1 discussed that storm duration controls runoff because it determines the survival length of the flow and in chapter 4 field recordings showed that the occurrence of runoff was related to the maximum rainfall intensity and the storm duration. In spite of the theoretic relation between rainfall characteristics and runoff amount and peak discharge respectively, these relations were not found in section 7.4 for the dataset in this study except for a weak but significant relation between runoff amount and rainfall amount. Rainfall characteristics can not be used to predict the runoff in the grouped studied catchments in the same way as the catchment characteristics were used. This section aims to analyse the relation with rainfall characteristics and the runoff in different sized catchments

The runoff expressed in total amount and peak discharge is partly controlled by the catchment surface. The selected catchments can be divided into three levels of scale (table 7.5) based on their stream order and catchment surface (table 2.2).

Table 7.5 Selected catchments and number of recorded rainfall-runoff events for every level of resolution.

Level of scale	Number of catchments	Stream order	Names of catchments	Catchment surface (ha)	Number of rainfall-runoff events
I	3	1	B7, B8, B9	0.7 – 2.2	18
II	4	2	B1, B2, A2, A5	9.2 – 13.3	19
III	1	3	Bt	110.6	9

If the runoff is influenced by the level of scale, the runoff recordings of total amount and peak discharge should differ significantly from each-other and the rainfall-runoff relation can be analysed for each level of scale separately. This way a better understanding is obtained of the factors other than the topographic index, channel width and the catchment surface, that control the rainfall-runoff relation at a smaller resolution.

The log-transformed amount of runoff and peak discharge of the recorded rainfall-runoff events (figure 7.12) show that is possible to make a distinction between the different levels of resolution. This distinction for the log-transformed runoff amounts as function of rainfall is clearer than it is for the log-transformed peak discharge as function of rainfall. This can be explained by the influence of discontinuities of the streambed that results in streambed storage by which the direct runoff response and hence the peak discharge is buffered. For very small rainfall events the log-transformed peak discharge is clearly not different per level of scale because only small parts of the streambed respond. The log-transformed runoff is clearly different per level of scale for small rainfall amounts (smaller than 20 mm) but for larger rainfall amounts scale level II and III respond more or less the same. This is probably caused by a complete usage of the infiltration capacity because when the rainfall increases surface water infiltrates at more parts of a hill slope.

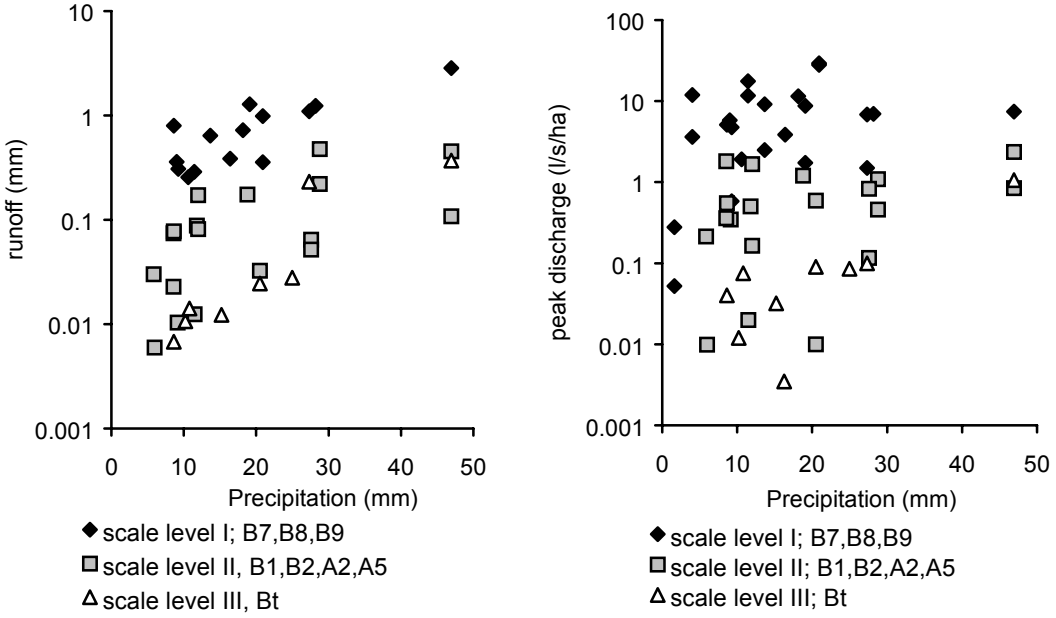

Figure 7.12 The total amount of runoff (left) and the peak discharge (right) for every level of resolution indicated by the dotted lines. Note; runoff amounts < 0.005 mm water column have been disregarded.

Cammeraat (in press) published minimum rainfall amounts needed to generate runoff at plots, hill slopes, subcatchments and catchments in the study area. The rainfall amounts for runoff generation increased with increasing surface area. Based on Cammeraat (in press) one would expect that the amount of rainfall needed to generate runoff at scale level III is higher than the amount of rainfall needed to generate runoff at scale level I. This is partly confirmed by the measurements in the study area (right graph of figure 7.12), however the differences are not very distinct. The indistinct differences in rainfall amount generating runoff at different levels of resolution, implies that only the amount of rainfall is not a valid parameter to characterise rainfall for runoff generation. It suggests that besides rainfall amount, rainfall should also be characterised by a combination of its maximum intensity and its duration.

Whether the rainfall-runoff recordings of figure 7.4 and 7.5 could indeed be subdivided per level of scale significantly, was tested statistically. The non-parametric Kolmogorov-Smirnov test was used to determine if the log-transformed runoff recordings were significantly different from runoff recordings at another level of resolution. This test is used because the variables are grouped per level of resolution and by this test the difference between the cumulative distributions is tested. The runoff amounts were expressed as the logit (runoff) to standardise the runoff amounts for the influence of precipitation.

The results showed that the logit-transformed runoff fractions of an event at one scale level were significantly ($p<<0.05$) different from each of the other levels of scale level (figure 7.13). The difference between scale level II and III is mainly the result of the

contribution of the runoff amounts measured under rainfall events with small amounts (< 27 mm) as was explained by figure 7.12.

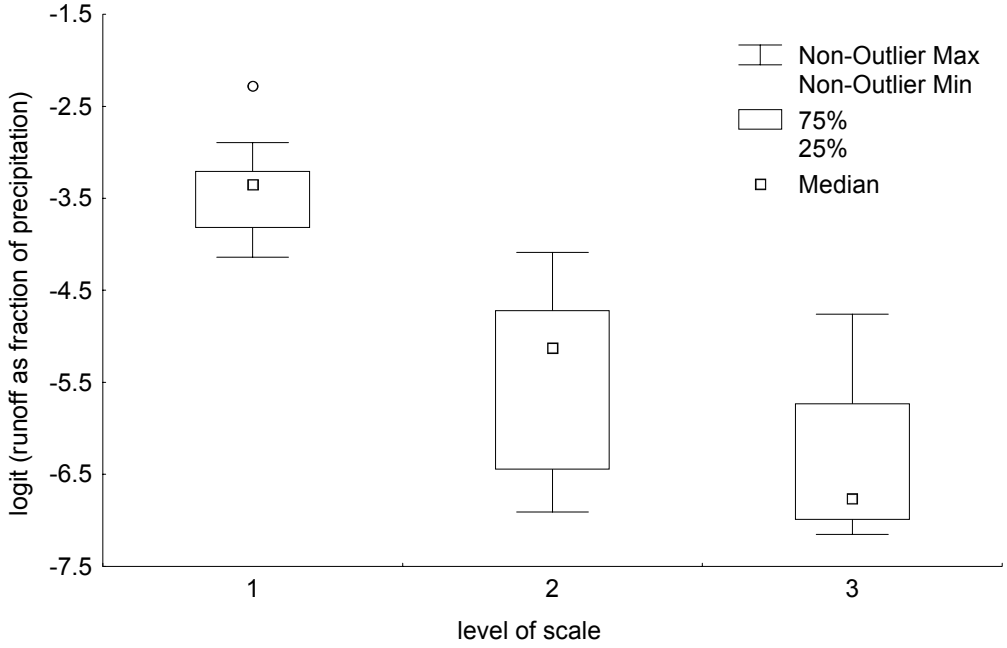

Figure 7.13 Box-Whisker plot of the log-transformed runoff at different levels of scale, outliers (indicated by a circle) differ more than one standard deviation from the mean. Note that this is a statistical representation of the data in which the different groups are plotted along the x-axis without indicating its magnitude, in contrast to figure 7.8.

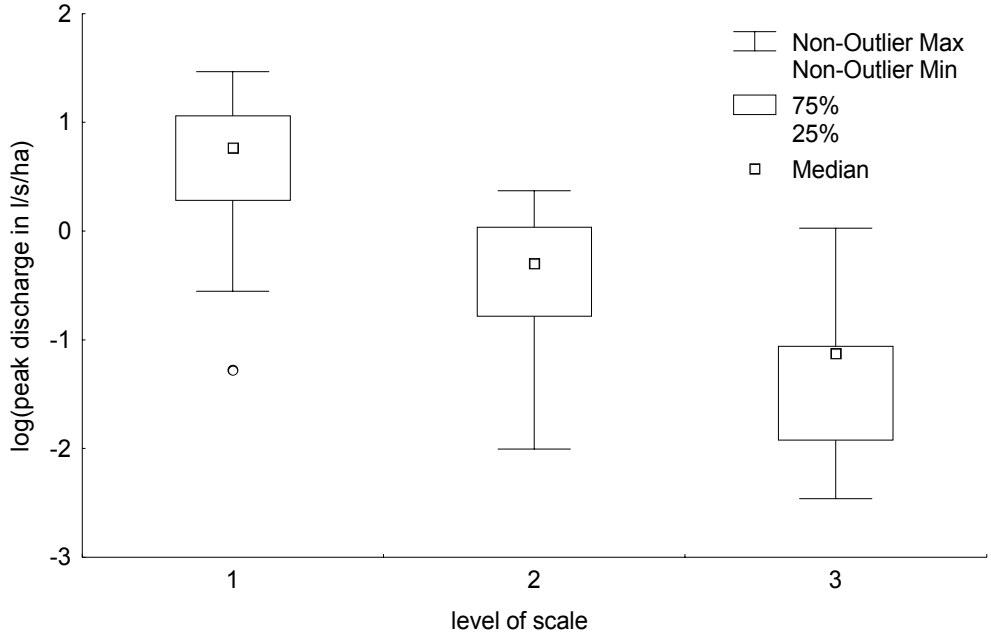

Figure 7.14 Box-Whisker plot of the logarithmic transformed peak discharge at different levels of scale, outliers (indicated by a circle) differ more than one standard deviation from the mean. Note that this is a statistical representation of the data in which the different groups are plotted along the x-axis without indicating its magnitude, in contrast to figure 7.8.

The recordings of the log-transformed peak discharge for all levels of scale were significantly ($p<<0.05$) different from recordings at other levels of scale (figure 7.14). The results (figure 7.13 and 7.14) suggest that the level of scale indeed influences the rainfall-runoff relation. For this reason the rainfall-runoff relation was further analysed at the separate levels of scale.

The recorded rainfall-runoff events were ordered per level of scale (figure 7.15 and figure 7.16). The runoff amounts (figure 7.15) for each level of scale show a linear relation with the rainfall amount. The runoff amounts in the smallest catchments were largest and decreased with increasing catchment size. In the smallest catchments the runoff response was controlled by the rainfall intensity. In larger catchments, the influence of the rainfall intensity and storm duration is less clear. In small catchments the travel distance of the runoff to the outlet of the catchments is small which explains the direct response of runoff towards rainfall characteristics. In larger catchments the runoff on hill slopes and in streambeds is often discontinuous by which the runoff responded indirectly on rainfall characteristics. It should be noted that the recordings of runoff amount at scale level I consist of recordings in B7 added with one event recorded in B8 and one in B9. The recordings at scale level III refer to only catchment Bt. For this reason the differences in runoff amounts at scale level II (B1, B2, A2, A5) were largest. These runoff amounts had the same order of magnitude as the recordings of Bt.

The scatterplots of the peak discharge (figure 7.16) as function of amount of precipitation, storm duration and maximum rainfall intensity did not show linear relations. The recorded peak discharges were largest at scale level I. At this level of scale, the peak discharge as function of the maximum intensity seems to have an asymptotical course by which it reaches a maximum value. Other relations except between the peak discharge of Bt and the rainfall amount, were not clear. For the recorded peak discharges, the dispersion in data is large at scale level II. The values of the recorded peak discharges at scale level II were in the same order of magnitude as the recordings of scale level III.

For each level of scale, the correlation coefficients were calculated between runoff and peak discharge on one hand and rainfall characteristics (amount, storm duration and intensity) on the other hand by simple correlation. For the log-transformed total runoff amounts and the rainfall amount or the storm duration the Pearson r correlation was calculated because a linear relation was assumed.

The correlation coefficient between the runoff amount and the rainfall intensity was calculated as the non-parametric Spearman r correlation because the scatterplots (figure 7.15) did not indicate a linear relation. This non-parametric correlation was also used for calculation of the correlation between the peak discharge and the rainfall characteristics because figure 7.16 did not indicate linear relation.

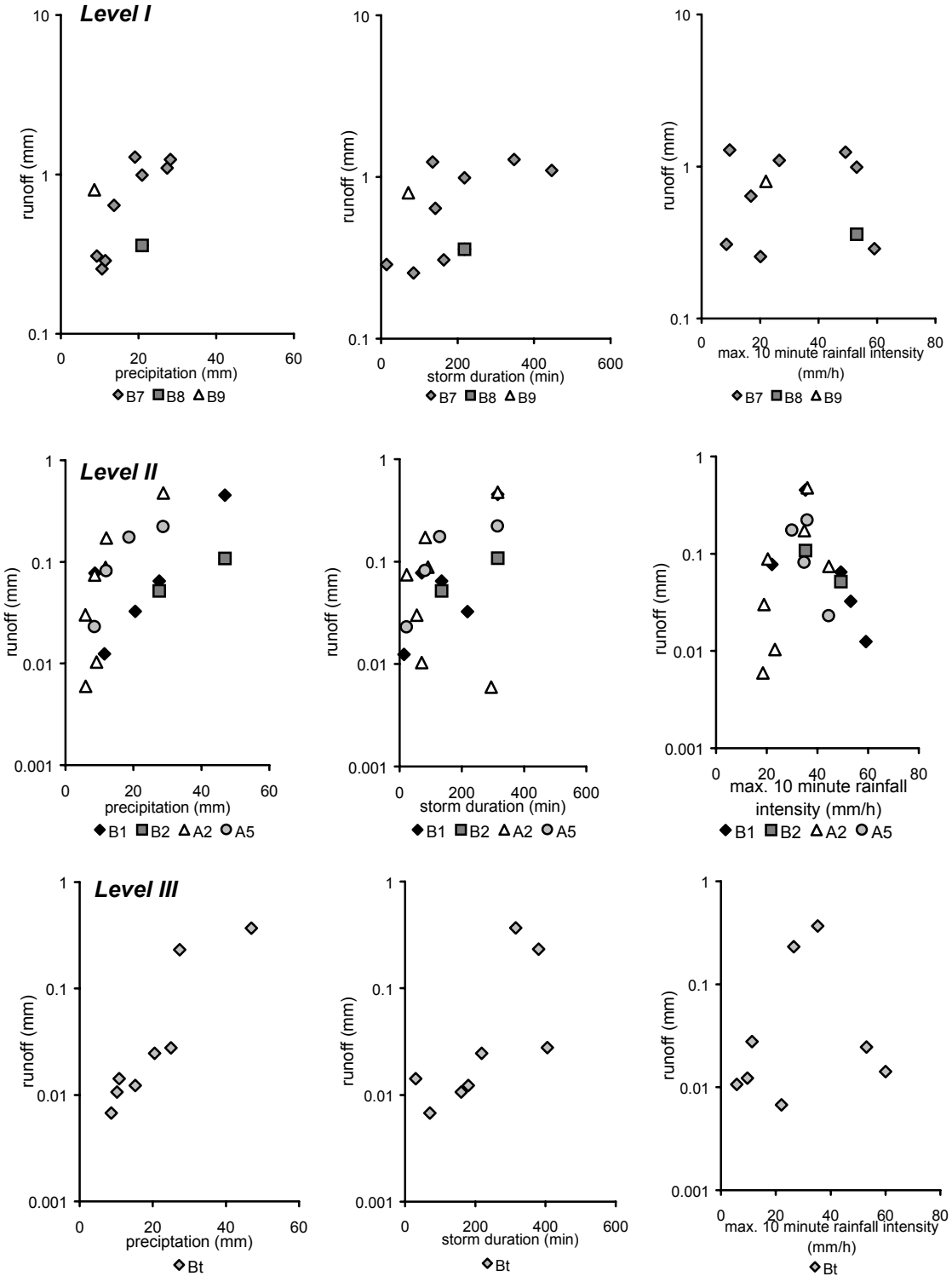

Figure 7.15 The runoff amounts as function of rainfall characteristics (amount of precipitation, storm duration and maximum intensity) ranging from scale level I (upper graphs) to scale level III (lowest graphs). Note the difference in magnitude of the y-axis for the different levels of scale.

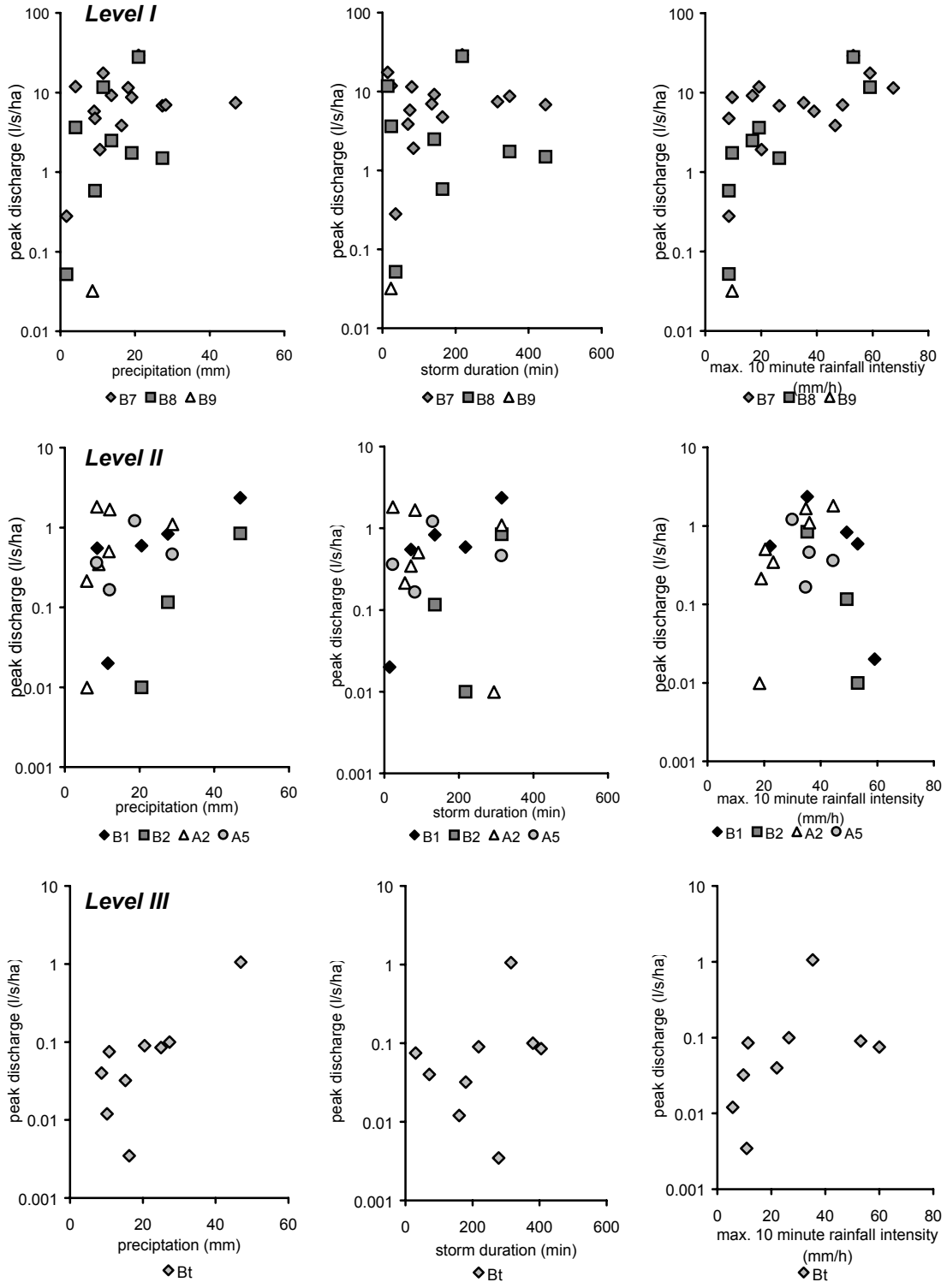

Figure 7.16 The peak discharge as function of rainfall characteristics (amount of precipitation, storm duration and maximum intensity) ranging from scale level I (upper graphs) to scale level III (lowest graphs). Note the difference in magnitude of the y-axis for the different levels of scale.

In contrast to the results of the rainfall-runoff analysis in section 7.3, the results (table 7.6) show that for all separate levels of scale significant correlation coefficients were obtained for runoff and the total amount of precipitation, and for scale level I and III for runoff and storm duration. It should be noted that the runoff recordings of scale level III were derived from only one catchment. At scale level I a significant correlation coefficient was calculated between the peak discharge and the maximum rainfall intensity. This is probably due to the rapid response of runoff on the rainfall in small catchments. This confirms the importance of measuring the maximum intensity over small time intervals in order to estimate the magnitude of the peak discharge in small catchments. At scale level III significant correlations were calculated between the peak discharge and the amount of rainfall. At this scale many small catchments contribute to the discharge of the total catchment and the peak discharge is a composite of several discharges. For scale level II it was not possible to establish significant relations between rainfall characteristics and the peak discharge. This suggests that except for rainfall characteristics, the peak discharge within the same level of scale is influenced by other factors. The influence of other factors will be discussed in the following section.

Table 7.6 The correlation coefficient of the significant relations ($p<0.05$) between rainfall characteristics and runoff for different levels of resolution (not significant correlations are printed between brackets). Note that the correlations between runoff amounts and rainfall amount or storm duration were calculated by Pearson r and the remaining correlations were calculated by Spearman r.

Correlation coefficients				
Rainfall characteristics (horizontal) and runoff (vertical)		Precipi-tation (mm)	Maximum intensity (mm/h)	Storm duration (min)
level of scale I	Log(Runoff (mm)) (n=15)	**0.80**	(-0.05)	**0.63**
	Log(Peak discharge (l/s/ha)) (n=23)	(0.36)	**0.69**	(-0.05)
level of scale II	Log(Runoff (mm)) (n=19)	**0.61**	(-0.02)	(0.41)
	Log(Peak discharge (l/s/ha)) (n=19)	(0.37)	(-0.02)	(0.18)
level of scale III	Log(Runoff (mm)) (n=9)	**0.92**	(0.43)	**0.72**
	Log(Peak discharge (l/s/ha)) (n=9)	**0.73**	(0.70)	(0.47)

The significant relations between runoff amount and peak discharge respectively with rainfall characteristics for the runoff recordings grouped per level of resolution, indicates that the rainfall-runoff relation is scale-dependent and cannot be used to predict the runoff in different sized catchments.

7.8 Discussion

The total data set analysed comprised 46 events. A few events were not considered in the analysis because calibration of the runoff recordings by the record gauge of B7 and B8 resulted in runoff amounts nearing zero. After exclusion of these events, only one rainfall-runoff event was recorded in sub-subcatchment B8 and one sub-subcatchment B9 at scale level I. Furthermore, runoff recordings at scale level III took place in only one

catchment. This might have reduced the variability in the recorded runoff amounts at scale level I and in the both the recorded runoff amounts and the peak discharges at scale level III.

The size of a REA was estimated based on the field recordings but runoff recordings of more than one catchments at scale level III were lacking. Given the large variability in runoff in the sub-subcatchments at scale level I, these are considered to be smaller than the REA but the runoff recordings were included to estimate the linear relations.

According the REA-concept, the spatial distribution of parameters should not influence the results of the hydrological analysis for catchments with sizes equal to or larger than a REA. For the analysis of the influence of the vegetation cover, the mean percentage of the percentage unvegetated surface cover per unit area was used which did not differ much for the different selected catchments because it was a value averaged over the different catchments. Furthermore, the spatial distribution of the unvegetated surface cover was disregarded while this is important for the hydrological response of catchments smaller than a REA.

The data set on which the analyses of this chapter are based, does not include extreme rainfall events because during the few extreme events logistic problems occurred and these events were not recorded. For this reason the data set is limited and gives insight in ordinary rainfall with a small recurrence period. Between the recorded runoff events at least several days elapsed and the soil dried. The equations presented in this chapter are not valid for rainfall conditions other than during the rainfall recordings of this study. It should be noted that the mean runoff and peak discharge used in the presented equations are based on the recordings of ordinary runoff events and as such do not include extreme runoff events. The large floods that cause damage occur under different rainfall conditions (Cammeraat, in press) consisting of several storms shortly after each other by which the soil is moist. When under these conditions extreme rainfall events occurs with high rainfall intensities, the results can be devastating.

7.9 Conclusions

Statistical hydrological analysis of the recorded runoff showed that variability of the runoff amount and peak discharge decreases with increasing catchment size. The runoff amounts and peak discharges of catchments ranging from 9.2 to 110.6 ha were in the same order of magnitude for all catchments. Because the variability in runoff had reached a minimum in these catchments, they fulfilled one of the constraints for the definition of a REA. Based on the decrease in variability of the runoff and peak discharge catchment A2 with a size of 9.2 ha, could be defined as a REA.

However, a power-law relation between the runoff and the catchment size was found (table 7.7) based on all catchments including the smallest catchments B7, B8 and B9 in which the variability in runoff had not reached a minimum. This relation indicates that the runoff amount and peak discharge are pseudo-fractals for which the variation of runoff as fraction of precipitation and peak discharge are self-similar. This means that the variation of the runoff amount and peak discharge of large catchments is similar to

the variation of a small catchment when it is transformed by a simple scaling parameter and therefore the variation depends on the catchment size. This is in contrast to the REA-concept, which states that the variability of runoff reaches a small constant value with increasing catchment size. The existence of the power-law relation indicated that the REA-concept may not be a valid tool for hydrological modelling after all.

Table 7.7 Estimated log-linear relations between runoff and catchments characteristics, P stands for Precipitation in mm and rainfall conditions exceed the threshold equation (4.1 and 4.2).

	Catchment Size (CS) in ha	Bottom width (BW) in m.	Logit (fraction afforested terraces and bare soil in catchment) (LAB)
Runoff (RO) in mm	Logit(RO_p)= -1.70* log(CS) -3.28 R^2=0.63 *RO_p is RO as fraction of P*	Log(RO)= 0.94-1.74*BW+0.03*P R^2=0.61	Log(RO)= -1.29+0.26*LAB+ 0.02*P R^2=0.39
Peak discharge (PD) in l/s/ha	Log(PD)= -0.93*log(CS) +0.62 R^2=0.47	Log(PD)= 2.32-2.13*BW+0.02*P R^2=0.59	No linear relation; Non-parametrically tested R^2=0.34

Next to the catchment size, the runoff amount and peak discharge in all catchments ranging from 0.4 – 111 ha. can quickly and easily be calculated by log-linear relations based on the bottom width and amount of land cover 'afforested terraces' and 'bare soil' (table 7.7). The use of the total amount of unvegetated soil per catchment is not a proper variable to estimate the influence of surface cover on runoff. Therefore vegetation types defined as percentage of surface cover were not found to control the runoff response of the selected catchments. The wetness index also significantly controlled the runoff amount and peak discharge but this variable incorporates the catchment surface and depends on the bottom width which are both more easily to estimate and more reliable than the wetness index. The log-linear relations are based on the runoff recordings of all catchments, including the smallest catchments B7, B8, B9. This indicates that the log-linear relations are valid for catchments ranging from 0.4 ha. to 111 ha.

When the recorded runoff and rainfall were analysed as one group, it was not possible to estimate rainfall-runoff relations for the runoff amount or the peak discharge. When the rainfall-runoff records are split in different scales of resolution, the rainfall amount is related significantly to the runoff amount per level of resolution. Other relations between rainfall characteristics were found such as at scale level I (B7, B8, B9) and III (Bt), the storm duration controlled the runoff amount. At scale level I the peak discharge was controlled by the maximum rainfall intensity and at scale level III the peak discharge was controlled by the precipitation amount. The presence of relations between rainfall characteristics and runoff per level of scale and the absence of these relations when the runoff recordings are combined in one group implies that the rainfall-runoff relation depends of the scale of resolution and cannot be used to the describe the runoff response in catchments with differing catchment size.

8 Hydrological modelling

8.1 Introduction

In chapter 7, it was shown that small catchments (B7, B8, B9) have a very variable runoff response. Simple lumped linear regression models cannot be used for runoff prediction at this spatial resolution, other than to make a rough estimation of the average runoff. As shown in section 7.6, the runoff response differs between the studied catchments within one level of resolution and is controlled by a set of parameters the influence of which is difficult to estimate. In this situation, a dynamic distributed model may be a useful tool to simulate runoff by including the spatial distribution of parameters within the REA. For this reason a 'semi-arid Mediterranean discharge model' (SAMDIM) was developed based on the knowledge and field data obtained in this study. After calibration, SAMDIM was used to test the remaining objectives of this study. The aims of this chapter are described as follows:

i. In the previous chapter the influence of land cover on the runoff of catchments was quantified by a lumped model. Here, the aim is to quantify the influence of land cover on runoff in different sized catchments by using a distributed model that includes the spatial distribution of the land cover.
ii. In chapter 7, the catchments defined as a REA were defined based on the decreasing variability of runoff with increasing catchment size. Another constraint of the REA-sized catchments is that the spatial distribution of model input parameters does not influence the runoff response. This means that the size of a REA can be estimated by finding the catchment sizes for which there is no change in runoff response to changes in the spatial distribution of the input parameters, with maintenance of its statistical mean and distribution (Beven & Wood, 1993). The aim is to test if the in chapter 7 as REA defined catchments fulfilled this constraint as well.
iii. Discontinuous runoff on hill slopes is characteristic for a semi-arid Mediterranean area. Given the discontinuous surface flow and the small runoff coefficients that decrease with increasing catchment surface, the hypothesis is that runoff at the outlet of the catchments is dominated by hydrological processes in and near the upstream located parts of the streambed. It means that the spatial distribution of the characteristics of REA-sized catchments is important because of the increased influence of the characteristics along the streambed. Discontinuity of runoff is not taken into account by the REA-concept. The aim is to test the hypothesis that the runoff at the outlet of the catchments only comes from the upstream streambed.

8.2 Hydrological model components

Despite the existence of numerous models that simulate the transport of water, the author chose to develop a model herself. This way the used principles and algorithms could be selected and implemented by the author. This implies that model is transparent and the author fully understands how the model acts. This way the model easily can be modified to the conditions of the study area.

The model SAMDIM includes the components of the water balance as outlined in chapter 1. The structure of the model is given in figure 8.1. The assumptions made for the different model components are outlined in the following sections.

SAMDIM is a distributed hydrological model that simulates the runoff by taking into account the spatial distribution of the used parameters. SAMDIM was developed in PCRaster© GIS (Wesseling et al., 1996) which is a Geographical Information System (GIS) with a programming language in which complex spatio-temporal models can be developed. By developing SAMDIM in a raster GIS, the spatial distribution of parameters and the dynamics of the hydrological processes can be visualised easily.

8.2.1 Precipitation

In chapter 4 the precipitation recordings were analysed and discussed. In section 4.9 it was concluded that the maximum rainfall intensity is an important rainfall characteristic for runoff generation and the time interval of the model should therefore be smaller or equal to than the time interval of the rainfall recordings. In the context of this study, this means that the time interval of the model has been set at 10 minutes, but a smaller time interval would be preferred due to the high dynamics of the Mediterranean rainfall events.

As discussed in chapter 4, the need to incorporate the spatial distribution of rainfall is widely accepted. The spatial distribution of the interpolated rainfall fractions of section 4.7 was used for the calculation (equation 8.1) of the rainfall amount per time step in the model.

Precipitation = Rainfall (1+standardised rainfall deviation of mean) equation 8.1

Using the data presented in chapter 4 served as input data for the hydrological model. Rainfall events that did not exceed the threshold conditions for runoff generation determined by its maximum intensity and duration (equation 4.1, section 4.4), were a priori excluded as input data.

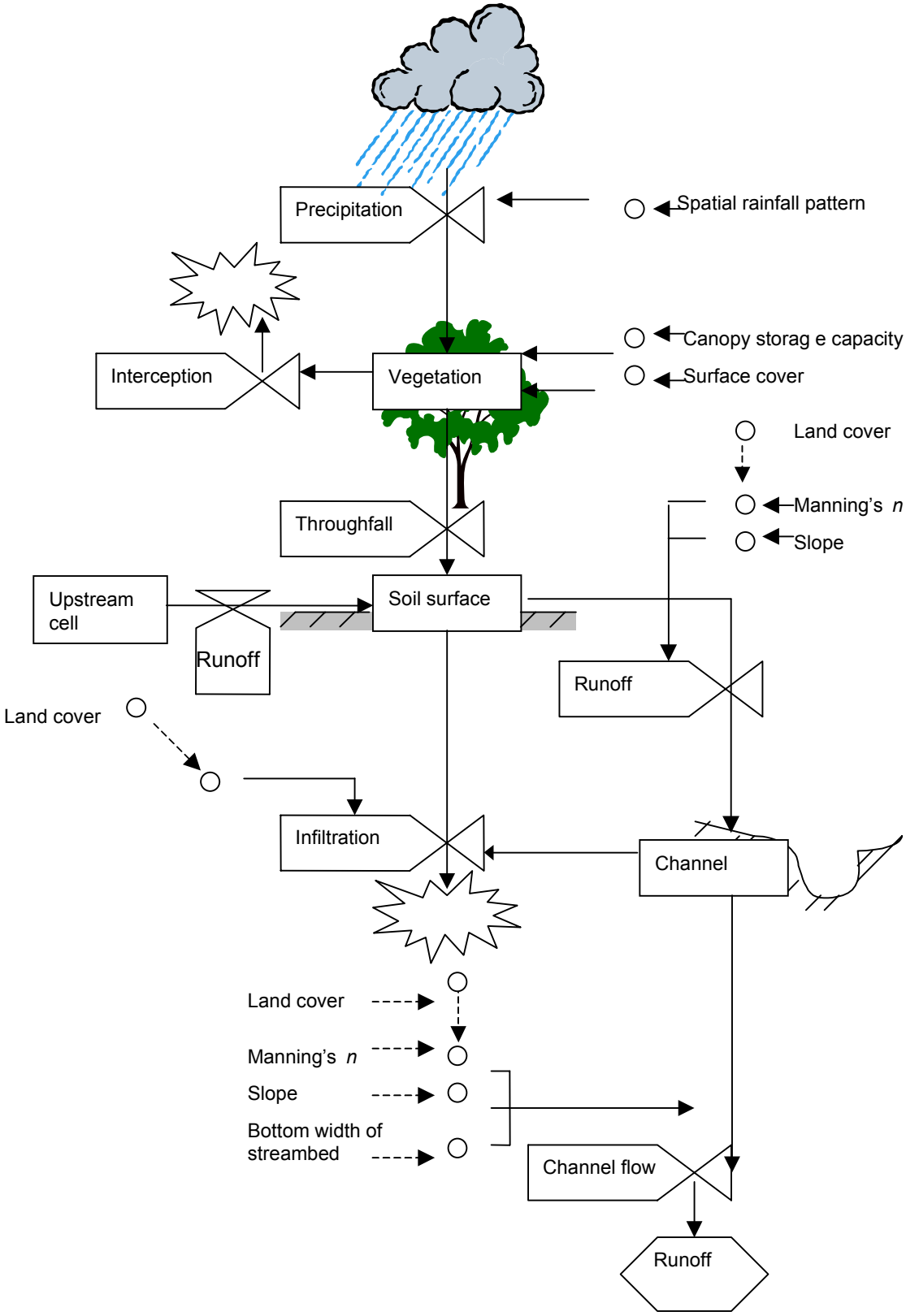

Figure 8.1 The model components of SAMDIM.

8.2.2 Interception

- *A general interception model*

For modelling the hydrological response of small catchments, the amount of rainfall that reaches the soil surface (throughfall) needs to be calculated. Therefore the amount of rainfall lost to interception to vegetation and evaporation needs to be quantified. Due to time, financial and logistic constraints, interception loss could not be estimated in the field. Therefore the interception was calculated using an interception model based on research results of others obtained in a similar semi-arid Mediterranean environment in southeast Spain (Belmonte Serrato, 1997; Domingo et al., 1998). The interception model accounts for the spatial variability of surface cover in the study area, as quantified in chapter 3. The temporal variability of the surface cover both seasonal and annual, was assumed to be negligible as illustrated in chapter 3 (figure 3.10). This interception model works as follows.

The process of interception is controlled by the canopy structure and type of the vegetation cover (Rutter et al., 1971). The flux of water reaching the soil surface directly or indirectly is called the throughfall T (mm/h) and is determined by the proportion p of rain R, which falls through the canopy without striking a surface added to water draining from the canopy to the soil D (mm/h) (equation 8.2). All water that does not reach the soil surface directly or indirectly is not available for the water balance of the soil and is not be taken into account.

$$T = p\,R + D \qquad \textit{equation 8.2}$$

The canopy drainage D is assumed zero when the canopy storage C_t at time t is less than the canopy storage capacity S. The canopy storage C_t can be temporarily larger than S if the rainfall is larger than the drainage flux D. Under these conditions the drainage flux D is a function of the storage surplus (Domingo et al., 1998) (equation 8.3);

$$D = 0 \quad \textit{when } C_t \le S$$
$$D = a(C_t - S)^b \quad \textit{when } C_t > S \qquad \textit{equation 8.3}$$

in which:
a and b are local empirical drainage parameters

Rutter's interception model (Rutter et al., 1971) assumes that the change in the amount of water stored in the canopy is proportional to rainfall, interception and evaporation (equation 8.4)

$$C_{t+dt} = C_t + dt((1-p)R - D - Ep) \qquad \textit{equation 8.4}$$

in which:
C_t : water stored on the canopy at time t per unit area of a canopy (mm)
t : time (h)

dt : time interval (h)
(1-p)R : rainfall that falls on the canopy (mm/h)
D : water draining from the canopy to the soil (mm/h)
Ep : evaporation (mm/h)

Because only rainfall events are used as model input that caused runoff, these rainfall amounts were very large compared to the amount of evapotranspiration during rainfall and for this reason the evapotranspiration is assumed to be negligible during rainfall. Because a rainfall event has been defined as a period of rain before which and after which at least 30 minutes no rain falls (chapter 4), it is possible that short dry periods occur during the rainfall event. For these periods of time evaporationtranspiration *Ep* is calculated. The evapotranspiration *Ep* depends on the potential evapotranspiration EVP_0 as described by equation 8.5;

$Ep = EVP_0$ *when* $C_t > S$
$Ep = EVP_0 * C_t/S$ *when* $C_t \leq S$ *equation 8.5*

in which:
Ep : actual evapotranspiration (mm/h)
C_t : actual canopy storage at time t (mm)
S : storage capacity (mm)
EVP_0 : potential evapotranspiration (mm/h)

The potential evapotranspiration in the study area is derived from monthly amounts of evapotranspiration (Alías Pérez, 1989) as calculated by Thornthwaite (1948). Figure 8.2 shows how equation 8.2 to 8.5 are linked for dynamic calculation of the canopy storage per timestep by using the Rutter model.

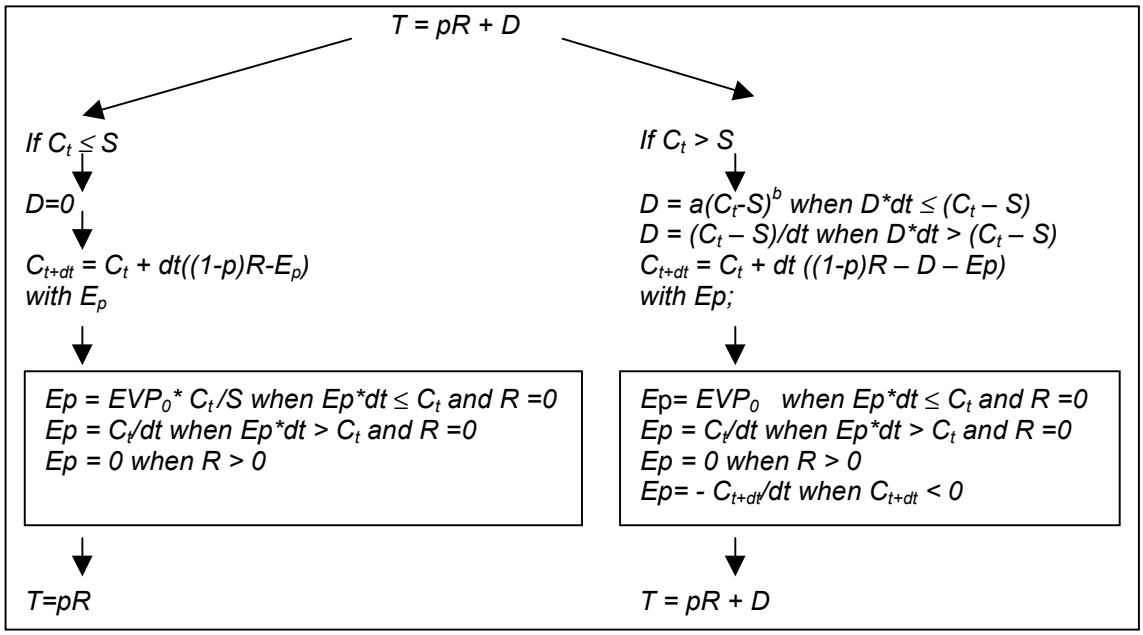

Figure 8.2 Calculating throughfall depending on the canopy storage at time t based on Rutter et al. (1971).

The SAMDIM model is event-based and does not calculate the interception loss because only the drip to the soil surface contributes to the runoff process and throughfall ceases soon after the end of a rain event. The rainfall events in the study area are so infrequent that all intercepted water will evaporate. The canopy storage at the end of an event can thus be seen as the interception loss.

Previous studies (Belmonte Serrato et al., 1996; Belmonte Serrato, 1997; Domingo et al., 1998) modified the Rutter model to match the dominant vegetation species in the study area i.e. *Stipa tenacissima* and *Pinus halepensis* (as described in chapter 2 and 3). In SAMDIM the adapted Rutter model was used to calculate the amount of throughfall for each rainfall event. The modifications are as follows:

- *Modifications for* Stipa tenacissima

For *Stipa tenacissima,* it is known that the proportion of rain *p* that falls freely through the plant without touching the canopy is about 10 percent of the rainfall at that moment (Domingo et al., 1998) so *p* equals 0.1. The storage capacity S of the *Stipa tenacissima* grass is 2.44 mm at the base of the projected canopy area (Domingo et al., 1998). At the moment the total storage capacity *S* is full, the plant starts to drain the surplus water. Domingo et al. (1998) were able to quantify the parameters *a* and *b* of equation 8.3. By using these parameters, the drainage *D* of the water from the canopy of *Stipa tenacissima* is described by equation 8.6 after which the amount of throughfall is calculated according figure 8.1.

$$D = 0.002\ (C_t - S)^{7.71} \qquad \textit{equation 8.6}$$

It should be noted that Domingo et al. (1998) quantified these parameters for timesteps *dt* of 10 seconds. Larger timesteps introduce an artifact, namely an overestimate of the drainage of the canopy storage, an underestimate of the actual evapotranspiration, and an overestimate of the water from the canopy D_t (Dorigo & van Groenendaal, 2000).

- *Modifications for* Pinus halepensis

No relation for the drainage from the canopy during time interval *dt* is available for *Pinus halepensis*. Belmonte Serrato (1997) established an empirical relation (equation 8.7) for closed canopies of adult trees of *Pinus halepensis* between the total throughfall T_{total} and total rainfall R_{total} of an event.

$$T_{total} = 0.917 * R_{total} - 2.035 \qquad \textit{equation 8.7}$$

Because no data is available on the drainage parameters *a* and *b* during an event, the actual amount of water draining of the canopy is assumed to be equal to the total surplus of the storage capacity $(C_t - S)$. The storage capacity *S* of an adult *Pinus halepensis* with a closed canopy is derived from equation 8.7. When T_{total} equals zero and the tree starts to drain, the storage capacity *S* is filled and *S* equals R_{total} which is 2.22 mm on the basis of the projected canopy area (Belmonte Serrato, 1997).

The fraction *p* of rain that falls freely through the *Pinus halepensis* tree was estimated in the field by the fraction of gaps in the canopy as defined in section 3.4, figure 3.4. The mean value of *p* is 0.69 (standard deviation 0.09) based on 859 measurements.

- *Incorporation of surface cover for dominant vegetation species*

The large difference in the fractions of water that can fall freely through the canopy between *Stipa tenacissima* and *Pinus halepensis* in combination with a larger storage capacity of *Stipa tenacissima* results in more water being intercepted by *Stipa tenacissima* than by *Pinus halepensis* according to the modified Rutter model. For this reason it is important to distinguish the surface cover of these two vegetation species from each other in the SAMDIM model.

This was done using the fraction maps with the percentage of surface cover per unit area for *Stipa tenacissima*, *Pinus halepensis* and unvegetated soil, given in chapter 3. These maps are used to calculate the weighted total net rain per timestep per square surface or throughfall (mm/h) that reaches the soil surface.

8.2.3 Infiltration

- *Philip's model*

In chapter 5 it was noted that infiltration capacity depends on several factors, including of the saturated hydraulic conductivity. There are various ways to describe the infiltration process using the hydraulic conductivity. Besides the saturated hydraulic conductivity, these also include the initial soil moisture content as an additional component.

The infiltration model developed by Philip (1957) was used to describe infiltration in the study area because it is easy using a straightforward relation (equation 8.8) to describe the infiltration process (figure 8.3) based on two parameters *A*, which describes the main part of the gravitational influence, and Sorptivity *S* which is a measure for the capacity of the soil to absorb water.

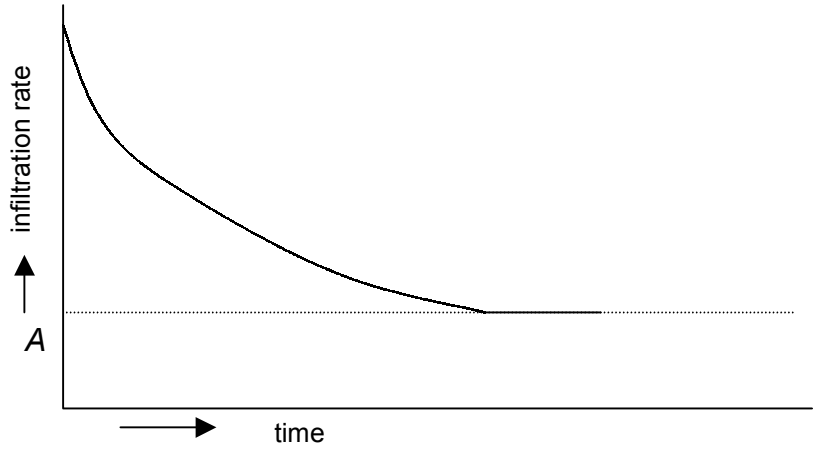

Figure 8.3 Infiltration rate as function of time.

$INF(t)=St^{1/2} + At$ *equation 8.8*

in which:
INF : cumulative infiltration (mm) at moment t
t : time of infiltration (s)
S : sorptivity (mm/$s^{1/2}$)
A : steady state infiltration (mm/s)

The infiltration rate is (equation 8.9),

$inf(t)=1/2St^{-1/2} + A$ *equation 8.9*

in which:
inf : infiltration rate (mm/s)

The steady state infiltration rate *A* depends on the saturated hydraulic conductivity K_s. Koorevaar et al. (1983) used a transformation of the infiltration model developed by Green and Ampt (1911) to estimate relation between *A* and K_s for the Philip equation case the constraints given in equation 8.10 are met.

$(-s_f / h_f)^2<1$ *equation 8.10*

in which:
s_f : depth of wetting front of a saturated moisture profile (cm)
h_f : pressure head at wetting front of a saturated moisture profile (cm)

- *Application in SAMDIM*

The Koorevaar et al. (1983) transformation (equation 8.11) was used in this study to transform the K_s estimates (chapter 5) into steady state infiltration rates *A* for the Philip equation (equation 8.8).

$A=2/3\ K_s$ *equation 8.11*

in which:
K_s : saturated hydraulic conductivity (mm/s)

Cammeraat (in press) has shown that normally h_f lies between -6 and –12 cm and various rainfall events in the study area meet the restrictions of equation 8.10. Only during extreme rainfall events, the soil moisture increases. Because the other input parameters for SAMDIM were not estimated under these specific rainfall conditions, the saturated hydraulic conductivity as measured in the field (chapter 5) was used for the infiltration module.

The sorptivity *S* depends on the initial soil moisture content, the porosity, the saturated hydraulic conductivity K_s and the water retention curve. Philip and Knight (1974) showed that *S* can be rewritten as a linear relation ($S = \alpha * \sqrt{K_s}$) as depending

on the saturated hydraulic conductivity K_s. The factor α is a bulked parameter that includes the influence of the storage capacity of the soil and the water retention curve. Both the S and the saturated hydraulic conductivity K_s were estimated in the study area by Odijk and Van Bemmel (1997) at 45 locations under dry conditions with the inverse auger hole method (figure 8.4). Based on their data, a linear relation was established (R^2=0.47) (equation 8.12).

$$S = 3.88 * \sqrt{K_s} \qquad \textit{equation 8.12}$$

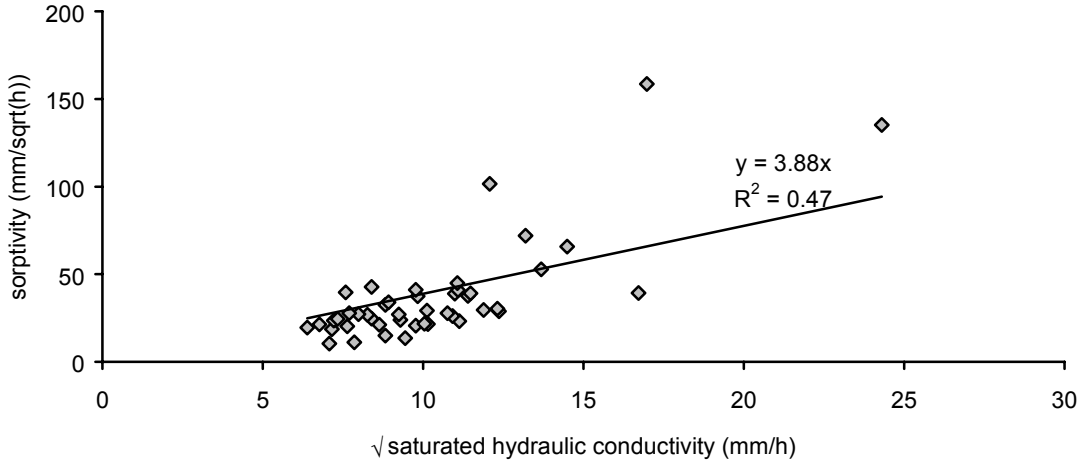

Figure 8.4 Sorptivity S as function of the square root of the saturated hydraulic conductivity K_s, based on data of Odijk & van Bemmel (1997).

In this study this relation was used to transform the estimated K_s (chapter 5) into the S needed for the infiltration module based on the Philip equation. When this relation is used, the water retention curve and the storage capacity of the soil, defined as the porosity minus the initial soil moisture content are assumed not to control the infiltration. Because soil texture in the study area is rather homogeneous (section 2.5) I assume that the porosity and the water retention curves do not vary much. The values of the K_s in the study area were presented in table 5.3 of chapter 5. These values were used to calculate S (table 8.1) by use of equation 8.12. The differences of K_s-values between land cover units were significant and the differences of K_s-values between plant and inter-plant areas was not significant. For this reason it is valid to assign a K_s value related to the land cover unit to a rastercell and not take the small-scale variability of plant and inter-plant areas into account.

Table 8.1 Estimated values for saturated hydraulic conductivity K_s and Sorptivity S.

Land cover	Ks (mm/h)	S (mm/√h)
Bare soil	3.5	7.3
Afforested terraces	64	31.0
Grassland/ natural woodland	137	45.4

For all events the initial soil moisture conditions were assumed to be constant. This assumption is based on the fact that the soil surface was dry (pF=4) before the rainfall events on which the data set is based (Imeson et al., 1999; Cammeraat, personal communication). This observation is supported by Imeson et al. (1999) who states that the soil surface is at wilting point or dryer for about 2/3 of the year. Provisional results of continuous soil moisture recordings in the study area around a *Stipa tenacissima* tussock (Imeson et al., 1999; Cammeraat, in press) show that the soil is mostly dry (pF = 4) before a rainfall event starts as might be expected in a warm, semi-arid environment. For rainfall events recorded during this study the soil moisture at 3.5 cm depth changed but at 9 cm depth change was only slight and the soil dries within in three to five days (Imeson et al., 1999; Cammeraat, in press). Only occasionally do large amounts of water fall within 24 hours causing dramatic changes in soil moisture but due to logistic problems these events were excluded from the data obtained in the study presented here.

Cammeraat's (in press) results were obtained on a small plot (about 1 m^2) in the study area. From a study of small catchments (6 – 24 ha.) in a corresponding area, Gómez Plaza, (2000) showed that for rainfall events with a small amount and intensity that only generate local runoff, the generation of runoff is controlled by the initial soil moisture content. For events with a large amount and intensity of rainfall, the initial soil moisture content and its spatial distribution are not important (Gómez Plaza, 2000). Subsequently, the influence of the sorptivity S in large events is minimal. Gómez Plaza (2000) used the return period of a rainfall event to arbitrarily classify the event as small (< 15 years) or large (> 15 years). However, it is questionable whether the recurrence interval of rainfall (based on the maximum of 24 hour precipitation) is a reliable index to express its magnitude in the context of runoff generation as was discussed in chapter 4.

SAMDIM assumes that the soil moisture content in the study area does not have a spatial correlation structure. This assumption is based on the initially dry soil surface conditions that dominate. For this reason the sorptivity can be estimated by the K_s which can be used as calibration factor. Because rainfall events used for the model were recorded under corresponding initial dry conditions of the soil, the initial soil moisture in the study area is assumed not to control the runoff.

Before the amount of infiltration can be calculated at time t, the amount of surface water must be calculated as the net precipitation resulting from precipitation and throughfall. Based on equation 8.9, the potential infiltration is calculated for time t. When the amount of surface water at time t exceeds the potential infiltration, the amount of infiltrated water at time t is determined by the potential infiltration. When the amount of surface water is less than the potential infiltration, the amount of surface water infiltrates at time t. The exact process and algorithms of the infiltration module according Philip used in the model, are described in Chow et al. (1988).

8.2.4 Routing of overland flow

SAMDIM is developed and programmed in a GIS-based simulation environment. Contour lines of elevation with an equidistance of 5 m of the topographical map (1:10000, Comunidad Autónoma de la región de Murcia) were digitised and rasterised in cells of 30 by 30 metre. The cell size equals the pixel size of the Landsat TM images which enables the implementation of remote sensing results in SAMDIM easily without transformation of spatial resolution which inevitably would lead to the reduction of accuracy. These cell sizes provide a suitable base to prevent SAMDIM from excessive processing time.

The rasterised topographical map was transformed into a Digital Terrain Model (*DTM*) with the program ISDD (Hazelhoff, 1999). This program uses a spreading algorithm to linearly interpolate the elevation based on the rasterised contour lines. It is able to interpolate the elevation based on a single point (for example the top of a hill) and the surrounding contour line and prevents the occurrence of step-wise elevation differences that can occur due to a large spatial distance between the contour lines.

The *DTM* was implemented in PCRaster© GIS (Wesseling et al., 1996) after which a 'local drain direction' map (*LDD*) was created (Van Deursen, 1995). For a 3 x 3 block of cells the *LDD* determines in which direction the overland flow is routed from the centre cell. Based on field observations of where the channel was cut into the bedrock, parts of the *LDD* were classified as streambed. For these cells, the properties of the streambed as explained in the equations 8.14 to 8.17, were used to describe the routing of runoff. In the smallest catchments B7, B8 and B9, the channel had the dimensions of a rill without clear incisions into the limestone. Therefore no streambed cells were classified in these catchments and the routing of the runoff was described as overland flow that covers the whole cell.

The REA-concept has been developed based on model simulations of a version of the TOPMODEL that calculates the runoff depth per rastercell and the catchment runoff as the arithmetic mean of the runoff in all rastercells of the catchment (Wood et al., 1988, 1990). This way routing and reinfiltration of surface water are not considered and the spatial variability of the runoff and the contribution of a particular tributary to the main stream have been neglected (Fan & Bras, 1995) while distributed models in fact derive their strength from the incorporation of a routing module and spatial diversity. By taking the routing of runoff into account, a REA can also be tested for peak discharges which is more sensitive to routing.

The routing of overland flow in SAMDIM is described by the 'kinematic wave' (Chow et al., 1988) which is commonly used to describe the transport of water in hydrological models. The lateral inflow into the channel or rastercell is determined by the change of the volume of streamflow per length of the channel or raster cells and by the change of the cross sectional surface of the flow during time (equation 8.14).

$$\frac{\partial Q}{\partial x} + \frac{\partial A}{\partial t} = q \qquad \textit{equation 8.14}$$

in which:
Q : streamflow through channel or raster cell (m^3/s)
x : channel length through cell (m)
A : cross sectional surface of flow (m^2)
t : timestep used in model (s)
q : inflow into the channel or raster cell (m^3/s)

The cross sectional surface A of the flow can be described as (equation 8.15):

$$A=\alpha Q^{\beta} \qquad \textit{equation 8.15}$$

in which:
α : coefficient determined by Manning's n, slope and wetted perimeter
β : coefficient with value 0.6

The value of α fluctuates during the flow through the channel and hence during running SAMDIM because it is related to the wetted perimeter P of the channel based on the Manning's equation (equation 8.16).

$$\alpha = \left(\frac{n}{\sqrt{Slope}} \right)^{\beta} * P^{\frac{2}{5}} \qquad \textit{equation 8.16}$$

in which:
n : Manning's roughness coefficient (-)
$Slope$: tangent of the slope angle of the channel or raster cell (-)
P : wetted perimeter (m)

The wetted perimeter is calculated based on an assumed rectangular channel profile (equation 8.17).

$$P = B_w + 2\,H \qquad \textit{equation 8.17}$$

in which:
B_w : Bottom width of streambed (m)
In cells without streambed, the cell length is used
H : height of water level in channel or raster cell (m)

Change in flow in the stream channel causes a change in the cross sectional surface of the flow. This results in an adjusted water level by which a new wetted perimeter is calculated. This serves as input for the recalculation of cross sectional surface that

can be used to calculate the inflow into the channel in the next time step of the model. Field estimates of the bottom width are assigned to the raster cells that include a stream channel (table 6.1). If the raster cell does not include a stream channel, the value of the bottom width equals the cell width.

Table 8.2 Manning's n for different types of land cover used in SAMDIM, modified from Arcement, (1989).

Type of land cover	Manning's *n*
natural woodland	0.055
grassland	0.035
afforested terraces	0.027
bare soil	0.020

For the determination of the Manning's roughness coefficient *n*, the stream channel was distinguished from the rest of the study area based on mapping of the field situation. In the stream channel the value of 0.025 was assigned to a second order stream channel and 0.020 was assigned to the third order stream channel. These values were arbitrarily chosen based on Arcement (1989). The Manning's *n* for the remaining areas without concentrated runoff but with overland flow, was also arbitrarily chosen based on land cover type (Arcement, 1989)(table 8.2).

The timestep used in SAMDIM was 15 seconds. The size of the timestep was estimated by manual optimalisation of the simulated hydrographs under condition that the surface water was not more than one raster cell per timestep transported in downslope direction. The choice of the combination of cell sizes and timesteps is important during the routing of the surface water in SAMDIM. With cell sizes of 30 by 30 metres and timesteps of 15 seconds, the '*Courant condition*' (equation 8.18, Chow et al., 1988) was met because the flow rate in the study area does not reach 2 m/s. The combination of the defined cell sizes and timesteps was therefore valid for runoff modelling.

$$\Delta t \leq \frac{\Delta x_i}{c_k} \qquad \textit{equation 8.18}$$

in which:

Δt : timestep

Δx : travel distance of wave

c_k : kinematic wave celerity; the flow rate at a point in time and space.

The bottom widths of the stream channels (table 6.1) are rather small compared to the size of the raster cells used by SAMDIM (30 x 30 m). The stream channel has different hydraulic properties than the remaining areas. For the raster cell consisting of the stream channel and remaining area, some assumptions have to be made (figure 8.5). Water infiltrates on the hill slopes as well as in the streambed of the channel, which results in transmission losses. All water that enters the cell containing the stream channel, i.e. both throughfall and overland flow from the cell

upstream, is used for the calculation of the total infiltration in the whole cell. The surplus is transported into the streambed within one timestep for further downstream transport. The infiltration characteristics in the channel are assumed to be equal to the characteristics outside the channels in the same raster cell.

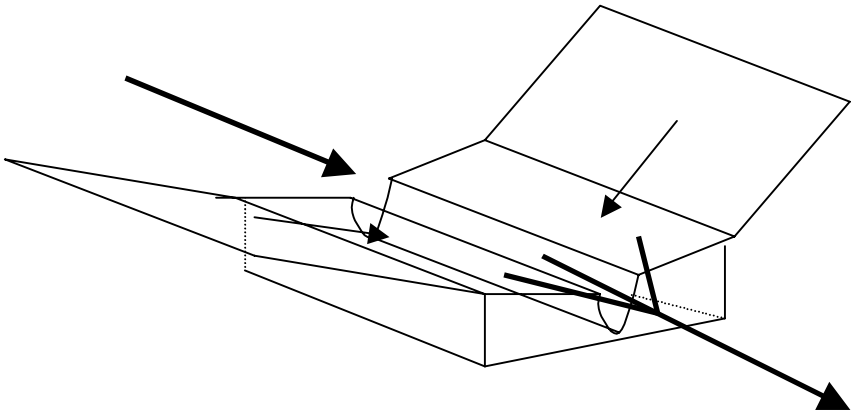

Figure 8.5 Schematic representation of water transport in a raster cell containing a streambed.

8.3 Model calibration

8.3.1 Calibration factor for effective K_s

When the K_s-values as estimated in chapter 5 were used for runoff simulation, little to no runoff was generated in the catchments by SAMDIM for the recorded rainfall events. As noted in chapter 5, the saturated hydraulic conductivity K_s measured in the study area by the inverse auger hole method is too large when compared with other known estimates (section 5.9). The relative differences between the K_s of the different land cover types however, seem to reflect the differences of the conductivity of the soil correctly. The lognormal distribution of the K_s values indicates that over a larger surface the chance increases that the infiltration capacity is completely utilised (Freeze, 1980; Corradini et al., 1998; Karssenberg, in prep).

The support of the saturated hydraulic conductivity is the test surface of the field measurements. The 'effective' saturated hydraulic conductivity K_{s_eff} is a parameter used to account for larger areas than the support size of the K_s. K_{s_eff} is defined as an area-average value (Kabat et al., 1997).

For this study the value of the K_{s_eff} was estimated by inverse modelling. The monitored rainfall-runoff data given in section 7.4 showed that runoff decreased as a fraction of the precipitation with increasing catchment size. This indicates an increase of K_{s_eff} with increasing catchment size. For the model presented here, the 'effective' saturated hydraulic conductivity for each studied catchment is used separately for calibration. This has been done by multiplying the K_s by a calibration factor x (equation 8.19).

$K_{s\_eff} = K_s * x$ *equation 8.19*

in which:

K_{s_eff}	:'effective' saturated hydraulic conductivity (mm/h)
K_s	: saturated hydraulic conductivity based on field measurements (chapter 6) (mm/h)
x	: calibration factor, defined per catchment size

8.3.2 Calibration by PEST

The model was run and the calibration was carried out for each catchment automatically by PEST2000© (Doherty et al., 1999) based on the peak discharge and the total amount of runoff at the same time per event. PEST generated the best suitable x for all catchments studied by minimising the root mean square error of the observed and predicted runoff amounts and peak discharges per catchment. It should be noted that the rainfall events used for calibration differed per catchment. Not every rainfall event was recorded in each catchment due to logistic problems and because not always in every catchment runoff was generated. Catchment B_9 was excluded from calibration because only one runoff event had been recorded during the study period.

PEST generates a correlation coefficient (equation 8.20) to indicate the measure of goodness of fit (Doherty et al., 1999). The correlation coefficient is calculated as:

$$R = \frac{\sum (w_i c_i - m)(w_i c_{0i} - m_0)}{\sqrt{\sum (w_i c_i - m)(w_i c_i - m) \sum (w_i c_{0i} - m)(w_i c_{0i} - m_0)}} \qquad \textit{equation 8.20}$$

in which:

R	: correlation coefficient
w_i	: weigth of i'th oberservation value
c_i	: the i'th observation value
c_{0i}	: the model-generated counterpart to the i'th observation value
m	: the mean value of weighted observations
m_0	: the mean of weighted model-generated counterparts to observations

The x-factor was calculated for each catchment (table 8.3). The corresponding correlation coefficients varied between good for the smallest (B7, B8) and the largest catchment (Bt) to bad for the middle-sized catchments B1, B2, A2 and A5. To analyse the goodness of fit per catchment, explained variances (R^2) were calculated by regression analyses of the observed versus the predicted total runoff amount (m^3) and peak discharge (l/s) (tables 8.4).

Table 8.3 The calibrated x-factors for different sized catchments, the correlation coefficient is based on the difference between the observed and predicted runoff amounts and peak discharges.

Catchment	*x*-factor	Upper boundary of 95% confidence interval	Lower boundary of 95% confidence interval	Correlation coefficient R
Bt	0.283	0.271	0.295	0.90
B1	0.284	0.307	0.262	0.41
B2	0.250	0.265	0.235	0.01
B7	0.218	0.237	0.200	0.79
B8	0.134	0.143	0.125	0.97
A2	0.145	0.176	0.113	0.12
A5	0.160	0.172	0.148	0.44

Table 8.4 The explained variances between the measured and modelled total amount of runoff (m^3) (left) and the peak discharge (l/s) (right) for the different catchments after calibration (n stands for the number of events).

R^2	Modelled						
Measured	qBt	qB1	qB2	qB7	qB8	qA2	qA5
qBt (n=8)	0.66						
qB1 (n=5)		0.48					
qB2 (n=3)			0.00				
qB7 (n=6)				0.71			
qB8 (n=2)					0.64		
qA2 (n=3)						0.79	
qA5 (n=3)							0.82

R^2	Modelled						
Measured	pBt	pB1	pB2	pB7	pB8	pA2	pA5
pBt (n=8)	0.83						
pB1 (n=4)		0.21					
pB2 (n=3)			0.00				
pB7 (n=7)				0.32			
pB8 (n=6)					0.93		
pA2 (n=4)						0.00	
pA5 (n=3)							0.73

In chapter 7 the differences in runoff response of catchments B1, B2, A2, and A5 were discussed and at this resolution relations between runoff and rainfall characteristics were not found except between rainfall amount and runoff amount. The simulations gave the same results and the lowest R^2 values between the predicted and observed runoff amounts and peak discharges were found for these catchments. The plots of the observed values against the predicted values for the catchment B1, B2, A2 and A5 showed over-predicted values of small peak discharges and under-predicted values for the total runoff amounts (figure 8.6). This tendency is well known and accepted for erosion models. It is caused by the natural variability of the measured data that cannot be explained by the model (Freeze, 1980; Nearing, 1998; Nearing, 2000).

Because the trend of the predicted runoff amounts and peak discharges, indicated by ✳ in figure 8.13 and 8.14, corresponded with the trend in the observed runoff amounts and peak discharges (figure 7.7) and the model performed well on the largest and smallest catchments, all calculated *x*-factor's were accepted and used for further model simulations. When the observed and predicted runoff recordings of all events in all catchments were compared, the explained variance for the runoff amounts was 0.63 and for the peak discharge was 0.62.

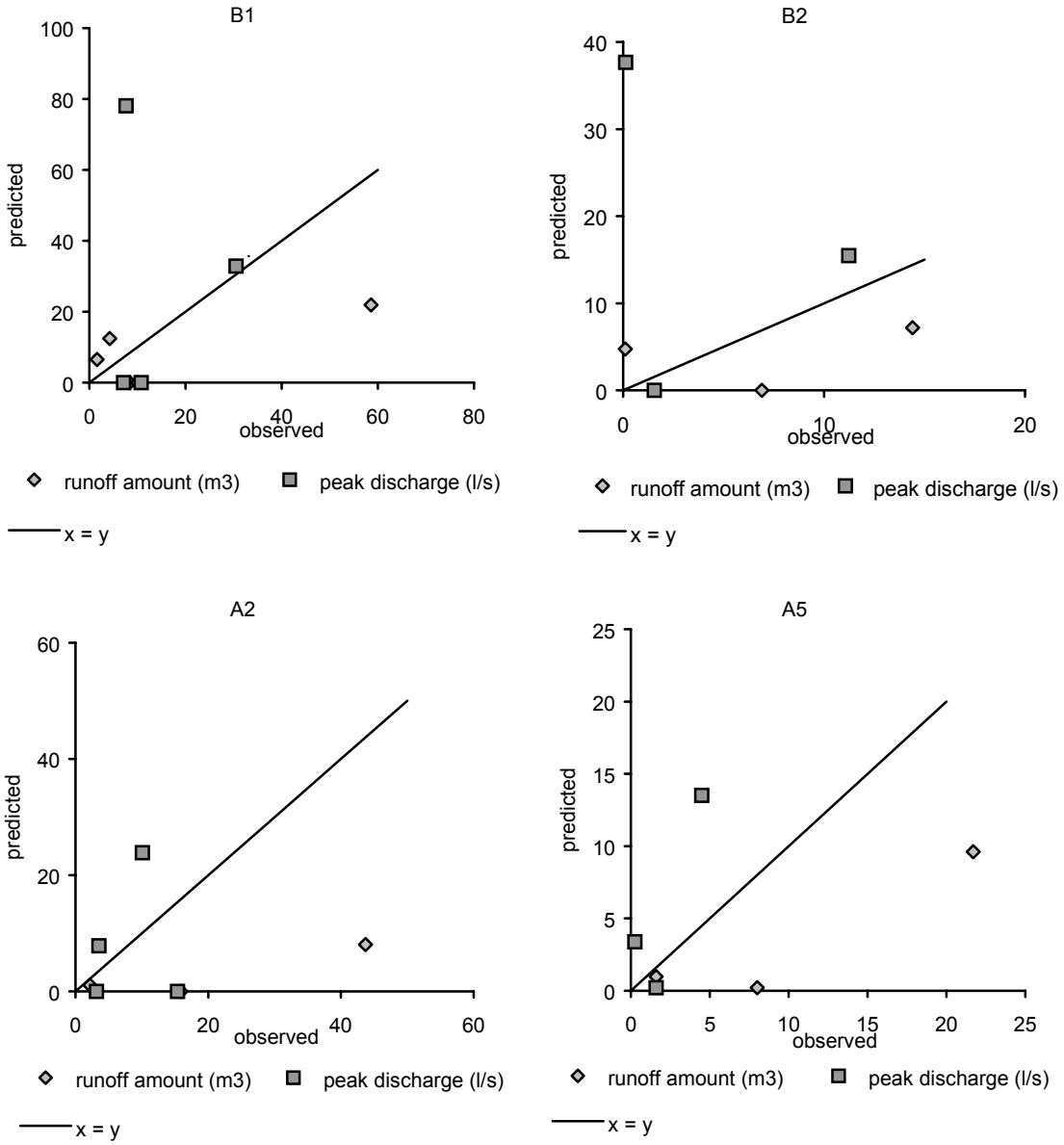

Figure 8.6 Observed versus predicted runoff amounts and peak discharges for the catchments B1 (top left) B2 (top right) A2 (bottom left) and A5 (bottom right).

The *x*-factor of the two Alqueria-catchments A2 and A5, is of the same magnitude as the B8-catchment and smaller than catchments B1 and B2 while catchments B1 and B2 are more or less the same size. This indicates that according SAMDIM in A2 and A5 less water infiltrates than in catchments B1 and B2 which was not found in the runoff recordings discussed in chapter 7. Catchments A2 and A5 consist for the majority (98 and 72% respectively) of land cover 'grassland' in contrast to the other studied catchments. The saturated hydraulic conductivity is known to be less in 'grassland' than in 'woodland' but (table 5.4) this could not be confirmed by field measurements. The difference in the calibration factor between catchments A2 and

A5 and catchments B1 and B2 might be a correction of the smaller K_s in 'grassland' than in 'woodland'.

8.3.3 Calibration factor depending on catchment surface

Binley et al (1989) show that the 'effective' saturated hydraulic conductivity (K_{s_eff}) of hill slopes under unsaturated flow conditions will be smaller than the geometric mean of the K_s field measurements that are lognormally distributed. The test surface of the K_s measurements was very small compared to the size of the catchments. If the support of the test surface increases, the variability of the K_s increases. Under conditions of infiltration excess runoff, the increasing variability will result in an increase of runoff because under these conditions the infiltration capacity at some locations is not completely utilised (Binley et al., 1989). Therefore I assumed the values of the K_{s_eff} were less than the values of the K_s. Indirectly the K_{s_eff} incorporates the influence of processes that were not included in the model like surface storage, initial soil moisture content etc.

In the study area, the recorded runoff amounts and runoff coefficients decreased with increasing catchments sizes. So in larger catchments more water can infiltrate than in smaller catchments and the K_{s_eff} of larger catchments will therefore be larger than for smaller catchments. The increase of the K_{s_eff} with the catchment size depends of the correlation length (i.e. range of the spatial structure) of the K_s (Karssenberg, in prep).

The results (table 8.3) confirm that x increases with increasing catchment size (figure 8.7). The increase of x is valid for catchments to 111 ha. For larger catchments, the value of x will probably reach a sill after which no further increase is expected.

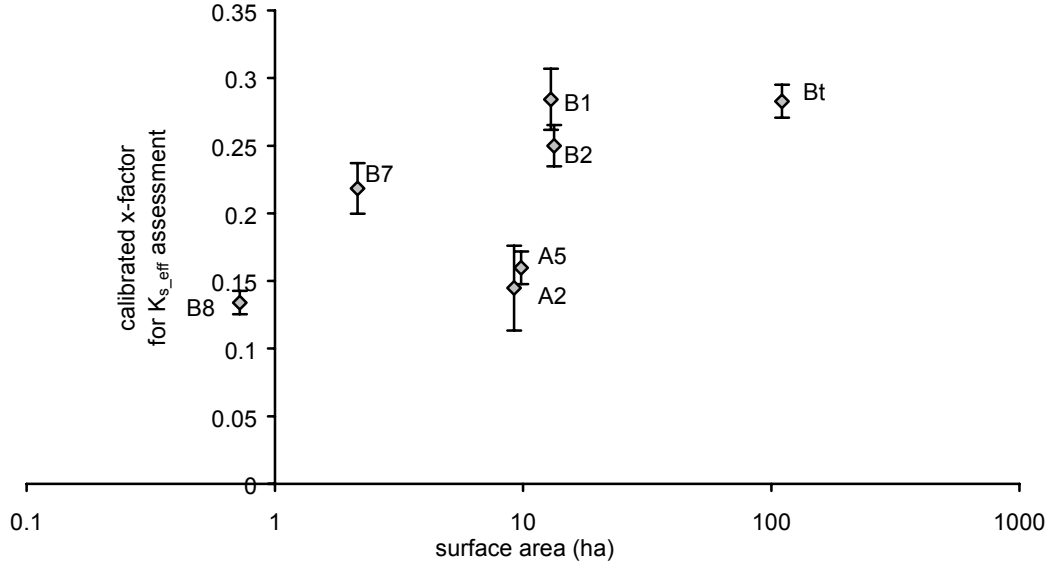

Figure 8.7 The calibrated x-factors for the different catchments.

8.3.4 Discussion of calibration results

The results for the individual catchments showed that not all rainfall-runoff events could be well predicted when using a single calibration factor per catchment for all events (table 8.4). The low explained variances between observed and predicted runoff for catchments B1, B2, A2 and A5 was accepted because this is often the case for events of different magnitude (De Roo & Jetten, 1999; Jetten et al., 1999) as catchments tend to behave differently for large and small events. Probably better results would be obtained when calibrating for individual events or groups of events. However, the small data set did not permit a further subdivision in groups of events of the same magnitude.

The difference between the observed and the predicted runoff (i.e. peak discharge and runoff amount) can generally be explained by various factors as uncertainties in the theoretical structure of the model leading to wrong assumptions, the introduction of an implementation error in the algorithms, a calibration error, uncertainties of representation of the data in the model and the use of an inaccurate spatial or temporal resolution of model parameters (Orekes et al., 1994; De Roo, 1996). Unbiased results are difficult to obtain due to these factors. Besides these general remarks, van Dijck (2000) showed that the saturated hydraulic conductivity is also controlled by the rainfall intensity. This relation was neglected in this study because it requires that first an 'effective' rainfall intensity should be calibrated for every event per studied catchment, after which calibration can take place for every event separately. This prevents a general approach to estimating one calibration factor x per catchment.

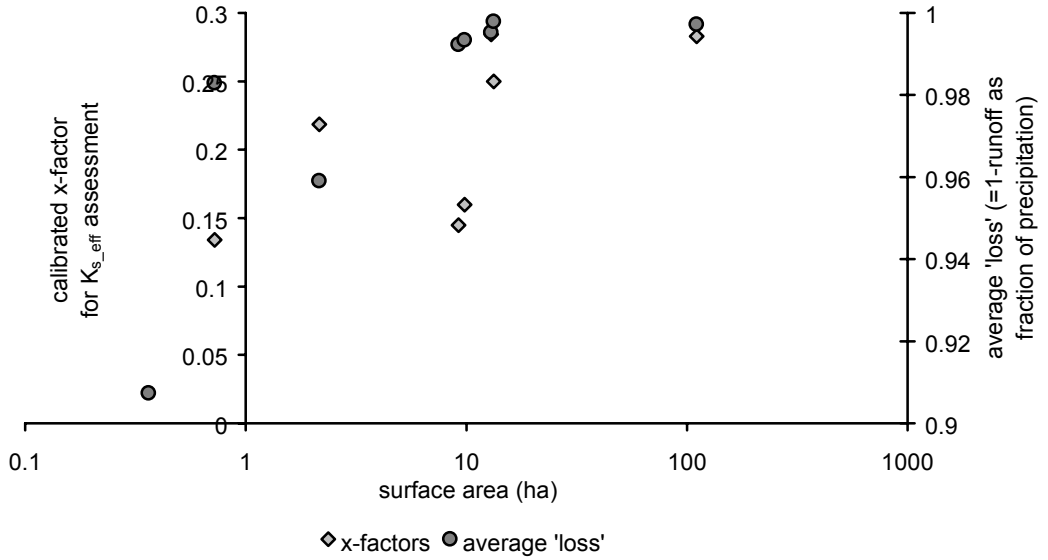

Figure 8.8 The calibrated x-factors for the different catchments with the corresponding average 'losses' as estimated in section 7.5.

The correlation coefficients of table 8.3 and the explained variances of table 8.4 indicated that the driving factors in the scatter of hydrologic response for the

different catchments are parameterised and the complex interaction of various parameters and relevant processes and their influence on the runoff are correctly translated in algorithmes. However the natural variability was not included which resulted in an over-prediction of small peak discharges and an under-prediction for large runoff amounts in catchment B1 and B2. Figure 8.8 shows that the relative differences in calibrated x-factors in figure 8.7 roughly correspond with the relative differences in average 'loss' given in figure 7.9. Therefore the calibrated x-factors were assumed to be valid and used for the simulation of runoff events by SAMDIM.

8.4 Model scenarios

Once the model has been set up and calibrated it can be used to examine different scenarios.

8.4.1 The influence of land cover on the runoff

The influence of land cover in different sized catchments is studied by simulating the runoff of the studied catchments with changing land cover. To determine the influence of afforestation on runoff, the effects of a hypothetical change of land cover have been simulated with the model. The hypothetical land cover change consists of the removal of the remaining natural vegetation (i.e. land cover 'grassland' and 'natural woodland') in catchments B7 and B8 and afforestation of these parts. Catchments B7 and B8 are located inside catchment B1 which is located inside catchment Bt. A land cover change in B7 and B8 means for these catchments that the land cover of a relative large part of the catchment surface changes while the relative land cover change for catchment Bt is small. By modifying only the land cover of catchments B7 and B8, the result of this change on the runoff response at different resolutions can be estimated

Table 8.5 The actual land cover and the hypothetical land cover of sub-subcatchments B7, B8 that are located within subcatchment B1, located within catchment Bt.

Catchment		B8	B7	B1	Bt
Catchment size (ha)		0.72	2.16	12.96	110.6
Actual land cover (% of catchment)	Natural woodland	12	0	9	13
	Grassland	38	17	34	55
	Bare soil	0	0	6	8
	Afforested terraces	50	83	51	24
Hypothetical land cover (% of catchment)	Natural woodland	0	0	4	12
	Grassland	0	0	33	55
	Bare soil	0	17	6	8
	Afforested terraces	100	83	57	25

For the simulations, the rainfall events were used, that were measured during the study period and also were used for the model calibration. The results (figure 8.9) show an increase in both runoff amount and peak discharge with increasing change

of land cover into afforested terraces 'compared' to the modelled runoff of the actual land cover. One percent of change from natural vegetation into 'afforested terraces' results in an increase of 4.7 percent larger runoff amount and 5.4 percent larger peak discharge. These results are based on implementation of afforestation corresponding to the afforestation in the study area. This means that terraces were created by bulldozers which caused deterioration of the soil conditions and hinder the growth of the small planted trees. For this reasons afforestation caused an increase of runoff which also resulted from the model simulations.

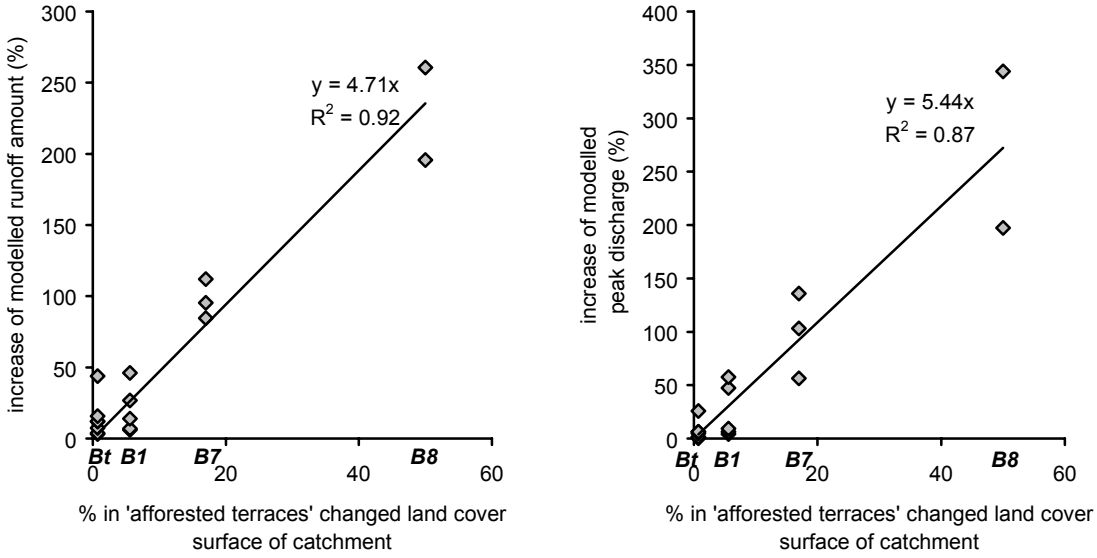

Figure 8.9 The increase of relative runoff amount (left) and peak discharge (right) for a change of natural vegetation into 'afforested terraces'.

It should be noted that for the catchments B1 and Bt, the land cover change is smaller than for the catchments B7 and B8 but also that the land cover change is located at a larger distance from the outlet of these catchments. Nevertheless, the increase of 'afforested terraces' resulted in a linearly related increase of the runoff amount and peak discharge for all catchments and the spatial location of the land cover change seemed not to control the runoff response. The land cover change model simulation illustrates the usefulness of models to anticipate the effects of land management measures.

8.4.2 Testing the REA-concept

As noted in the previous chapter, catchments B1, B2, A2, A5 and Bt fulfilled the constraints of a REA with respect to a decrease in variability of runoff with increasing catchment size. In this section it was tested whether these catchments also fulfilled the other constraint of a REA, which is that the runoff in these catchments is independent of the spatial distribution of the parameters. If the REA-concept is

valid, it will be useful to assist modelling by using it as a fundamental building block for hydrological modelling at various resolution and hence it can be used to predict the runoff in larger areas with corresponding environmental conditions. In SAMDIM both the infiltration parameters K_s and S and the routing parameter Manning's n are related to the land cover units. By varying the spatial distribution of the land cover units with maintenance of the amount of cover per unit, the REA-concept in the study area was tested.

This exercise has been carried out for hill slopes by Freeze (1980) and Corradini et al (1998). The introduction of a heterogeneous K_s had an attenuating effect on the overland flow of a hill slope compared to the use of a homogeneous Ks (Freeze, 19800). Corradini et al. (1998) showed an increasing overestimation of the rising limb of the hydrograph with an increasing spatial correlation of K_s. They included in their analyses 'runon' which is defined as the amount of infiltration after the rain has stopped. Runon reduced the sensivity of the hydrograph to the level of spatial correlation of K_s. In SAMDIM 'runon' is also included. The effect of different spatial distributed infiltration parameters K_s and S is more complex than for hillslopes because catchments are studied which include both hillslope and streambed processes.

The effect of the spatial distribution of land cover of different sized catchments on the runoff was quantified by using different land cover maps as model input. The land cover map of each catchment was modified in three different ways with preservation of the amount of cells per land cover unit but with a change of its location.

1. A land cover map was generated with land cover units in the sequence natural woodland, grass, afforested terrace, bare soil ordered from the streambed slope upwards to the border of the catchment (figure 8.10).

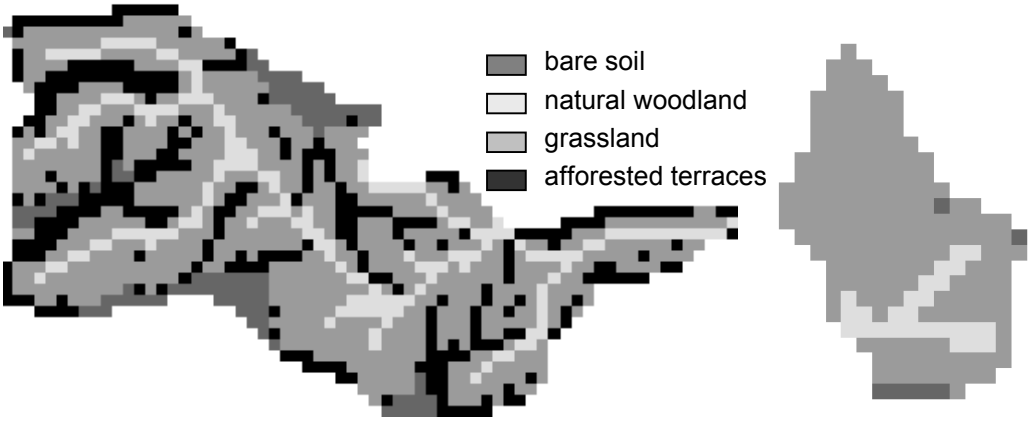

Figure 8.10 The modified land cover maps of the Buitre catchment (left) and the Alqueria catchment (right) ordered in a sequence of natural woodland, grass, afforested terraces, bare soil from the streambed to the catchment border.

2. A land cover map was generated with land cover units in the sequence natural woodland, grass, afforested terraces, bare soil ordered from the border of the catchment slope downwards to the streambed (figure 8.11).

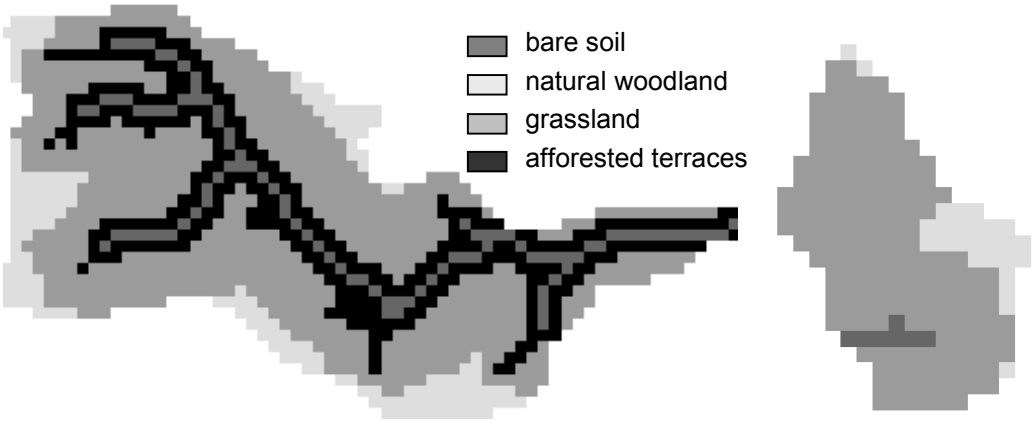

Figure 8.11 The modified land cover maps of the Buitre catchment (left) and the Alqueria catchment (right) ordered in a sequence of natural woodland, grass, afforested terraces, bare soil from the catchment border to the streambed.

3. A land cover maps was generated with land cover units randomly distributed over the catchment (figure 8.12).

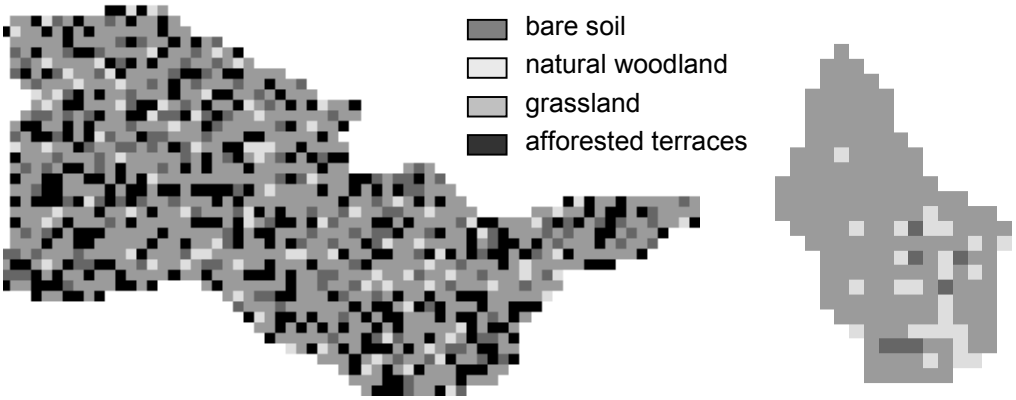

Figure 8.12 The modified land cover maps of the Buitre catchment (left) and the Alqueria catchment (right) with randomly distributed land cover maps.

The sequence of the land cover units in the modified maps from the streambed to the border of the catchment is based on the estimated saturated hydraulic conductivity values and the Manning's *n*. These are largest in natural woodland and smallest in bare soil.

By running SAMDIM with the estimated calibration factors and these modified land cover maps, the variation in runoff as fraction of precipitation was estimated for the different sized catchments and compared to the simulated runoff with the actual or 'original' land cover.

The model simulations of all three different land cover distributions in the smallest catchments (B7 and B8) showed the largest variations in the runoff as a fraction of precipitation (figure 8.13) and as peak discharge (l/s/ha) (figure 8.14). The variability in the simulated runoff for the larger catchments A2, A5, B2 and Bt decreased which corresponds with the field estimates as discussed in chapter 7 and for which was concluded that a REA-constraint was met for these catchments.

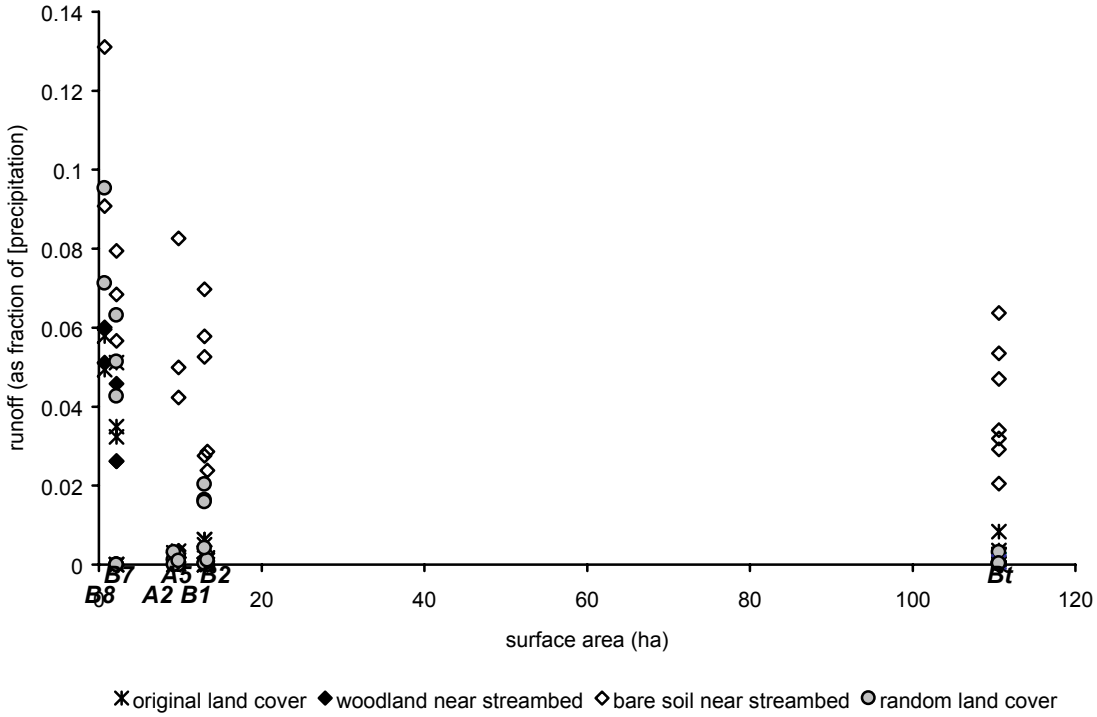

Figure 8.13 Modelled runoff as fraction of precipitation for the studied catchments with varying land cover distributions.

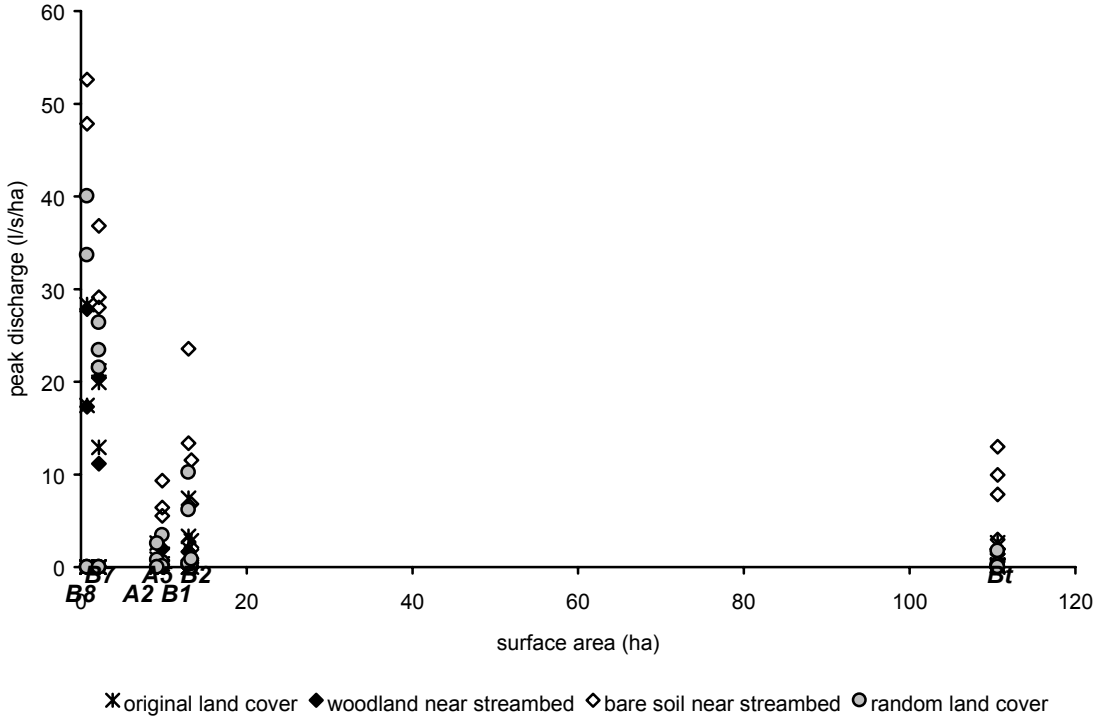

Figure 8.14 Modelled peak discharge for the studied catchments with varying land cover distributions.

The magnitude and variation in the runoff amount and peak discharge in the catchments A2, A5, B1, B2 and Bt with a random land cover distribution or a land cover distribution with 'natural woodland' next to the streambed corresponded with the original land cover distribution. The land cover map with 'bare soil' located next to the streambed resulted in all catchments in larger runoff amounts and peak discharges compared to runoff with the 'original' land cover map. In catchment B1 the runoff amount and peak discharge increased both with a random land cover distribution and with a land cover of 'bare soil' next to the streambed.

In chapter 7 was shown that the catchments B1, B2, A2, A5 and Bt fulfilled the REA-constraint of decreasing variability in runoff response with increasing catchment size. The model simulations however, showed that these catchments did not fulfil the other REA-constraint of the runoff being independent of the spatial distribution of the input model parameters controlled by the land cover units.

SAMDIM illustrated that the magnitude and variability of the runoff response remained unchanged with different land cover distributions as long as the areas near the streambed were vegetated and the total of the catchment covered with 'afforested terraces' and 'bare soil' did not exceed 32 % based on catchments Bt, B2, A2 and A5 (table 7.1). The runoff response in the study area is controlled by the near-channel areas and is very sensitive for 'bare soil' located next to the streambed. In catchments B1, B7 and B8, 50% or more percentage of the catchment surface consists of the land cover 'bare soil' and 'afforested terraces' (table 7.1). In these catchments the runoff increased when the original land cover distribution was changed in a random land cover distribution. By this land cover change the percentage of raster cells with a land cover of 'bare soil' and 'afforested terraces' located next to the streambed was more than in the other catchments.

Because of the influence of the land cover in the areas located next to the streambed, the REA-concept cannot be applied in the study area. This concept proved not to be a suitable tool for hydrological modelling in a semi-arid Mediterranean environment because of the major influence of the areas located next to the streambed on the runoff, which is disregarded by the REA-concept. Based on the assumptions underlying the REA-concept, Fan & Bras (1995) already concluded that the REA-concept is not a robust measure to use for large-scale hydrology. The peak discharge and runoff amounts simulated by SAMDIM, illustrate that also with the incorporation of a routing module and spatial distribution of parameters a REA cannot be defined.

8.4.3 The influence of the channel on the runoff

The runoff coefficients measured in the study area were very low, varying between 9% (catchment B9) and 0.14% (catchment B2) (table 6.2). The runoff amount and peak discharge in the streambed were assumed to be small because the runoff in semi-arid Mediterranean environments is known to be discontinuous. For this reason only the upstream parts of the streambed were assumed to contribute to the

discharge of the outlets and the runoff of the hill slope was assumed not to contribute to the runoff at the outlet of the catchments.

To test this hypothesis that only the streambed and its adjacent areas (i.e. the size of a raster cell) contribute to the runoff at the outlet of the different sized catchments, the runoff was simulated for two scenarios.

1. A map consisting of only rastercells containing a channel. Note that the streambed is relatively small compared with the used rastercells and therefor these cells consist for the majority of non-channel area (figure 8.15).

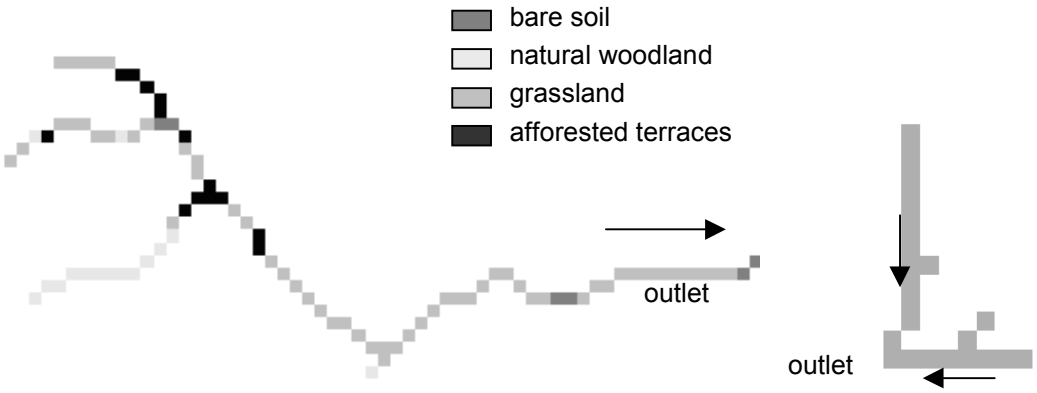

Figure 8.15 The used maps with channel cells for the Buitre catchment (left) and the Alqeuría catchment (right).

2. A map in which the extended-channel cells because during large rainfall events more flow paths of concentrated surface water exist by which the surface water reaches the streambed and can contribute to the runoff at the outlet of the catchments. The extended channel cells were defined as the area downstream of the locations where two different drain directions in the *LDD*-map join each-other (figure 8.16).

Figure 8.16 The used maps with extended-channel cells defined by their drainage pattern for the Buitre catchment (left) and the Alquería catchment (right).

For each catchment, the runoff was simulated only in the areas defined by the map of figure 8.15 and 8.16. The properties of these maps for each catchment are given in table 8.5. For each catchment the simulated runoff was compared with the simulated runoff of the total catchment surface.

Table 8.6 The selected area as part of the total catchment surface, note that in catchment B7 and B8 no channel cells were defined as discussed in section 8.2.4.

Catchment	Total number of rastercells	Number of channel cells	Number of extended-channel cells	% of channel cells in catchment	% of extended-channel cells in catchment
B8	8	-	3	-	0.38
B7	24	-	13	-	0.54
A2	102	13	15	0.13	0.15
A5	109	9	12	0.08	0.11
B1	144	11	47	0.08	0.33
B2	144	12	37	0.08	0.26
Bt	1242	92	324	0.07	0.26

The contribution of simulated runoff of the channel cells and extended-channel cells to the simulated runoff of the total catchments was expressed as fractions of the total amount of runoff and of the peak discharges (figure 8.17).

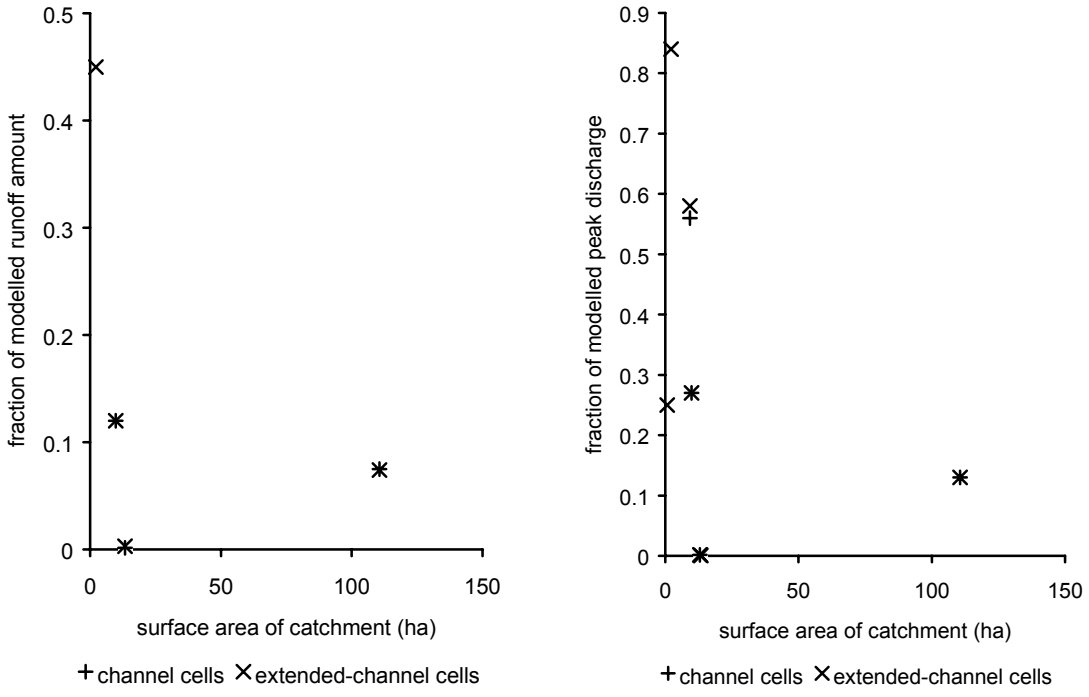

Figure 8.17 The fraction of runoff amount (left) and peak discharge (right) of the total cachment explained by channel cells and extended-channel areas. The fractions calculated based on explained variances less than 0.84 are not indicated in the graphs, see text.

The fractions that were calculated with $R^2 < 0.84$ were not indicated in figure 8.17. These were the fraction of runoff amount in channel and extended-channel cells in catchment B1, A2 and the fraction of runoff amount in the extended-channel cells in catchment B8. Also the explained variance of the fraction of peak discharge of channel cells calculated for catchment B2 was less than 0.84 and therefore left out of the plot in figure 8.17.

The contribution of the extended-channel cells to the runoff amount and peak discharge is largest in catchments B7 in which the land cover near the channel mainly consisted of 'afforested terraces'. In catchment B2, the land cover of channel cells and most of the extended -channel cells consisted of 'natural woodland' and the contribution of these cells to the runoff amount and peak discharge of the total catchment was smallest. The resulting fractions of the total amount of runoff and of the peak discharges (figure 8.17) did not differ between channel cells and the extended-channel cells for most catchments. Only in catchment A2 the peak discharge of the channel cells differed slightly from the peak discharge of the extended-channel cells.

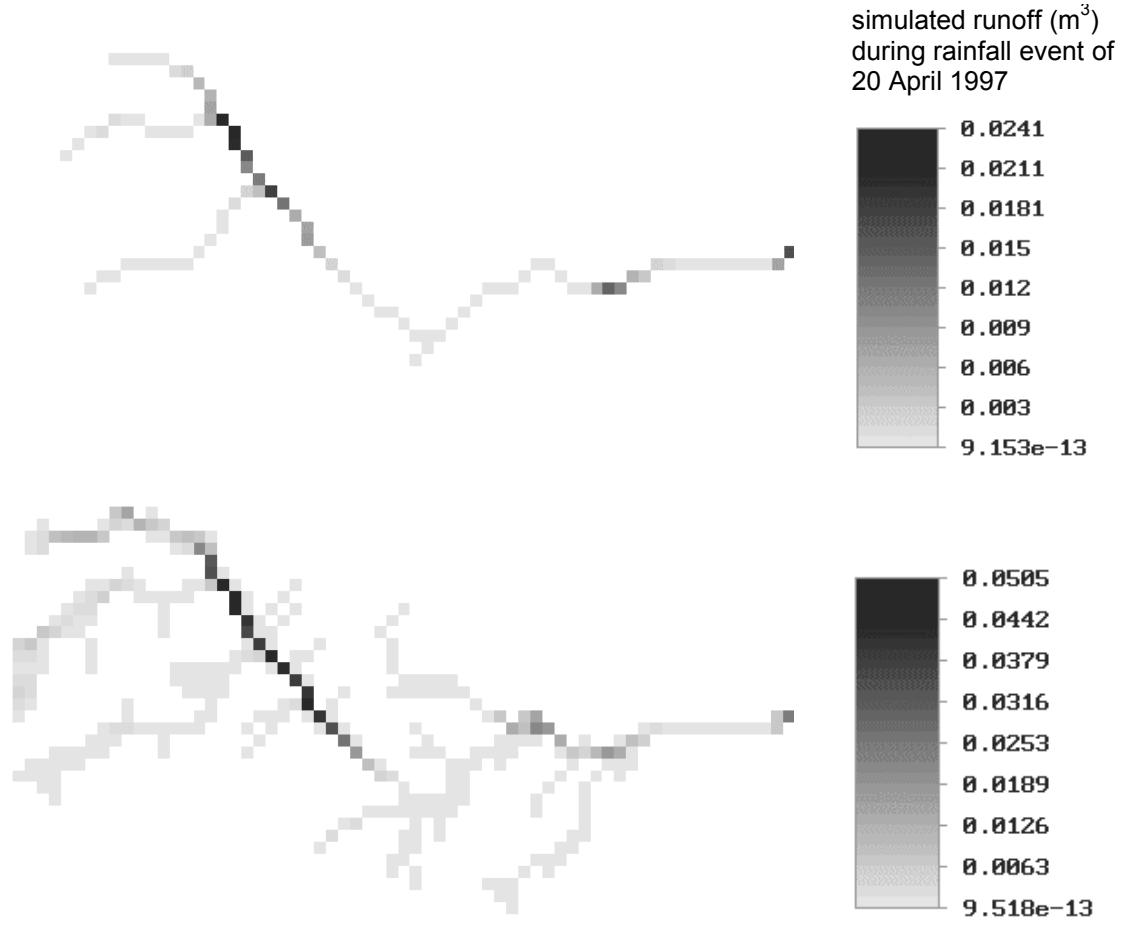

Figure 8.18 The spatial distribution of the runoff at timestep 765 during simulation of rainfall event 20 April 1997 by SAMDIM in the channel cells (at top) and the extended-channel cells (at bottom) of catchment Bt.

Because the extended-channel cells cover a larger area than the channel cells, more water is generated that contributes to the peak discharge. Both the channel cells and the extended-channel cells of catchment A2 have a land cover consisting of 'grassland' while the channel cells and extended-channels cells of the other catchments consist a combination of land cover units. The combination of land cover units in the channel and extended-channel cells, smoothened the increasing channel area and for this reason no differences were observed in the peak discharges of the other catchments.

The runoff at the outlet of catchment Bt modelled with the maps of the channel cells and the extended-channel cells, is controlled by the channel area located near the outlet. Runoff generated in the upstream part of the catchment does not reach the outlet as is shown in figure 8.18. This means that runoff generated in the total catchment area of Bt, not all surface water in the upstream parts of the catchment will reach the outlet of Bt. This result corresponds with the field measurements of the runoff. The runoff recordings showed that the runoff of the subcatchments cannot be extrapolated to a larger catchment by summation of the discharge of smaller catchments. This implied that transmission losses control the runoff in the streambed (section 7.5.2).

The model exercise showed that the contribution of the channel cells and the extended-channel cells to the simulated runoff varied between 0 and 45% for the runoff amount and 0 to 84 % for the peak discharge. For the second and third order catchments the differences in runoff and peak discharge between channel cells and near-channel cells were almost zero. The runoff simulated in the channel or extended-channel cells is smaller than the runoff measured and simulated for the total catchments. This indicates that the hill slope part of the catchments contribute to the runoff in the streambeds which is in contrast to the hypothesis of this section. Larger contributing areas result in larger amounts of water per timestep in the streambed.

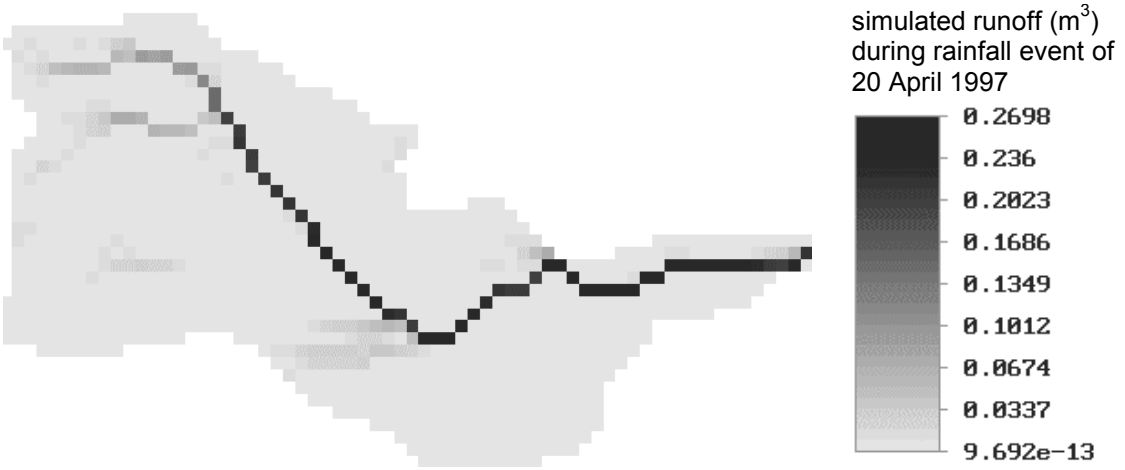

Figure 8.19 The spatial distribution of the runoff at timestep 765 during simulation of rainfall event 20 April 1997 by SAMDIM in the whole catchment Bt.

More important is the spatial distribution of the runoff contributing areas (figure 8.19) because the runoff of the contributing areas leads to the connection of streambed parts with runoff. This causes an increase of the survival length of the runoff in the streambed. Therefore the location of the hill slope areas that contribute to the runoff in the streambed controls the magnitude of the runoff.

8.5 Discussion

As for any model, assumptions had to be made to describe the processes in SAMDIM because it is a simplification of the reality. In this study SAMDIM is used to identify the driving factors of runoff at different resolution and to compensate the limited amount of field measurements. One should be aware of the assumptions and simplifications when interpreting the model results.

The hydrological processes in the study area are tried to be understood by use of SAMDIM. It is based on field measurements during the study period which do not include extreme rainfall events with damaging effects. Therefore SAMDIM cannot be used to predict these extreme conditions. It assumes initially dry soil moisture conditions (pF=4) as discussed in section 8.2.3. and cannot be used to simulate wet initial conditions, should they occur. As no data were available, surface storage was not included and its effect is assumed to be included in the infiltration and runoff routing modules. Because the discharge events in the semi-arid Mediterranean and in the study area do not last very long, SAMDIM is event-based and the total amount of evapotranspiraton during an event is assumed to be negligible.

In SAMDIM the land cover and surface cover determine the interception, infiltration and routing module. The information of land cover and surface cover has been derived from satellite images as described in chapter 3. When information of satellite images is derived and combined with digitised maps, the raster cells of the images and the maps are not necessary co-located. The geometric correction of the satellite images was tested as discussed in chapter 3. Based on these results, the raster cells of the images were moved to match the co-ordinates of the digitised map when they were combined.

Because of the infrequent rainfall and the dry periods before the rain was recorded, all runoff was assumed to be Hortonian and subsurface flow was not considered. The streambed, located in the channel cells had a width of several metres which is small compared to the width of the channel cells i.e. 30 x 30 metres. The water flowing downstream and entering the raster cell from all directions is used to calculate the infiltration. For the infiltration in these cells, a K_s-value is used that was assigned to the raster cell based on its land cover. Inherently this value is also assigned to the streambed. This might lead to small delay in the response of the channel flow because during the first time step a water film enters the raster cell, the water will infiltrate depending on the infiltration capacity of the raster cell. Under the conditions of channel flow, the runoff amount in the channel cell will be far more than the infiltration capacity. The amount of water that infiltrates in the channel cell

might be over-estimated by SAMDIM but the decrease of runoff due to the overestimated infiltration in these cells will be very small. Because the surface water entering a channel cell form upstream direction, uses the total channel cell for its infiltration, the infiltration capacity of the channel cell is used completely during discharge. This means that within the raster cell also infiltration capacity of the areas that are located adjacent to the streambed is complete used. Under these conditions runoff from the cells located adjacent to the channel cell will contribute to the runoff in the channel cell while in reality this water might have infiltrated in the areas adjacent to the streambed. This might result in an overestimation of the runoff contribution of the cells located adjacent to the channel cells, but this increase of runoff will also be very small compared to the total amount of runoff in the channel cells. Technically channel flow can be incorporated in SAMDIM apart from the routing of runoff but it will complicate the model, introduce errors and the time needed to run the model will increase considerably. The calibration of the model and large model simulations model will be almost impossible due to these increasing run time and lack of reliable field data.

Calibration by use of PEST offers the opportunity to assign weights to the observed versus predicted values. For the calibration of SAMDIM weights nor standardised values were used because the runoff amounts and peak discharges were in the same order of magnitude (figure 8.6). The calibration results have been discussed in section 8. A2 and A5 were difficult to calibrate and the only reason to accept the calibrated x-factor was because simulated runoff amounts and peak discharges of A2 and A5 fitted in the general trend of the field measurements. SAMDIM worked well for all resolutions of the Buitre catchment and for this reason the results of the model simulations were accepted to be valid for the conditions of the study area.

The rainfall data used for the model simulations was discussed in chapter 4 and is limited because extreme events were not included and hence the conclusions are related to limited rainfall conditions.

8.6 Conclusion

A dynamic distributed model SAMDIM was developed. To incorporate the influence of land cover and surface cover on the runoff in SAMDIM, the relations found in the previous chapter, were used. Land cover was incorporated based on the relations between for K_s and land cover units. From literature is known that land cover controls the surface roughness and hence the velocity of the surface water which is incorporated in the Manning's n. Based on the values assigned to the K_s and the Manning's n the infiltration capacity of natural woodland is equal to that of grassland but the roughness of grassland is larger. The fraction maps of surface cover estimated in chapter 3 were used to calculate the throughfall in SAMDIM. The explained variances of the predicted runoff amounts and peak discharges versus the observed values were slightly better than the results obtained by the use of the linear equations defined in chapter 7.

A hypothetical land cover change by which natural vegetation is changed into afforested terraces results in increasing runoff amounts and peak discharges. An increase of one percent afforested terraces resulted in 4.7% increase of the runoff amount and 5.4% increase of the peak discharge regardless the catchment size.

The REA-concept was tested for its sensitiveness of the spatial distribution of runoff controlling factors. For this purpose three different land cover maps were used with an identical statistical distribution and mean of land cover units but with a different spatial distribution. The catchments (B1, B2,A2, A5 and Bt) that in chapter 7 had been defined to fulfil the constraints of a REA based on the decreasing variability of runoff, responded with an increase of runoff amount and peak discharge in case the original land cover was spatially changed by locating bare soil near the streambed. In case the catchment surface covered with 'afforested terraces' and 'bare soil' was 50% or more, the increase of variability in runoff response also occurred with a random distribution of land cover with maintenance of its statistical distribution. The REA-theory does not account for the spatial distribution of 'bare soil' areas. These areas proved to be important in controlling the runoff response in various sized catchments. For this reason the REA-concept is not suitable to use in a semi-arid Mediterranean environment in which large areas consisting of 'bare soil' are common. For the various sized catchments located in this environment the spatial location is of 'bare soil' is very important and should be taken into account for runoff modelling.

The influence of the areas located near the streambed was further analysed by model simulations of runoff in only the channel cells or in the near-channel cells. The contribution of these areas to the runoff was smallest in the smallest catchments. In the largest catchment Bt, the channel cells and near-channel cells both contributed for 13% to the peak discharge and 7.5% to the total runoff amount. In larger catchments the spatial distribution of the near-channel areas is very important because it determines the survival length of the runoff. The development of a methodology to define these near-channel areas in the field and to quantify the contribution of these areas to the runoff in catchments would provide a large insight in the survival length of the flow. This way it would contribute to tackle the problem of resolution in runoff in various sized large catchments.

9 Conclusions

Progressing land degradation processes are a general accepted problem in the semi-arid Mediterranean and it is now recognised that land degradation is mainly caused by excessive runoff. The contributing factors are precipitation, the limited infiltration capacity, the vegetation type and cover and the discontinuity of runoff both on hillslopes and in streambeds. These factors make land degradation a complex problem because they have impact at different levels of resolution and with their non-linearity and mutual feedback they form a set of complex interactions. To understand the processes that underlie excessive runoff in a semi-arid Mediterranean environment, this study focused on the main factors that control the runoff in various sized catchments with a semi-natural vegetation cover

To fulfil the aims of this study, a series of nested catchments was selected ranging in size from 0.4 to 111 ha, rainfall-runoff recordings were analysed and a distributed hydrological model was developed. The analyses of the estimation of the vegetation cover and the runoff measurements were carried out at varying resolutions of scale. This implied that for both the vegetation cover and the runoff measurements the spatial level of detail varied during these analyses. The results of the analyses are based on a data set of which extreme rainfall events and successive rainfall events were not included due to logistic problems.

The objectives of this study were given in Chapter 1, section 1.6, and the reader should refer to them when reading the following conclusions.

9.1 The influence of vegetation on runoff

Before the influence of vegetation on runoff could be analysed (i.e. objective 1), the vegetation types needed to be parameterised. In the context of this study, the vegetation was parameterised at two different levels of resolution by use of Landsat TM satellite images:

- classified as land cover units consisting of various image pixels to account for large spatial variability. In the study area these land cover units were 'natural woodland', 'grassland', 'afforested terraces' and 'bare soil'.
- as percentage surface cover per unit area (one image pixel) to account for small scale variability. In the study area these surface cover types were *Pinus halepensis*, *Stipa tenacissima* and unvegetated soil.

The spectra mixture analysis (SMA) of Landsat TM images proved valuable to unravel the spectral information into abundance maps of surface cover per entity per unit area. However, the method was hampered by the limited number of spectral bands of TM and the similar spectral reflectance of the selected entities.

The estimates of the saturated hydraulic conductivity K_s showed that the land cover units could be used to map the K_s over the study area. 'Bare soil' had the

smallest value and 'natural woodland' and 'grassland' both the largest value of K_s. Because the variability of K_s within a land cover unit was larger than the variability of the K_s between plant and inter-plant areas, the K_s could not be related to the percentage of surface cover per unit area.

Runoff analysis of the recorded rainfall-runoff events showed that vegetation defined as surface cover did not control the runoff response of the catchments ranging from 0.4 – 111 ha. This can be explained by the 'smoothing effect' of the use of the total amount of unvegetated soil per catchment and because the unvegetated soil controls the runoff in an area smaller than the fairly large cell size (i.e. 30 by 30 m) of which the amount of unvegetated soil was calculated. Therefore the resolution of the surface cover estimates did not provide a useful tool to analyse the influence of vegetation at the scale of catchments.

Vegetation defined as classified land cover units, proved to be a useful variable for the runoff analysis of the selected catchments. By use of this variable the influence of vegetation cover on runoff could be estimated. For this purpose the land cover units were placed in two groups based on the infiltration capacity and the routing of surface water. Due to the limited number of catchments, the influence of the individual land cover units on the runoff could not be estimated. The land cover units 'afforested terraces' and 'bare soil' were grouped because the disturbed soil of the 'afforested terraces' has lead to deterioration of the infiltration capacity and vegetation growth by which the hydrological conditions of these areas resemble the hydrological conditions of 'bare soil'. The grouped land cover units 'afforested terraces' and 'bare soil' were used as variable for runoff analysis of the recorded rainfall-runoff events. The analysis showed that the runoff amount in all catchments ranging from 0.4 – 111 ha. for the present environmental conditions of the study area is related log-linearly to the catchment surface covered with 'afforested terraces' and 'bare soil' (table 7.7).

By using a distributed runoff model in which land cover determined the K_s and the routing of the runoff, the possible effect of land management measures was anticipated. The model simulations showed that a change of natural vegetation (grassland or woodland) into afforested terraces of one percentage of the catchment surface results in an increase of runoff amount by 4.7% and 5.4% of peak discharge, which is in contrast to the purpose of afforestation. The implementation of afforestation in the study area in the past by which natural vegetation was removed, has resulted in an increase of runoff. In order to decrease the runoff it would be better to preserve the natural vegetation and to afforest only the 'bare soil' areas by planting trees individually without creating terraces.

9.2 Testing the REA-concept

The REA-concept was originally developed for a humid area. The validity of the REA-concept in a semi-arid Mediterranean environment was investigated (i.e. objective 2) based on field measurements in eight small catchments ranging from 0.4 – 111 ha. and model simulations.

The rainfall-runoff recordings showed that the variability of runoff decreased when the runoff responses were arranged according to catchment size. The variability and magnitude of runoff amount and peak discharge for four catchments with sizes from 9.2 to 13.0 ha was of the same order of magnitude as of the catchment with a size of 111 ha. Based on this, it was concluded that a catchment of 9.2 ha is the smallest area in which the runoff has reached a minimum of variability and therefore can be defined as an REA.

The second REA-constraint defined as the runoff being independent of the spatial distribution of controlling characteristics (i.e. objective 3), was tested by distributed modelling of the runoff response with varying spatially distributed land cover units. The results of these model scenarios showed that the seven catchments ranging from 0.7 ha to 111 ha responded with an increase of runoff and peak discharge when the original land cover was spatially modified by locating the land cover unit 'bare soil' near the streambed. If the catchment originally was covered for 50% or more by the land cover units 'afforested terraces' and 'bare soil', a spatially random distribution with retaining the statistical distribution of these land cover units would also increase the variability in runoff response.

Besides the amount of the catchment covered by 'bare soil' and 'afforested terraces', the spatial distribution of these land cover units appeared to be very important in controlling the runoff in the various sized small catchments. The runoff contribution of these areas to the main stream, controls the survival length of the flow to the main stream. This dependence of runoff on the internal structure of the catchment is a violation of the REA-concept. Because this kind of situation is common in a semi-arid Mediterranean environment I conclude that the REA is not of much value in semi-arid areas. The impact of the spatial distribution of these land cover units on runoff severely hampers the development of reliable models.

Another violation of the REA-concept are the power-law relations between the runoff amount or peak discharge and the catchment size valid for catchments ranging from 0.4 –111 ha. These relations are based on average rainfall recordings and indicate that within the limits of this study the runoff response is self-similar which means that the variation in runoff response is dependent of the scale of resolution and therefor does not reach a minimum value. This means that a REA does not exist and therefore in this area it is not a useful concept for hydrological modelling. This conclusion corresponds with the conclusions of Fan & Bras (1995) regarding the use of the REA-concept.

9.3 Runoff controlling factors in various sized catchments

Although the REA-concept proved not to be a useful tool, it yielded some interesting insights into the runoff response in the semi-arid Mediterranean type of environment:

For the present environmental conditions of the study area it was possible to set up straightforward log-linear relations that predict the runoff amount and peak discharge based on simple variables (i.e. objective 4). These relations are defined in

table 7.7 given that the rainfall conditions exceeded the threshold conditions defined by equations 4.1 and 4.2. These variables were catchment size, bottom width of the outlet and the percentage of catchment covered by the land cover units 'afforested terraces' and 'bare soil'. Although the runoff was also controlled by the wetness index, this variable was not considered because it incorporates the catchment size and depends on the bottom width which are both more easily and more reliable than the wetness index. The relations of table 7.7 are valid for catchments sizes ranging from 0.4 – 111 ha and so for this range they are independent of resolution. Due to their simplicity, the linear relations provide quick and easy rough estimates of the magnitude of the moderate runoff that can be expected in these catchments.

The Desertification Response Unit (DRU)-theory focuses on the understanding of the driving factors that control water redistribution at various spatial and temporal scales. The defined variables provide useful tools for further development of the DRU-theory in larger areas than a hillslope.

The rainfall characteristics were defined as rainfall amount, rainfall intensity and the duration of the rainfall event. The relation between rainfall characteristics and runoff amount or peak discharge depended of the scale of resolution. The three smallest catchments ranging from 0.4 – 2.2 ha. and the largest catchment of 111 ha responded cleary to rainfall. The runoff response of the four catchments ranging from 9.2 – 13.3 ha. was very variable and was not clearly related to rainfall characteristics; only a relation between the rainfall amount and the runoff amount was found. When all rainfall-runoff recordings were combined in one group, no relation with rainfall characteristics was found. The presence of the rainfall-runoff relation within the different groups of catchments sizes means that the rainfall-runoff relation is related to the resolution of scale and therefore cannot be used to predict in different sized catchments.

9.4 General conclusions and recommendations for future research

This study has resulted in some understanding of the runoff controlling factors in small catchments in semi-arid Mediterranean areas. The controlling factors of the magnitude of the runoff amount and peak discharge under modal rainfall conditions have been identified. The results showed a decrease of runoff with increasing catchment size mainly caused by discontinuous runoff. Unfortunately no data on excessive rainfall-runoff events were recorded during this study. With respect to the rainfall-runoff relations, the results of this thesis depend on the analysis of a limited data set and therefore the conclusions cannot easily be extrapolated to runoff predictions of larger rainfall events with recurrence intervals of more than one year.

The results of this study showed that the percentage of catchment area consisting of 'afforested terraces' and 'bare soil', can be used to estimate the magnitude of the expected runoff of various sized catchments under normal rainfall circumstances. At a hill slope, the amount and location of unvegetated soil is expected to control runoff. For hydrological studies that focus at this finer level of

resolution, it is recommended to take the spatial pattern of the surface cover into account by use of hyper-spectral images with a fine spectral and spatial resolution.

The results of this study can be translated to a larger scale of resolution, which consists of catchments with various land use. In these catchments extreme successive rainfall events are one of the controlling factors of catastrophic floods during which continuous runoff conditions occur in the studied catchments. The amount and location of 'bare soil' and 'afforested terraces' are a controlling factor for runoff in the studied catchments. Likewise the location of outlets of the small draining catchments in the larger catchment is a controlling factor for the runoff in large catchments because it controls the survival length of the flow in these large catchments. When the survival length of the flow is long enough to reach the outlet of catchments having a size of 1 – 50 km^2 that consist of various types of land use, the runoff can have dramatic effects. For this reason further research to understand and predict catastrophic floods should focus on the survival length of the runoff in these larger catchments.

In a semi-arid Mediterranean environment rainfall events that result in runoff in the small catchments are not very frequent. For this reason research projects should be developed with a long-term strategy that cover at least five years or more of monitoring. When scientific research aims to get more insight in the results of extreme rainfall events that cause severe damage, the used rainfall-runoff recordings should cover an even larger period up to decades.

Runoff controlling factors in various sized catchments in a semi-arid Mediterranean environment in Spain

Summary

Understanding land degradation in a semi-arid Mediterranean environment is very difficult because of the contributing factors: precipitation, infiltration vegetation cover and discontinuity of flow and the temporal and spatial levels of resolution at which these factors are acting. Therefore it is sensible to attempt to linearize these relations to make them more amenable to research. One way, used in this thesis is the Representative Elementary Area (REA). The value of the REA-concept was investigated as a tool to overcome the problem of different levels of resolution of the factors contributing to the runoff in various sized catchments. Based on the REA, it is possible to define a resolution at which runoff can be described by simple equations because;

- The variability in runoff response of the catchment size has reached a minimum compared to smaller sized areas with a more variable runoff response.
- The runoff response of this area is independent the spatial distribution of the characteristics that control runoff and only dependent of its statistical distribution.

The study area in Southern Spain was selected because its geomorphological setting, soil types and vegetation patterns are representative for large areas in the Mediterranean basin. The 9 studied catchments were selected in an area that is known to channel runoff though well-developed streambeds in limestone. The measurement set-up was nested: first order catchments with in them second and third order catchments were selected varying in size between 0.4 and 111 ha. They are covered by natural vegetation with an open structure. In some parts they are covered by afforested terraces, which consist of disturbed soils planted with indigenous pine trees that have not been developed well so far. At some parts, the terraces are not installed according the contour lines.

The vegetation cover of the catchment was parameterised at two levels of resolution by the use of satellite images;

- As classified land cover units.
- As percentage surface cover per unit area.

The land cover units 'natural woodland', 'grassland', 'afforested terraces' and 'bare soil' were obtained by conventional supervised classification of the available Landsat imagery. The images were used for Spectral Mixture Analysis (SMA) by which information was obtained on the percentage of cover of the dominant vegetation species *Pinus halepensis* and *Stipa tenacissima* per pixel. The Landsat TM images have only six broad wavelength bands. Furthermore the spectral reflectance

of the dominant vegetation species *Pinus halepensis*, *Stipa tenacissima* and the unvegetated soil surface resemble each other. This lead to limited results of SMA.

The most important components of the water balance, precipitation, infiltration and runoff, were studied by detailed fieldwork. The precipitation was characterised by a large number of small rainfall events. Both the storm duration and the rainfall intensity had a skew distribution. The log-transformed rainfall intensity and storm duration resulted in a power-law relation by which the threshold conditions for the occurrence of runoff in second and third order streambeds could be defined. The spatial distribution of rainfall could not be related to topographic features such as aspect and altitude but showed variability within the studied catchments.

Infiltration was characterised by the estimation of the saturated hydraulic conductivity (K_s). Proxies were used to find a proper method to map the K_s over the study area. The *Ks* values were significantly related to the classified units of the land cover map. The variability of K_s within a land cover unit was larger than the variability of the K_s between plant and interplant areas, so it was concluded that K_s was not related to surface cover.

Runoff was recorded at the outlet of 9 catchments of which several were nested within each other. The runoff coefficients were very small and decreased with increasing catchment surface which indicated the loss of runoff during transmission in the streambed. Based on the grouped rainfall-runoff recordings it was not possible to define a rainfall-runoff relation which can be used for all catchments. When the rainfall-runoff recordings were grouped into levels of resolution based on the catchment sizes, rainfall-runoff relations were found for each level of resolution which means that the rainfall runoff relation depends on the catchment size.

Based on the decreasing variability of runoff with increasing catchment size, the catchments varying from 9.2 – 111 ha. were defined as the catchments in which the variability of runoff had reached a low value, which was one of the constraints for the definition of a REA. This implies that the size of a REA in the study area would be 9.2 ha. For the all catchments ranging from 0.4 – 111 ha. log-linear equations were found by which a rough but quick prediction of runoff was possible based on the channel bottom width, the catchment size and the percentage of the catchment surface that consisted of 'bare soil' and 'afforested terraces'. The relation between the catchment size and the runoff amount or the peak discharge was a power-law relation which indicated that the variation of runoff was self-similar at all levels of resolution, also in the catchment sizes ranging from 0.4 – 2.2 ha. that did not match the REA-constraints.

A distributed hydrological model was developed to test the influence of the spatial distribution of land cover units on the runoff amount and peak discharge. The results showed that the peak discharge and runoff amount would increase if 'bare soil' and 'afforested terraces' were to be located nearer the streambed than in the present situation. When the land cover units 'bare soil' and 'afforested terraces' cover 50 % or more of the catchment, a random spatial distribution of these land cover units also results in an increasing runoff amount and peak discharge. Obviously, an increase of the areas of 'afforested terraces' and 'bare soil' will result

in an increase of the runoff amount and the peak discharge because the terraces had compacted soils and the minimal development of the vegetation. The contribution of the near channel areas to the runoff in the main stream determined the survival length of the flow in the streambed.

As shown by runoff modelling with different spatial distributed land cover units, the REA-concept proved not to be a useful tool for hydrological modelling because the runoff response depends on the internal structure of the catchment and therefore violates the REA-concept. Furthermore the power-law relations between the runoff and the catchment size, which are valid for all studied catchments ranging from 0.4 – 111 ha. indicate that the runoff response is self-similar and the variation in the runoff response depends on the resolution, which in contrast to the REA-concept. A rough estimate of the moderate runoff amount and peak discharge in all studied catchments under average rainfall conditions and present environmental conditions is easily provided by linear relations based on catchment size, bottom width and the percentage of catchment covered by the land cover units 'bare soil' and 'afforested terraces'.

Factores que controlan la generación de escorrentía en cuencas de distinto tamaño en una ambiente semiárido mediterráneo en España

Resumen

La comprensión de los procesos de degradación del suelo en ambientes semiáridos mediterráneos es difícil debido a la cantidad de factores que contribuyen a dichos procesos (precipitación, infiltración, características de la cubierta vegetal, cauces de naturaleza efímera,...) y a la resolución espacio temporal a la que dichos factores están actuando. Por este motivo, es interesante intentar desarrollar métodos para linealizar estas relaciones con el fin de hacer más sencillo su estudio. Uno de los métodos utilizados en la presente tesis, es la del "Área Representativa Elemental" (REA). El concepto de la REA fue desarrollado como un instrumento, mediante el cual resolver el problema de los diferentes niveles de resolución de los factores que contribuyen a los procesos de escorrentía en cuencas de distinto tamaño. Basándose en la REA, es posible definir un nivel de resolución en el cual los procesos de escorrentía pueden ser definidos mediante ecuaciones sencillas, ya que:

- La variabilidad en los procesos de escorrentía alcanza un mínimo, comparada con la que se da en áreas más pequeñas, en las que la respuesta hidrológica es mucho más variable.
- La respuesta hidrológica en esta área, es independiente de la distribución espacial de las características que controlan la escorrentía, y tan solo depende de su distribución estadística.

Se seleccionó el área de estudio en el sureste de España, ya que sus tipos de suelo y características geomorfológicas y de cubierta vegetal, son representativas de amplias zonas de la cuenca mediterránea. Las nueve cuencas estudiadas se seleccionaron en una zona en la cual, la escorrentía se concentra en cauces bien desarrollados, con un lecho calizo. Cuencas del orden primero contenían cuencas del segundo y tercero orden. El tamaño de las cuencas varíen entre las 0.4 y las 111 ha. Su cobertura vegetal es de tipo natural, con una estructura abierta, existiendo en algunas partes repoblaciones de pinos autóctonos en terrazas que en algunos partes no son construido conforme a las curvas de nivel. Las terrazas consistir del suelo perturbado y las repoblaciones de pinos autóctonos estan en este momento mal desarrollado.

La cobertura vegetal de las cuencas se parametrizó a dos niveles de resolución, mediante el uso de imágenes de satélite:

- Como unidades de terreno cubierto
- Como porcentaje de superficie cubierta por unidad de área.

Las unidades de terreno definidas mediante la clasificación convencional obtenida de imágenes del satélite Landsat, fueron: " vegetación natural leñosa", " herbáceas", "terrazas de repoblación" y "suelo desnudo". Las imágenes fueron tratadas

mediante "Spectral Mixture Analysis" (SMA) mediante el cual se obtuvo información del porcentaje cubierto por la vegetación dominante (*Pinus Halepensis* y *Stipa tenacissima*) por pixel. La reflectancia espectral de las especies de vegetación dominante *Pinus halepensis, Stipa tenacissima*, y la zona sin vegetación, es bastante parecida. Además las imágenes del Landsat TM tan solo tienen seis bandas de longitudes de onda que acabó en resultados limitados.

Los componentes más importantes del balance hídrico, precipitación, infiltración y escorrentía, fueron estudiados detalladamente en campo. La precipitación fue caracterizada por un gran número de eventos lluviosos. Tanto la duración del evento lluvioso como su intensidad presentaron una distribución bastante sesgada. La transformada logarítmica de la intensidad y la duración, dio como resultado una relación exponencial mediante la cual pudieran ser definidas las condiciones umbrales para la ocurrencia de escorrentía en cauces de segundo y tercer orden. La distribución espacial de la lluvia no pudo relacionarse con las características topográficas tales como altitud y orientación, pero se observó que existía variabilidad entre las cuencas estudiadas.

La infiltración fue caracterizada mediante la estimación de la conductividad hidráulica saturada (K_s). Se procuró encontrar un método adecuado mediante el cual cartografiar la K_S en el área de estudio. Se encontró que los valores de K_S estaban significativamente relacionados con las unidades de clasificación de los mapas de cobertura vegetal. La variabilidad de K_S dentro de una misma unidad de cobertura vegetal fue mayor que la encontrada entre zonas e interzonas de vegetación, por lo que se concluyó que la K_S no estaba relacionada con la cubierta vegetal.

La escorrentía se midió a la salida de las nueve cuencas, de las cuales, algunas eran subcuencas de las otras. Los coeficientes de escorrentía encontrados fueron bastante bajos, y estos decrecían conforme aumentaba el tamaño de las cuencas, lo que era un indicador de las pérdidas de transmisión a lo largo de los cauces. Basándose en los datos registrados de escorrentía-precipitación, no fue posible definir una relación que pudiera ser utilizada para todas las cuencas. Cuando se intentó agrupar los registros precipitación-escorrentía en distintos niveles de resolución según el tamaño de las cuencas, se encontró que existían relaciones precipitación-escorrentía para cada nivel de resolución, lo cual quiere decir que la relación precipitación-escorrentía es dependiente del tamaño de la cuenca.

Basándose en el descenso de la variabilidad de la escorrentía con el aumento del tamaño de la cuenca, las cuencas con una superficie de entre 9.2 y 111 ha fueron definidas como las cuencas en las que la variabilidad de la escorrentía alcanzó un pequeño valor, lo cual es uno de los conceptos que definen la REA. En la zona de estudio una REA será una cuenca con una superficie de 9.2 ha. Par las cuencas cuya superficie oscila entre los 0.4 y 11 ha, fue posible definir ecuaciones lineales mediante las que obtener una tosca pero rápida predicción de la escorrentía. Dichas ecuaciones se basaron en la anchura del lecho del cauce, el tamaño de la cuenca y el porcentaje de suelo de la cuenca desnudo o aterrazado para repoblación. La relación entre el tamaño de la cuenca y la cantidad de escorrentía o caudal pico fue una relación exponencial la cual indicaba que la variación de escorrentía era similar en

todos los niveles de resolución, también en las cuencas cuyo tamaño oscilaba entre las 0.4 y 2.2 ha, lo cual no se ajustaba con el concepto de la REA.

Se desarrolló un modelo hidrológico de tipo distribuido con el fin de comprobar la influencia de la distribución espacial de la cobertura vegetal sobre la escorrentía generada y los caudales pico alcanzados. Los resultados mostraron que tanto la cantidad de escorrentía como los caudales pico, se verían incrementados si las unidades "terrazas de repoblación" y "suelo desnudo" se situasen más cerca del cauce que en la situación actual. Las aportaciones de las áreas cercanas al lecho del cauce principal determinaban la presencia de escorrentía en el cauce.

Como se mostró mediante la modelización de la escorrentía con distintas distribuciones espaciales de unidades de cubierta vegetal, el concepto de la REA se reveló como una herramienta poco útil para la modelización hidrológica ya que la respuesta hidrológica depende de la estructura interna de la cuenca, lo cual contradice el concepto de la REA. Más aún, las relaciones encontradas entre la escorrentía y el tamaño de la cuenca, las cuales son válidas para todas las cuencas estudiadas con un tamaño de entre 0.4 y 111 ha, indican que la variabilidad en la generación de escorrentía depende de la resolución considerada, lo cual contradice el concepto REA. Es posible obtener fácilmente una estimación de la escorrentía generada, y de los caudales punta alcanzados en todas las cuencas, bajo unas condiciones de precipitación medias y las actuales condiciones ambientales, mediante una serie de ecuaciones lineales basadas en el tamaño de la cuenca, anchura del lecho del cauce y el porcentaje de cobertura vegetal obtenido de las unidades "suelo desnudo" y "terrazas de repoblación".

Runoff controlling factors in various sized catchments in a semi-arid Mediterranean environment in Spain

Summary

Understanding land degradation in a semi-arid Mediterranean environment is very difficult because of the contributing factors: precipitation, infiltration vegetation cover and discontinuity of flow and the temporal and spatial levels of resolution at which these factors are acting. Therefore it is sensible to attempt to linearize these relations to make them more amenable to research. One way, used in this thesis is the Representative Elementary Area (REA). The value of the REA-concept was investigated as a tool to overcome the problem of different levels of resolution of the factors contributing to the runoff in various sized catchments. Based on the REA, it is possible to define a resolution at which runoff can be described by simple equations because;

- The variability in runoff response of the catchment size has reached a minimum compared to smaller sized areas with a more variable runoff response.
- The runoff response of this area is independent the spatial distribution of the characteristics that control runoff and only dependent of its statistical distribution.

The study area in Southern Spain was selected because its geomorphological setting, soil types and vegetation patterns are representative for large areas in the Mediterranean basin. The 9 studied catchments were selected in an area that is known to channel runoff though well-developed streambeds in limestone. The measurement set-up was nested: first order catchments with in them second and third order catchments were selected varying in size between 0.4 and 111 ha. They are covered by natural vegetation with an open structure. In some parts they are covered by afforested terraces, which consist of disturbed soils planted with indigenous pine trees that have not been developed well so far. At some parts, the terraces are not installed according the contour lines.

The vegetation cover of the catchment was parameterised at two levels of resolution by the use of satellite images;

- As classified land cover units.
- As percentage surface cover per unit area.

The land cover units 'natural woodland', 'grassland', 'afforested terraces' and 'bare soil' were obtained by conventional supervised classification of the available Landsat imagery. The images were used for Spectral Mixture Analysis (SMA) by which information was obtained on the percentage of cover of the dominant vegetation species *Pinus halepensis* and *Stipa tenacissima* per pixel. The Landsat TM images have only six broad wavelength bands. Furthermore the spectral reflectance

of the dominant vegetation species *Pinus halepensis*, *Stipa tenacissima* and the unvegetated soil surface resemble each other. This lead to limited results of SMA.

The most important components of the water balance, precipitation, infiltration and runoff, were studied by detailed fieldwork. The precipitation was characterised by a large number of small rainfall events. Both the storm duration and the rainfall intensity had a skew distribution. The log-transformed rainfall intensity and storm duration resulted in a power-law relation by which the threshold conditions for the occurrence of runoff in second and third order streambeds could be defined. The spatial distribution of rainfall could not be related to topographic features such as aspect and altitude but showed variability within the studied catchments.

Infiltration was characterised by the estimation of the saturated hydraulic conductivity (K_s). Proxies were used to find a proper method to map the K_s over the study area. The *Ks* values were significantly related to the classified units of the land cover map. The variability of K_s within a land cover unit was larger than the variability of the K_s between plant and interplant areas, so it was concluded that K_s was not related to surface cover.

Runoff was recorded at the outlet of 9 catchments of which several were nested within each other. The runoff coefficients were very small and decreased with increasing catchment surface which indicated the loss of runoff during transmission in the streambed. Based on the grouped rainfall-runoff recordings it was not possible to define a rainfall-runoff relation which can be used for all catchments. When the rainfall-runoff recordings were grouped into levels of resolution based on the catchment sizes, rainfall-runoff relations were found for each level of resolution which means that the rainfall runoff relation depends on the catchment size.

Based on the decreasing variability of runoff with increasing catchment size, the catchments varying from 9.2 – 111 ha. were defined as the catchments in which the variability of runoff had reached a low value, which was one of the constraints for the definition of a REA. This implies that the size of a REA in the study area would be 9.2 ha. For the all catchments ranging from 0.4 – 111 ha. log-linear equations were found by which a rough but quick prediction of runoff was possible based on the channel bottom width, the catchment size and the percentage of the catchment surface that consisted of 'bare soil' and 'afforested terraces'. The relation between the catchment size and the runoff amount or the peak discharge was a power-law relation which indicated that the variation of runoff was self-similar at all levels of resolution, also in the catchment sizes ranging from 0.4 – 2.2 ha. that did not match the REA-constraints.

A distributed hydrological model was developed to test the influence of the spatial distribution of land cover units on the runoff amount and peak discharge. The results showed that the peak discharge and runoff amount would increase if 'bare soil' and 'afforested terraces' were to be located nearer the streambed than in the present situation. When the land cover units 'bare soil' and 'afforested terraces' cover 50 % or more of the catchment, a random spatial distribution of these land cover units also results in an increasing runoff amount and peak discharge. Obviously, an increase of the areas of 'afforested terraces' and 'bare soil' will result

in an increase of the runoff amount and the peak discharge because the terraces had compacted soils and the minimal development of the vegetation. The contribution of the near channel areas to the runoff in the main stream determined the survival length of the flow in the streambed.

As shown by runoff modelling with different spatial distributed land cover units, the REA-concept proved not to be a useful tool for hydrological modelling because the runoff response depends on the internal structure of the catchment and therefore violates the REA-concept. Furthermore the power-law relations between the runoff and the catchment size, which are valid for all studied catchments ranging from 0.4 – 111 ha. indicate that the runoff response is self-similar and the variation in the runoff response depends on the resolution, which in contrast to the REA-concept. A rough estimate of the moderate runoff amount and peak discharge in all studied catchments under average rainfall conditions and present environmental conditions is easily provided by linear relations based on catchment size, bottom width and the percentage of catchment covered by the land cover units 'bare soil' and 'afforested terraces'.

References

Adams, J.B., Smith, M.O., Gillespie, A.R. (1993) Imaging Spectroscopy: Interpretation based on Spectral Mixture Analysis. In: Pieters, C.M., Englert, P. (Eds.) Remote Geochemical Analysis: Elemental and Mineralogical Composition. Topics in Remote Sensing 4. New York: Cambridge University Press, pp.145-166

Ahnert, F. (1987) An approach to the identification of morphoclimates. In: V. Gardiner (ed.) International Geomorphology 1986, Volume II, Chichester: Wiley, pp. 159-188

Alías Pérez, J. (Ed) (1989) Proyecto Lucdeme, Mapa de Suelos, Escala 1:100.000 Lorca-953. Madrid: ICONA, Universidad de Murcia, Ministerio de Agricultura Pesca y Alimentacion

Arcement, G.J. (1989) Guide for selecting Manning's roughness coefficients for natural channels and flood plains. Water-supply paper, Denver: United States Geological Survey 2339

Barrow, C.J. (1991) Land degradation, Development and Breakdown of Terrestrial Environments. Cambridge: Cambridge University Press

Belmonte Serrato, F., Romero Díaz, A., López Bermúdez, F. (1996) Volumen y variabilidad espacial de la lluvia trascolada bajo bosque y matorral mediterraneo semiarido. Ecología 10, pp. 95-104

Belmonte Serrato, F. (1997) Interceptión en bosque y matorral mediterráneo semiárido: balance hídrico y distribución espacial de la lluvia neta. Ph.D. thesis, Murcia: Universidad de Murcia

Bergkamp, G., Cammeraat, L.H., Martinez-Fernandez, J. (1996) Water movement and vegetation patterns on shrubland and an abandoned field in two desertification-threatened areas in Spain. Earth Surface Processes and Landforms 21, pp. 1073-1090

Beven, K.J., Kirkby, M.J. (1979) A physically-based variable contributing area model of basin hydrology. Hydrological Science Bulletin, 24 (1) pp. 43-69

Beven, K.J., Wood, E.F., Sivapalan, M. (1988) On hydrological heterogeneity – catchment morphology and catchment response. In: Journal of Hydrology 100, pp. 353-375

Beven, K., Wood, E.F. (1993) Flow routing and the hydrological response of channel networks. In: K. Beven, M.J. Kirkby (Eds.) Channel Network Hydrology, Chichester: Wiley, pp. 99-128

Beven, K.J. (1995) Linking parameters across scales: subgrid parameterizations and scale dependent hydrological models. Hydrological Processes 9, pp. 507-525 /In: J.D. Kalma, M. Sivapalan (Eds.) Advances in Hydrological Processes, Scale Issue in Hydrological Modelling, Chichester: Wiley, pp. 263-281

Beven, K.J., Fisher, J. (1996) Remote sensing and scaling in hydrology. In: Stewart, J.B., Engman, E.T., Feddes, R.A., Kerr, Y. (Eds.) Scaling up in hydrology using remote sensing. Institute of Hydrology, Chichester: Wiley, pp.1-18

Bierkens, M.F.P., Van der Gaast, J.W.J. (1998) Upscaling hydraulic conductivity: theory and examples from geohydrological studies. Nutrient Cycling in Agroecosystems 50, pp. 193-207

Biermann, C. (1995) The Beltic Cordilleras (SE Spain). Anatomy of a dualistic collision-type orogenic belt. Geologie en Mijnbouw 74, pp. 167-182

Binley, A., Beven, K., Elgy, J. (1989) A physically based model of heterogeneous hillslopes, 2. Effective Hydraulic Conducitivities. Water Resources Research 25, pp. 1227-1233

Blalock, H.M. (1985) Social Statistics, Revised Second Edition, international student edition. Singapore: McGraw-Hill Book Company

Blöschl, G. Sivapalan, M. (1995) Scale issues in hydrological modelling: a review. In: J.D. Kalma, M. Sivapalan (Eds.) Scale Issues in Hydrological Modelling, Advances in Hydrological Processes, Chichester: Wiley, pp. 10-48

Blöschl, G., Grayson, V.B., Sivapalan, M. (1995) On the representative elementary area (REA) concept and its utility for distributed rainfall-runoff modelling. In: J.D. Kalma, M. Sivapalan (Eds.) Scale Issues in Hydrological Modelling, Advances in Hydrological Processes, Chichester: Wiley, pp. 71-88

Boardman, J.W., Kruse, F.A., Green, R.O. (1995) Mapping target signatures via partial unmixing of AVIRIS data. Summaries, fifth JPLAirborne Earth Science Workshop, JPL Publication 95-1, v.1, pp.23-26

Bochet, E. (1996) Interactions sol – vegetation et processus d'erosion hydrique dans le microenvironnement de trois especes du matorral mediterraneen. Ph.D. thesis, Leuven: Katholieke Universiteit Leuven, departement geografie-geologie,.

Bochet, E., Rubio, J.L., Poesen, J. (1998) Relative efficiency of three representative matorral species in reducing water erosion at the microscale in a semi-arid climate (Valencia, Spain). Geomorphology 23, pp. 139-150

Boer, M., Puigdefabregas, J. (1995) Assessing spatial patterns of precipitation and moisture in dry Mediterranean landscapes using digital terrain analysis. In: Ibáñez, J.J. & Machado, C. (Eds.) Anális de la variabilidad espacio-temporal y procesos caóticos en ciencias medioambientales. Logroño: Geoforma Ediciones, pp. 259-276

Boer, M.M. (1999) Assessment of dryland degradation; linking theory and practice through site water balance modelling. Utrecht: Koninklijk Nederlands Aardrijkskundig Genootschap/Unversiteit Utrecht (Nederlandse Geografische Studies 251)

Bos, M.G. (1978) Discharge measurements structures. Wageningen:International Institute for Land Reclamation and Improvement/ILRI

Bosch, J.M., Hewlett, J.D. (1982) A review of catchment experiments to determine the effect of vegetation changes on water yield and evapotranspiration. Journal of Hydrology 55, pp. 3-23

Buishand, T.A., Velds, C.A. (1980) Neerslag en verdamping. Klimaat van Nederland 1, KNMI, De Bilt

Bull, L.J., Kirkby, M.J., Shannon, J., Hooke, J.M. (1999) The impact of rainstorms on floods in ephemeral channels in southeast Spain. Catena 38, pp. 191-209

Burke, S., Thornes, J.B. (1998) Actions taken by national governmental and non-governmental organisations to mitigate desertification in the Mediterranean. Environment and climate programme. Luxembourg: Concerted Action Report 1, EC,

Burrough, P.A. (1993) Fractals and geostatistical methods in landscape studies, chapter 5. In: Lam, N.S-N., De Cola, L. (Eds.) Fractals in Geography. Englewood Cliffs: PTR Prentice-Hall Inc., pp. 87-121

Burrough, P.A., McDonnell, R.A. (1998) Principles of Geographical Information Systems. Oxford: Oxford University Press

Butcher, G.C., Thornes, J.B. (1978) Spatial variability in runoff processes in an ephemeral channel. In: Zeitschrift für Geomorphologie Supplement Band 29, pp. 83-92

Cammeraat, L.H. (in press) Scale dependent thresholds in hydrological and erosion response of a semi-arid catchment. Agriculture, Ecosystems and Management

Cerdà, A. (1997a) Seasonal changes of infiltration rates in a Mediterranean scrubland on limestone. Journal of Hydrology 198, pp. 209-225

Cerdà, A. (1997b) The effect of patchy distribution of *Stipa tenacissima* L. on runoff and erosion. Journal of Arid Environments 36, pp. 37-51

Cerdà, A., Schnabel, S., Ceballos, A., Gomez-Amelia, D. (1998) Soil hydrological response under simulated rainfall in the Dehesa land system (Extremadura, SW Spain) under drought conditions. Earth Surface Processes and Landforms 23, pp. 195 - 209

Chorley, R.J., Schumm, S.A., Sugden, D.E. (1984) Geomorphology. London: Methuen

Chow, V.T., Maidment, D.R., Mays, L.W. (1988) Applied Hydrology. Singapore: McGraw-Hill.

Conacher, A.J., Sala, M. (1998) Land degradation in Mediterranean environments of the world, nature and extent, causes and solutions. Chichester: Wiley

Corradini, C., Morbidelli, R., Melone, F. (1998) On the interaction between infiltration and Hortonian runoff, Journal of Hydrology 204, pp. 52-67

Crist, E.P., & Cicone, R.C. (1984) A physically based transformation of thematic mapper data: the TM tasseled cap. IEEE Transactions on Geoscience and Remote Sensing, GE-22(3), pp. 256-263

Crist, E.P., Kauth, R.J. (1986) The tasseled cap de-mystified. Photogrammetric Engineering and Remote Sensing 53 (1), pp. 81-86

Crist, E.P., Laurin, R., Cicone, R.C. (1986) Vegetation and soils information contained in transformed thematic mapper data. In: Proceedings of the International Geoscience and Remote Sensing Symposium (IGARSS'86), Zurich, 8-11 September, pp. 1465-1470

Cropscan Inc. (1994) Multispectral radiometer (MSR)'s datalogger controller, user's manual and technical reference, Rochester

Darcy, H. (1856) Les fontaines publiques de la ville de Dijon. Paris: Dalmont

De Jong, K. (1991) Tectono-metamorphic studies and radiometric dating in the Betic Cordilleras (SE Spain) –with implications for the dynamics of extension and compression in the Western Mediterranean area. Ph.D. thesis, Amsterdam: Vrije Universiteit

De Jong, S.M. (1994) Applications of Reflective Remote Sensing for Land Degradation Studies in a Mediterranean Environment. Utrecht: Koninklijk Nederlands Aardrijkskundig Genootschap/Unversiteit Utrecht (Nederlandse Geografische Studies 177)

De Jong, S.M. (1994) Derivation of vegetative variables from a Landsat TM image for modelling soil erosion. In: Earth Surface Processes and Landforms 19, pp. 165-178

De Jong, S.M., Paracchini, M.L., Bertolo, F., Folving, S., Megier,J., De Roo, A.P.J. (1999) Regional Assessment of Soil Erosion using the Distributed Model SEMMED and Remotely Sensed Data. Catena 37, pp. 291-308

De Pijper, I. (1999) Soil mapping in the South East of Spain. Doctoraal verslag, Vakgroep fysische geografie en bodemkunde, Amsterdam: Universiteit van Amsterdam

De Ploey, J., Kirkby, M.J., Ahnert, F. (1991) Hillslope erosion by rainstorms – a magnitude-frequency analysis. Earth Surface Processes and Landforms, 16, pp. 399-409

De Roo, A. (1996) Validation problems of hydrologic and soil-erosion catchment models: examples from a dutch erosion project. In: Anderson, M.G., Brooks, S.M. (Eds.) Advances in Hillslope Processes, 1, Chichester: Wiley, pp.669-683

De Roo, A.P.J., Jetten, V.G. (1999) Calibrating and validating the LISEM model for two data sets from the Netherlands and South Africa. Catena 37, pp. 477-493

De Wit, A.M.W., Brouwer, L.C. (1998) The effect of afforestation as a restoration measure in a degraded area in a Mediterranean environment near Lorca (Spain). In: Usó, J.L., Brebbia, C.A., Power, H. (Eds.) Ecosystems and Sustainable Development, *Advances in Ecological Sciences*, Vol.1. Southampton, Boston: Computational Mechanics Publications. pp. 165-170

Doherty, J., Brebber, L, Whyte, P. (1999) PEST Model-Independent Parameter Estimation, Corinda: Watermark Numerical Computing

Domingo F., Sánchez, G., Moro, M.J., Brenner, A.J., Puidefábregas, J. (1998) Measurement and modelling of rainfall interception by three semi-arid canopies. Agricultural and Forest Meteorology 91, pp. 275-292

Dorigo, W., Groenendaal, Y. (2000) Modelling interception loss in a semi-arid environment, a study using remotely sensed data performed in South Eastern Spain. Doctoraal verslag, Vakgroep Fysische Geografie, Utrecht: Universiteit Utrecht

Fan, Y., Bras, R.L. (1995) On the concept of a representative elementary area in catchment runoff. Hydrological Processes, 10th anniversary issue, pp. 69-80

FAO (1988) FAO/Unesco, Soil map of the world, revised legend, Technical paper 20, Rome

Faurès, J., Goodrich, D.C., Woolhiser, D.A., Sorooshian, S. (1995) Impact of small-scale spatial rainfall variability on runoff modelling. Journal of Hydrology 173, pp. 309-326

Faust, D., Díaz del Olmo, F. (1997) Paläogeographie Süsapaniens in den letzten 30000 Jahren: eine Zusammenstellung. Petermanns Geographische Mitteilungen 141 (4), pp. 279-285

Fitzjohn, C., Ternan, J.L., Williams, A.G. (1998) Soil moisture variability in a semiarid gully catchment: implications for runoff and erosion control. Catena 32, pp. 55-70

Francis, C.F., Thornes, J.B., Romero Díaz, A., López Bermúdez, F., Fisher, G.C. (1986) Topographic control of soil moisture, vegetation cover and land degradation in a moisture stressed Mediterranean environment. Catena 13, pp. 211-225

Francis, C.F. (1990) Soil Erosion and Organic Matter Losses on Fallow Land: a case study from Southeast Spain. In: Boardman, J., Foster, D.L., Dearing, J.A. (Eds.) Soil Erosion on Agricultural Land. Chichester: Wiley, pp. 331-338

Francis, C.F., Thornes, J.B. (1990a) Matorral: erosion and reclamation. In: Albaladejo, J., Stocking, M., Diaz, M. (Eds.) Soil degradation and rehabilitation in Mediterranean environmental conditions. Murcia: CSIC, pp. 87-115

Francis, C.F. (1994) Plants on desert hillslopes. In: Abrahams, A.D., Parsons, A.J. (Eds.) Geomorphology of Desert Environments. London: Chapman & Hall, pp. 243-254

Freeze, R.A. (1980) A stochastic-conceptual analysis of rainfall-runoff processes on a hillslope. Water Resources Research 16 (2), pp. 391-408

Gandullo, J.M., Sánchez Palomares, O. (1994) Estaciones ecológicas de los pinares españoles. Colección Técnica ICONA, Madrid: Ministerio de agricultura, pesca y alimentacion,

García Salmerón, J. (1990) La repoblación forestal: tecnicas y repercusion en la mejora de la calidad del suelo. In: Albaladejo, J., Stocking, M.A., Díazm E. (Eds.) Degradacion y regeneracion del suelo en condiciones ambientales Mediterraneas/Soil Degradation and rehabilitation in Mediterranean environmental conditions. Murcia: CSIC, pp. 117-137

Geel, T. (1973) The geology of the Betic of Málaga, the Subbetic, and the zone between these two units in the Vélez Rubio area (southern Spain). Ph.D. thesis, Amsterdam: Universiteit van Amsterdam (GUA Papers of Geology, Series 1, no. 5)

Geel, T., Roep, Th.B., ten Kate, W., Smit, J. (1992) Early-Middle Miocene stratigraphic turning poiints in the Alicante region (SE Spain): reflections of Western Mediterrranean plate-tectonic reorganizations. Sedimentary Geology 75, pp. 223-239

Geel, T. (1996) Palaeogene to early Miocene sedimentary history of the Sierra Espuña (Malaguide Complex, internal zone of the Betic Cordilleras, SE Spain). Evidence for Extra-Malaguide (Sardinian?) Provenance of Oligocene conglomerates: Paleogeographic implications. Estudios Geologicos 52, pp. 211-230

Geerlings, I.P.A. (1978) Geologie van het gebied ten noordoosten van Fuensanta la Parroquia, Murcia, zuid-oost Spanje. Doctoraal verslag, Amsterdam: Universiteit van Amsterdam

Gillespie, A.R., Smith, M.O., Adams, J.B., Willis, S.C., Fischer, A.F.III, Sabol, D.E. (1990) Interpretation of residual images: spectral mixture analysis of AVIRIS images, Owens Valley, California. In: Proceedings of the Second Airborne Visible/Infrared Imaging Spectrometer (AVIRIS). Pasadena: JPL Publication 90-54, pp. 243-270

Gillespie, A.R., Smith, M.O., Sabol, D.E. (1992) A field measure of the 'shade' fraction. In: Green, R. (Ed.) Summaries of the third annual JPL Airborne Geoscience Workshop, Volume 1, AVIRIS Workshop, JPL Publication 92-14 Vol 1, pp.32-34

Gil Olcina, A. (1989) Causas climáticas de las riadas. In: A.Gil Olcina & A. Morales Gil (Eds) Avenidas Fluviales e Inundaciones en la Cuenca del Mediterráneo. Guadalajarra: Instituto Universitario de Geografía de la Universidad de Alicante y Caja de Ahorros del Mediterráneo, pp.15-30

Gómez-Plaza, A. (2000) Variabilidad espacio-temporal del contenido de humedad del suelo en una zona miditerránea semiárida, efectos de las condiciones antecendentes en la respuesta hidrológoca, PhD-thesis, Madrid: Departamento de Proyectos y Planificación rural escuela técnica superior de ingenieros de montes, Universidad Politécnica de Madrid

González del Tánago, M., Blanco, R., Ternan, L., Williams, A., Elmes, A. (1998) Afforestation effects on runoff and infiltration processes (Guadalajara, Central Spain). Geoökodynamik, Band XIX, pp. 153-163

Goovaerts, P. (1999) Using elevation to aid the geostatistical mapping of rainfall erosivity. Catena, Vol. 34, pp. 227-242

Green, W.H., Ampt, G.A. (1911) Studies on soil physics, part I, the flow of air and water through soils. J. Agr. Sc. 4 (1), pp. 1-24

Gupta, V.K., Rodríguez-Iturbe, I., Wood, E.F. (1986) Scale problems in hydrology, runoff generation and basin response. Water science and technology library, Dordrecht: D. Riedel Publishing Company

Gupta, V.K., Waymire, E.C. (1998) Spatial Variability and Scale Invariance in Hydrologic Regionalization. In: G. Sposito (Ed.) Scale Dependence and Scale Invariance in Hydrology, Cambridge: Cambridge University Press, pp.88-135

Hazelhoff, L. (1999) ISDD&EDA, http://web.inter.nl.net/users/HAZEL/page1.html

Hein, L. (1997) Socio-economic Risk Assessment of Erosion in the Alqueria Region, South East Spain. Amsterdam: Foundation of Sustainable Development.

Hernández Franco,J.,Gris Martínez, J., Mula Gómez A.J.(1989) Avenidas y obras hidráulicas en el Guadalentín (Siglos XVII-XIX). In: A.Gil Olcina & A. Morales Gil (Eds) Avenidas Fluviales e Inundaciones en la Cuenca del Mediterráneo. Guadalajarra: Instituto Universitario de Geografía de la Universidad de Alicante y Caja de Ahorros del Mediterráneo, pp.435-446

Horton, R.E. (1933) The role of infiltration in the hydrologic cycle, Trans. American Geophysical Union 14, pp. 446-460

Horton, R.E., (1945) Erosional development of streams and their drainage basins: hydrophysical approach to quantitative morphology. Geological Soc. Am. Bult. 56, pp. 275-370
Houkes, G.H.M. (1998) The influence of vegetation patterns on soil erodibitily determined by aggregate stability and infiltration characteristics on semi-arid slopes. Doctoraal verslag, Fysische geografie en bodemkunde, Amsterdam: Universiteit van Amsterdam
Huete, A.R. (1988) A Soil-Adjusted Vegetation Index (SAVI). Remote Sensing and Environment 25, pp. 295-309
Imeson, A.C., Emmer, I.M. (1992) Implications of climatic change on land degradation in the Mediterranean. In: Jeftic, L. Milliman, J.D., Sestini, G. (Eds.) Climatic change in the Mediterranean, UNEP, London: Edward Arnold, pp. 95-128
Imeson, A.C., Cammeraat, L.H., Pérez-Trejo, F. (1995) Desertification response units. In: Fantechi, R., Peter, D., Balabanis, P., Rubio, J.L. (Eds.) Desertification in an European Context: Physical and Socio-economic Aspects. Luxembourg: Office for Official Publications of the European Communities, pp. 263-277
Imeson, A.C., Pérez-Trejo, F., Cammeraat, L.H. (1996) The Response of Landscape Units to Desertification. In: Brandt, C.J., Thornes, J.B. (Eds.) Mediterranean Desertification and Land Use, Chichester: Wiley, pp. 447-469
Imeson, A.C., Cammeraat, L.H., (1999) Scaling up from field measurements to large areas using the Desertification Response Units and Indicator Approaches. In: Arnalds, O., Archer, S. (Eds.) Rangeland Desertification, Advances in Vegetation Science 19, Dordrecht: Kluwer Academic Publishers, pp. 99-114
Imeson, A.C., Cammeraat, L.H., Coppus, R., Hein, L., Lambrechts, C., Mantel, M. (1999) Hierarchy of land degradation dynamics in the Guadalentín Basin. In: MEDALUS III Final Reports; Project 2. Thatcham: http://www.medalus.leeds.ac.uk, pp. 241-289
Instituto Géologico y Minero de España (IGME), (1981) Mapa Géologico de España, Escala 1:50.000, Hoja 953 (25-38) Lorca, Segunda Serie, Madrid
Jetten, V., De Roo, A., Favis-Mortlock, D. (1999) Evaluation of field-scale and catchment-scale soil erosion models. Catena 37, pp. 521-541
Kabat, P., Hutjes, R.W.A., Feddes, R.A. (1997) The scaling characteristics of soil parameters: From plot scale heterogeneity to subgrid parameterization. Journal of Hydrology 190, pp. 363-396
Kalma, J.D., Sivapalan, M. (1995) Scale issues in hydrological modelling, advances in hydrological processes. Chichester: Wiley.
Karssenberg, D. (in prep.) Modelling effective saturated conductivity across scales under steady state conditions of Hortonian runoff
Kauth, R.J., Thomas, G.S. (1976) The Tasseled Cap, a Graphic Description of the Spectral-Temporal Development of Agricultural Crops as Seen by Landsat. Proc. Symp. On Machine Processing of Remotely Sensed Data. West Lafayette, Indiana: Purdue University, pp. 41-51
Kessler, J., Ossterbaan, R. (1974) Determining hydraulic conductivities of soils. In: Drainage principles and applications. Publication 16, III. Wageningen: International Institute for Land Reclamation and Improvement, pp. 253-296
King, H.V. (1954) Handbook of Hydraulics, New York: McGraw Hill
Kirkby, M.J., Imeson, A.C., Bergkamp, G., Cammeraat, L.H. (1996) Scaling up processes and models from the field plot to the watershed and regional areas. Journal of soil and water conservation 51 (5), pp. 391-396
Kneubuehler, M., Schaepman, M., Schlaepfer, D., Itten, K., (1998) Endmember selection procedures for partial spectral unmixing of DAIS 7915 imaging spectrometer data in highly vegetated areas. In: Schaepman, M., Schläpfer, D., Itten, K. (Eds.) First EARSeL Workshop on Imaging Spectroscopy. EARSeL, Zurich: RSL, pp. 255-261
Kniveton, D.R., De Graff, P.J., Granica, K., Hardy, R.J. (2000) The development of a remote sensing based technique to predict debris flow triggering conditions in the French Alps. International Journal of Remote Sensing 21 (3) pp. 419-434
Koorevaar, P., Menelik, G., Dirksen, C. (1983) Elements of Soil Physics, developments in Soil Science 13. Amsterdam: Elsevier,

Kutílek, M., Nielsen, D.R. (1994) Soil Hydrology. GeoEcology textbook. Cremlingen-Destedt: Catena Verlag

Lacaze, B. (1996) Spectral characteristics of vegetation communities and practical approaches to vegetation cover changes monitoring. In: Hill, J., Peter, D. (Eds.) The use of remote sensing for land degradation and desertification monitoring in the Mediterranean basin, State of the art and future research. Luxembourg: European Commision EUR 16732 EN, pp.149-166

Lambregts, C. (1999) The impact of harvesting ants on soil surface properties of a degraded Mediterranean ecosystem. Doctoraal verslag, Department of geography, Amsterdam: Universiteit van Amsterdam

Lane, L.J. (1982) Distributed model for small semiarid watersheds. Journal Hydraulics Division, Proceeding of the American Society of Civil Engineers 108, pp. 114-1131

Lillesand, T.M., Kiefer, R.W. (1979) Remote sensing and image interpretation, second edition. Toronto: Wiley

Linacre, E. (1992) Climate, Data and Resources, a reference guide. London: Routledge

Loague, K., Gander, G.A. (1990) R-5 revisited: 1. Spatial variability of infiltration on a small range and catchment. IWater Resources Research 26, pp. 957-971

Lopes, V.L. (1996) On the effect of uncertainty in spatial distribution of rainfall on catchment modelling. Catena 28, pp. 107-119

López Bermúdez, F. (1971) Las precipitaciones en Murcia de 1982 – 1971. Papeles de Departamiento de Geografía 3, Universidad de Murcia, pp. 171-187

López-Bermúdez, F., Romero-Díaz, M.A., Ruiz García, A., Fisher, G.C., Francis, C.F., Thornes, J.B. (1984) Erosión y ecologia en la España esmiárida (Cuenca de Mula, Murcia). Cuadernos de Investigación Geografica X, p. 113-126

López Bermúdez, F., Albaladejo, J. (1990) Factores ambientales de la degradacion del suelo en el area mediterranea. In: Albaladejo, J., Stocking, M.A., Díaz, E. (Eds.) Degradacion y regeneracion del suelo en condiciones ambientales Mediterraneas/Soil Degradation and rehabilitation in Mediterranean environmental conditions. Murcia: CSIC, pp. 15-45

López-Bermúdez, F., Romero-Díaz,.A., Martínez-Fernández, J., Martínez-Fernández, J. (1996) El Ardal Field Site: Soil and Vegetation Cover. In: Brandt, C.J., Thornes, J.B. (Eds.) Mediterranean Desertification and Land Use, John Wiley & Sons, Chichester, pp. 169-188

López Bermúdez, F, Romero Diaz, A., Hernandez Laguna, E., Belmonte Serrato, F., Tobarra Ochoa, P. (1999) Regional Economic and Social Approaches to Desertification. In : MEDALUS III Final Report, Project 3., Thatcham: http://www.medalus.leeds.ac.uk, pp.171-196

López Gómez, A. (1989) Aguaceros extraordinarios e inundaciones en la costa mediterránea española (1957-1982) In: A.Gil Olcina & A. Morales Gil (Eds) Avenidas Fluviales e Inundaciones en la Cuenca del Mediterráneo. Guadalajarra: Instituto Universitario de Geografía de la Universidad de Alicante y Caja de Ahorros del Mediterráneo, pp.31-50

Lyford, F.P. and Qashu, H.K. (1969) Infiltration rates as affected by desert vegetation. Water Resources Research, 5, pp.1373-1376

Markham, B.L., Baker, J.L. (1986) EOSAT Landsat Technical Notes, No. 1, EOSAT, Lanham, Maryland, pp. 1-8

Martínez de Azagra Paredes , A. (1996) Diseño de Sistemas de Recolección de Agua para la Repoblación Forestal. Madrid: Ediciones Mundi-Prensa

Martinez-Mena Garcia, M. (1995) Respuesta Hidrologica en Medios Semiaridos: Factores de Control y Modelizacion. PhD thesis, Murcia: Universidad de Murcia

Medalus (1993) Research project on Mediterranean desertification and land use. Presentation of research area: Guadalentín Basin, Spain. Murcia: Universidad de Murcia, Confederación Hidrografica del Segura, Instituto Nacional para la Conservación de la Naturaleza (Medalus II Report, Project 4)

Melía, J. (1996) Use of soil and rock spectral signatures for natural vegetation cover estimation. In: Hill, J., Peter, D. (Eds.) The use of remote sensing for land degradation and desertification monitoring in the Mediterranean basin, State of the art and future research. Luxembourg: European Commision EUR 16732 EN, pp.183-198

Merz, B., Plate, E.J., (1997) An analysis of the effects of spatial variability of soil and soil moisture on runoff. Water resources research 33, pp. 2909-2922
Moore, I.D., Lewis, A., Gallant, J.C. (1993) Terrain Attributes: Estimation Methods and Scale Effects. In: A.J. Jakeman, M.B. Beck, M.J. McAleer (Eds.) Modelling Change in Environmental Systems, Chichester: Wiley, pp.189-214
Melía, J. (1996) Use of soil and rock spectral signatures for natural vegetation cover estimation. In: Hill, J., Peter, D. (Eds.) The use of remote sensing for land degradation and desertification monitoring in the Mediterranean basin, State of the art and future research. Luxembourg: European Commision EUR 16732 EN, pp.183-198
Moran, M.S., Humes, K.S., Pinter, P.J.Jr. (1997) The scaling characteristics of remotely-sensed variables for sparsely-vegetated heterogeneous landscapes. Journal of Hydrology 190, pp. 337-362
Mosch, W. (1999) Study on the genesis of landforms in the Guadalentín catchment (Prov. Murcia, SE-Spain). Doctoraal verslag, Vakgroep Fysische Geografie en Bodemkunde, Amsterdam: Universiteit van Amsterdam
Navarro Hervás, F. (1991) El Sistema Hidrográfico del Guadalentín. Cuadernos Tecnicos 6. Murcia: Región de Murcia, Consejería de Política Territorial, Obras Públicas y Medio Ambiente
Nearing, M.A. (1998) Why soil erosion models over-predict small soil losses and under-predict large soil losses. Catena 32, pp. 15-22
Nearing, M.A. (2000) Evaluating Soil Erosion Models using Measured Plot Data: Accounting for Variability in the Data. Earth Surface Processes and Landforms 25, pp. 1035-1043
Nonhebel, M. (1999) Infiltration properties in soils developed in different parent materials in SE Spain. Doctoraal verslag, Fysische geografie en bodemkunde, Amsterdam: Universiteit van Amsterdam.
Odijk, M., Van Bemmel, S. (1997) De invloed van stenen op hydrologische processen en bodemerosie op verschillende schaalniveaus in een semi-aride gebied in zuidoost-Spanje. Doctoraal verslag, Vakgroep Fysische Geografie, Utrecht: Universiteit Utrecht
O'Niell, R>V>, DeAngelis, D.L., Waide, J.B., Allen, T.F.H. (1986) A hierarchical concept of ecosystems. Princeton, New Jersey: Princeton University Press
Orekes, N., Shrader-Frechette, K., Belitz, K. (1994) Verification, Validation, and Confirmation of Numerical Models in the Earth Sciences. Science 263, pp. 641-646
Pebesma, E.J., (1995) GSTAT: geostatistical modelling, prediction and simulation. Computer program manual. Available from http://www.geog.nl.uu.nl/gstat/
Pérez Pujalte, A. (Ed.) (1993) Proyecto Lucdeme, Mapa de Suelos, Escala 1:100.000 Velez Blanco-952. Madrid: ICONA, Universidad de Murcia, Ministerio de Agricultura Pesca y Alimentacion
Perry Jr., C.R., Lautenschlager, L.F. (1984) Functional Equivalence of Spectral Vegetation Indices. Remote Sensing of Environment 14, pp. 169-182
Philip, J.R. (1957) The theory of infiltration: 1. The infiltration equation and its solution. Soil Science 83, pp. 345-357
Pickup, G., Chewings, V.H. (1996) Identifying and measuring land degradation processes using remote sensing. In: Hill, J., Peter, D. (Eds.) The use of remote sensing for land degradation and desertification monitoring in the Mediterranean basin, State of the art and future research. Luxembourg: European Commision EUR 16732 EN, pp.135-147
Pilgrim, D.H., Chapman, T.G., Doran, D.G. (1988) Problems of rainfall-runoff modelling in arid and semiarid regions. Hydrological Sciences – Journal – des Sciences Hydrologiques 33, pp. 379-400
Poesen, J. (1996) Effects of rock fragments on soil degradation processes in Mediterranean environments. In: Rubio, J.L., Calvo, A. (Eds.) Soil degradation and desertification in Mediterranean environments. Logroño: Geoforma Ediciones, pp. 185-222
Poesen, J.W.A, Hooke, J.M. (1997) Erosion, flooding and channel managment in Mediterranean environments of southern Europe. Progress in Physical Geography, 21,2, pp. 157-199
Prinsen, H.A.M. (in prep.) Soil-water-vegetation interactions at different scales: consequences for land degradation processes in semi-arid environments, PhD thesis, Amsterdam: Universiteit van Amsterdam
Puigdefábregas, J., Sánchez, G. (1996) Geomorphological implications of vegetation patchiness on semi-arid slopes. In: Anderson, M.G., Brooks, S.M. (Eds.) Advances in Hillslope Processes, Volume 2. Chichester: Wiley, pp. 1027-1060

Puigdefábregas, J., Alonso, J.M., Delgado, L., Domingo, F., Cueto, M., Gutiérrez, L., Lázaro, R., Nicolau, J.M., Sánchez, G., Solé, A, Vidal, S., Aguilera, C., Brenner, A., Clark, S., Incoll, L, (1996) The Rambla Honda field site: Interactions of soil and vegetation along a catena in semi-arid southeast Spain. In: Brandt, C.J., Thornes, J.B. (Eds.) Mediterranean Desertification and Land Use. Chichester: Wiley pp. 137-168

Puigdefabregas, J., Sole, A., Gutierrez, L., del Barrio, G., Boer, M. (1999) Scales and processes of water and sediment redistribution in drylands: results from the Rambla Honda field site in Southeast Spain. Earth-Science Reviews 48, pp. 39-70

Quinn, P.F., Beven, K.J., Lamb, R. (1995) The ln(a/tan□) index: how to calculate it and how to use it within the TOPMODEL framework. Hydrological Processes 9, pp. 161-182

Quinton, J.N., Edwards, G.M., Morgan, R.P.C. (1997) The influence of vegetation species and plant properties on runoff and soil erosion: results from a rainfall simulation study in south east Spain. Soil Use and Management 13, pp. 143-148

Richardson, A.J., Wiegand, C.L. (1977) Distinguishing vegetation from soil background information. Photogrammetric Engineering and Remote Sensing 43, pp. 1541-1552

Rojo Serrano, L., Carrera Morales, J.A., Martinez Artero, J.A. (1993) Guadalentín Basin. In: First Annual report MEDALUS III, Project 4, Research and policy interfaces in selected regions, Thatcham, http://www.medalus.leeds.ac.uk, pp. 30-37

Rojo Serrano, L. (1995) Spanish National Plan to combat desertification. In: Desertification in an European context: physical and socio-economic aspects. Luxembourg, Report EUR 15414 EN, pp.357-358

Rojo Serrano, L., García Robredo, F., Martínez Artero, J-A., (1999) Economic Assessment of Watershed Restoration Actions. In: MEDALUS III Final Report, Project 3, Thatcham, http://www.medalus.leeds.ac.uk, pp., 131-169

Roméro Díaz, M.A., Lopéz Bermúdez, F., Silva, P.G., Rodriguez Estrella, T., Navarro Hervas, F., Díaz del Olmo, F., Goy, J.L., Zazo, Cl, Baena Escudero, R, Somoza, L., Mather, A., Borja Barrera, F. (1992) Geomorfología de las cuencas neogeno-cuaternatias de Mula y Guadalentín. Cordilleras Beticas, Sureste de España. In: Lopéz Bermúrdez, F., Conesa García, C., Roméro Díaz, M.A. (Eds.) Estudios de Geomorfología en España. Murcia: Actas de la II Reunión Nacional de Geomorfología, Sociedad Española de Geomorfología, pp.749-786

Romero-Díaz, A., Cammeraat, L.H., Vacca, A., Kosmas, C. (1999) Soil erosion at three experimental sites in the Mediterranean. Earth Surface Processes and Landforms 24, pp.1243-1256

Rubio, J.L. and Calvo, A. (1996) Mechanisms and processes of soil erosion by water in Mediterranean Spain. In: Rubio, J.L., & Calvo, A. (Eds) Soil Degradation and desertification in Mediterranean environments. Logroño: Geoforma Ediciones, pp.37-48

Rubio, J.L. (1998) The Spanish experience in combating desertification and its impacts. In: UNEP convention to combat desertification, http://www.unep.ch/incd/partvi.html

Rutter, A.J., Kershaw, K.A., Robins, P.C., Morton, A.J. (1971) A predictive model of rainfall interception in forests, 1 Deriviation of the model from observations in a plantation of corsican pine. Agricultural Meteorology 9, pp. 367-384

Scoging, H. (1989) Runoff generation and sediment mobilisation by water. In: Thomas, D.S.G. (Ed.) Arid zone geomorphology, London: Belhaven, pp. 87-116

Selby, (1985) Earth's Changing Surface, an introduction in geomorphology, Oxford: Clarendon Press

Settle, J.J., Drake, N.A., (1993) Linear mixing and the estimation of ground cover proportions. International Journal of Remote Sensing 14 (6), pp. 1159-1177

Seyfried, M.S., Wilcox, B.P. (1995) Scale and the nature of spatial variability: Field examples having implications for hydrologic modelling. Water Resources Research 31 (1), pp. 173-184

Shaw, E.M. (1988) Hydrology in Practice, second edition. London: VNR International

Singh, V.P. (1997) Effect of spatial and temporal variability in rainfall and watershed characteristics on stream flow hydrograph. Hydrological Processes, 11, pp. 1649-1669

Smith, R.E., Parlange, J.-Y. (1978) A parameter-efficient hydrologic infiltration model. Water Resources Research 14 (3), pp. 533-538

Smith, M.O, Ustin, S.L., Adams, J.B., Gillespie, A.R. (1990) Vegetation in Deserts: I. A regional measure of abundance from multispectral images. Remote Sensing of Environment 31. pp.1-26

Space Imaging EOSAT (1998) Digital Number (DN) to Radiance Conversion Procedures. http:/www.spaceimage.com/home/pubs/tech_papers/radiance.html
Soediono, H. (1971) Geological inverstigations in the Chirivel Area, Province of Almeria – south eastern Spain, Ph.D. thesis, Amsterdam: Universiteit van Amsterdam
Solé-Benet, A., Calvo, A., Cerdà, A., Lázaro, R., Pini, R., Barbero, J. (1997) Influences of micro-relief patterns and plant cover on runoff related processes in badlands from Tabernas (SE Spain). Catena 31, pp. 23-38
Sorriso-Valvo, M., Bryan, R.B., Yair, A., Iovino, F., Antronico, L. (1995) Impact of afforestation on hydrological response and sediment production in a small Calabrian catchment. Catena 25, pp. 89-104
Strahler, A.N. (1964) Quantitative geomorphology of drainage basins and channel networks. In: Chow, V.T. (Ed.) Handbook of applied hydrology. New York: McGraw-Hill, pp. 4.39-4.76
Sullivan, M., Warwick, J.J., Tyler, S.W. (1996) Quantifying and delineating spatial variations of surface infiltration in a small watershed. Journal of Hydrology 181, pp. 149 - 168
Ternan, J.L., Elmes, A., Gonzalez del Tanago, M., Williams, A.G. BLanco, R. (1997) Conversion of mattoral land to *Pinus* forest: some hydrological and erosional impacts (Reboisement de matorral en *Pinus*: quelques impacts hydrologiques et érosifs) Méditerranée 1.2, pp. 77-84
Thomas, D.S.G., Middleton, N.J. (1994) Desertification, Exploding the Myth. Chichester: Wiley
Thornes, J.B. (1976) Semi-arid erosional systems. Geographical Papers No. 7 London School of Economics and Political Science.
Thornes, J.B. (1977) Channel Changes in Ephemeral Streams: Observations, Problems and Models. In: K.J. Gregory (Ed.) River Channel Changes, Chichester: Wiley, pp. 317-335
Thornes, J.B. (1985) The ecology of erosion. Geography, pp.222-235
Thornes, J.B. (1994) Catchment and channel hydrology. In: A.D Abrahams & A.J. Parsons, (Eds.) Geomorphology of desert environments, pp. 257-287
Thornes, J., Shannon, J., Richardson, R. (1999) Modelling flow regimes in ephemeral channels. In: MEDALUS III Final Reports; Project 4. Thatcham, http://www.medalus.leeds.ac.uk, pp. 197-244
Thornthwaite, C.W. (1948) An approach towards a rational classification of climate. Geographical review 38, pp. 55-94
Thornthwaite, C.W., Mather, J.R. (1957) Instructions and tables for computing potential evapotranspiration and the water balance. Publications in Climatology Vol. X no. 3, Centerton, New Jersey: Drexel Institute of technology laboratory of climatology
Turcke, M.A, Kueper, B.H., (1996) Geostatistical analysis of the Borden aquifer hydraulic conductivity field. Journal of Hydrology 178, pp. 223-240
Tucker, C.J. (1979) Red and Photographic Infrared Linear Combinations for Monitoring Vegetation. Remote Sensing of Environment 8, pp. 127-150
Twomey, S. (1977) Introduction to the mathematics of inversion in remote sensing and indirect measurements. Developments in Geomathematics 3, Amsterdam: Elsevier
Van Deursen, W.P.A. (1995) Geographical Information Systems and Dynamic Models, development and application of a prototype spatial modelling language. Utrecht: Koninklijk Nederlands Aardrijkskundig Genootschap/Unversiteit Utrecht (Nederlandse Geografische Studies 190)
Van Dijck, S.J.E. (2000) Effects of agricultural land use on surface runoff and erosion in a Mediterranean area. Utrecht. Koninklijk Nederlands Aardrijkskundig Genootschap/Unversiteit Utrecht (Nederlandse Geografische Studies 263)
Vera, J.A. (1983) Las Zonas Externas de las Cordilleras Beticas. In: Geología de España (libro jubilar J.M. Rios) Tomo II, IGME, pp. 218-251
Webster, R., Oliver, M.A. (1990) Statistical Methods in Soil and Land Resource-Survey (Spatial Information Systems). Oxford: Oxford University Press
Wesseling, C.G., Karssenberg, D., Van Deursen, W.P.A., Burrough, P.A. (1996) Integrating dynamic environmental models in GIS: the development of an dynamic modelling language. Transactions in GIS 1, pp. 40-48
Wood, E.F., Sivapalan, M., Beven, K., Band, L. (1988) Effects of spatial variability and scale with implications to hydrologic modeling. Journal of Hydrology 102, pp. 29-47

Wood, E.F., Sivapalan, M., Beven, K. (1990) Similarity and scale in catchment storm response. Reviews of Geophysics, 28,1, pp.1-18
Wood, E.F. (1995) Scaling behaviour of hydrological fluxes and variables: empirical studies using a hydrological model and remote sensing data. In: J.D. Kalma, M. Sivapalan (Eds.) Scale Issues in Hydrological Modelling, Advances in Hydrological Processes, Chichester: Wiley, pp. 89-104
Wood, E.F. (1998) Scale analyses for land-surface hydrology. In: G. Sposito (Ed.) Scale dependence and scale invariance in hydrology. Cambridge: Cambridge University Press, pp. 1-29
Woods, R., Sivapalan, M., Duncan, M. (1995) Investigating the representative elementary area concept: an approach based on field data. In: J.D. Kalma, M. Sivapalan (Eds.) Scale Issues in Hydrological Modelling, Advances in Hydrological Processes, Chichester: Wiley, pp. 49-70
Woolhiser, D.A., Smith, R.E., Giraldez, J.-V. (1996) Effects of spatial variability of saturated hydraulic conductivity on Hortonian overland flow. Water Resources Research 32 (3), pp. 671-678
Yair, A., Lavee, H. (1985) Runoff generation in arid and semi-arid zones, chapter 8. In: M.G. Anderson, T.B. Burt (Eds.) Hydrological Forecasting, Chichester: Wiley, pp. 183-200
Yin, Z., Lee Williams, T.H. (1997) Obtaining Spatial and Temporal Vegetation Data from Landsat Mss and AVHRR/NOAA Satellite Images for a Hydrologic Model. Photogrammetric Engineering & Remote Sensing 63 (1), pp. 69-77

Appendix 1 Variogram models of surface cover estimates

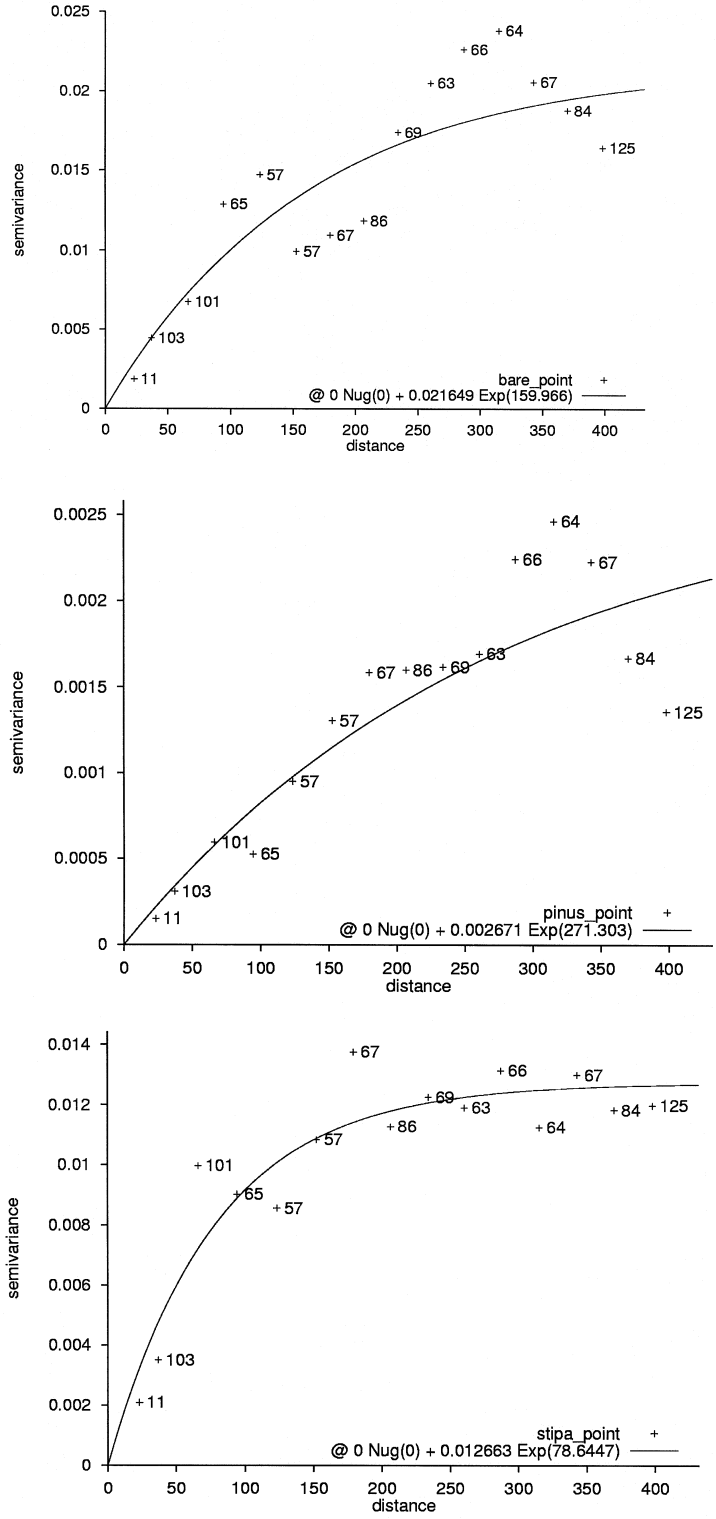

A1 Variogram models of field estimates; unvegetated soil (top), *Pinus halepensis* (middle) and *Stipa tenacissima* (bottom), distance in meters.

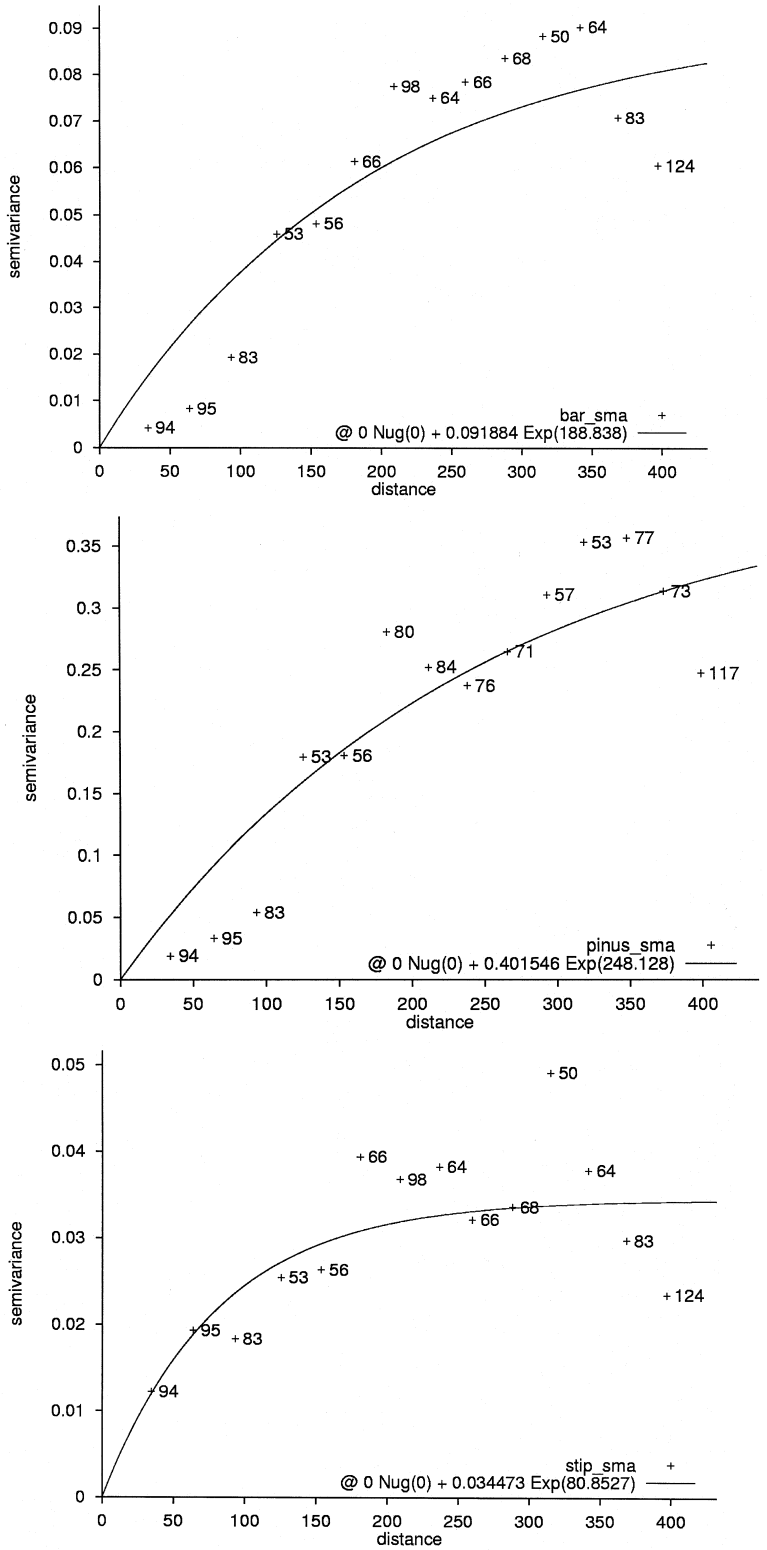

A2 Variogram models of SMA of TM070493; unvegetated soil (top), *Pinus halepensis* (middle) and *Stipa tenacissima* (bottom), distance in meters.

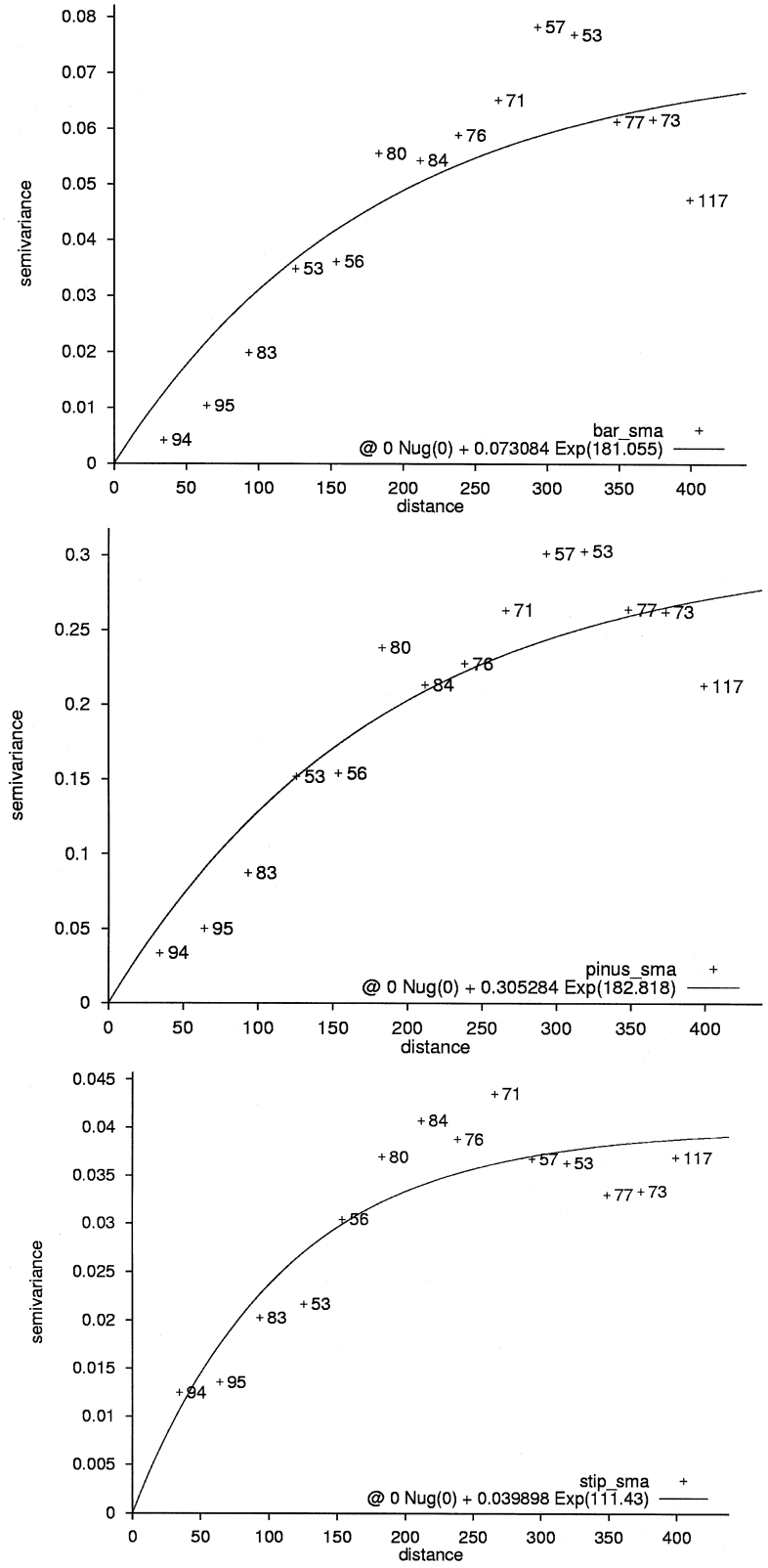

A3 Variogram models of SMA of TM140993; unvegetated soil (top), *Pinus halepensis* (middle) and *Stipa tenacissima* (bottom), distance in meters.

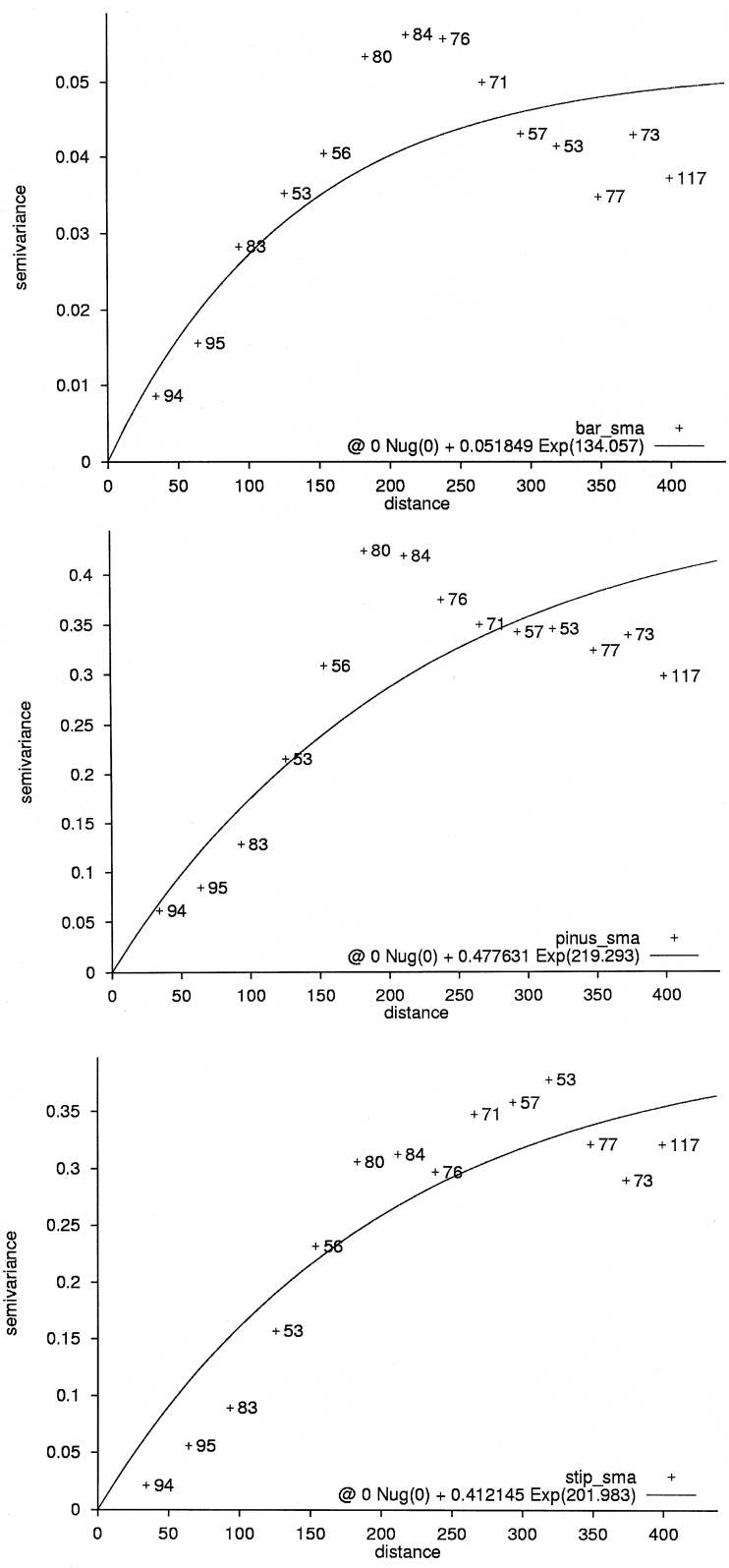

A4 Variogram models of SMA of TM031293; unvegetated soil (top), *Pinus halepensis* (middle) and *Stipa tenacissima* (bottom), distance in meters.

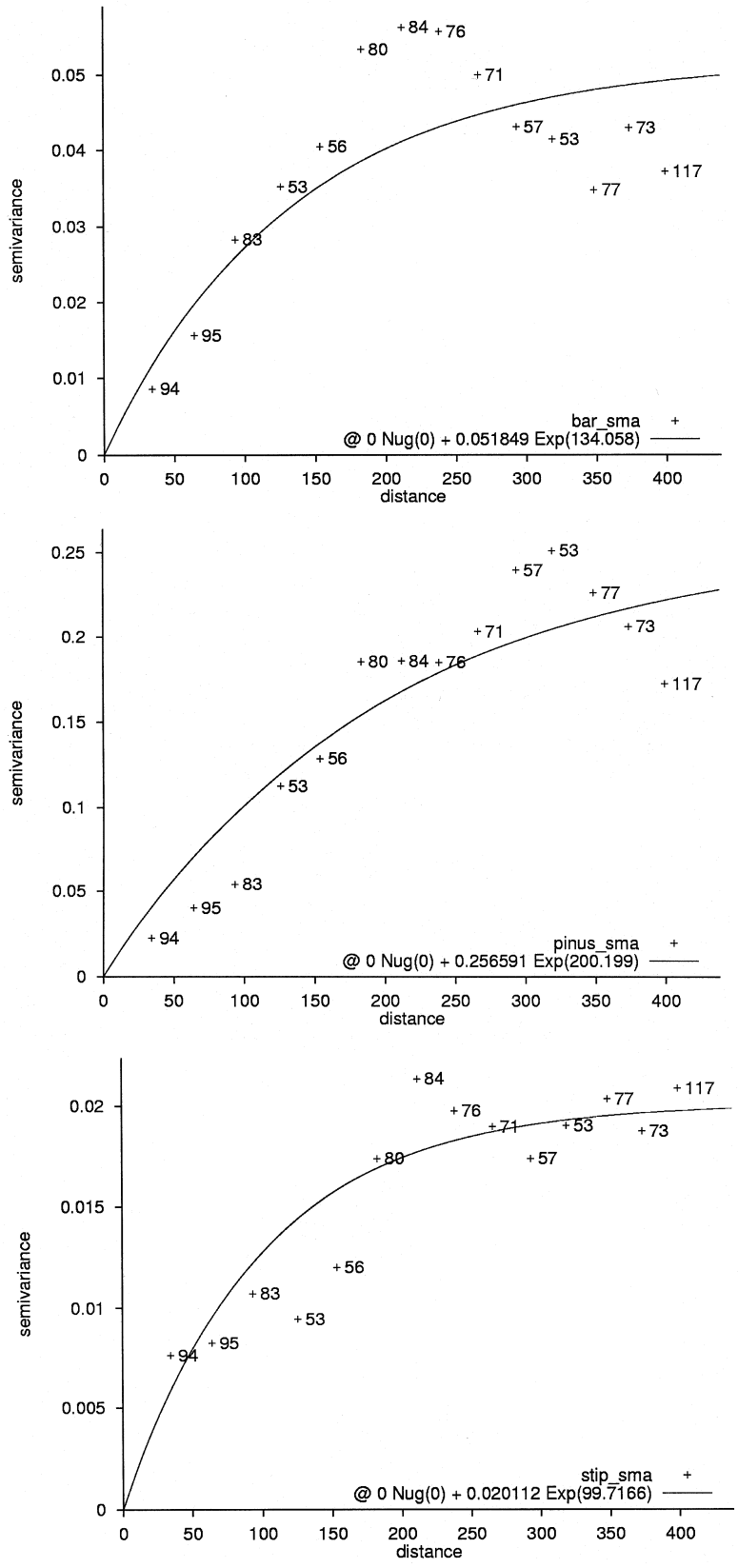

A5 Variogram models of SMA of TM290394; unvegetated soil (top), *Pinus halepensis* (middle) and *Stipa tenacissima* (bottom), distance in meters.

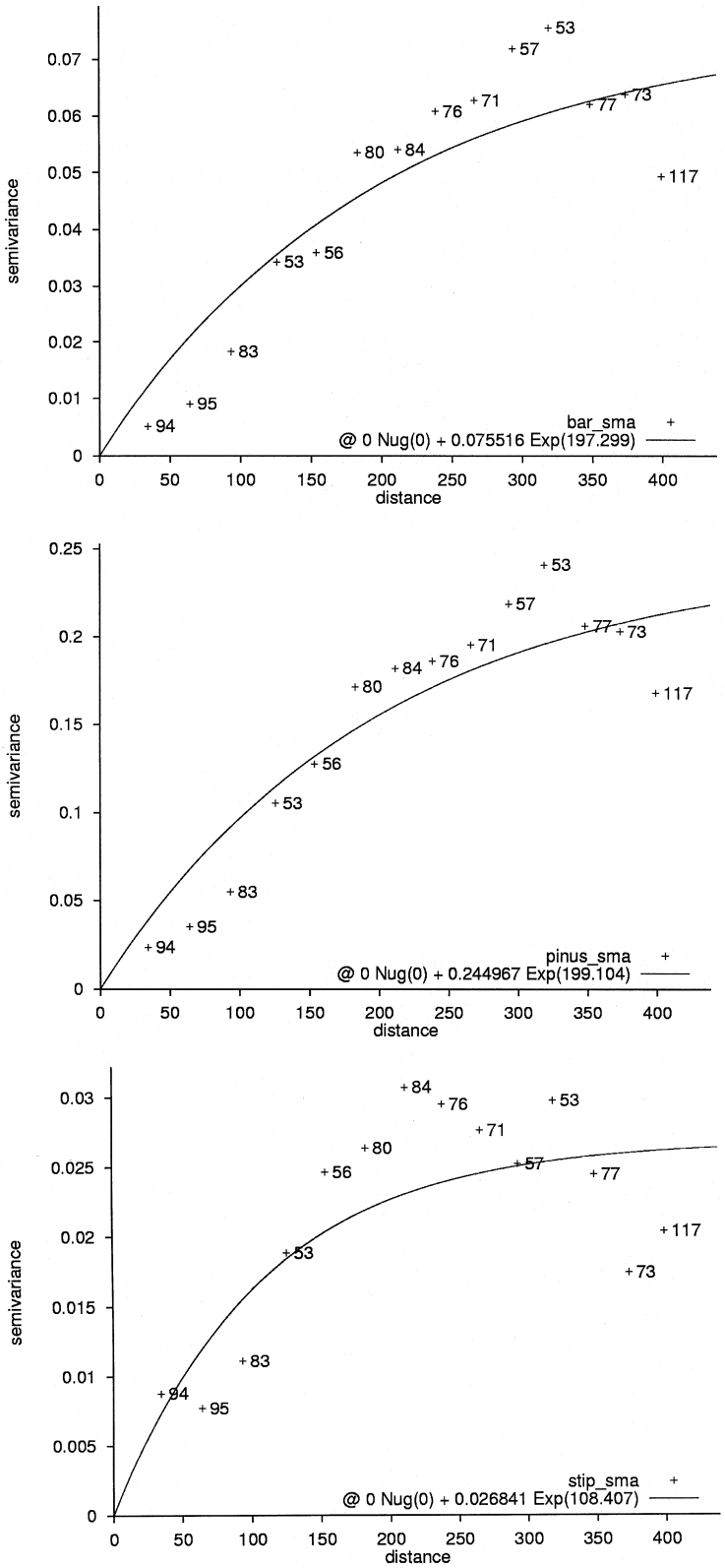

A6 Variogram models of SMA of TM270494; unvegetated soil (top), *Pinus halepensis* (middle) and *Stipa tenacissima* (bottom), distance in meters.

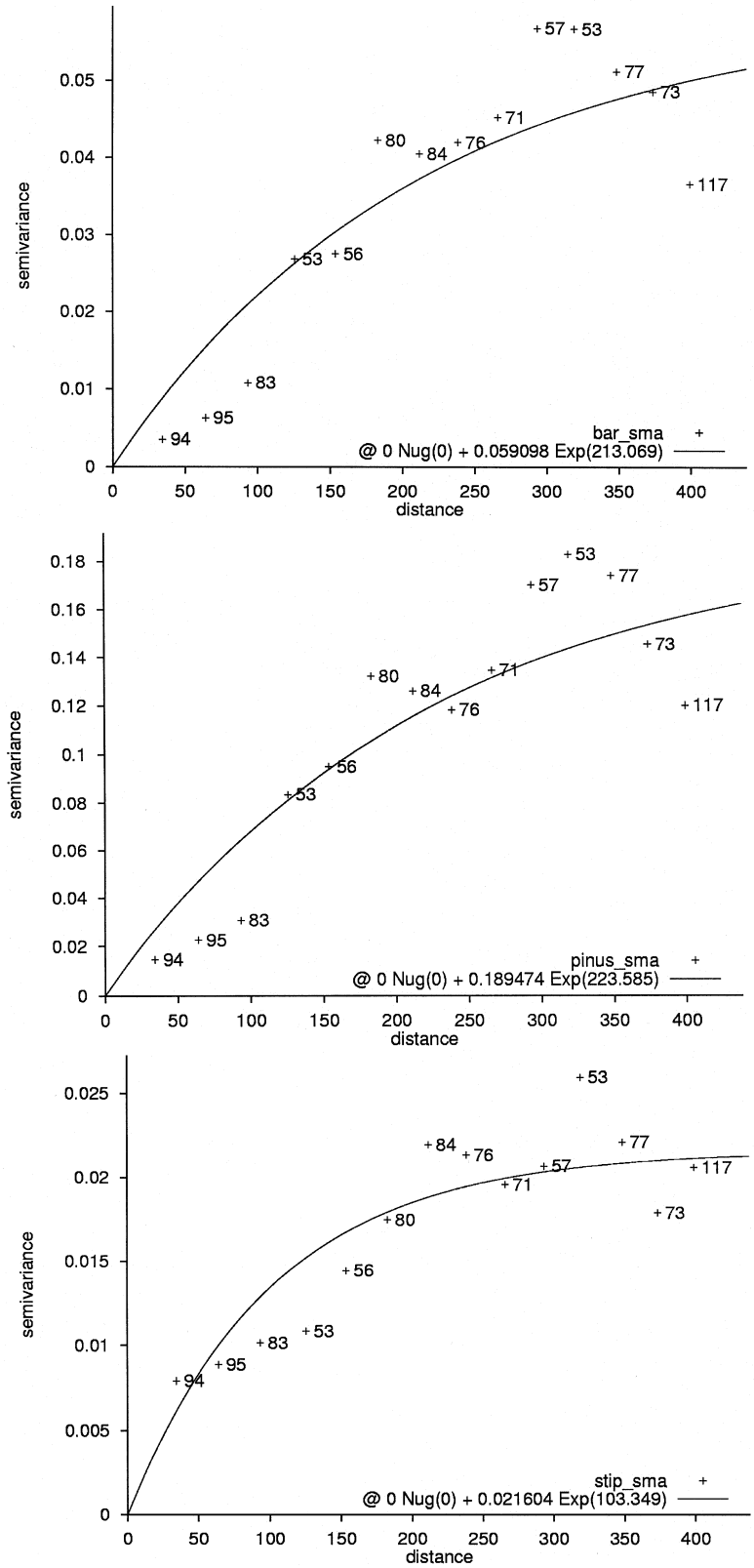

A7 Variogram models of SMA of TM280594; unvegetated soil (top), *Pinus halepensis* (middle) and *Stipa tenacissima* (bottom), distance in meters.

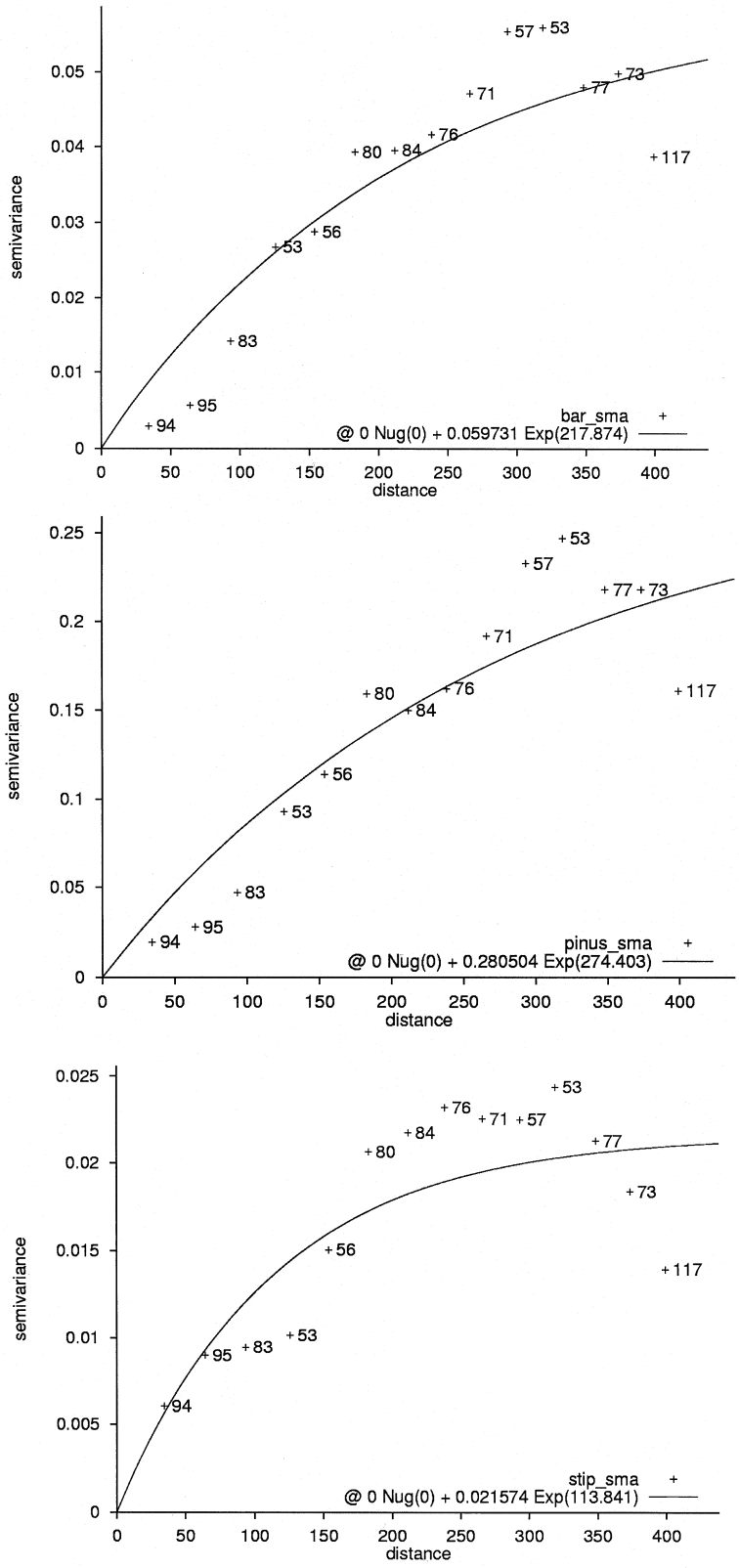

A8 Variogram models of SMA of TM310794; unvegetated soil (top), *Pinus halepensis* (middle) and *Stipa tenacissima* (bottom), distance in meters.

Curriculum vitae

Anja de Wit werd op 5 september 1968 geboren te Schalkwijk. In 1985 behaalde zij haar HAVO diploma aan de St. Gregorius scholengemeenschap in Utrecht. Vervolgens behaalde ze in 1987 haar diploma OVWO aan het St. Bonifatius college in Utrecht.

Ze ging in 1987 technische natuurkunde studeren aan de Technische Universiteit Twente. Ze veranderde in 1988 van studie en begon met fysische geografie aan de Universiteit Utrecht. In 1989 behaalde ze haar propedeuse. Tijdens haar vervolgdoctoraal koos ze landdegradatie als specialisatie. Ze deed een groot bijvak bodem- en waterconservering aan de Wageningen Universiteit waarvoor ze in Burkina Faso de vochtbeschikbaarheid voor de groei van de *acacia seyal* bestudeerde. Vervolgens deed ze haar vervolgdoctoraal veldwerk in Botswana waar ze de geschiktheid voor regenafhankelijke en geïrrigeerde landbouw onderzocht. In 1994 rondde ze haar studie fysische geografie af.

In 1995 werd ze aangenomen als onderzoeker in opleiding bij de vakgroep fysische geografie van de Universiteit Utrecht waar ze deel uitmaakte van het project: 'Hierarchy of land degradation processes in a Mediterranean environment'. Binnen dit project heeft Anja onderzoek uitgevoerd naar de factoren die runoff bepalen op verschillende schaalniveaus in het semi-aride gedeelte van Spanje. Dit onderzoek staat beschreven in dit proefschrift.